The Chemistry of Cyclopropylarene Radical Cations

by

Yonghui Wang

Dissertation submitted to the Faculty of the Virginia Polytechnic Institute and State University in partial fulfillment of the requirements for the degree of

DOCTOR OF PHILOSOPHY

IN

CHEMISTRY

APPROVED:

_____

James M. Tanko, Chair

_____

Neal Castagnoli, Jr. Richard D. Gandour

_____

David G. I. Kingston Mark R. Anderson

May, 1997

Blacksburg, Virginia

Key words: Cyclopropylarene, Radical Cation, Ring Opening, Deprotonation, Anodic Oxidation, Ce(IV) Oxidation, Voltammetry, Reaction Mechanism and Kinetics

THE CHEMISTRY OF CYCLOPROPYLARENE RADICAL CATIONS

by

Yonghui Wang

James M. Tanko, Chairman

Chemistry

(ABSTRACT)

Cyclopropane derivatives are frequently utilized as "probes" for radical cation intermediates in a number of important chemical and biochemical oxidation. The implicit assumption in such studies is that if a radical cation is produced, it will undergo ring opening. Through a detailed examination of follow-up chemistry of electrochemically and chemically generated cyclopropylarene radical cations, we have shown that the assumption made in the use of these substrates as SET probes is not necessarily valid. While cyclopropylbenzene radical cation undergoes rapid methanol-induced ring opening (e.g., $k = 8.9 \times 10^7\ s^{-1}M^{-1}$), the radical cations generated from 9-cyclopropylanthracenes do not undergo cyclopropane ring opening at all. The radical cations generated from cyclopropylnaphthalenes disproportionate or dimerize before undergoing ring opening. Utilizing cyclic, derivative cyclic, and linear sweep voltammetry, it was discovered that decay of radical cations generated from cyclopropylnaphthalenes in CH_3CN/CH_3OH is second order in radical cation and zero order in methanol. Anodic and Ce(IV) oxidation of all these naphthyl substrates in CH_3CN/CH_3OH led to cyclopropane ring-opened products. However, the rate constant for methanol-induced ring opening ($Ar\text{-}c\text{-}C_3H_5^{+\cdot} + CH_3OH \rightarrow$

$ArCH(\bullet)CH_2CH_2O(H^+)CH_3$) is extremely small (<20 s^{-1} M^{-1} for 1-cyclopropylnaphthalenes) despite the fact that ring opening is exothermic by nearly 30 kcal/mol. These results are explained on the basis of a product-like transition state for ring opening wherein the positive charge is localized on the cyclopropyl group, and thus unable to benefit from potential stabilization offered by the aromatic ring. Reactions of radical cations generated from 9-cyclopropylanthracenes in CH_3CN/CH_3CN have also been investigated electrochemically. The major products arising from oxidation of these anthryl substrates are attributable to CH_3OH attack at the aromatic ring rather than CH_3OH-induced cyclopropane ring opening. Ce(IV) oxidation of 9-cyclopropyl-10-methylanthracene and 9,10-dimethylanthracene further showed that radical cations generated from these anthryl substrates undergo neither cyclopropane ring opening nor deprotonation but nucleophilic addition. Side-chain oxidation products from Ce(IV) oxidation of methylated anthracenes arose from further reaction of nuclear oxidation products under acidic and higher temperature conditions. An analogous (more product-like) transition state picture can be applied for cyclopropane ring opening and deprotonation of these anthryl radical cations. Because of much higher intrinsic barrier to either nucleophile-induced cyclopropane ring opening or deprotonation of these anthryl radical cations, nucleophilic addition predominates. Stereoelectronic effects may be another additional factor contributing to this intrinsic barrier because the cyclopropyl group in these anthryl systems adopts a perpendicular conformation which may not meet the stereoelectronic requirements for cyclopropyl ring opening at either the radical cation or dication stage.

ACKNOWLEDGEMENTS

I would like to express my sincere gratitude to Dr. James M. Tanko for his patience, guidance and friendship during my graduate career. I am very grateful to all of my committee members for their generous donation of time and critical reviews of my work and progress. I would like to thank the other faculty members and graduate students (past and present) in the Department of Chemistry who made my stay at Virginia Tech very pleasant.

A special thanks goes to NSF (CHEM-9412814) and the Department of Chemistry at Virginia Tech for financial support.

Finally, and perhaps most importantly, I would like to thank my entire family (my parents and my brothers and sisters) for their unyielding support and understanding. An extremely warm and loving thanks is given to my dearest wife, Ailian, my lovely son, Tony and my mother-in-law, Xiulan Li, who keeps me sane through all these years.

TABLE OF CONTENTS

LIST OF SCHEMES

LIST OF FIGURES

LIST OF TABLES

CHAPTER 1. HISTORICAL

1.1 INTRODUCTION

Organic radical cations, their structures and their reactions have been attracting ever increasing attention for the last two decades.[1,2] Radical cations are important intermediates in a variety of chemical and biological processes, encompassing photosynthesis[3] and interstellar chemistry[4] and ranging from conducting polymers[5] to synthetically useful reactions, such as electron transfer induced anti-Markovnikov additions,[6] radical cation Diels-Alder reactions,[7] or nucleophilic substitution reactions.[8]

"The Formation, Properties and Reactions of Radical Cations in Solution" was extensively reviewed by Bard et al. in 1976.[9] Since then, there have been a number of other good reviews such as "Electron Transfer Reactions in Organic Chemistry" by Eberson (1982),[10] "The Kinetics and Mechanism of Reactions of Organic Cation Radicals in Solution" by Hammerich and Parker (1984),[11] and "The Structure and Reactivity of Organic Radical Cations" by Roth (1992).[12] Other important reviews dealing with cyclopropane chemistry are "Photochemistry of Cyclopropanes" by Hixson (1979)[13] and "Cyclopropane Radical Cations" by Boche and Walborsky (1990).[14]

1.1.1 Generation, Detection and Methods for Studying Radical Cations

Generation. A radical cation is generated by the removal of one electron from a neutral molecule. The resulting species is at the same time a cation (the positive charge

caused by the loss of an electron) and a radical (the remaining unpaired electron). One-electron oxidation can be achieved by a variety of methods such as chemical oxidation, photochemical oxidation, electrochemical oxidation, and other methods like pulse radiolysis and electron impact ionization.

Chemical Oxidation. A variety of chemical oxidizing reagents has been applied for the generation of radical cations. The principal types of reagents include: Bronsted and Lewis acids; the halogens; certain peroxide anions or radical anions; numerous metal ions or oxides; nitrosonium and dioxygenyl ions; stable organic (aminium) radical cations; some semiconductor surfaces; and certain zeolites.

Photochemical Oxidation. A mild and versatile method for the generation of radical cation-radical anion pairs in solution is based on photoinduced electron transfer (PIET).[15] This method utilizes the fact that the oxidative power of an acceptor or the reductive power of a donor is substantially enhanced by photoexcitation. Thus, for donor and acceptor pairs with negligible or weak interactions in the ground state, electronic excitation of either reactant may lead to the generation of radical ion pairs via electron transfer. The resulting pairs have limited lifetimes since they readily undergo intersystem crossing and recombination. For the study of radical cations it is advantageous to excite the acceptor. Singlet excited state electron acceptors are likewise used as organic photooxidants. The most frequently used singlet state electron acceptors are aromatic hydrocarbons bearing one or more cyano groups.

Electrochemical Oxidation. Anodic oxidation is one of most important methods to generate radical cations.[16] An electrode is fundamentally an electron transfer agent so that, given the proper solvent system, anodic oxidation allows formation of the radical

cation without formation of a reduced species in the immediate vicinity of the radical cation. Moreover, because the potential of the electrode can be adjusted precisely, its oxidizing power can be controlled and further oxidation of the radical cation can be avoided. A variety of electrochemical techniques has been developed for the generation and study of organic radical cations.[16]

Detection. The methods for detection of radical cations are mostly physical methods such as mass spectrometry (MS), ultraviolet photoelectron spectroscopy (UV-PES), optical spectroscopy, electron spin resonance (ESR), fluorescence detected magnetic resonance (FDMR), and nuclear magnetic resonance (NMR) methods (e.g. chemically induced dynamic nuclear polarization, or CIDNP). Among the techniques available to study free radicals or radical ions in solution, ESR stands out as a technique with sufficient resolution to provide detailed information about the identity and structure of the intermediate in question. CIDNP is the technique most recently introduced to study radical cations. It is based on transient enhanced NMR signals, in absorption or emission, shown by some diamagnetic products of radical reactions. The signal can be related to ^{1}H hyperfine couplings which reveal structural features of the intermediates. The results from CIDNP can be expected to reflect the equilibrium structure of the intermediates. This method has been successfully applied to the investigation of cyclopropane radical cations.[12]

Methods for Studying Radical Cations. The decay kinetics and mechanism of radical cations can be studied by laser flash photolysis (LFP), spectroelectrochemistry (e.g. UV-visible spectroelectrochemistry),[17] direct and indirect electrochemistry[18] as well as conventional stop flow method. Electrochemical methods, such as cyclic voltammetry

(CV), derivative cyclic voltammetry (DCV), linear sweep voltammetry (LSV), chronoamperometry and homogenous redox catalysis, have been employed extensively in studies of follow-up reactions of radical cations. Besides, both the general nature and the detailed structure of an intermediate are frequently inferred from the reaction conditions and from the type and structure of the reaction products. Also, molecular orbital calculations at different levels of sophistication have become an integral part in the characterization of organic radical cations in general and those of strained molecules like cyclopropanes in particular.[12,14]

1.1.2 Properties and Reactions of Radical Cations

Radical cations, like other paramagnetic species such as free radicals or radical anions, are much more reactive than the corresponding neutral species. A simple change in oxidation state of a molecule can drastically affect its reactivity. For example, toluene is an extremely weak acid with a pKa of 41. If toluene is oxidized to its radical cation, its pKa plummets to –13[19] (Scheme 1-1).

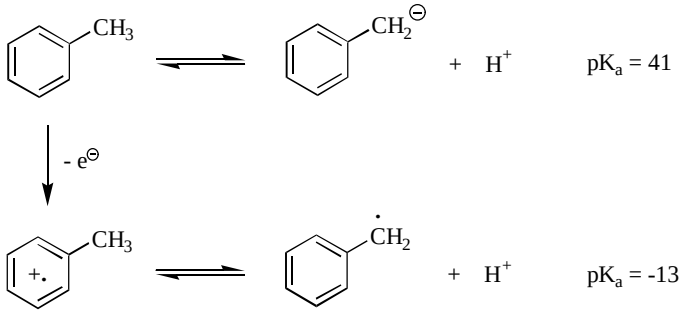

Scheme 1-1. Acidity comparison between toluene and its radical cation

Organic radical cations undergo a rich variety of reactions, including both unimolecular processes and bimolecular reactions. Among the unimolecular reactions are geometric isomerization, rearrangement, cycloreversion, as well as fragmentation and other bond cleavage reactions. In bimolecular reactions, radical cations can react with neutral reagents, ionic substrates (especially nucleophiles), free radicals and radical ions of like and opposite charge. These reactions include a) ion-molecule reactions, such as cycloadditions, hole transfer, or complex formation; b) nucleophile capture; c) spin labeling; and d) dimerization or disproportionation, and reverse electron transfer, proton transfer, atom or group transfer reactions, or coupling. Some typical reactions of organic radical cations which are frequently met in our studies are shown in Scheme 1-2.

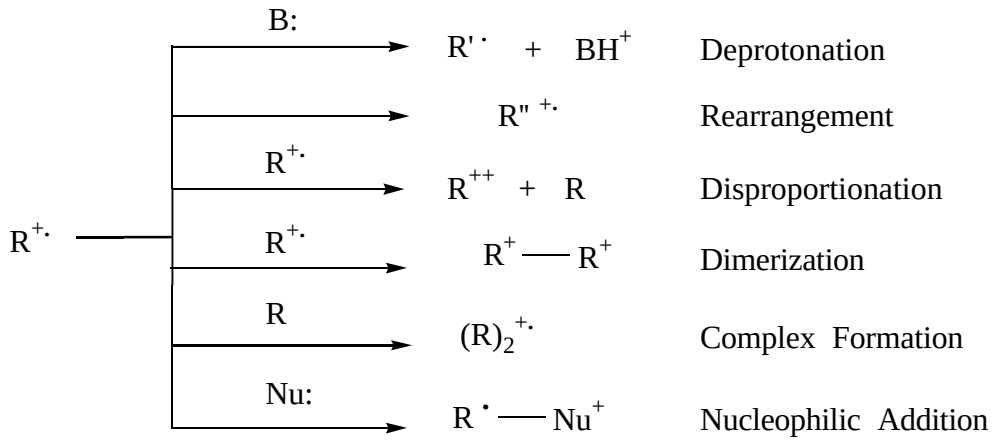

Scheme 1-2. Typical reactions of organic radical cations

Deprotonation. Deprotonation of radical cations in the gas phase is a high energy process due to the formation of a "naked" proton. In solution, however, the large solvation energy of the proton may provide the driving force for radical cation deprotonation, and this reaction is expected to play an important role in the chemistry of a large range of radical cations. The deprotonation of alkylbenzene radical cations has been studied in detail in nonaqueous solvents under aprotic and acidic conditions.

Rearrangement. Unimolecular rearrangements of radical cations, especially of those generated from hydrocarbons containing strained-ring moieties (e.g., cyclopropyl group), have been attracting ever increasing attention over the last two decades.[12] Radical cations generated from strained-ring compounds may undergo rearrangement because of ring strain. Consequently, the unusually low oxidation potential of strained rings were noted.

Disproportionation. In disproportionation, two molecules of radical cation undergo single electron transfer to produce a neutral (parent) molecule and a dication. The reaction is usually detected kinetically, spectroscopically or by electrochemical techniques. Many reactions of radical cations with nucleophiles have the stochiometry of Eq. 1-1:

$$2\ M^{+\cdot} + Nu^{-} \rightarrow M + M\text{-}Nu^{+} \qquad (1\text{-}1)$$

Without the aid of kinetics it is not possible to say what the mechanism is, and two important possibilities exist, namely, direct reaction with the radical cation (Eq. 1-2 and Eq. 1-3):

$$M^{+\cdot} + Nu^{-} \rightarrow M\text{-}Nu^{\cdot} \qquad (1\text{-}2)$$

$$M\text{-}Nu^{\cdot} + M^{+\cdot} \rightarrow M\text{-}Nu^{+} + M \qquad (1\text{-}3)$$

or reaction with a dication formed via disproportionation (Eq. 1-4 and Eq. 1-5):

$$2\ M^{+\cdot} \rightarrow M + M^{2+} \qquad (1\text{-}4)$$

$$M^{2+} + Nu^{-} \rightarrow M\text{-}Nu^{+} \qquad (1\text{-}5)$$

Dimerization and Complex Formation. Two molecules of radical cation may dimerize to form a dimer dication (Eq. 1-6), while a radical cation associates with a parent molecule to form a complex, dimer radical cation (Eq. 1-7):

$$2\ M^{+\cdot} \rightarrow M\text{-}M^{2+} \qquad (1\text{-}6)$$

$$M^{+\cdot} + M \rightarrow M\text{-}M^{+\cdot} \qquad (1\text{-}7)$$

The paramagnetic dimer radical cation is usually characterized by an ESR spectrum with twice as many lines and half the splitting constant of $M^{+\cdot}$, while dimer dication results in spin pairing and the disappearance of the ESR signal.

Nucleophilic Reactions. Radical cations react with a variety of nucleophiles. There are many reactions named on the basis of the nucleophile involved, such as hydroxylation, methoxylation, acetoxylation, acetamidation, pyridination, cyanation, halogenation, etc.. Reactions of these types were classified according to the nature of the reaction: substitution, addition and electron transfer reaction. By virtue of the fact that the initial reaction between a radical cation and a nucleophile produces an unstable radical intermediate, the reactions are inevitably complex. Further electron-transfer reactions accompanied by a proton transfer or reaction with a nucleophile are necessary in order to reach a stable product. These multi-step reactions can give rise to complicated rate laws and the observed mechanism can be highly dependent upon the reaction conditions,

especially on the magnitudes of the concentrations of the reactants. While some nucleophilic reactions occur at the stage of radical cations (Eq. 1-2), others may occur at the stage of dication (Eq. 1-5). The detailed mechanisms were discussed by Parker.[11] Eberson has provided a theoretical explanation for a number of nucleophilic reactions, based on the Dewar-Zimmerman rules.[20]

1.2. BACKGROUND

1.2.1 Ring Opening Reactions of Cyclopropylarene Radical Cations

Among reactions of cyclopropylarene radical cations, cyclopropane ring opening reactions have been the subject of numerous investigations. The methods for studying these reactions ranged from anodic oxidation, photoinduced electron transfer to metal-mediated oxidation. The most frequently employed substrates are cyclopropylbenzene and its derivatives.

Electrochemical Oxidation. Extensive studies have been focused on oxidative cleavage of cyclopropane rings by electrochemical methods in the past and recent years because of the unique reactivity of the strained σ-bonds, easy availability of cyclopropane compounds and the usefulness of the resulting products in organic synthesis. Anodic oxidation of cyclopropylbenzene and derivatives in methanol was studied by Shono, et al.[21] in 1970. The cyclopropane ring-opened products (1,3-dimethoxy ether) were obtained from the bulk electrolysis (Scheme 1-3).

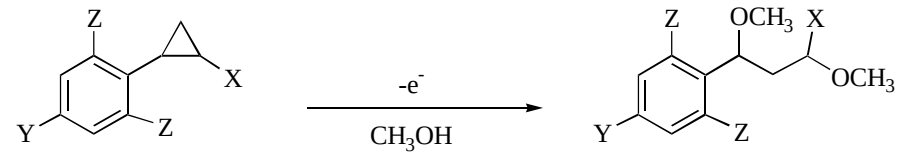

X = H, CH_3, C_6H_5, OCH_3
Y = H, CH_3, OCH_3, Cl
Z = H, CH_3

60~74%

Scheme 1-3. Anodic oxidation of cyclopropylbenzene and derivatives in CH_3OH

Controlled potential oxidation and product analysis suggested that the reaction was initiated by the oxidation of the aromatic nucleus to a radical cation. Half-wave polarographic oxidation potentials of cyclopropylbenzenes were measured in CH_3CN and plotted against Hammett's σ^+. The results indicated that the electron was transferred to the anode not from the cyclopropane ring but from the phenyl ring, and that opening of the cyclopropane ring was through the conjugate interaction of the cyclopropyl group and adjacent carbonium ion in the intermediate. Thus, the mechanism of oxidation was believed to involve initial one-electron oxidation yielding a radical cation, which subsequently underwent cyclopropane ring opening, as shown in Scheme 1-4.

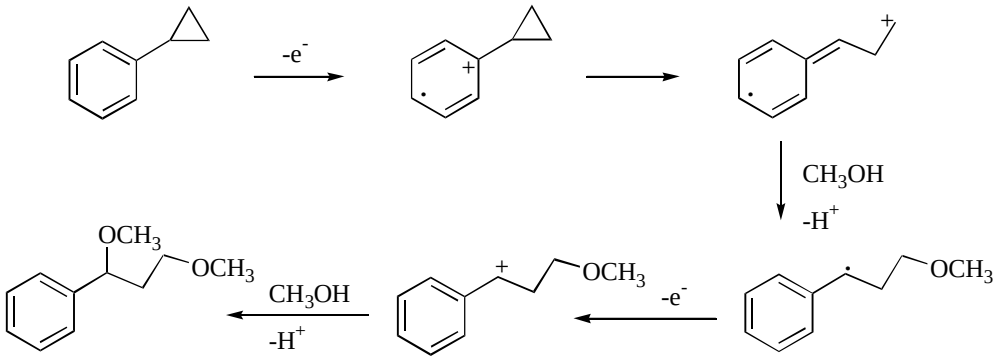

Scheme 1-4. Anodic oxidation mechanism of cyclopropylbenzene in CH_3OH

The anodic oxidation of polyalkyl-substituted cyclopropanes and spiro[2, n]alkanes was carried out in methanol by Shono et al. in 1975.[22] Monomethoxyolefin and dimethoxy compounds resulted from the selective cleavage at the most substituted carbon-carbon bond. In the same year, anodic oxidation of several other cyclopropane derivatives was studied by Klehr et al.[23] and by Brettle et al.[24,25] Electrolysis of cyclopropylbenzene in methanolic sodium methoxide gave 1,3-dimethoxy-1-phenylpropane, which was also formed together with 3-methoxy-3-phenylpropan-1-ol and 3-methoxy-1-phenylpropan-1-ol in methanolic sodium methyl carbonate. Electrolysis of 2-(2-methyl-1-propenyl)-1,1-dimethylcyclopropane in either system gave 4,6-dimethoxy-2,6-dimethylhept-2-ene and (E)-2,6-dimethoxy-2,6-dimethylhept-3-ene.

In 1985, Uchida, et al.[26] found that anodic oxidation in acetic acid of polycyclic cyclopropanes, namely tricyclene, cyclofenchene, and longicyclene, followed by hydrolysis

brought about stereo- and regioselective formation of the corresponding homoallylic alcohols as the main product in good yields (76~85%). Later in 1990, Uchida, et al.[27] reported a facile and efficient synthesis of exo-5,5-dimethyl-6-methylenebicyclo[2,2,1]heptan-2-ol, named “nojigiku alcohol”, based on the same cyclopropane ring opening reaction.

The electrochemical oxidation of 1,1,2,2-tetraphenylcyclopropane was reported in detail by Wayner and Arnold.[28] The products obtained from controlled potential electrolysis were 1,3,3-triphenylindene, tetraphenylallene and 3-methoxy-1,1,3,3-tetraphenylpropene, depended on the medium systems employed. Studied by cyclic voltammetry and other photochemical methods, 1,1,2,2-tetraphenylcyclopropane was observed to oxidize irreversibly at 1.36V (in CH_3CN vs. SCE) via a two-electron process leading to 1,1,3,3-tetraphenylpropenyl cation,[29] which subsequently cyclizes to form 1,3,3-triphenylindene or deprotonates to give tetraphenylallene, depending on the basicity of the medium, or is captured by methanol to produce 3-methoxy-1,1,3,3-tetraphenylpropene (Scheme 1-5). The effects of multiple substitution by methoxy and cyano in the 4-position(s) of 1,1,2,2-tetraphenylcyclopropane on the oxidation potential have also been measured. The results indicated that the oxidation process for the cyclopropanes is irreversible and the substituent effect on the potential is essentially additive and correlates reasonably well with $\Sigma\sigma^+$. A slow electron transfer process, with a transition state resembling the ring-opened radical cation, compromises with this observation (Scheme 1-5).[30]

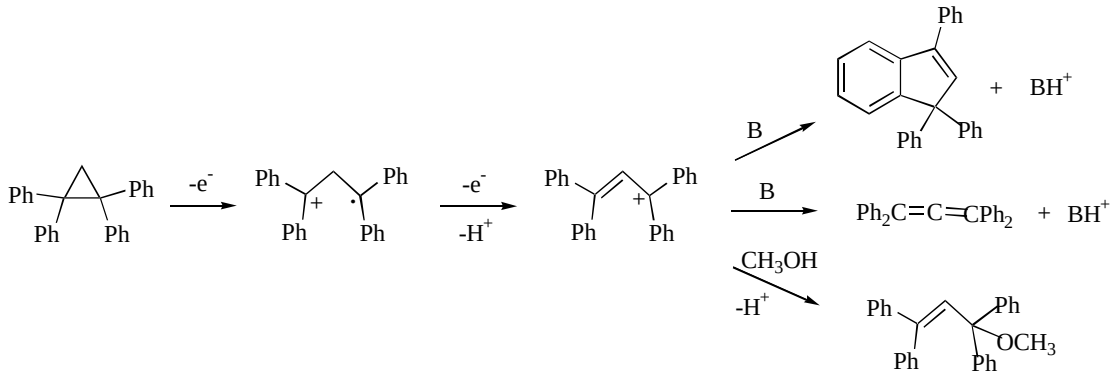

Scheme 1-5. Electrochemical oxidation of 1,1,2,2-tetraphenylcyclopropane

Photochemical Oxidation. For the past decade, much attention has been focused on the reactivity of radical cations generated via photoinduced electron transfer from cyclopropylarenes. The radical cations thus generated are subject to a nucleophilic attack if an appropriate nucleophile is present in the system. Photocleavage of cyclopropane ring in cyclopropylbenzene and derivatives is a subject of increasing interest mainly from mechanistic viewpoints. Rao and Hixson,[31] in 1979, reported photolysis of several cyclopropylbenzenes in CH_3OH/CH_3CN using 1,4-dicyanobenzene (DCB) as a sensitizer. In most cases, a novel "anti-Markownikoff" addition of methanol to the cyclopropane ring resulted (Scheme 1-6).

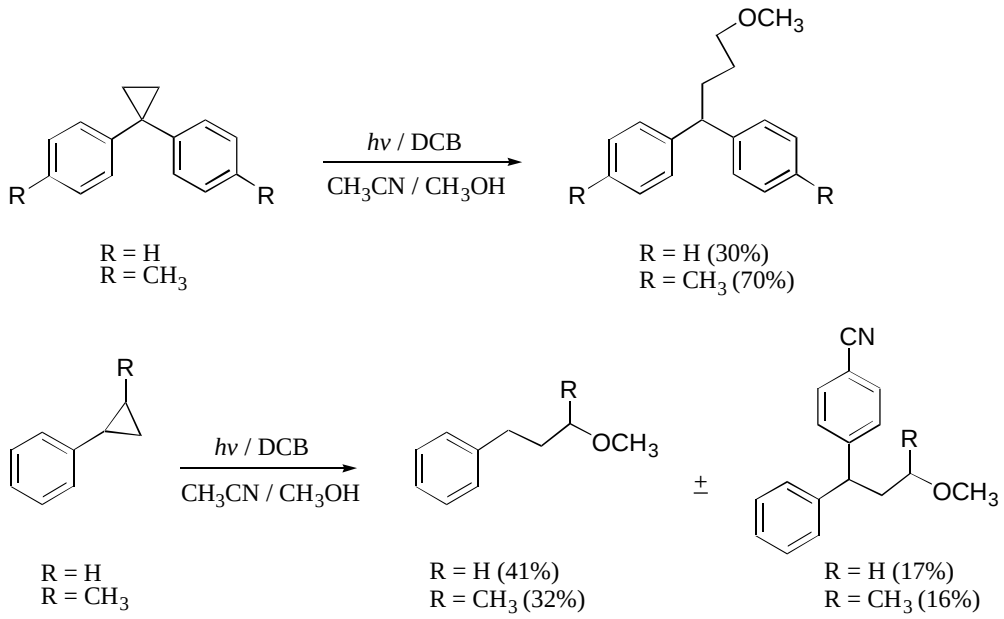

Scheme 1-6. DCB sensitized photolysis of cyclopropylbenzenes in CH_3CN/CH_3OH

The reactions observed were best rationalized as proceeding via initial electron transfer from the cyclopropanes to the excited DCB to give the cyclopropylbenzene radical cations. Two mechanisms for cyclopropane ring opening of the intermediate radical cations were proposed: unimolecular rearrangement of the cyclopropylarene radical cation to the ring-opened distonic radical cation ("S_N1") and/or methanol induced ("S_N2", bimolecular) ring opening (Scheme 1-7).

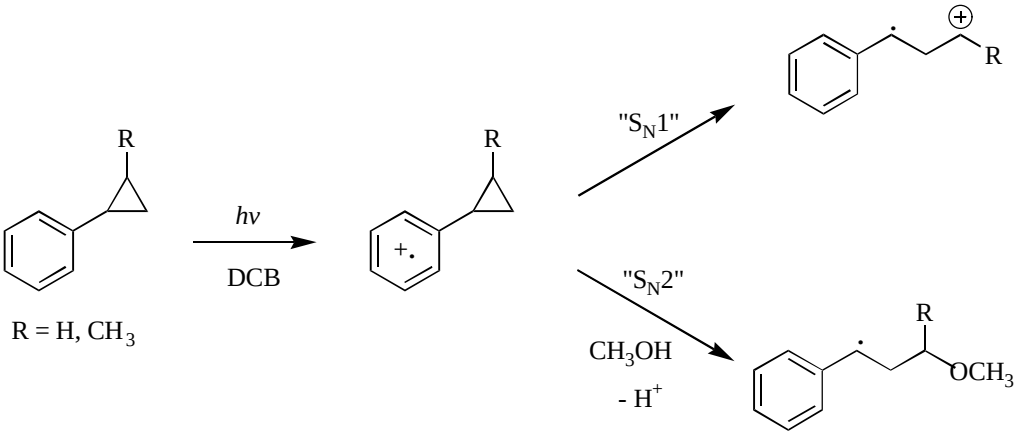

Scheme 1-7. Two mechanisms for ring opening of cyclopropylbenzene radical cations

Although the fact that attack occurs at the most substituted carbon of cyclopropylbenzene radical cation supports "S_N1" pathway, the finding that only a very small amount of *trans*-*cis* isomerization occurs when *trans*-1-methyl-2-phenylcyclopropane is reacted in the absence of methanol is not readily accommodated by this mechanism. Most likely the radical cation of *trans*-1-methyl-2-phenylcyclopropane undergoing attack by methanol has a significantly weakened yet not broken C_1-C_2 bond.

Mizuno, al et.[32] independently reported their results on the polar addition of various nucleophiles to cyclopropylarenes through a photoinduced electron transfer and on the reactivity feature of radical cations produced as intermediates. Mizuno, al et.[33] also in 1981 reported the photoinduced nucleophilic attack of methanol on cyclopropylbenzene in the presence of copper (II) ions, which proceed via one-electron transfer from excited substrate to Cu(II) ions. The 1,3-dimethoxy-1-phenylpropane was isolated as major

product in this reaction (70%). Later in 1983, Mizuno, al et.[34] reported in detail the 9,10-dicyanoanthracene (DCA)-sensitized two-electron oxidation of cyclopropylbenzene and aromatic olefins in the presence of Cu(II) ions, in which 1,3-dimethoxy-1-phenylpropane was formed in a yield of 84% .

Based upon the work of Rao and Hixson, several cyclopropylarenes were chosen by Dinnocenzo, et al.[35] as substrates for determining the stereochemistry of nucleophilic one-electron σ-bond cleavage. The 1-cyanonaphthalene (1-CN) photosensitized oxidation of these cyclopropylarenes in the presence of nucleophiles (e.g., CH_3OH, H_2O, KCN) yielded exclusively ring opened products. The reactions were characterized as occurring with essentially complete inversion of configuration at carbon undergoing nucleophilic substitution, based on stereochemical analysis of the products (Scheme 1-8).

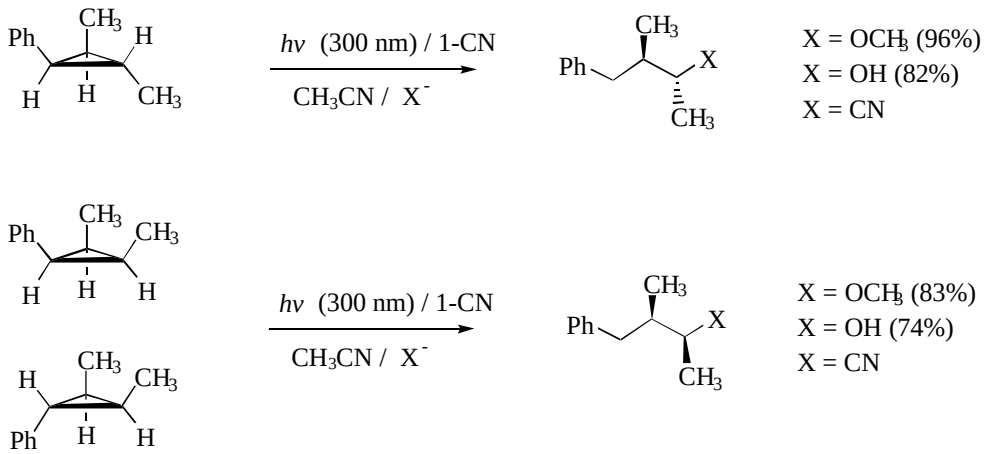

Scheme 1-8. Photolysis of cyclopropylbenzenes in the presence of nucleophiles

This observation was consistent with a ring-closed radical cation intermediate proposed by Rao and Hixson.[31] There were other reports dealing with ring-closed radical cations and nucleophilic substitution with inversion of configuration.[36] The explanation as to why these nucleophilic cleavage reactions proceed with inversion of configuration was provided by the valence-bond curve crossing model.[37] The model predicts that the stereochemical course of nucleophilic displacements on σ one electron bonds will be governed by the σ* (LUMO) orbital of the one-electron bond and will therefore proceed with conversion of the configuration at the site of attack.

The rate constants for the alcohol cleavage of the one-electron σ-bond in the cyclopropylbenzene radical cation was measured in CH_3CN, CH_2Cl_2 and dichloroethane by laser flash photolysis.[38] The detailed mechanism for three-electron S_N2 reactions of cyclopropylarene radical cations was reported.[38]

In 1993, Dinnocenzo and coworkers[39] reported several examples of three-electron S_N2 reactions that exhibit greatly diminished steric effects and occur with preferential substitution at the more hindered carbon atom, even when it is tertiary or neopentyl. The 1-cyanonaphthalene-sensitized photooxidations of 1,1-diphenyl-2-methylcycloproane, 1,1-diphenyl-2,2-dimethylcyclopropane and 1,1-diphenyl-2-*tert*-butylcyclopropane in degassed methanol yielded exclusively corresponding cyclopropane ring-opened products (98%, 93% and 60%, respectively) with substitution at more hindered carbon. The steric effects were evaluated by measuring rate constants for the reactions of methanol with various 1,1-diphenyl-2-alkylcyclopropane radical cations with laser flash photolysis (Table 1-1). The data reveal steric effects in the three-electron S_N2 reactions much smaller than those found

in most four-electron S_N2 reactions. This can be explained by Hammond's postulate.[40] On the basis of the large rate constants for these reactions, a early transition state is expected. The alkyl substituents stabilize positive charge at the carbon atom undergoing substitution, thereby reversing the normal regiochemistry of substitution. The electronic effects apparently overwhelm the smaller steric effects in three-electron S_N2 transition states.

Table 1-1 Rate constants for the reaction of methanol with various 1,1-diphenyl-2-alkylcyclopropane radical cations in CH_2Cl_2 at 22 °C

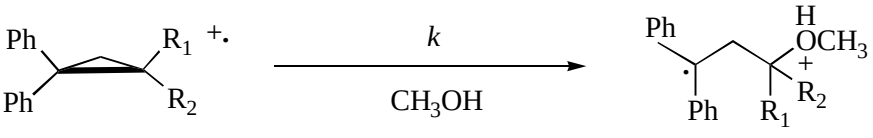

Substituents at C_2		k ($M^{-1}s^{-1}$)	k_{rel}
R_1	R_2		
Me	H	$1.5(1) \times 10^8$	31
Et	H	$8.3(4) \times 10^7$	17
Pr^i	H	$3.0(1) \times 10^7$	6.3
Bu^t	H	$4.8(2) \times 10^6$	1
H	H	$1.7(2) \times 10^7$	1
Me	H	$1.5(1) \times 10^8$	8.8
Me	Me	$3.2(1) \times 10^8$	19

The detailed studies of steric and electronic effects on the three-electron S_N2 substitution of cyclopropylarene radical cations were reported recently by Dinnocenzo, et al. using a combination of methods including product analysis, time-resolved laser flash photolysis, kinetic isotope effects and quantum chemical calculations.[41]

Mazzochi, al et.[42] first reported the cycloaddition of photochemically generated N-methylphthalimide (NMP) and N-methylnaphthalimide (NMN) radical anions to cyclopropylbenzene radical cations to give the corresponding spiroethers. The reaction of NMP radical anion and cyclopropylbenzene radical cation was illustrated in Scheme 1-9. Other research workers[43] also studied electron transfer photoreactions of quinone with cyclopropylbenzenes and similar cycloaddition products were obtained.

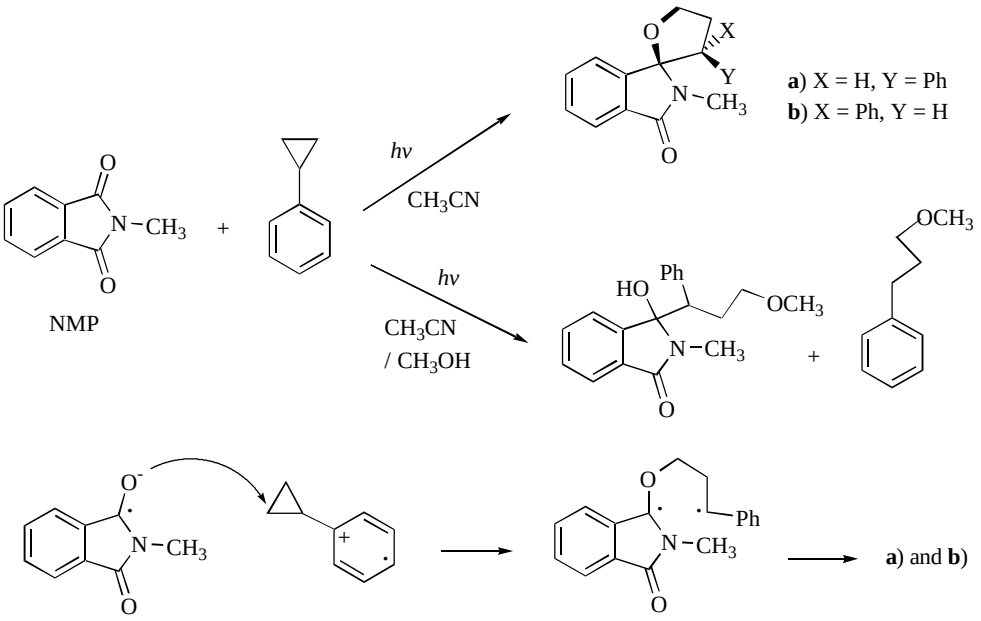

Scheme 1-9. Cycloaddition of photogenerated $NMP^{-\cdot}$ to cyclopropylbenzene radical cation

Besides the photoaddition of nucleophiles to cyclopropylarene radical cations, the photosensitized *cis* → *trans* isomerization[44] and photo-oxygenation[45] of 1,2-diphenylcyclopropane (and other disubstituted cyclopropanes) were explained to involve cyclcopropane radical cations via photoinduced electron transfer.

Metal-mediated Oxidation. Cyclopropane ring cleavage by electrophiles to yield adducts has been known since the 19th century. Ouellette, al et.[46] reported cleavage of cyclopropylbenzene by lead tetraacetate, thallium triacetate and mercuric acetate, and S_E2 mechanism for the ring opening was proposed based on kinetic studies. Although electrophilic attack on the cyclopropane ring is well established, very few examples that certain cyclopropanes are readily susceptable to reaction with one-electron oxidizing reagents have been reported. Young[47] first reported ceric(IV) ammonium nitrate (CAN) cleavage of of cyclopropylbenzenes and ring opened 1,3-disubstituted products were obtained (Scheme 1-10). Specifically, he found that the Ce(IV) oxidation of 1,1-dimethyl-2-phenylcyclopropane results in exclusively cleavage between the phenyl- and gem-dimethyl-substituted carbons. However, the mechanism of Ce(IV) oxidation of cyclopropylbenzenes remained vague although Young pointed that the reaction pathway of Ce(IV) oxidation of cyclopropanes must be quite different from lead, thallium, and mercury acetate oxidations because Ce(IV) is not amenable to metal-carbon bond formation.

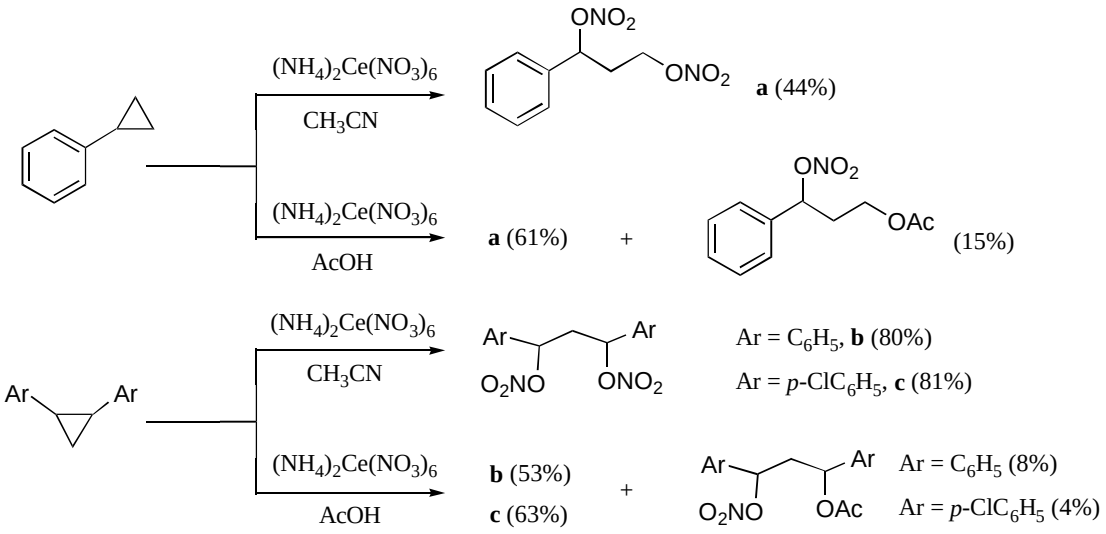

Scheme 1-10. Ce(IV) oxidation of cyclopropylbenzenes in CH_3CN and in AcOH

1.2.2 Deprotonation of Alkylarene Radical Cations

The side-chain oxidation of alkyl aromatic compounds is one of the most important organic reactions and accordingly, it has been the subject of intense investigation, both from the practical and the theoretical point of view. In particular, oxidation occurring by a electron transfer mechanism has attracted the most attention. It is generally accepted that side-chain oxidation of an alkylarene (e.g., Ar-CH_3) by an one-electron oxidant (e.g., Ce(IV)) often involves initial oxidation of the alkylarene to a radical cation. The radical cation then undergoes loss of a benzylic proton (called deprotonation or proton transfer), and the resulting radical is further oxidized to a benzylic carboncation, which can be trapped by a nucleophile or solvent present in the solution to lead to final product (Eq. 1-8 $\rightarrow$ 1-11).

$$Ar\text{-}CH_3 + Ce(IV) \rightarrow Ar\text{-}CH_3^{+\cdot} + Ce(III) \quad (1\text{-}8)$$

$$Ar\text{-}CH_3^{+\cdot} \rightarrow H^+ + Ar\text{-}CH_2^{\cdot} \quad (1\text{-}9)$$

$$Ar\text{-}CH_2^{\cdot} + Ce(IV) \rightarrow Ar\text{-}CH_2^{+} + Ce(III) \quad (1\text{-}10)$$

$$Ar\text{-}CH_2^{+} + Nu^{-} \rightarrow Ar\text{-}CH_2\text{-}Nu \quad (1\text{-}11)$$

While most of substrates chosen for studies on deprotonation reactions of alkylaromatic radical cations are alkylbenzenes, a few of them also come from alkylnaphthalenes and alkylanthracenes. The oxidants employed in these studies are mainly higher valence metals or other reagents, such as ceric (IV) ammonium nitrate, peroxydisufate-Cu(II), tris(phenanthroline) iron(III) complex, etc.. Other radical cation generating methods include anodic oxidation and photochemical oxidation.

Alkylbenzenes. Baciocchi, et al.[48] have extensively studied mechanism of oxidation of alkylbenzenes. The orientation, positional and substrate selectivity in the side-chain oxidation of some alkylbenzenes by Ce(IV) in acetic acid was determined. The reaction was found to be very sensitive to the electronic effects of substituents, a strong accelerating effect being produced by the progressive introduction of methyl groups. Hexamethylbenzene is revealed as ca. 10^5 fold more reactive then mesitylene.

The relative reactivity of C_α-H bonds of methyl, ethyl and isopropyl groups in mono- or *p*-disubstituted benzenes, namely intermolecular or intramolecular TSP (Tertiary, Secondary and Primary) selectivity, was determined and it was found that secondary C-H bond is the most reactive one and tertiary center can be either more or less reactive then the primary one, which was not expected for a free radical chain reaction (^{i}Pr

> Et > Me). This reactivity order may provide a tool to distinguish electron transfer mechanism from hydrogen atom transfer mechanism.[49]

The deuterium isotope effect in the side-chain oxidation of alkyl aromatic compounds with Ce(IV) was determined. The results fully confirm the mechanism of the Eq. 1-8 → 1-11 for the reaction of this metal and also show that the slow step of the reaction can change depending on the substrate structure.[50]

Fujita and Fukuzumi[51] in 1993 found that the isopropyl group has no significant stereoelectronic effect on inter- and intramolecular competition in deprotonation from alkylbenzene radical cations in the photoaddition of alkylbenzenes derivatives with 10-methylacridinium ion via photoinduced electron transfer from alkylbenzene derivatives to the singlet excited state of 10-methylacridinium ion, followed by the deprotonation of alkylbenzene radical cations. This result was somewhat controversial to that Schultz, et al.[52] reported many years ago. Schultz, et al. proposed that a conformation in which the isopropyl group bisects the plane of *p*-cymene would hinder deprotonation from the tertiary center of the radical cation, although steoroelectronic effects in the gas phase has been shown not to exist by Baciocchi, et al..[53]

The electronic and stereoelectronic effects of α-substituents on the deprotonation rate from the benzylic position of alkyl aromatic radical cations, $k(CH_2Z)/k(CH_3)$, has been investigated by determining the intramolecular selectivity in the anodic oxidation in acetic acid of α-Z-substituted *p*-xylenes.[54] It has been found that, with the exception of when Z is *tert*-butyl, the deprotonation rate of *p*-xylene radical cations is always faster from the CH_2Z group than from the CH_3 group, independently of the electron-donating or electron-

withdrawing nature of Z. The negligible deprotonation rate from CH_2-*t*-Bu has been ascribed to stereoelectronic effects.

In 1986, Baciiocchi, et al. reported substituent effects on intramolecular selectivity and free energy relationships in anodic and metal ion oxidation of 5-X-1,2,3-trimethylbenzenes. In Ce(IV) promoted and electrochemical reactions, very similar substituent effects on the k_2/k_1 (reactivity of the 2- and 1-methyl group) were observed. In the reactions of $Co(OAc)_3$ k_2/k_1 values were much less sensitive to the nature of substituents than former reactions and very close to those determined for the side-chain bromination of the same substrates by NBS.

The rates of deprotonation for a number of α-substituted *p*-methoxytoluene radical cations have also determined by a laser photolysis technique in CH_3CN.[55] The radical cations have been generated from the corresponding neutral substrates ether by biphenyl/9,10-dicyanoanthracene photosensitized oxidation or by reaction with $NO_3^{\cdot}$. It has been found that all α-substituents increase the deprotonation rates, with the rate constant almost reaching diffusion-controlled limit when X = CN and the base is NO_3^-. A kinetic study of the side-chain oxidation of α-substituted 4-methoxytoluenes by potassium 12-tungstocobalt(III)ate in $AcOH/H_2O$ (55:45) has been carried out by Baciocchi, et al..[56] The reaction follow complex kinetics, suggesting that both the electron transfer and the radical cation deprotonation steps affect the reaction rate.

The distribution between nuclear and side-chain substitution in the oxidation of *m*-methoxytolulene, 2-methylnaphthalene, mesitylene, and fluorene by Ce(IV) and Co(III) acetate in acetic acid has been determined by Baciocchi, et al.[57] Two oxidants exhibit

remarkably different behaviors, the propensity for nuclear substitution being much stronger with Ce(IV) than with $Co(OAc)_3$. Recently, side-chain fragmentation (C-C and C-H bond) of arylalkylanol radical cations and the role of α- and β-OH groups were studied by Baciocchi, et al.[58] as well.

Kochi, et al.[59] also extensively investigated the kinetics and mechanism of oxidation of alkylbenzenes by metal ions. An electron transfer pathway in side-chain substitution of alkyl aromatics under electrophilic conditions was suggested by Kochi in 1974, based on ESR studies of intermediates. Oxidative substitution of methylarenes by tris(phenanthroline)iron(III) complexes proceeds via initial electron transfer to afford benzylic products in excellent yields.[60] The growth and decay of radical cation $ArCH_3^{+\cdot}$ were observed directly by its ESR spectrum. Marcus theory was applied to these organic processes[61] in the endergonic region. The fast rate of proton transfer from various methylbenzene radical cations to a series of substituted pyridine bases are successfully measured in acetonitrile solution.[62] The deprotonation rate constants were found to range from 3×10^2 to more than 2×10^7 $M^{-1}s^1$. The relative acidities of these methylbenzene radical cations can be obtained from the Bronsted correlation of the deprotonation rate constants with pyridine strengths and the standard oxidation potentials of the methylarenes.

During the oxidation of methylarenes such as toluene, studies of the proton transfer reaction are complicated by competing nucleophilic attack and coupling reactions. The kinetics of the deprotonation reactions of the radical cations of several methylarenes were studied by DCV and DLSV in acetonitrile by Parker, et al.[63] The kinetic data indicate a second order rate law with rate constants of the order of $10^7M^{-1}s^{-1}$ (Eq. 1-12).

The kinetic isotope effect data as well as the apparent negative activation energies suggest a mechanism consisting of reversible dimerization (Eq. 1-13) followed by rate-determining deprotonation (Eq. 1-14).

$$\text{rate} = k_{app}[\text{Ar-CH}_3^{+\cdot}]^2 \qquad (1\text{-}12)$$

$$2\ \text{Ar-CH}_3^{+\cdot} = \text{dimer}(2+) \qquad (1\text{-}13)$$

$$\text{dimer}(2+) + \text{B} \rightarrow \text{Ar-CH}_3^{+} + \text{Ar-CH}_3 + \text{BH}^{+} \qquad (1\text{-}14)$$

A symmetrical dimer dication or a dimeric π-complex are possiible structures for the intermediate. The fact that a first-order deprotonation takes place in other types of experiments, i.e., metal-ion oxidation or pulse radiolysis, is a consequence of the large differences in radical cation concentrations and in some cases the more basic medium that the reactions are carried out in.

The oxidation of a variety of alkylbenzenes, (hydroxyalkyl)benzenes, and styrene derivatives by $S_2O_8^{2-}$-Cu^{II} in acetic acid and acetonitrile was studied by Walling, et al..[64] $SO_4^{-\cdot}$ generated from $S_2O_8^{2-}$ serves as an one-electron oxidant to oxidize arenes to radical cations. One of the interesting results is that oxidation of cyclopropylbenzene in acetic acid yielded 1-phenyl-1-acetoxycyclopropane as a major products. It suggests that the rate of proton transfer from the radical cation exceeds that of ring opening.[65]

The methods of estimating the pK_a of a organic radical cation using thermochemical cycles were reported by Arnold, et al.[19] Calculation showed that the toluene radical cation is an extremely strong acid (pK_a = -10 → -13) and the benzene radical cation a moderately strong acid in acetonitrile solution (pK_a = -2 → -4). These estimates indicate that the radical cations of benzene and toluene should deprotonate even

in moderate acidic media if alternative pathways for decay do not exist. The gas phase acidity of several hydrocarbon radical cations was also determined by thermochemical cycles.[19]

The reactions of the radical cations of methylated benzene derivatives in aqueous solution were studied in detail by Sehested and Holcman.[66] The rate constants for deprotonation were found to decrease by three orders of magnitude as the number of methyl groups increases from one to five. The rate constants can be correlated with the ionization potential of the parent compound. In neutral solution the reverse reaction to the acid-catalyzed OH adduct conversion occurs and the radical cations react with water to form the OH adduct. In slightly alkaline solution the radical cations of the higher methylated benzenes (n >= 3) react with hydroxide ions forming the OH adduct.

Alkylnaphthalenes. Baciocchi, et al.[67] investigated the reactions of 1-methyl-, 1-ethyl-, and 1-methyl-4-ethylnaphthalenes, induced by Ce(IV) in acetic acid. Product analysis showed that the oxidation of 1-ethylnaphthalene and 1-methyl-4-ethylnaphthalene leads exclusively side-chain substitution products. For oxidation of 1-methylnaphthalene, the side-chain substitution products were accompanied by products of nuclear acetoxylation (30%). The mole ratio of two side-chain oxidation products (methylacetate to ethylacetate) for oxidation of 1-methyl-4-ethylnaphthalene was found to be 1.38, from which a C_2H_5 : CH_3 reactivity ratio of 2 to 1 was calculated. The mechanism for the oxidation of alkylnaphthalenes follows those proposed for alkylbenzenes.

Alkylanthracenes. Chemical and biomimetic oxidation of 9,10-dialkylanthracenes in acetonitrile/water was studied by Tolbert, et, al. [68] Treatment of 9,10-dimethylanthracene (DMA), 9, 10-diethylanthracene (DEA) and 9-ethyl-10-

methylanthracene (EMA) with tris(phenanthroline)tris(hexafluorophosphate)iron in 10:90 water acetonitrile under argon proceeded cleanly to give > 90% yields of oxidized products. Formation of these products is readily interpreted as involving the intermediacy of the dialkylanthracene radical cation, in accord with the works of Kochi, et al. When a methyl group is present, rapid deprotonation followed by a second one-electron oxidation and hydration of the resulting cation occurs, provided a suitable proton carrier (H_2O) is available. With an ethyl group, stereoelectronic effects inhibit deprotonation. Rather, elimination of ethylene via an unprecedented seven-member transition state was proposed, facilitated by conversion of a benzhydryl radical to an a-hydroxybenzhydryl radical. Stereoelectronic effects in the deprotonation of alkylarene radical cations were further investigated by Tolbert, al et. in 1990.[69] It was confirmed that unlike 9-methylanthracenes, which are oxidized by one-electron oxidants to hydroxymethyl derivatives, 9-ethylanthracenes undergo a facile chemical or biochemical oxidative elimination of ethylene to yield an anthrone. The rationale for this dramatic selection between methyl and ethyl reactivity is a stereoelectronic effect on radical cation deprotonation. For the ethyl group, C_α-H bond is not perpendicular to aromatic ring due to *peri*-interactions, and thus inhibits deprotonation. In 1991, Tolbert, et al.[70] reported that oxidation of 9-methylanthracene by pyridine/iodine proceeds mainly through nucleophilic attack on the intermediate anthracene radical cation rather than deprotonation and replacement of a methyl proton by trimethylsilyl completely reverses the regiochemistry. Recently, Guengerich and Tolbert, et al.[71] reported the oxidation of 9-alkylanthracenes by cytochrome P450 2B1, horseradish peroxidase, and iron

tetraphenylporphine/iodosylbenzene systems. Anaerobic and Aerobic mechanisms were proposed.

The Cu(II)-$S_2O_8^{2-}$ oxidation of 9-methylanthracene was studied in refluxing CH_3CN/acedic acid and aqueous CH_3CN by Camaioni, et al..[72,73] Side-chain and nuclear oxidation products and the dimeric compound lepidopterene were produced. A mechanism is proposed where the initially formed radical cation undergoes competing proton loss and reversible nucleophile addition reactions to form respectively the anthracenylmethyl radical and nucleophile adduct radicals, which is oxidized by Cu(II) or $S_2O_8^{2-}$ to yield the corresponding cations that react to form the products (Scheme 1-11).

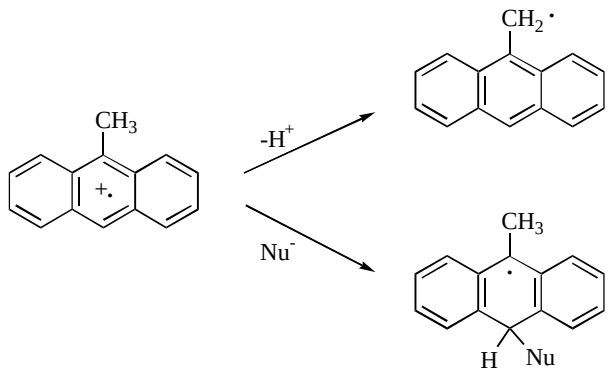

Scheme 1-11. Two competing reaction pathways of 9-methylanthracene radical cation

The results suggest that nucleophilic addition is faster than proton loss and that it is more reversible in CH_3CN/HOAc than in CH_3CN/H_2O. The Cu(II)-$S_2O_8^{2-}$ oxidation of 9-acylanthracenes and 9-acyl-10-methylanthracenes was also studied by Camaioni, et al.[74]

Obviously, proton loss from methyl or formyl groups was not a competing reaction path for these anthracene radical cations in contrast to those benzene radical cations.

1.3 DISSERTATION DESCRIPTION

Radical Cation "Probes", An Assumption. The fate of a cyclopropyl group incorporated into a substrate participating in a chemical process often provides useful mechanistic information about the importance of radicals and/or radical ions as intermediates along the reaction pathway. Consequently, cyclopropane-containing substrates have frequently been utilized to "probe" for radical cation intermediates in a number of important chemical and biochemical oxidation (Scheme 1-12).[75,76,77,78] For example, in Dr. Castagnoli's group, MAO oxidation of CpPTP was extensively studied. The cyclopropane ring opening of CpPTP during MAO oxidation may provide some information about the enzymatic oxidation mechanism (SET or HAT).

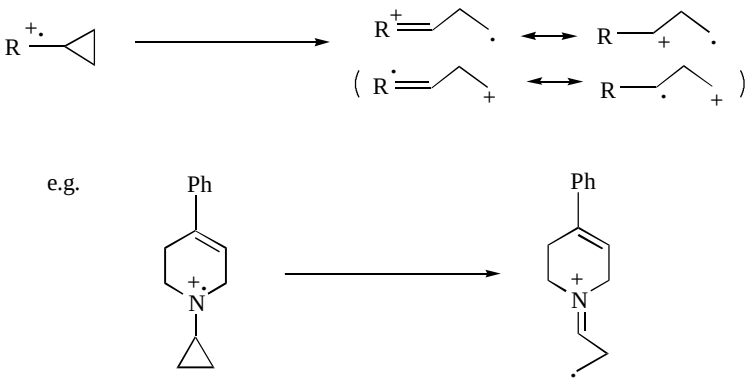

Scheme 1-12. Radical cation rearrangement used as "designer probes" for SET

It is frequently assumed that incorporation of a cyclopropyl group into a substrate will result in ring-opened products if a radical cation is an important reactive intermediate in the reaction pathway. A difficulty associated with this approach is that there is surprisingly little actually known about the chemistry of these cyclopropane radical cations.

In earlier work dealing with radical *anions* generated from cyclopropylketones, it was found that many of the analogous assumptions pertaining to the facility of ring opening of these species were incorrect (Scheme 1-13).[79] Rates of ring opening of these species were shown to be dramatically retarded by phenomena such as delocalization of spin and charge in the ring-closed form, and by stereoelectronic factors.

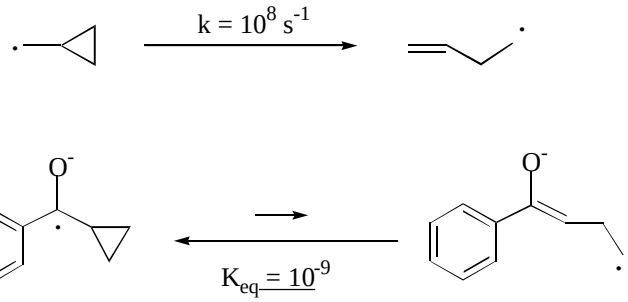

Scheme 1-13. Free radical and ketyl anion rearrangement

The information regarding the rate of ring opening of cyclopropane-containing radical cations (and the effects substituents on the mechanism on that rate) is somewhat scarce.

To address this issue, we initiated an investigation of the chemistry of radical cations generated from cyclopropylarenes.

Stereoelectronic Factors, A Hypothesis. As introduced in 1.2.1, anodic, photochemical and metal ion oxidation of cyclopropylbenzenes all led to cyclopropane ring-opened products. The mechanism was believed to involve initial one-electron oxidation yielding a radical cation, which subsequently underwent cyclopropane ring opening. Obviously, cyclopropylbenzenes can be regarded as radical cation "probes".

In 1990, it was shown that S_H2 ring-opening of cyclopropylarenes by bromine atom was sensitive to stereoelectronic factors.[80] For example, whereas the free radical bromination of cyclopropylbenzene and cyclopropylnaphthalene led to cyclopropane ring-opened products (1,3-dibromide), the free radical bromination of 9-cyclopropylanthracene and derivatives yielded exclusively hydrogen abstraction products (Scheme 1-14).

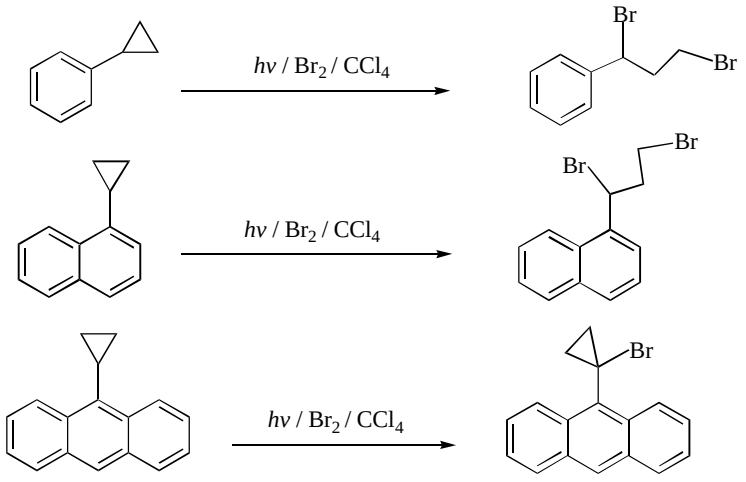

Scheme 1-14 Free radical bromination of cyclopropylarenes

This observed variation in the chemoselectivity of bromination of cyclopropylarenes is attributable to stereoelectronic factors. For 9-cyclopropyanthracene, the cyclopropyl group adopts a perpendicular conformation since the normally preferred bisected conformation is destabilized by unfavorable steric interactions between the *peri*-hydrogen and *cis*-hydrogens in cyclopropyl group. However, for cyclopropylbenzene, the cyclopropyl group is essentially freely rotating with a slight preference for the bisected conformation. The lowest energy conformation of 1-cyclopropylnaphthalenes is midway between the bisected and the perpendicuclar (Scheme 1-15).

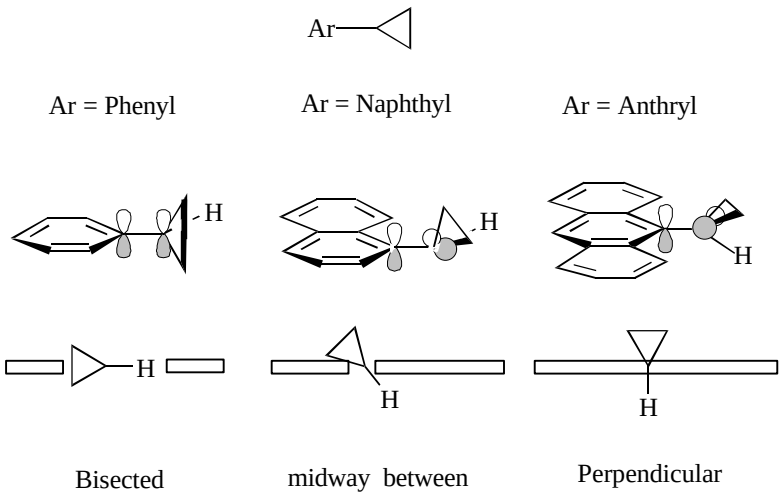

Scheme 1-15. Lowest energy conformations of cyclopropylarenes

Since the π-component of the vicinal C_1-C_2 and C_1-C_3 bonds in the bisected conformation is perfectly aligned with the aromatic π-system, ring opening is facilitated by benzylic stabilization in the transition state. In the perpendicular conformation, it is the C-

H bond that is aligned with the aromatic π-system; abstraction of hydrogen by the bromine atom leads to a transition state in which full benzylic stabilization can be realized (Scheme 1-16). other conformational studies of cyclopropylarenes were reported as well.[81]

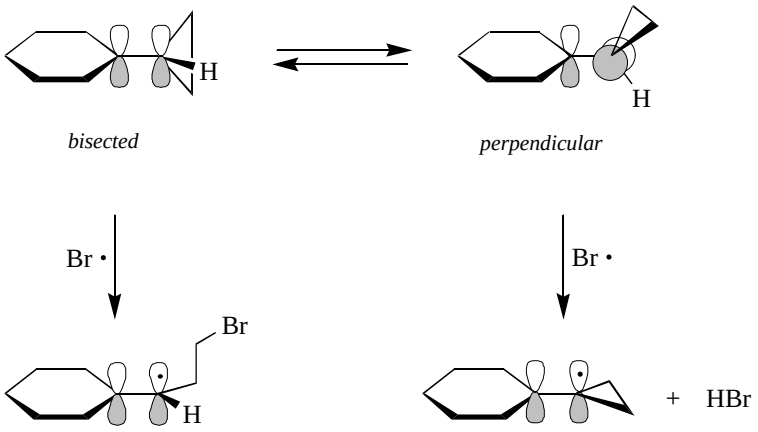

Scheme 1-16. Stereoelectronic effects on the chemoselectivity of the free radical bromination of cyclopropylarenes

The transition state for the reaction of a cyclopropylarene with a neutral free radical is isoelectronic to that of the reaction of its radical cation with a nucleophile (Ar-*c*-$C_3H_5^{+\bullet}/X^-$ vs. Ar-*c*-$C_3H_5/X^\bullet$). Consequently, it is our hypothesis that the same stereoelectronic factors should pertain to both processes.

Dissertation Development, Questions. The dissertation was designed to answer the questions of whether or not the stereoelectronic effect on the reactivity of cyclopropylarene radical cations is important and what other factors will affect this reactivity. The tasks to complete this dissertation are summarized in the following three

aspects: 1) Perform electrochemical and chemical oxidations of cyclopropylarenes: What are the products? What is the fate of cyclopropyl group? 2) Examine decay kinetics of these radical cations: Can the mechanism of oxidation be derived by electrochemical methods? 3) Analyze structure and reactivity relationships for these radical cations: Are stereoelectronic factors important in these systems? The main substrates employed in these studies are shown in the Scheme 1-17.

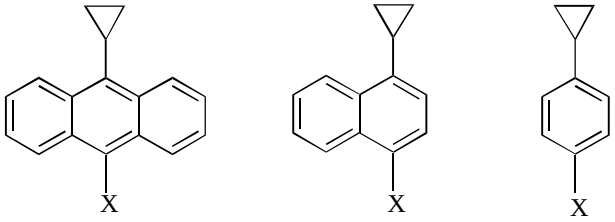

X = H, Br, CH_3

Scheme 1-17. Substrates used in studies on chemistry of cyclopropylarene radical cations

CHAPTER 2. ANODIC OXIDATION OF CYCLOPROPYLNAPHTHALENES

2.1 INTRODUCTION

The fate of a cyclopropyl group incorporated into a substrate participating in a chemical process often provides useful mechanistic information about the importance of radicals and/or radical ions as intermediates along the reaction pathway. In earlier work, Tanko et al. examined the chemistry of radical anions which undergo ring opening in analogy to the cyclopropylcarbinyl → homoallyl neutral free radical rearrangement, and the suitability of these reactions as "probes" for single electron transfer (SET) (Scheme 1-13).[79]

Cyclopropane derivatives are also frequently employed as probes for radical cation intermediates in a number of important chemical and biochemical oxidations.[75,76,77,78] However, information regarding the rate of ring opening of cyclopropane-containing radical cations (and the effect of substituents on that rate) is somewhat scarce. To address this issue, we initiated a study of the chemistry of radical cations generated from cyclopropylarenes.

Dinnocenzo, et al. have shown that ring opening of the cyclopropylbenzene radical cation occurs via a nucleophile-assisted (i.e., S_N2) pathway (Scheme 1-8).[35,37,38,39,41] This process has been well-characterized in terms of its stereochemistry (inversion of configuration at carbon), kinetics (first-order each in radical cation and nucleophile), regiochemistry, and kinetic isotope effects. The rate of ring opening has been found to be

highly sensitive to substituents on the aromatic ring. For a series of substituted cyclopropylbenzene radical cations, a correlation to σ^+ was observed ($\rho \approx +2.2$).

In the series of aromatic hydrocarbons, naphthalene systems occupy some properties (e.g., ionization potential, stability of radical cations) between those of benzene systems and anthracene systems. It is our expectation that results from oxidation of cyclopropylnaphthalenes will help us to know more about the chemistry of cyclopropylarene radical cations.

Molecular mechanics calculations[80,105] suggest that the lowest energy conformer of 1-cyclopropylnaphthalene is in-between a purely bisected and perpendicular conformation ($\theta = 67^o$) (Scheme 1-15), which agrees with the X-ray crystal structure of 4-cyclopropyl-1-naphthalenecarboxylic acid ($\theta = 54^o$), a closely related derivative of 1-cyclopropylnaphthalene. The bisected conformation is 1.2 kcal/mol higher in energy, with 1.4 kcal/mol barrier to inter-conversion. The free radical bromination of 1-cyclopropylnaphthalene gave only cyclopropane ring-opened products (Scheme 1-14), but the rate of this process is diminished due to unfavorable stereoelectronic factors. For 2-cyclopropylnaphthalene, the bisected conformation is preferred and like cyclopropylbenzene, ring opening predominates. Does this stereoelectronic factor also hold true for reactivity of cyclopropylnaphthalene radical cations?

Anodic nuclear substitution of naphthalenes[82] have been performed in the presence of strong nucleophiles such as methoxyation[83] in CH_3OH/KOH, cyanation[84] in CH_3CN/NaCN, nitration[85] in CH_3CN/N_2O_4 and halogenation[86] in CH_3CN/Et_4NX. The mechanism of oxidation is complicated mainly due to oxidation of most strong nucleophiles prior to naphthalenes. Photochemical oxidation of a number of methyl-

substituted naphthalenes has been studied by means of ESR spectroscopy.[87] Radical cations and/or dimer radical cations[88] were detected as reactive intermediates in the reaction.

Electrochemical techniques have been found to be powerful tools to trace follow up reactions of radical ions generated by heterogeneous electron transfer. A number of these studies has been focused on anthracene systems, mainly due to relative stability of these radical cations. In this chapter, the kinetics and mechanism of the follow-up reaction of radical cations generated from 1-cyclopropylnaphthalene (**1**), 1-bromo-4-cyclopropylnaphthalene (**2**) and 2-cyclopropylnaphthalene (**3**) in the presence of methanol are examined electrochemically.

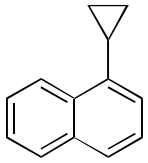

1

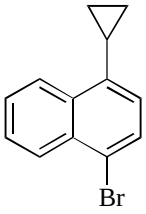

2

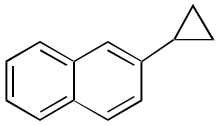

3

Voltammetric Methods. A thorough description of the voltammetric techniques employed in this study and their application to the elucidation of the mechanism of electrode generated intermediates have been reviewed by Saveant[89] and Parker.[90] In summary, voltammetric techniques such as cyclic voltammetry, derivative cyclic voltammetry (CV, DCV) or linear sweep voltammetry (LSV) permit assignment of the rate law for the decay of species generated (reversibly) by heterogeneous electron transfer (Scheme 2-1), where **A** represents the neutral substrate, **B** the radical cation, and **X**

another chemical entity in solution which may be involved in the reaction (e.g., nucleophile).

$$\mathbf{A} \longrightarrow \mathbf{B} + e^-$$

$$a\,\mathbf{A} + b\,\mathbf{B} + x\,\mathbf{X} \xrightarrow{k} \text{product(s)}$$

$$\frac{-d[\mathbf{B}]}{dt} = k\,[\mathbf{A}]^a\,[\mathbf{B}]^b\,[\mathbf{X}]^x$$

Scheme 2-1. Rate law expression for decay of radical cation **B**

In cases where no reverse wave is observed in the cyclic voltammogram, linear sweep voltammetry (LSV) is a powerful technique for studying the follow-up chemistry of the electrogenerated intermediate. Put briefly, the observed variation in the forward peak potential (E_P) as a function of sweep rate v, substrate concentration [**A**], and auxiliary reagent (nucleophile) concentration [**X**] can be related to the individual reaction order in **A**, **B**, **X** according to Eq. 2-1, 2-2, 2-3.

$$\partial E_P/[\partial \log(v)] = [1/(b + 1)]\log(RT/nF) \quad (2\text{-}1)$$

$$\partial E_P/(\partial \log[\mathbf{A}]) = -[(a + b - 1)/(b + 1)]\log(RT/nF) \quad (2\text{-}2)$$

$$\partial E_P/(\partial \log[\mathbf{X}]) = -[x/(b + 1)]\log(RT/nF) \quad (2\text{-}3)$$

When a reverse wave is observed, cyclic and derivative cyclic voltammetry (CV, DCV) and the "reaction order approach" advocated by Parker, et al.[90] are applicable. The reaction order approach provides a means of assessing the rate law for radical ion decay by observing the variation of the cathodic to anodic derivative peak current ratio (I'_{pc}/I'_{pa})

as a function of [**A**], [**X**], and v. A plot of log v_c *vs.* [**A**] yields a straight line whose slope is related to the combined reaction order in **A** and **B**, named $\mathbf{R}_{A/B}$ according to Eq. 2-4, where v_c represents the sweep rate needed to keep the derivative current ratio at a constant value (typically 0.5). Similarly, $\mathbf{R}_X$ is the reaction order of the auxiliary reagent according to Eq. 2-5.

$$R_{A/B} = a + b = \partial\log(v_c)/(\partial\log[\mathbf{A}]) + 1 \quad (2\text{-}4)$$

$$R_X = x = \partial\log(v_c)/(\partial\log[\mathbf{X}]) \quad (2\text{-}5)$$

Table 2-1 showed some typical theoretical LSV and CV (or DCV) responses for corresponding rate law of radical cation decay according to the published works.[90]

Table 2-1 Theoretical LSV and CV (or DCV) responses for rate law of decay of radical cation generated (reversibly) by heterogeneous electron transfer (25 °C)

rate law	LSV $\partial E_P/\partial\log v$	LSV $\partial E_P/\partial\log[A]$	LSV $\partial E_P/\partial\log[X]$	CV (or DCV) $\partial\log v_c/\partial\log[A]$	CV (or DCV) $\partial\log v_c/\partial\log[X]$
k[B]	29.6	0	0	0	0
k[B][X]	29.6	0	-29.6	0	1
k[B][A]	29.6	-29.6	0	1	0
k[A][B][X]	29.6	-29.6	-29.6	1	1
$k[B]^2$	19.7	-19.7	0	1	0
$k[B]^2[X]$	19.7	-19.7	-19.7	1	1
$k[B]^2[X]$ / [A]	19.7	0	-19.7	0	1

2.2 RESULTS AND DISCUSSION

2.2.1 Kinetic Analysis from Voltammetry

Radical cations generated from **1**, **2**, and **3** in the presence of methanol were studied electrochemically. Voltammetric techniques such as CV, DCV or LSV were employed to determine the rate law for the decay of $\mathbf{1}^{+\cdot}$, $\mathbf{2}^{+\cdot}$, and $\mathbf{3}^{+\cdot}$. The results are summarized below.

1-Cyclopropylnaphthalene (1). The cyclic voltammogram of **1** in CH_3CN is characterized by an initial oxidation wave (E_P = ~1130 mV at 400 mV/sec) and continuous indistinguishable oxidation waves located at more positive potentials (Figure 2-1). Addition of methanol does not shift the position (i.e., peak potential) of the initial oxidation wave, but does seems to affect those at more positive potentials.

Figure 2-1. Cyclic voltammogram of **1** in CH_3CN (0.5 M $LiBF_4$, 1.14×10^{-3} M **1**, v = 400 mV/sec)

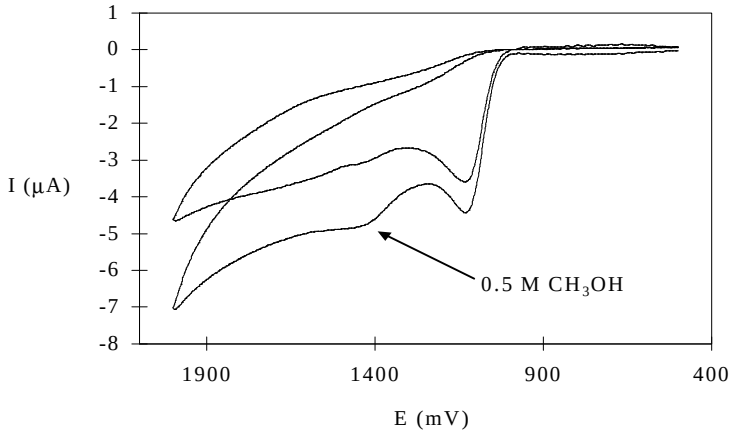

Because the initial wave is irreversible, LSV was employed to study the decay of $\mathbf{1}^{+\cdot}$. The peak potential (E_P) of the initial oxidation wave was found to vary as a function of both sweeprate (v) and substrate concentration ([**A**]), but was independent of methanol concentration ([**X**]). The results are summarized in Figures 2-2→2-13 and Table 2-2. These observations are in excellent agreement with a second-order rate law for radical cation decay (Eq. 2-6),

$$-d[\mathbf{1}^{+\cdot}]/dt = k[\mathbf{1}^{+\cdot}]^2 \qquad (2\text{-}6)$$

for which the theoretical response is $\partial E_P/\partial\log(v) = 19.7$, $\partial E_P/\partial\log[\mathbf{A}] = -19.7$, and $\partial E_P/\partial\log[\mathbf{X}] = 0$ (all in units of mV/decade, where **A** = substrate and **X** = CH_3OH).

Table 2-2. Observed LSV response for the electrochemical oxidation of **1** in CH_3CN

electrolyte	$\partial E_P/\partial\log(v)$[a]	$\partial E_P/\partial\log[\mathbf{1}]$[b]	$\partial E_P/\partial\log[CH_3OH]$[c]
0.5 M $LiBF_4$	19.5 ± 0.3 (1.19) 18.8 ± 1.0 (2.26) 22.2 ± 0.9 (9.52)	-18.2 ± 2.9 (1.19→9.52) -23.1 ± 1.3 (0.476→9.52)	-0.34 ± 0.57 (1.19)
0.5 M $LiClO_4$	18.7 ± 0.3 (0.595) 20.0 ± 0.9 (9.52)	-20.9 ± 2.8 (0.595→9.52) -19.3 ± 1.0 (1.67→12.9)	1.50 ± 1.07 (6.85) -0.20 ± 1.11 (1.25)

[a] 0.5 M CH_3OH, v = 100→3000 mV/sec, [**1**] (mM) appears in parentheses;

[b] 0.5 M CH_3OH, v = 400 mV/sec, [**1**] (mM) range appears in parentheses;

[c] 0.025→0.5 M CH_3OH, v = 400 mV/sec, [**1**] (mM) appears in parentheses.

Figure 2-2. LSV analysis of **1**, $\partial E_P/\partial \log(v)$. (0.5 M $LiBF_4$, 0.5 M CH_3OH, 1.19×10^{-3} M **1**, v = 100→3000 mV/sec)

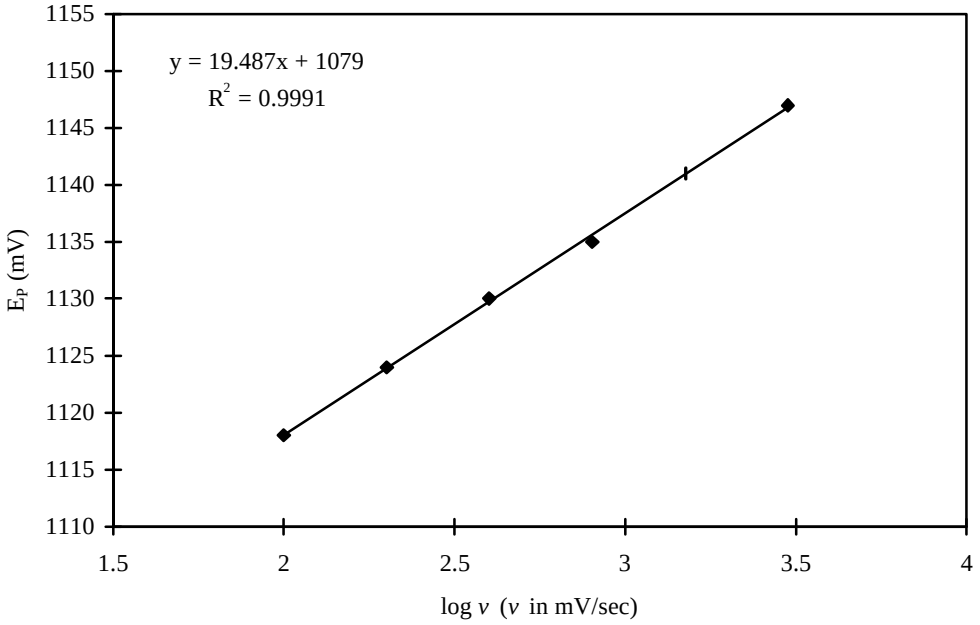

Figure 2-3. LSV analysis of **1**, $\partial E_P/\partial \log[\mathbf{1}]$. (0.5 M $LiBF_4$, 0.5 M CH_3OH, 1.19→9.52×10^{-3} M **1**, v = 400 mV/sec)

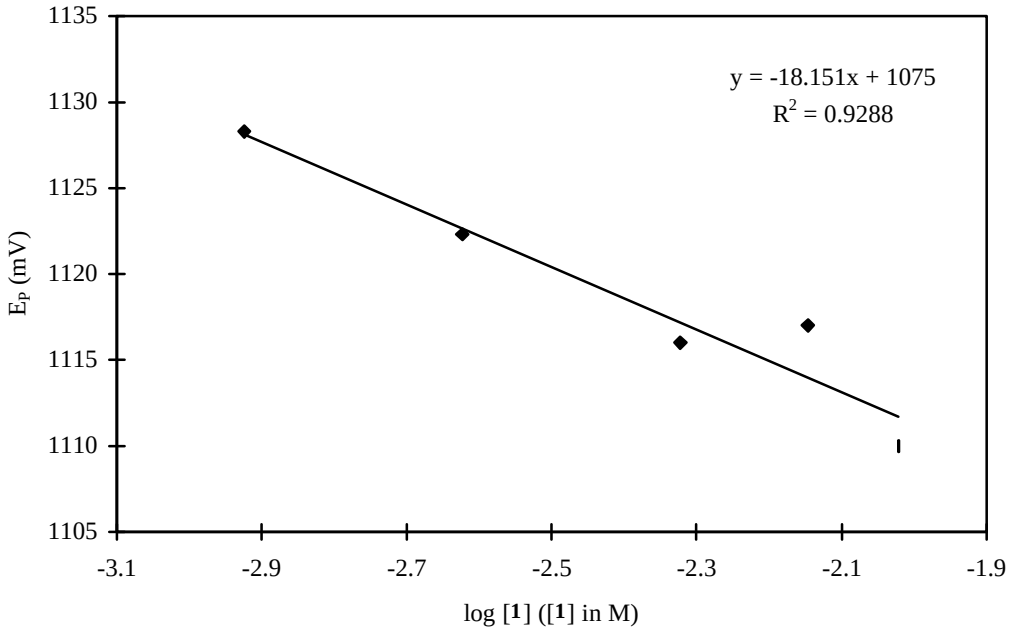

Figure 2-4. LSV analysis of **1**, $\partial E_P/\partial \log[CH_3OH]$. (0.5 M $LiBF_4$, 0.0125→0.5 M CH_3OH, 1.19×10^{-3} M **1**, ν = 400 mV/sec)

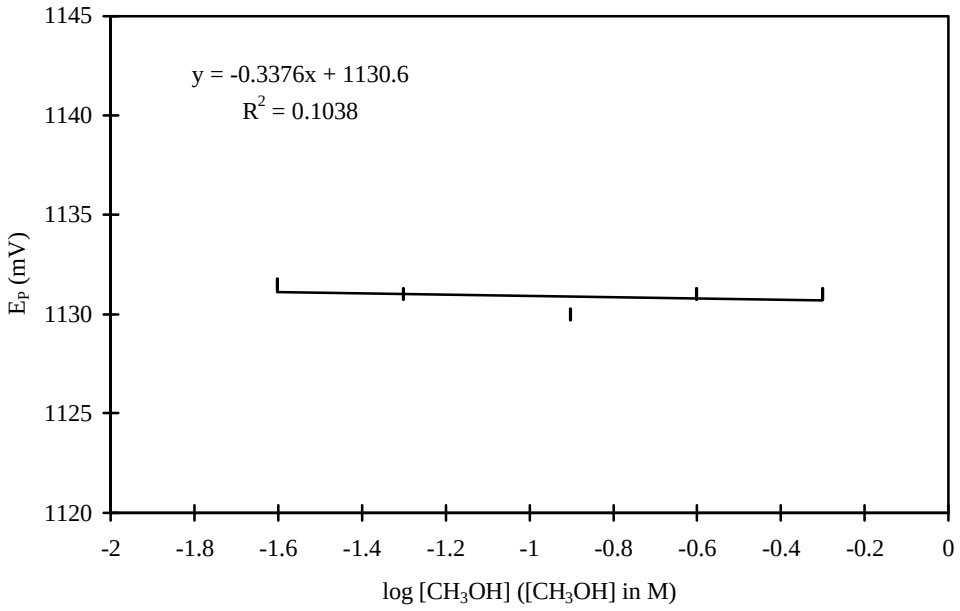

Figure 2-5. LSV analysis of **1**, $\partial E_P/\partial \log(\nu)$. (0.5 M $LiBF_4$, 0. 5 M CH_3OH, 2.26×10^{-3} M **1**, ν = 100→3000 mV/sec)

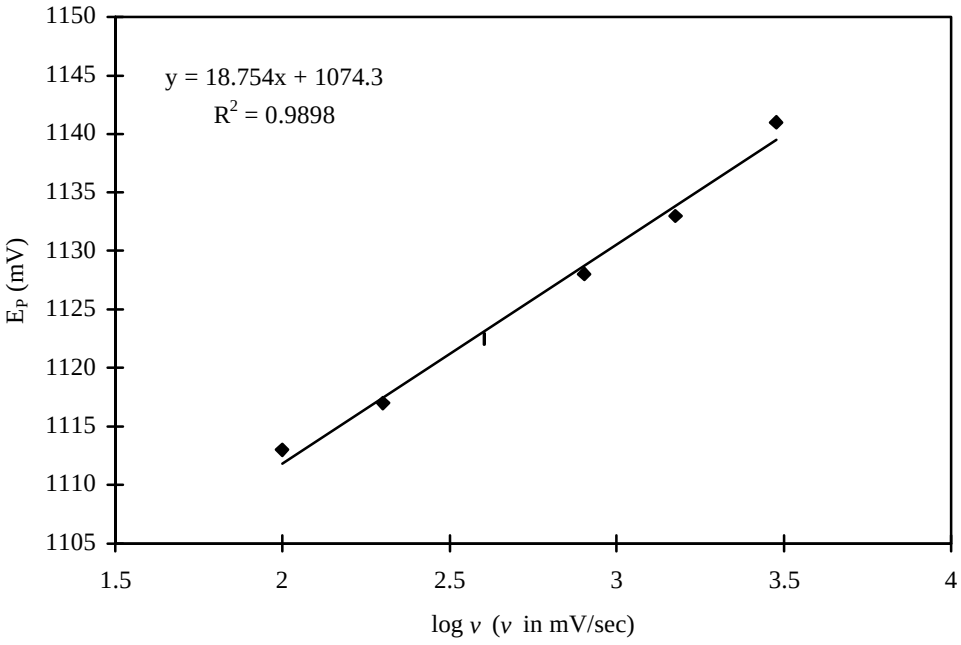

Figure 2-6. LSV analysis of **1**, $\partial E_P/\partial \log(v)$. (0.5 M $LiBF_4$, 0.5 M CH_3OH, 9.52×10^{-3} M **1**, v = 100→3000 mV/sec)

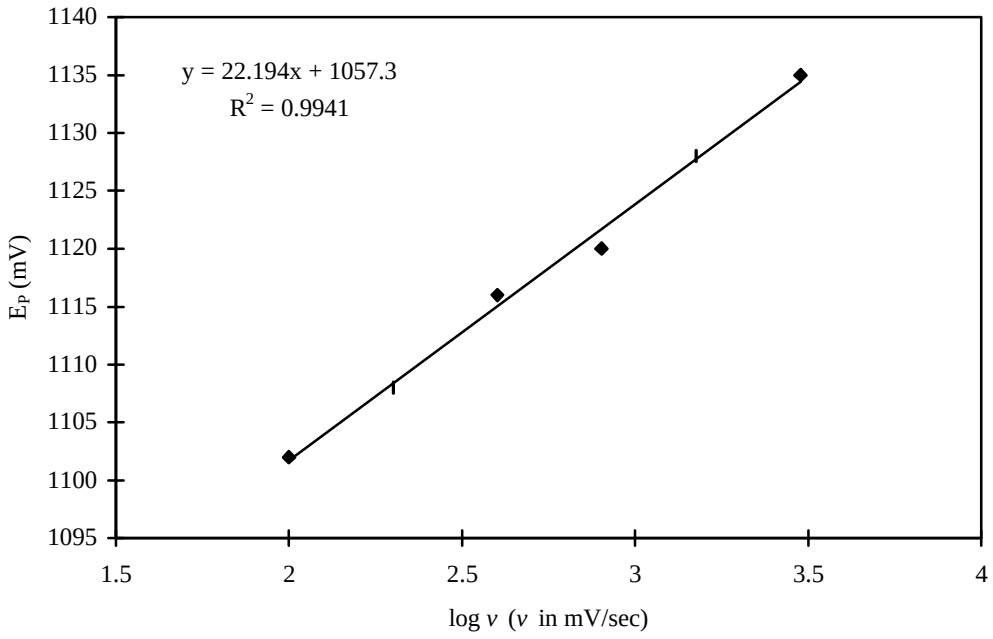

Figure 2-7. LSV analysis of **1**, $\partial E_P/\partial \log[\mathbf{1}]$. (0.5 M $LiBF_4$, 0.5 M CH_3OH, 0.476→9.52×10^{-3} M **1**, v = 400 mV/sec)

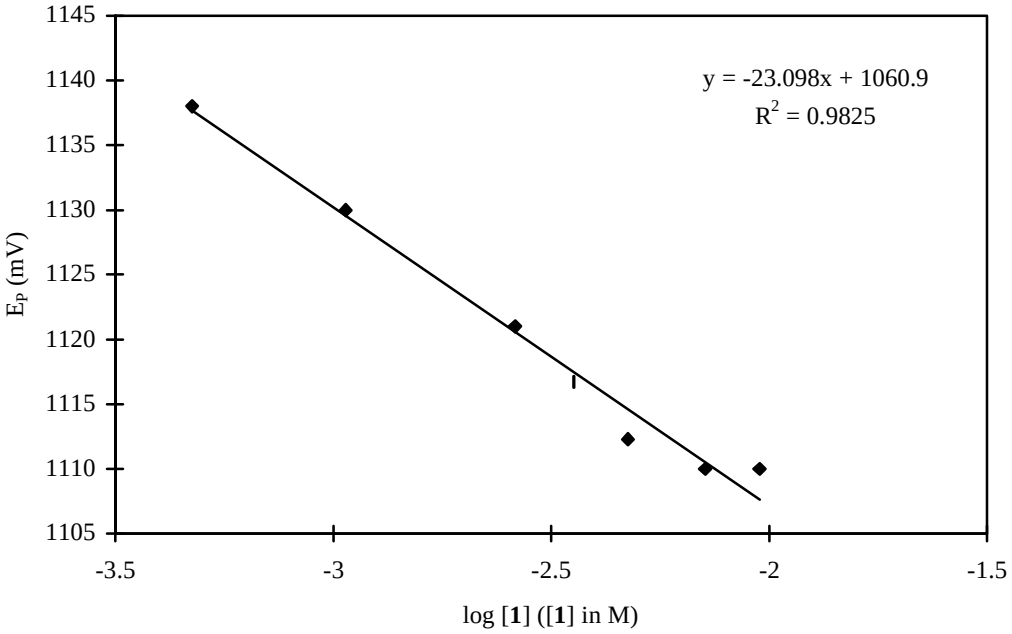

Figure 2-8. LSV analysis of **1**, $\partial E_P/\partial \log[\mathbf{1}]$. (0.5 M $LiClO_4$, 0.5 M CH_3OH, 0.595→9.52 $\times 10^{-3}$ M **1**, ν = 400 mV/sec)

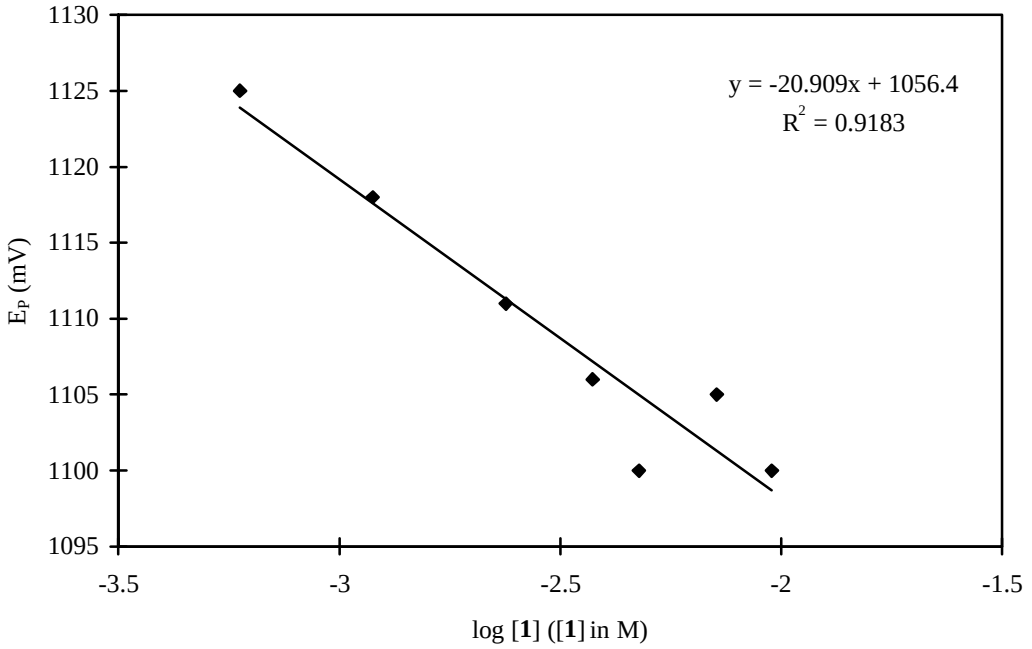

Figure 2-9. LSV analysis of **1**, $\partial E_P/\partial \log(\nu)$. (0.5 M $LiClO_4$, 0.5 M CH_3OH, 5.95×10^{-3} M **1**, ν = 100→3000 mV/sec)

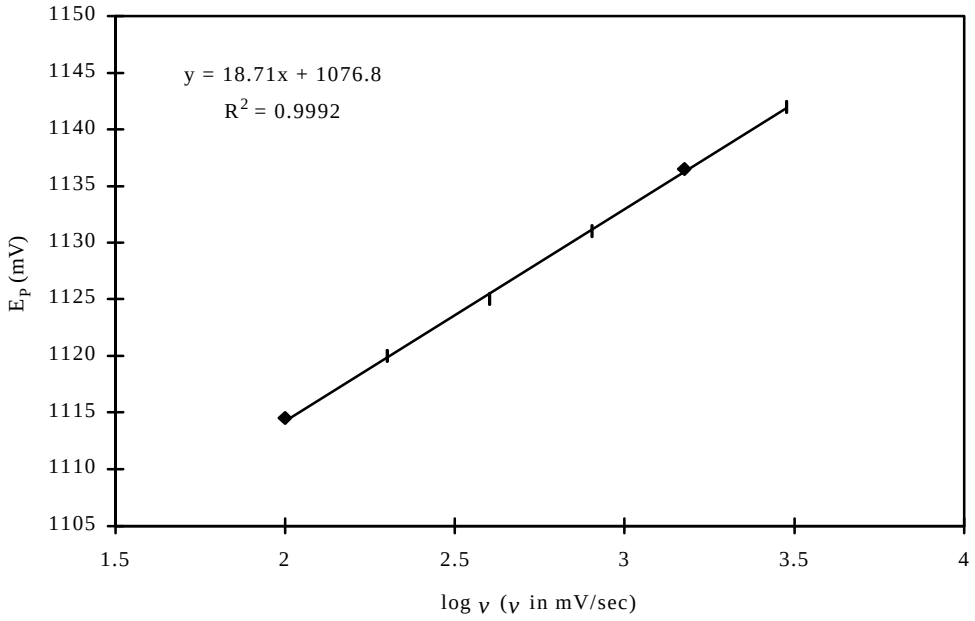

Figure 2-10. LSV analysis of **1**, $\partial E_P/\partial \log(\nu)$. (0.5 M $LiClO_4$, 0.5 M CH_3OH, 9.52×10^{-3} M **1**, ν = 100→3000 mV/sec)

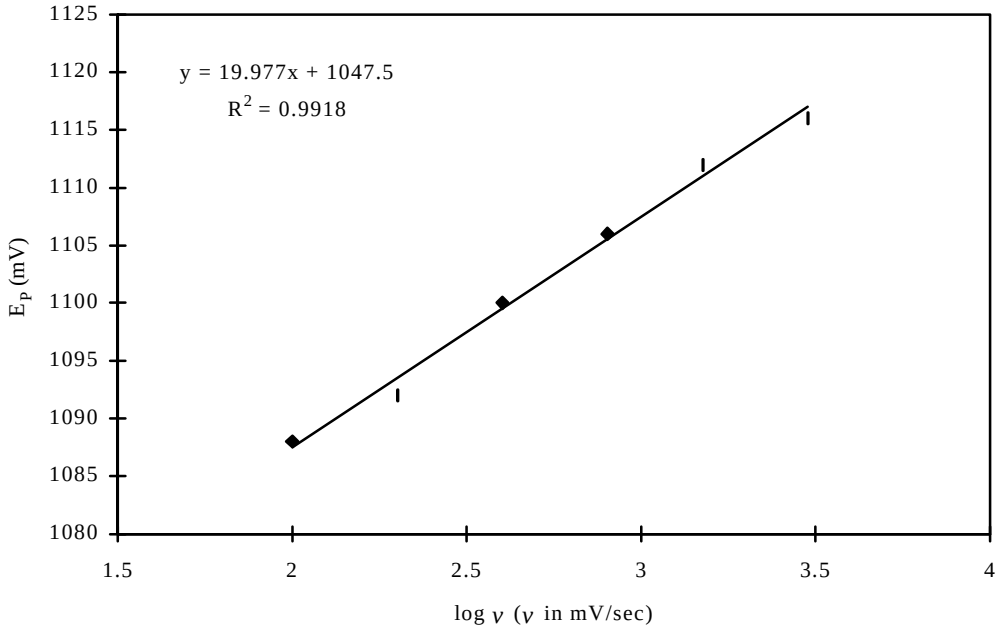

Figure 2-11. LSV analysis of **1**, $\partial E_P/\partial \log[CH_3OH]$. (0.5 M $LiClO_4$, 0.025→0.5 M CH_3OH, 6.845×10^{-3} M **1**, ν = 400 mV/sec)

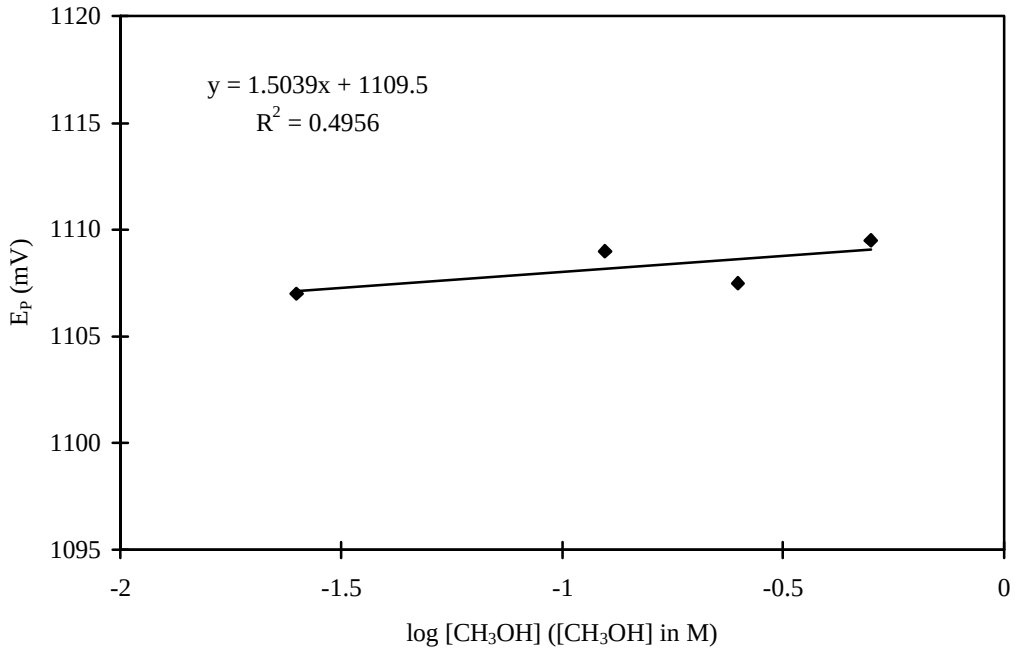

Figure 2-12. LSV analysis of **1**, $\partial E_P/\partial \log[CH_3OH]$. (0.5 M $LiClO_4$, 0.025→0.5 M CH_3OH, 1.25×10^{-3} M **1**, ν = 400 mV/sec)

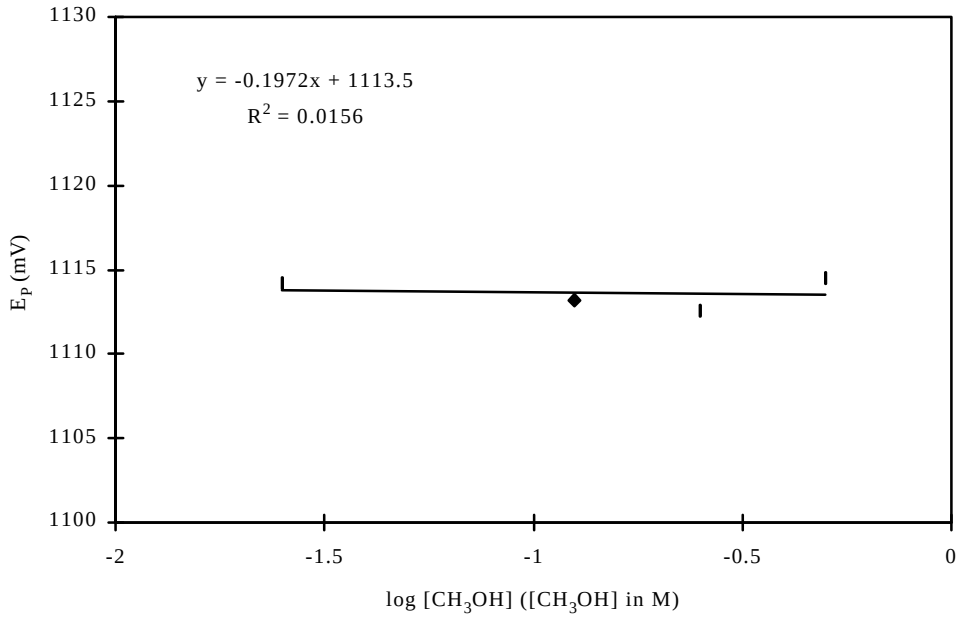

Figure 2-13. LSV analysis of **1**, $\partial E_P/\partial \log[\mathbf{1}]$. (0.5 M $LiClO_4$, 0.5 M CH_3OH, 1.67→12.9 $\times 10^{-3}$ M **1**, ν = 400 mV/sec)

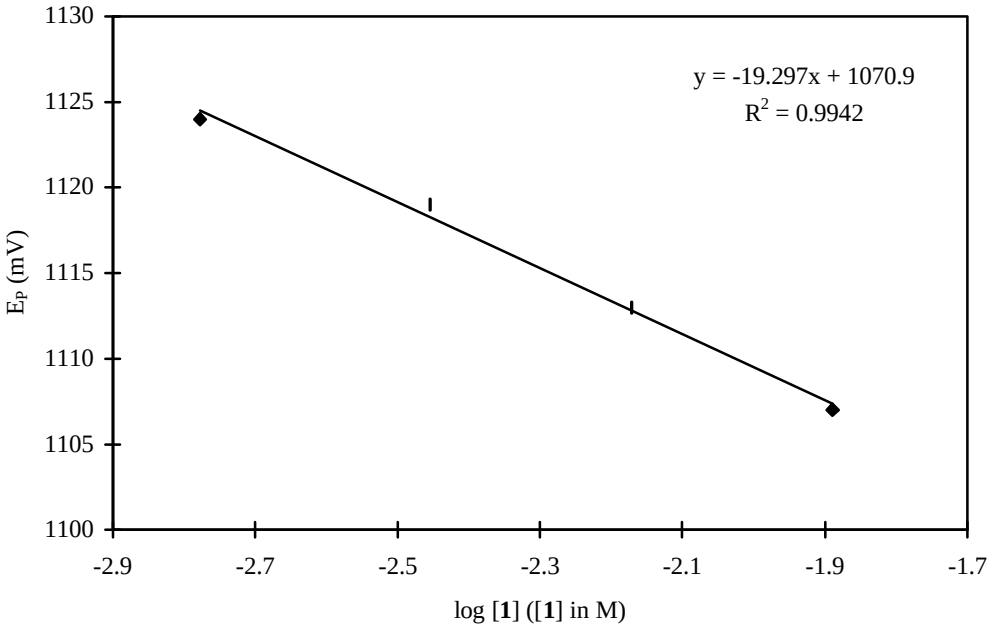

1-Bromo-4-cyclopropylnaphthalene (2). The cyclic voltammogram of **2** in CH_3CN is characterized by an initial oxidation wave (E_P = ~1245 mV, at 400 mV/sec) and other subsequent oxidation waves located at much more positive potentials (Figure 2-14). In the presence of methanol, the waves at more positive potentials appear to shift in the negative direction, but the initial oxidation wave is not affected.

Figure 2-14. Cyclic voltammogram of **2** in CH_3CN (0.5 M $LiBF_4$, 2.36×10^{-3} M **2**, v = 400 mV/s)

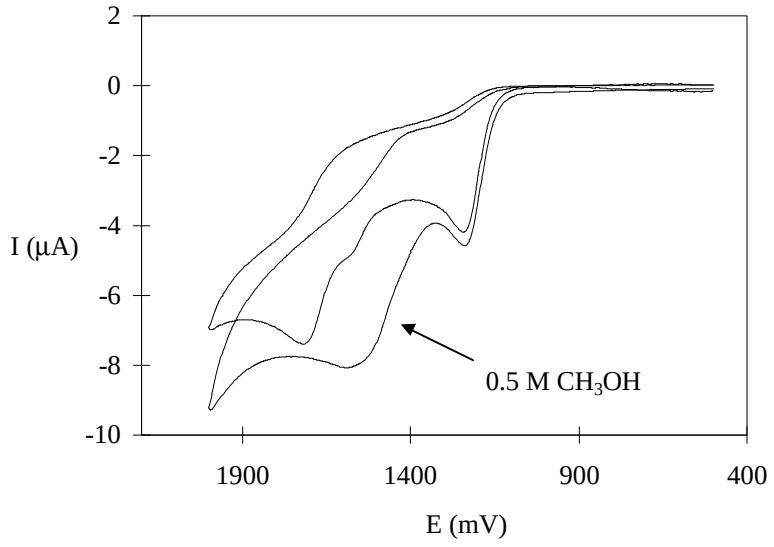

As was observed for **1**, the initial oxidation wave of **2** in CH_3CN is irreversible and thus, LSV is applicable. E_P was found to vary as a function of both sweeprate and substrate concentration, but was independent of methanol concentration. The LSV results for the electrochemical oxidation of **2** appear in Figures 2-15→2-31 and Table 2-3, and are also consistent with a mechanism that is second order in radical cation and zero order in

methanol (Eq. 2-7). Different supporting electrolytes and solvents do not alter the observed rate law.

$$-d[\mathbf{2}^{+\cdot}]/dt = k[\mathbf{2}^{+\cdot}]^2 \qquad (2\text{-}7)$$

Table 2-3 Observed LSV response for the electrochemical oxidation of **2** in several solvent/electrolyte combinations

electrolyte/solvent	$\partial E_P/\partial \log(v)$[a]	$\partial E_P/\partial \log[\mathbf{2}]$[b]	$\partial E_P/\partial \log[CH_3OH]$[c]
0.5 M $LiBF_4$/ CH_3CN	19.5 ± 0.9 (6.79) 19.4 ± 0.7(2.36)	-20.9 ± 2.8 (2.36→9.07) -21.5 ± 2.8 (1.59→13.8)	-1.2 ± 0.7 (6.79)
0.5 M $LiClO_4$/ CH_3CN	20.3 ± 0.4 (2.36) 20.7 ± 0.6 (9.44)	-19.5 ± 1.0 (0.59→9.44)	-0.27 ± 0.6 (5.67)
0.25 M $^nBu_4NPF_6$/ CH_3CN	20.7 ± 0.5 (1.18) 20.8 ± 0.4 (9.44)	-18.1 ± 1.1 (1.18→9.44)	-5.9 ± 1.0 (1.18)
0.25 M $^nBu_4NPF_6$/ 1:1CH_3CN:CH_2Cl_2	19.3 ± 0.4 (2.96) 21.1 ± 0.4 (9.44)	-17.4 ± 2.0 (1.18→9.44)	-0.64 ± 0.5 (2.36)

[a] 0.5 M CH_3OH, v = 100→6000mV/s, [**2**] (mM) appears in parentheses;

[b] 0.5 M CH_3OH, v = 400 mV/sec, [**2**] (mM) range appears in parentheses;

[c] 0.025→0.5 M CH_3OH, v = 400 mV/sec, [**2**] (mM) appears in parentheses.

Figure 2-15. LSV analysis of **2**, $\partial E_P/\partial \log[CH_3OH]$. (0.5 M $LiBF_4$, 0.025→0.5 M CH_3OH, 6.79×10^{-3} M **2**, ν = 400 mV/sec)

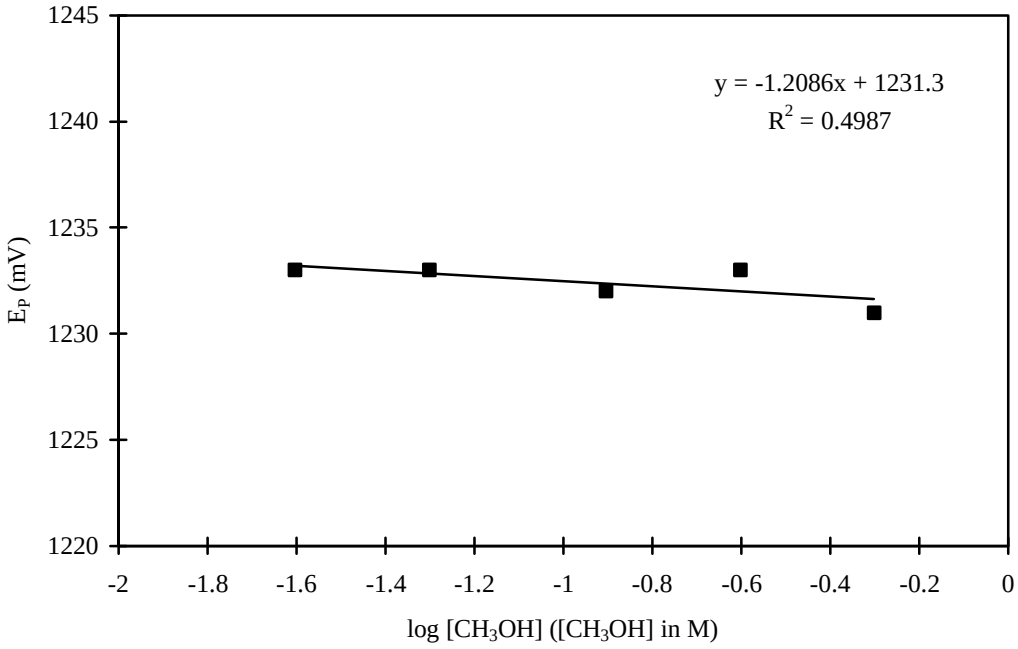

Figure 2-16. LSV analysis of **2**, $\partial E_P/\partial \log(\nu)$. (0.5 M $LiBF_4$, 0.5 M CH_3OH, 6.79×10^{-3} M **2**, ν = 100→6000 mV/sec)

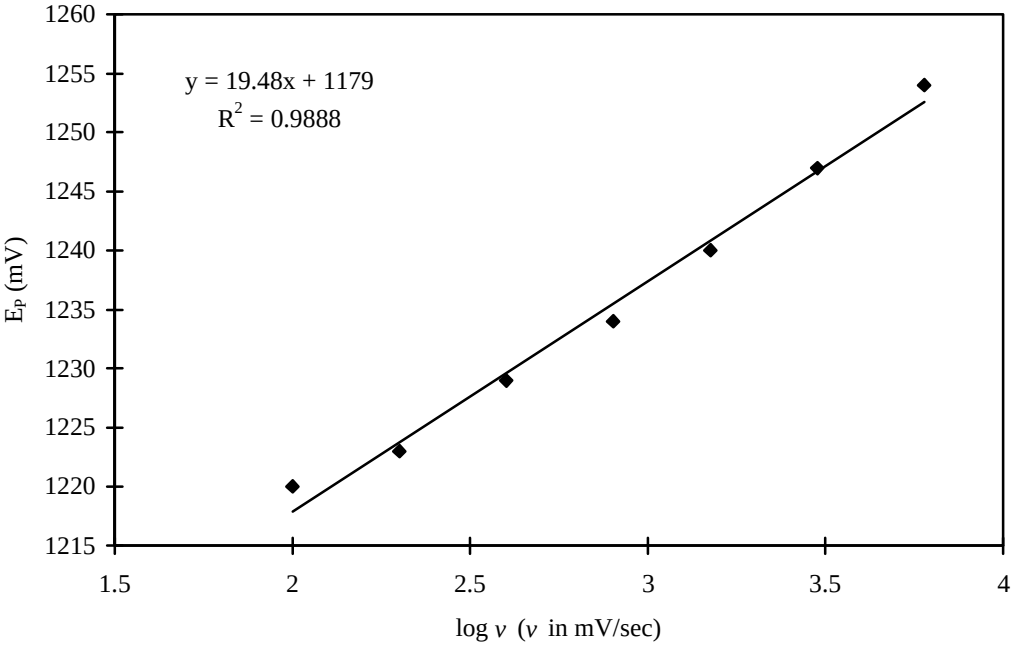

Figure 2-17. LSV analysis of **2**, $\partial E_P/\partial \log[CH_3OH]$. (0.5 M $LiClO_4$, 0.025→0.5 M CH_3OH, 5.67×10^{-3} M **2**, ν = 400 mV/sec)

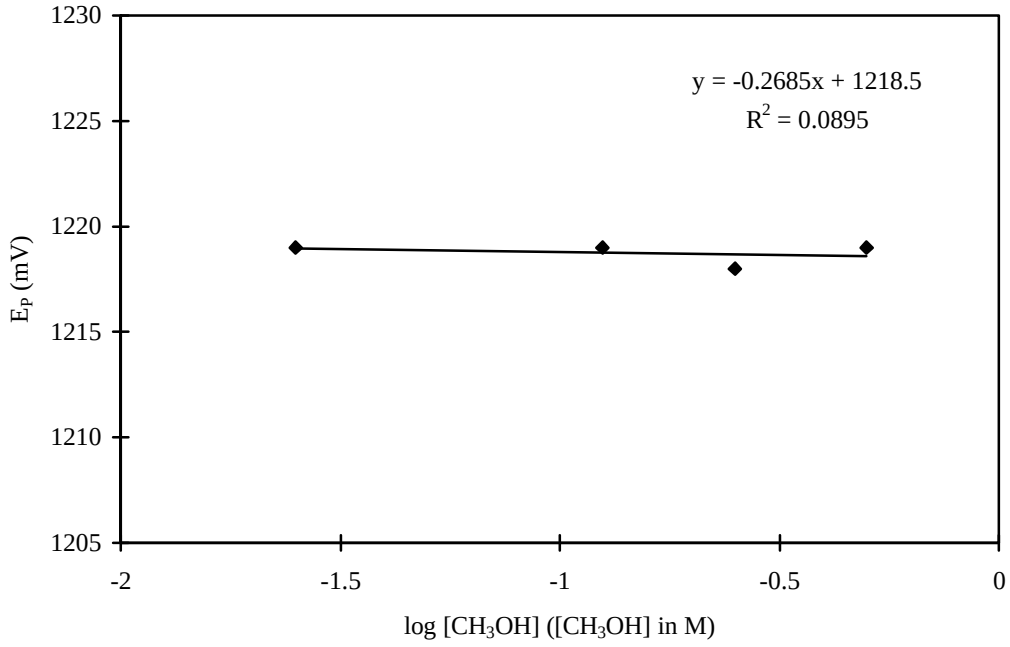

Figure 2-18. LSV analysis of **2**, $\partial E_P/\partial \log(\nu)$. (0.5 M $LiBF_4$, 0.5 M CH_3OH, 2.36×10^{-3} M **2**, ν = 100→6000 mV/sec)

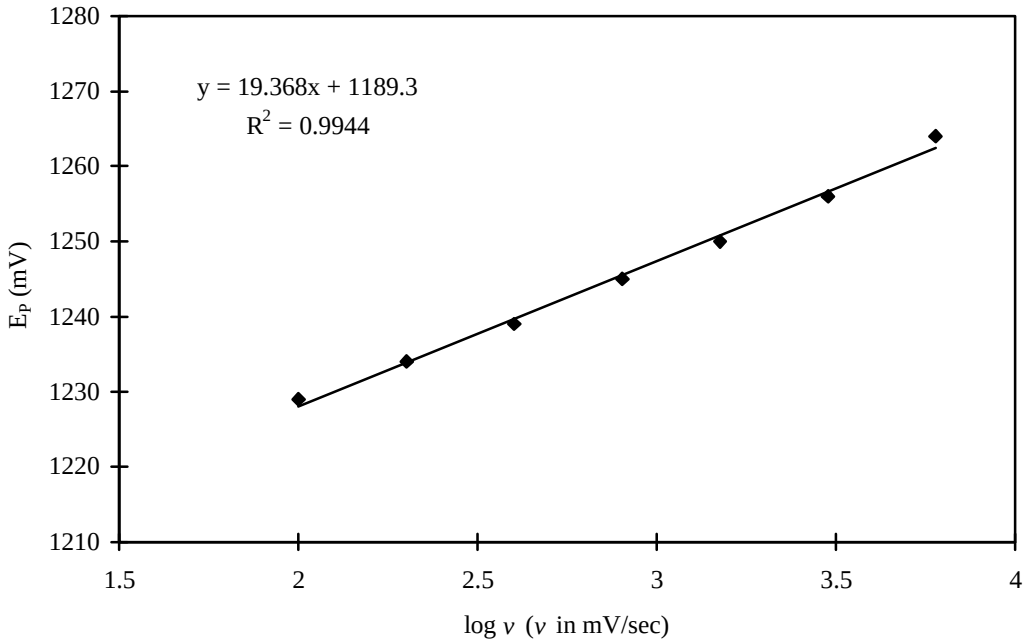

Figure 2-19. LSV analysis of **2**, $\partial E_P/\partial \log[\mathbf{2}]$. (0.5 M $LiBF_4$, 0.5 M CH_3OH, 2.36→9.07 × 10^{-3} M **2**, v = 400 mV/sec)

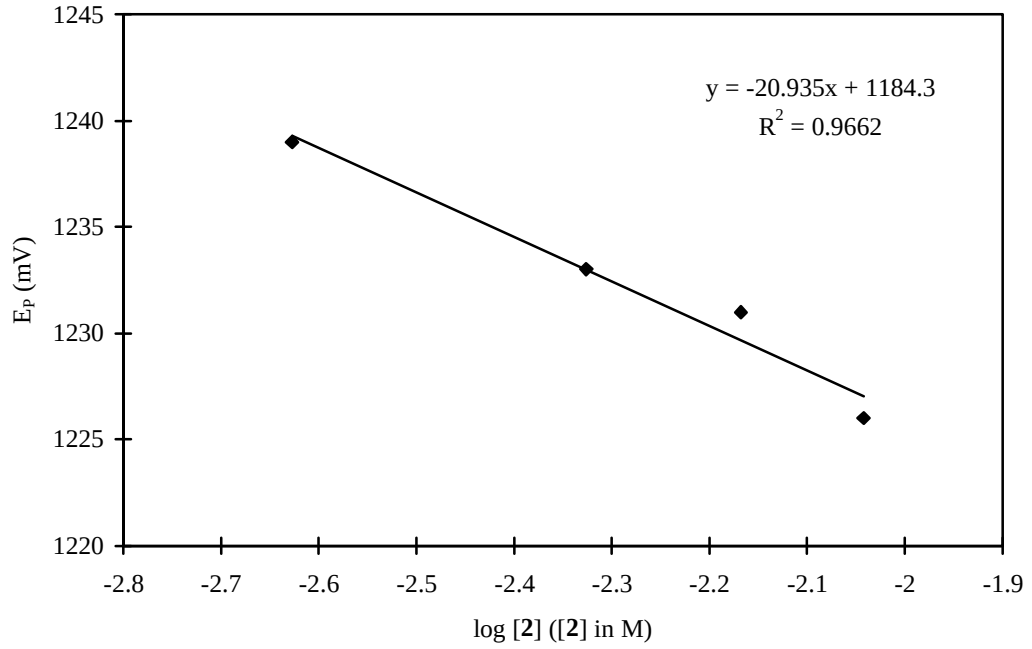

Figure 2-20. LSV analysis of **2**, $\partial E_P/\partial \log[\mathbf{2}]$. (0.5 M $LiBF_4$, 0.5 M CH_3OH, 1.59→13.8 × 10^{-3} M **2**, v = 400 mV/sec)

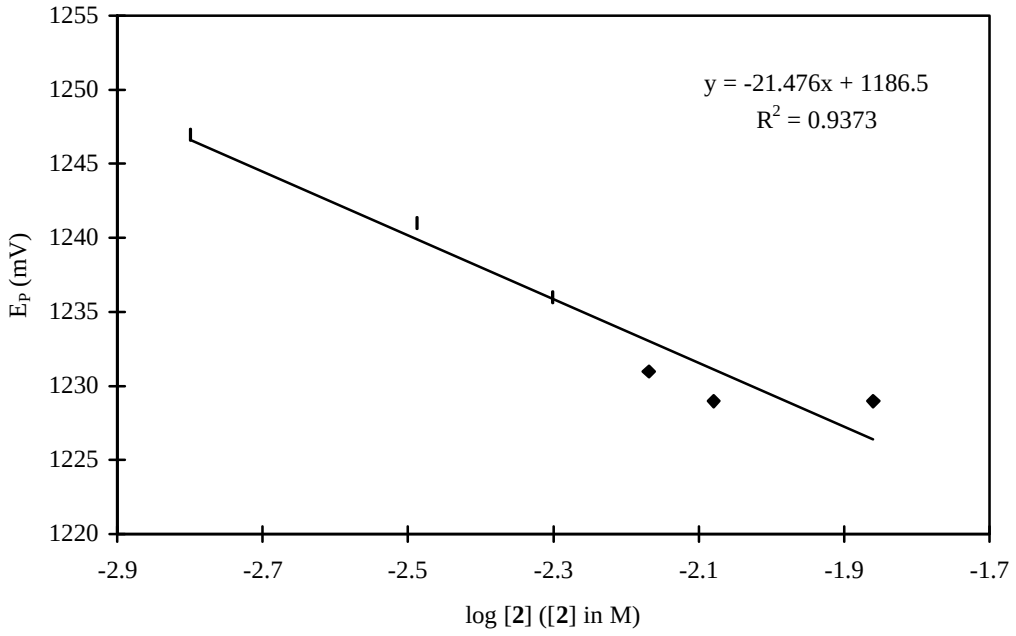

Figure 2-21. LSV analysis of **2**, $\partial E_P/\partial \log[\mathbf{2}]$. (0.5 M $LiClO_4$, 0.5 M CH_3OH, 0.59→9.44 $\times 10^{-3}$ M **2**, v = 400 mV/sec)

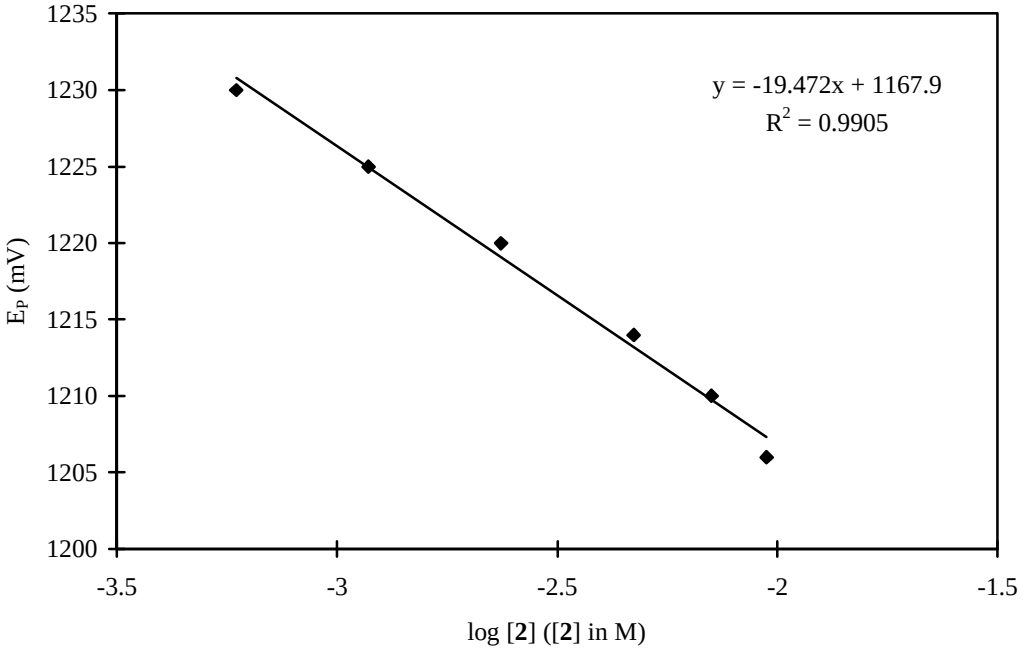

Figure 2-22. LSV analysis of **2**, $\partial E_P/\partial \log(v)$. (0.5 M $LiClO_4$, 0.5 M CH_3OH, 2.36 $\times 10^{-3}$ M **2**, v = 100→6000 mV/sec)

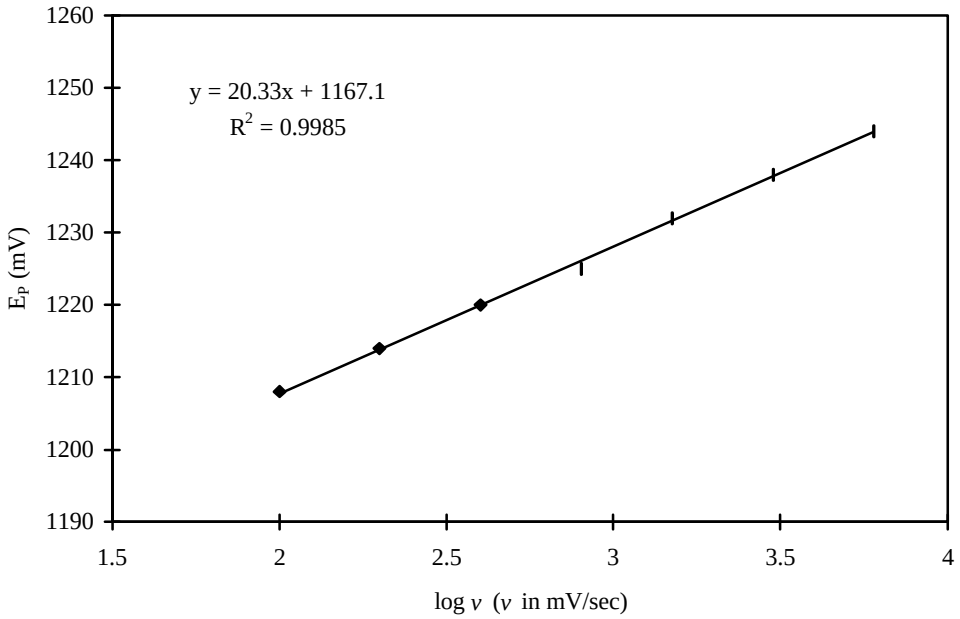

Figure 2-23. LSV analysis of **2**, $\partial E_P/\partial \log(v)$. (0.5 M $LiClO_4$, 0.5 M CH_3OH, 9.44×10^{-3} M **2**, v = 100→6000 mV/sec)

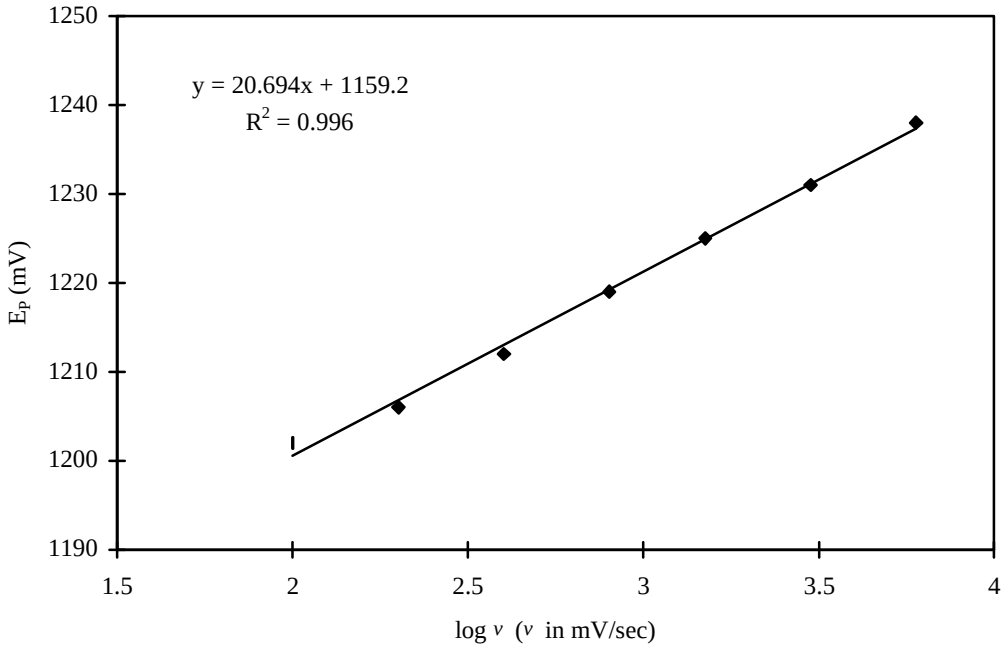

Figure 2-24. LSV analysis of **2**, $\partial E_P/\partial \log[CH_3OH]$. (0.25 M $^nBu_4NPF_6$, 0.025→0.25 M CH_3OH, 1.18×10^{-3} M **2**, v = 400 mV/sec)

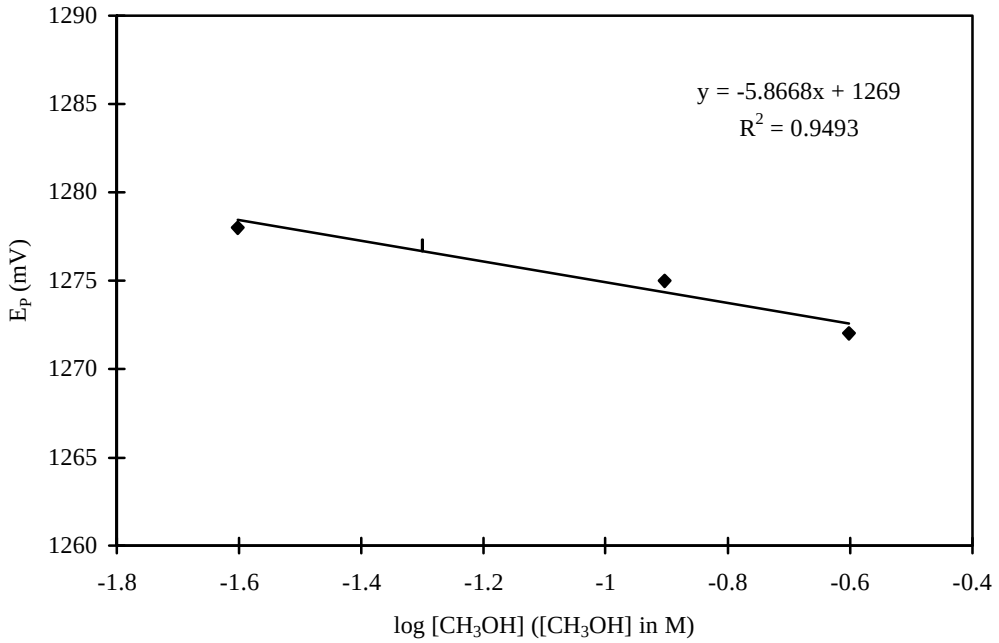

Figure 2-25. LSV analysis of **2**, $\partial E_P/\partial \log[\mathbf{2}]$. (0.25 M $^nBu_4NPF_6$, 0.25 M CH_3OH, $1.18 \rightarrow 9.44 \times 10^{-3}$ M **2**, ν = 400 mV/sec)

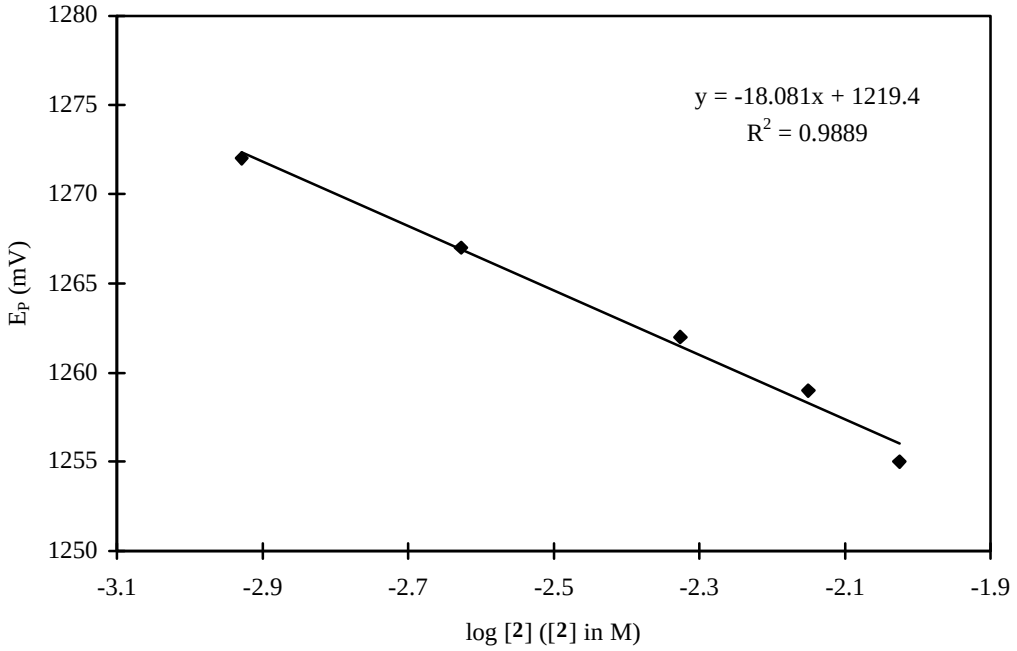

Figure 2-26. LSV analysis of **2**, $\partial E_P/\partial \log(\nu)$. (0.25 M $^nBu_4NPF_6$, 0.25 M CH_3OH, 1.18×10^{-3} M **2**, ν = 100→3000 mV/sec)

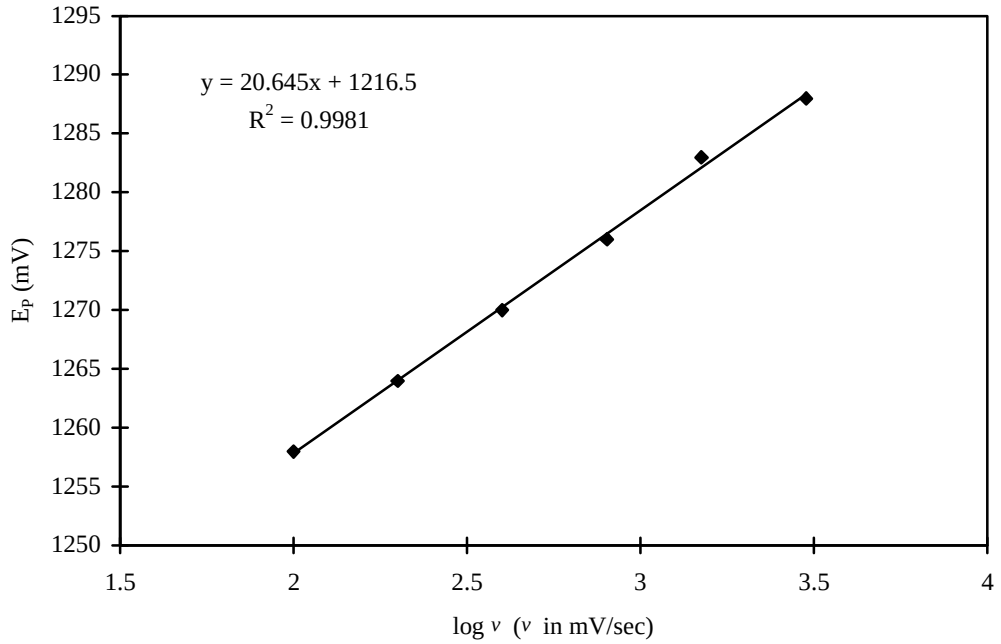

Figure 2-27. LSV analysis of **2**, $\partial E_P/\partial \log(v)$. (0.25 M $^nBu_4NPF_6$, 0.25 M CH_3OH, 9.44×10^{-3} M **2**, v = 100→3000 mV/sec)

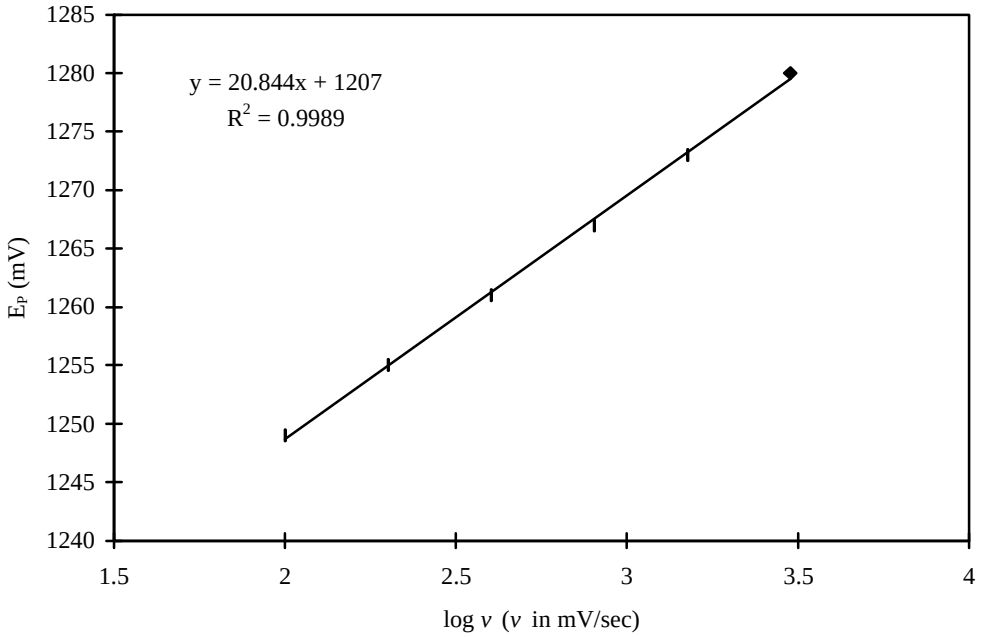

Figure 2-28. LSV analysis of **2**, $\partial E_P/\partial \log(v)$. (0.25 M $^nBu_4NPF_6$, CH_2Cl_2/CH_3CN (1:1), 2.36×10^{-3} M **2**, v = 100→6000 mV/sec)

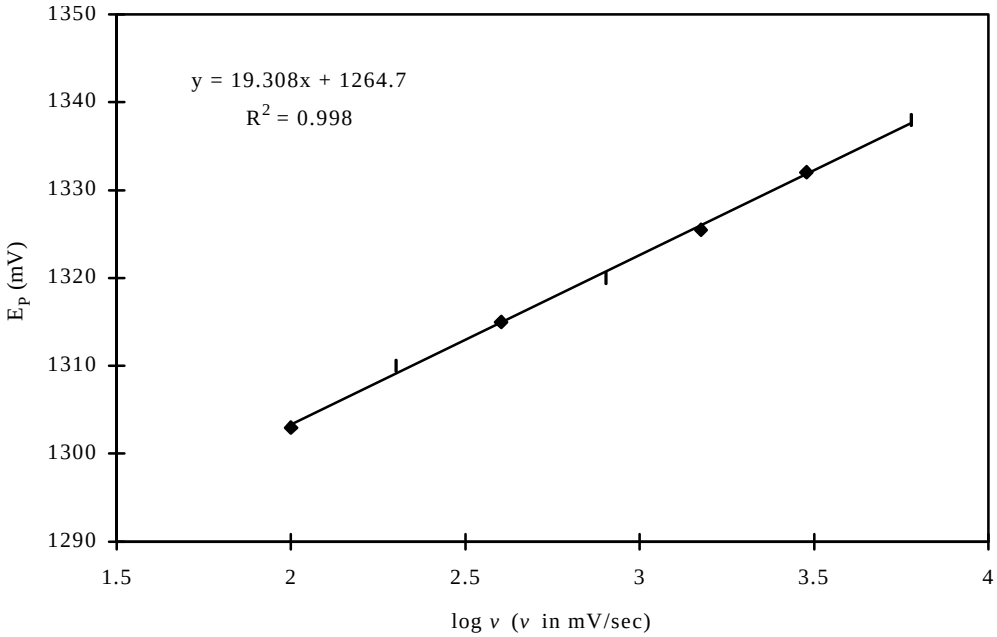

Figure 2-29. LSV analysis of **2**, $\partial E_P/\partial \log[CH_3OH]$. (0.25 M $^nBu_4NPF_6$, 0.0125→0.125 M CH_3OH, CH_2Cl_2/CH_3CN (1:1), 2.36×10^{-3} M **2**, ν = 400 mV/sec)

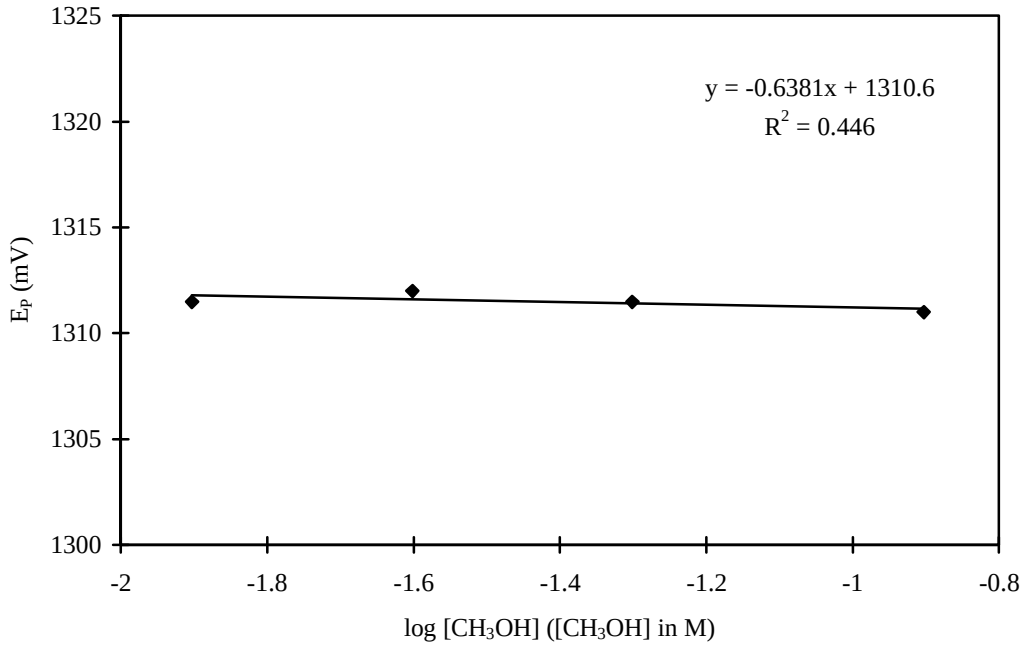

Figure 2-30. LSV analysis of **2**, $\partial E_P/\partial \log[\mathbf{2}]$. (0.25 M $^nBu_4NPF_6$, 0.25 M CH_3OH, CH_2Cl_2/CH_3CN (1:1), 1.18→9.44×10^{-3} M **2**, ν = 400 mV/sec)

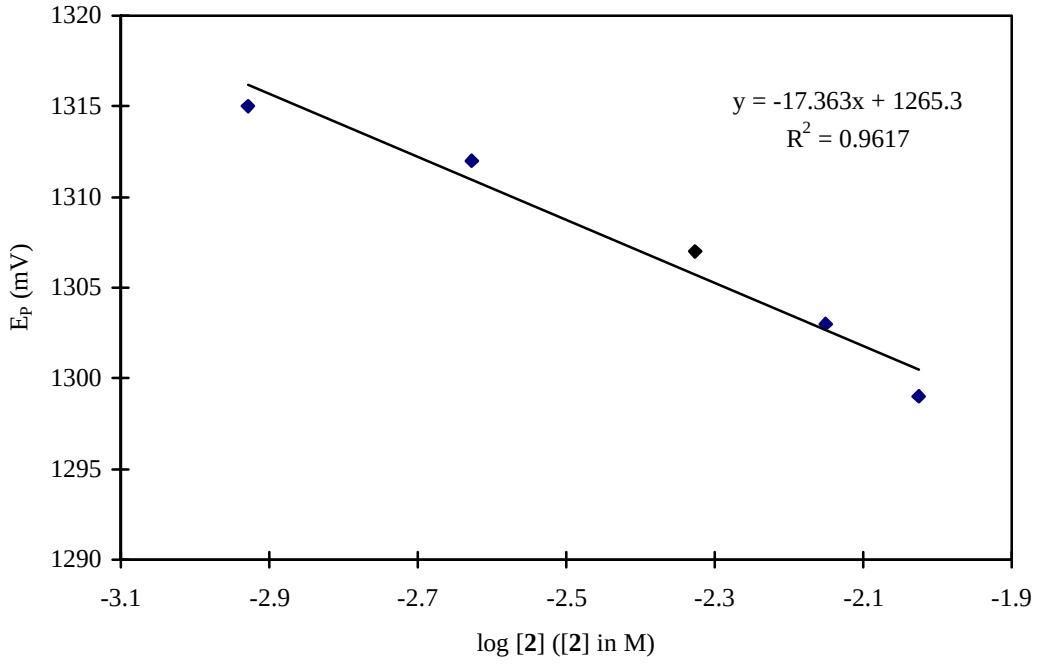

Figure 2-31. LSV analysis of **2**, $\partial E_P/\partial \log(\nu)$. (0.25 M $^nBu_4NPF_6$, CH_2Cl_2/CH_3CN (1:1), 9.44×10^{-3} M **2**, ν = 100→3000 mV/sec)

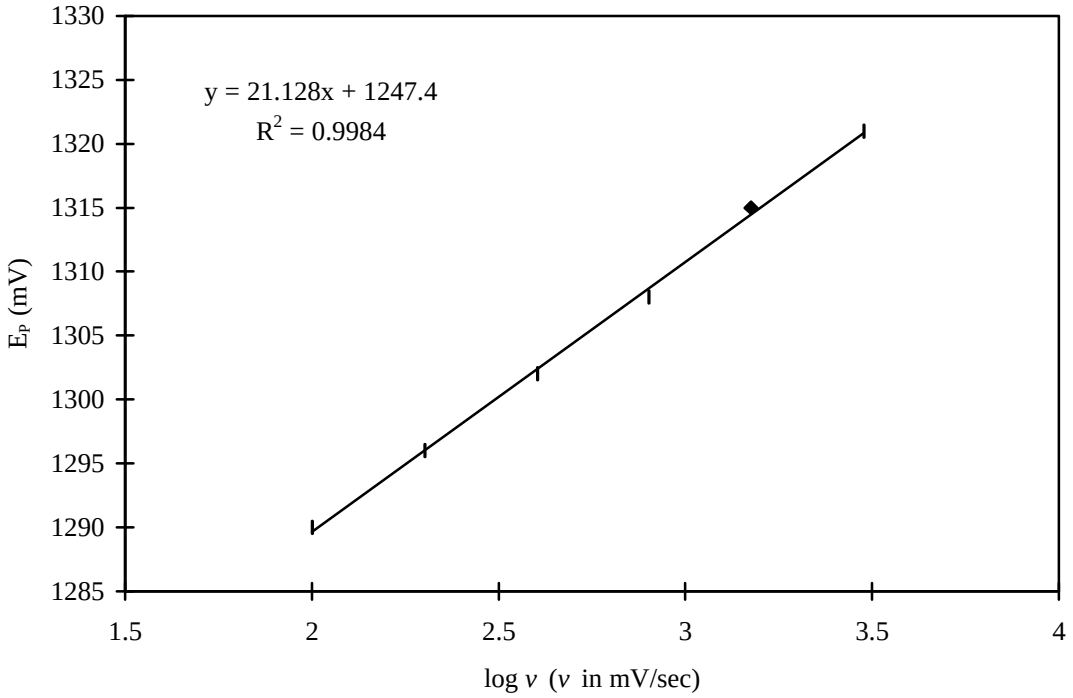

When CH_2Cl_2 is used as solvent, the cyclic voltammogram of **2** changes significantly. The initial oxidation wave shifts to a more positive potential (ΔE_P = ~130 mV) and begins to merge with the subsequent oxidation waves (Figure 2-32, curve a). Unlike in CH_3CN, at higher sweeprates in CH_2Cl_2, the initial wave of **2** becomes reversible (Figure 2-32, curve b) indicating that $\mathbf{2}^{+\cdot}$ is longer-lived in CH_2Cl_2 than in CH_3CN. The DCV "reaction order approach" was employed to study decay of $\mathbf{2}^{+\cdot}$ (Figures 2-33 ~ 35 and Table 2-4). The results obtained from this analysis are also consistent with a bimolecular decay of $\mathbf{2}^{+\cdot}$ in CH_2Cl_2.[91]

Figure 2-32 Cyclic voltammogram of **2** in CH_2Cl_2 (0.5 M $^nBu_4NPF_6$, 2.36×10^{-3} M **2**)

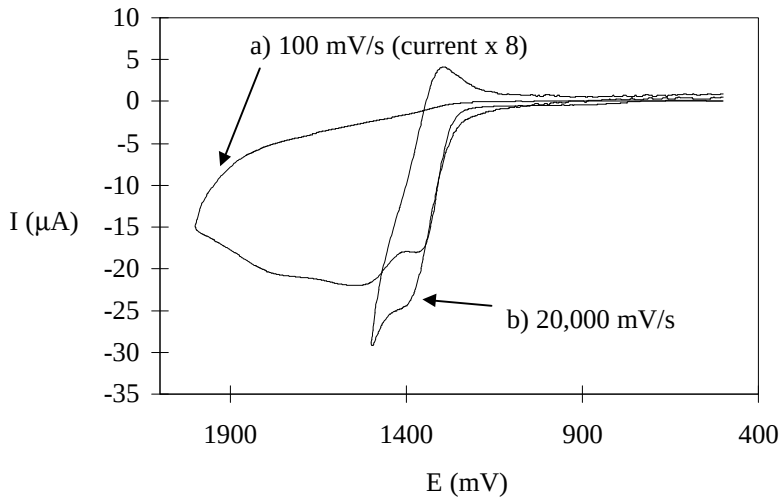

Table 2-4. Observed DCV response for the electrochemical oxidation of **2** in CH_2Cl_2 and in the presence of CH_3CN or CH_3OH

$\partial\log(v_c)/\partial\log[\mathbf{2}]$	$\partial\log(v_c)/\partial\log[\mathbf{X}]$
1.04 ± 0.04[a]	0.30 ± 0.01 (X = CH_3OH)[b] 0.27 ± 0.01 (X = CH_3CN)[c]

[a] 0.25 M $^nBu_4NPF_6$, 0.00059→0.0059 M **2**;

[b] 0.5 M $^nBu_4NPF_6$, 0.00236 M **2**, 0.125→1.25 M CH_3OH;

[c] 0.25 M $^nBu_4NPF_6$, 0.00177 M **2**, 0.0958→3.83 M CH_3CN.

Figure 2-33. DCV analysis of **2**, $\partial\log(v_c)/\partial\log[\mathbf{2}]$. (0.25 M $^{n}Bu_4NPF_6$-CH_2Cl_2, 0.59→5.9 × 10^{-3} M **2**, v = 200→8000 mV/sec, I'_{pc}/I'_{pa} = 0.6)

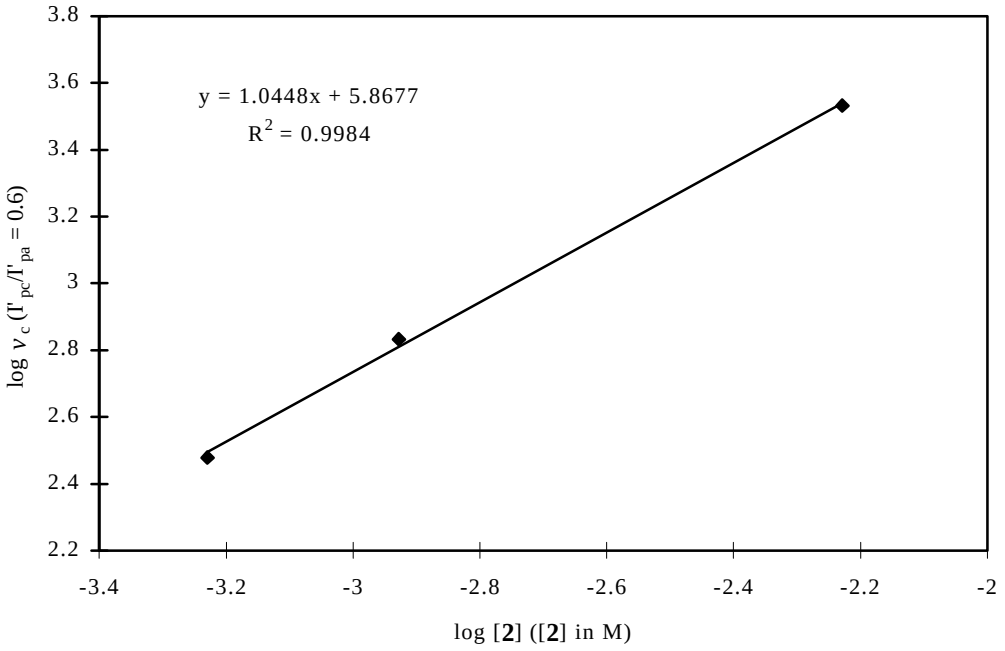

Figure 2-34. DCV analysis of **2**, $\partial\log(v_c)/\partial\log[CH_3OH]$. (0.5 M $^{n}Bu_4NPF_6$-CH_2Cl_2, 0.125→1.325 M CH_3OH, 2.36 × 10^{-3} M **2**, v = 5→50 V/sec, I'_{pc}/I'_{pa} = 0.7)

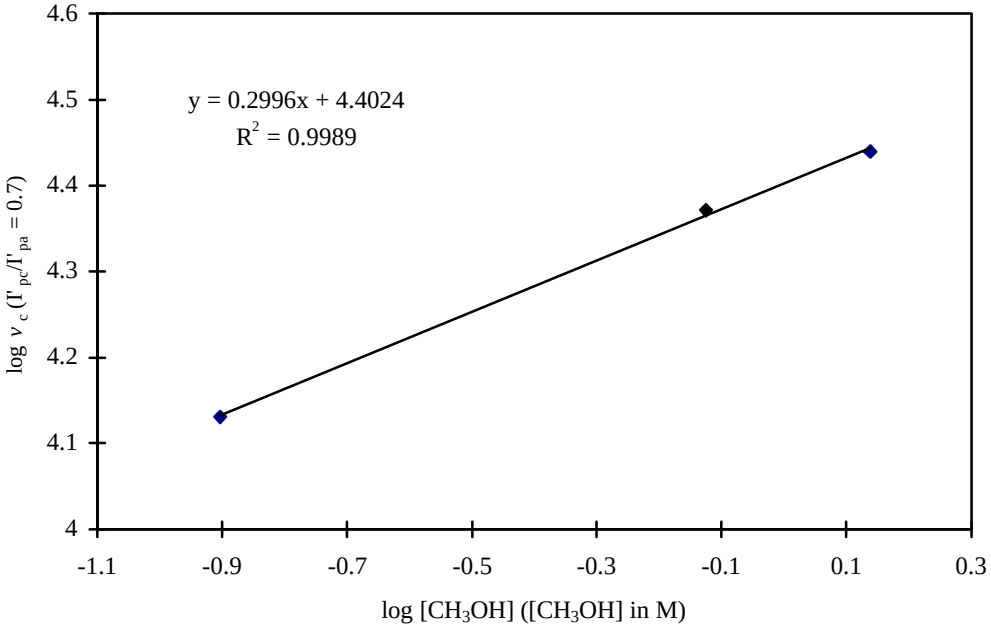

Figure 2-35. DCV analysis of **2**, $\partial\log(v_c)/\partial\log[CH_3CN]$. (0.25 M $^nBu_4NPF_6$-CH_2Cl_2, 0.985→3.83 M CH_3CN, 1.77×10^{-3} M **2**, v = 100→8000 mV/sec, I'_{pc}/I'_{pa} = 0.6)

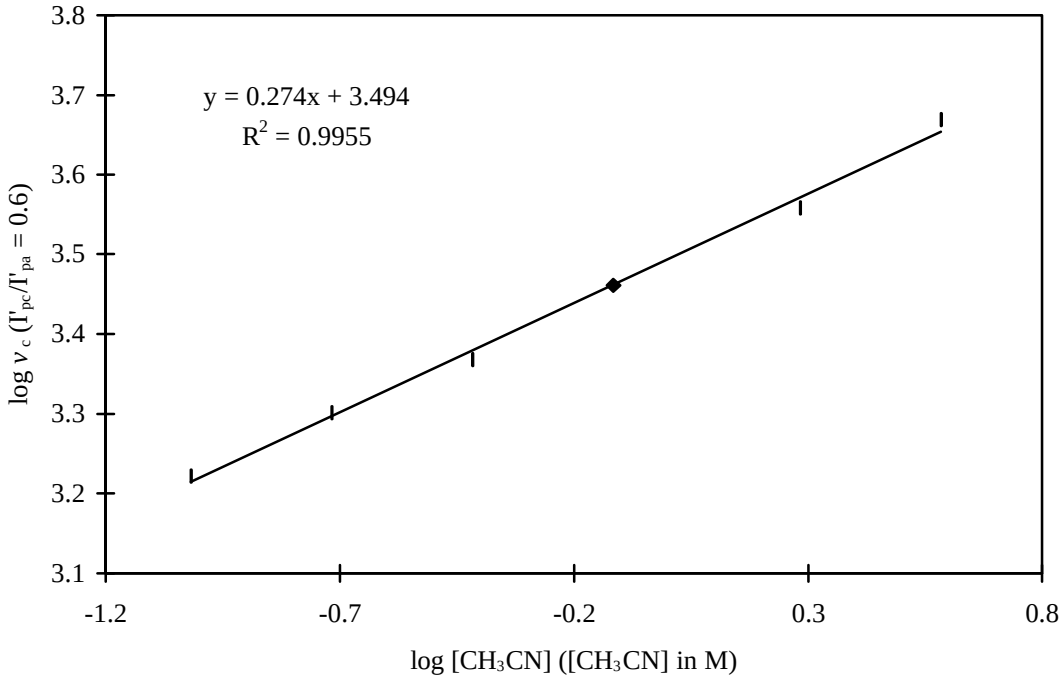

Addition of CH_3CN or CH_3OH (to CH_2Cl_2 solvent) slightly affects the cathodic to anodic derivative current ratio (I'_{pc}/I'_{pa}), resulting in an apparent reaction order of ca. 0.3. However, this small change in the derivative current ratio, coupled with the LSV results which show no change in E_P with CH_3OH concentration (in CH_3CN or 1:1 CH_3CN:CH_2Cl_2 solvents) suggest these observations are more the result of a solvent effect on the rate constant for dimerization (or disproportionation) of $\mathbf{2}^{+\cdot}$, rather than any significant participation of either CH_3OH or CH_3CN in the decay mechanism.

Because the rate law for the decay of $\mathbf{2}^{+\cdot}$ is now known, it becomes possible to calculate the rate constant for dimerization of $\mathbf{2}^{+\cdot}$ in CH_2Cl_2. DCV was employed to obtain the experimental derivative peak current ratio (I'_{pc}/I'_{pa}) at various sweeprates for a

given concentration of substrate. The data in the region of I'_{pc}/I'_{pa} = 0.4 ~ 0.8 were used in this analysis. Theoretical working curve was generated via digital simulation (Figure 2-36).[92] Equations for k_{dim} from this working curve at 298 K is $k_{dim} = 4.0\nu_{0.7}/C_A$, $k_{dim} = 6.8\nu_{0.6}/C_A$, $k_{dim} = 12.5\nu_{0.5}/C_A$, where ν_c in V/s, C_A in M. The rate constant for dimerization of $\mathbf{2}^{+\cdot}$ is found to be 3.9 ($\pm$ 0.2) $\times 10^3$ $M^{-1}s^{-1}$ in CH_2Cl_2. Similarly, rate constants for dimerization of $\mathbf{2}^{+\cdot}$ in CH_2Cl_2 at various concentrations of CH_3CN or CH_3OH were obtained (Table 2-5). With an increase of CH_3CN or CH_3OH concentration, the rate constants for dimerization of $\mathbf{2}^{+\cdot}$ increase.

Figure 2-36. Dimensionless working curve for EC_{dim} mechanism (A - e^- = B, 2B = C, rate = $k_{dim}C_A^2$)

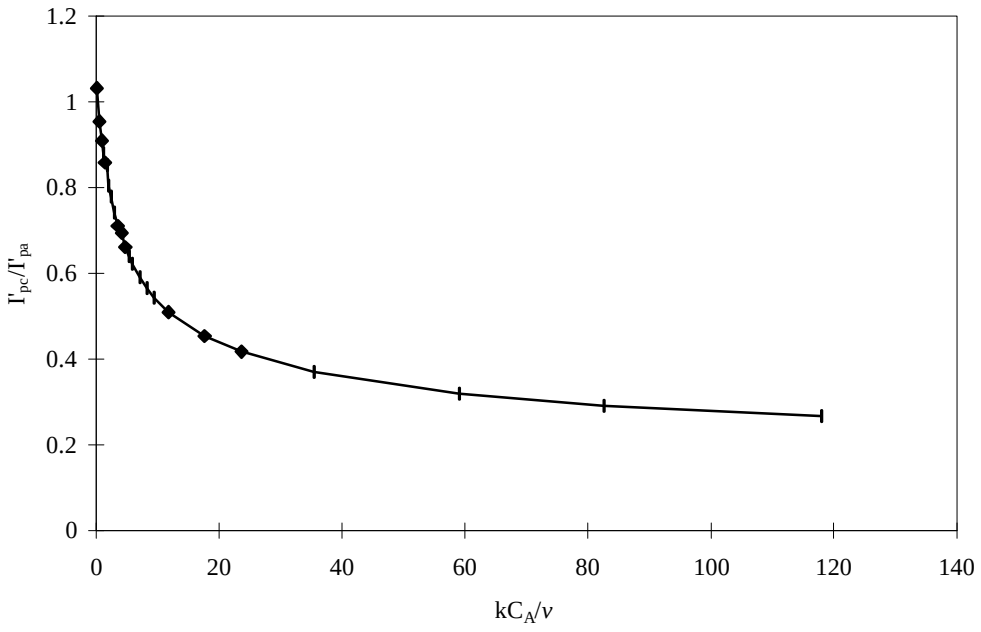

Table 2-5. Rate constant for dimerization of $\mathbf{2}^{+\cdot}$ (CH_2Cl_2 solvent mixed with varying amounts of CH_3OH or CH_3CN)

$[CH_3CN]$ (M)	$v_{0.6}$ (mV/sec) (C_A = 0.00177 M)	k_{dim} ($M^{-1}s^{-1}$)	C_{MeOH} (M)	$v_{0.7}$ (mV/sec) (C_A = 0.00236 M)	k_{dim} ($M^{-1}s^{-1}$)
0		3900	0.125	13500	22900
0.0958	1670	6400	0.75	23500	39800
0.192	2000	7700	1.38	27500	46600
0.383	2330	8900			
0.766	2890	11100			
1.92	3610	13800			
3.83	4670	17900			

2-Cyclopropylnaphthalene (3). The cyclic voltammogram of **3** in CH_3CN is similar to that of **1,** characterized by an initial oxidation wave (E_P = ~1157 mV at 400 mV/sec) which is not affected by the addition of methanol (Figure 2-37).

Figure 2-37. Cyclic voltammogram of **3** in CH_3CN (0.5 M $LiClO_4$, 1.19×10^{-3} M **3**, v = 400 mV/s)

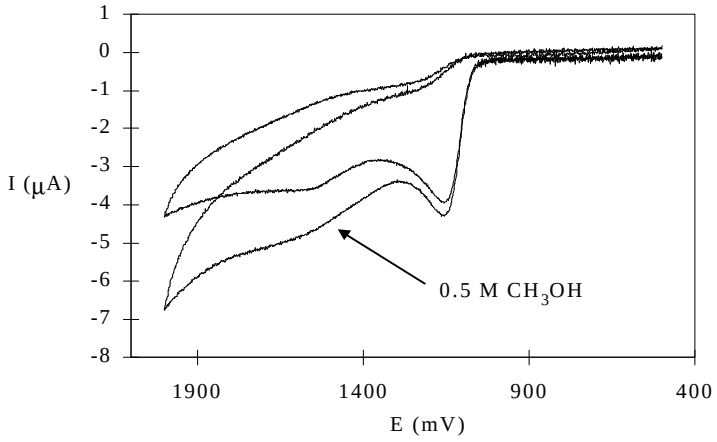

Because the initial oxidation wave is completely irreversible at sweeprates under 8000 mV/sec in CH_3CN, LSV was used to study the decay of $\mathbf{3}^{+\cdot}$. Figures 2-38→2-48 and Table 2-6 summarize the LSV results for the electrochemical oxidation of **3**. As was found for $\mathbf{1}^{+\cdot}$ and $\mathbf{2}^{+\cdot}$, the decay of $\mathbf{3}^{+\cdot}$ is second order in radical cation and zero order in methanol (Eq. 2-8):

$$-d[\mathbf{3}^{+\cdot}]/dt = k[\mathbf{3}^{+\cdot}]^2 \qquad (2\text{-}8)$$

Table 2-6. Observed LSV response for the electrochemical oxidation of **3** in CH_3CN

electrolytes	$\partial E_P/\partial \log(v)$[a]	$\partial E_P/\partial \log[\mathbf{3}]$[b]	$\partial E_P/\partial \log[CH_3OH]$[c]
0.5 M $LiBF_4$	16.8 ± 1.0 (1.2) 18.4 ± 0.5 (7.1)	-20.5 ± 3.0 (1.19→7.14)	-0.54 ± 0.33 (1.2)
0.5 M $LiClO_4$	18.6 ± 0.4 (1.2) 20.9 ± 0.4 (7.1)	-22.0 ± 0.6 (1.19→7.14)	1.19 ± 0.37 (10)

[a] 0.5 M CH_3OH, v = 100→3000 mV/s, [**3**] (mM) appears in parentheses;

[b] 0.5 M CH_3OH, *v* = 400 mV/sec, [**3**] (mM) range appears in parentheses;

[c] 0.025→0.5 M CH_3OH, *v* = 400 mV/sec, [**3**] (mM) appears in parentheses.

Figure 2-38. LSV analysis of **3**, $\partial E_P/\partial \log[\mathbf{3}]$. (0.5 M $LiBF_4$, 0.5 M CH_3OH, 1.19→7.14 × 10^{-3} M **3**, ν = 400 mV/sec)

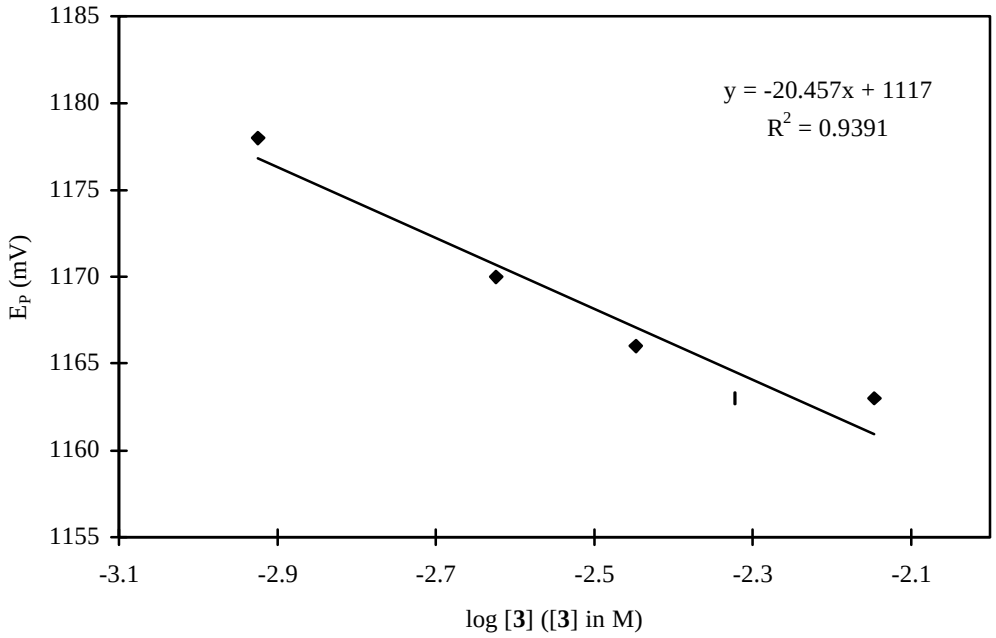

Figure 2-39. LSV analysis of **3**, $\partial E_P/\partial \log(\nu)$. (0.5 M $LiBF_4$, 0.5 M CH_3OH, 1.19 × 10^{-3} M **3**, ν = 200→6000 mV/sec)

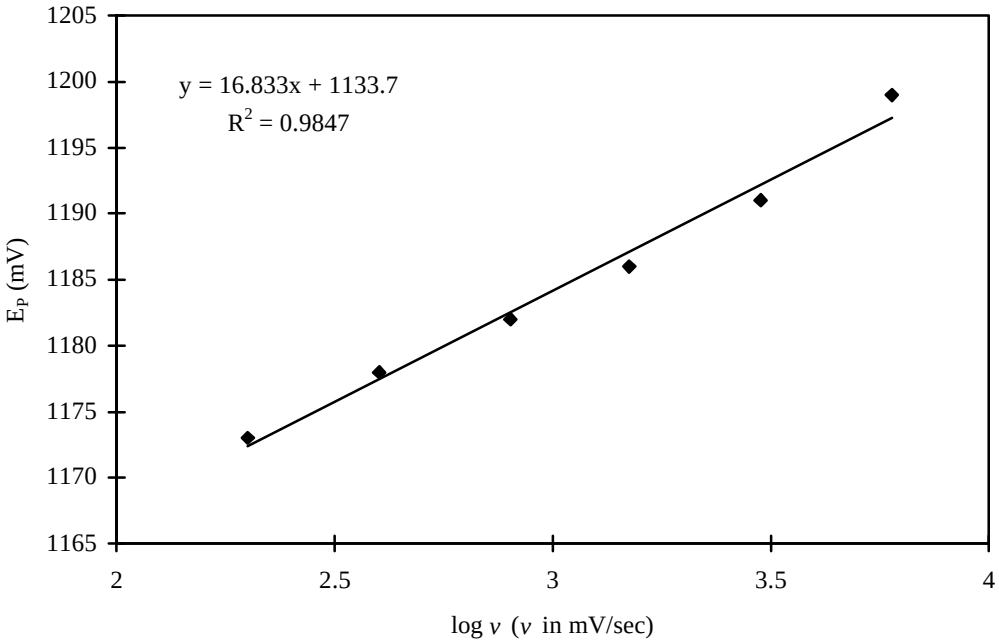

Figure 2-40. LSV analysis of **3**, $\partial E_P/\partial \log(v)$. (0.5 M $LiBF_4$, 0.5 M CH_3OH, 7.14×10^{-3} M **3**, v = 200→6000 mV/sec)

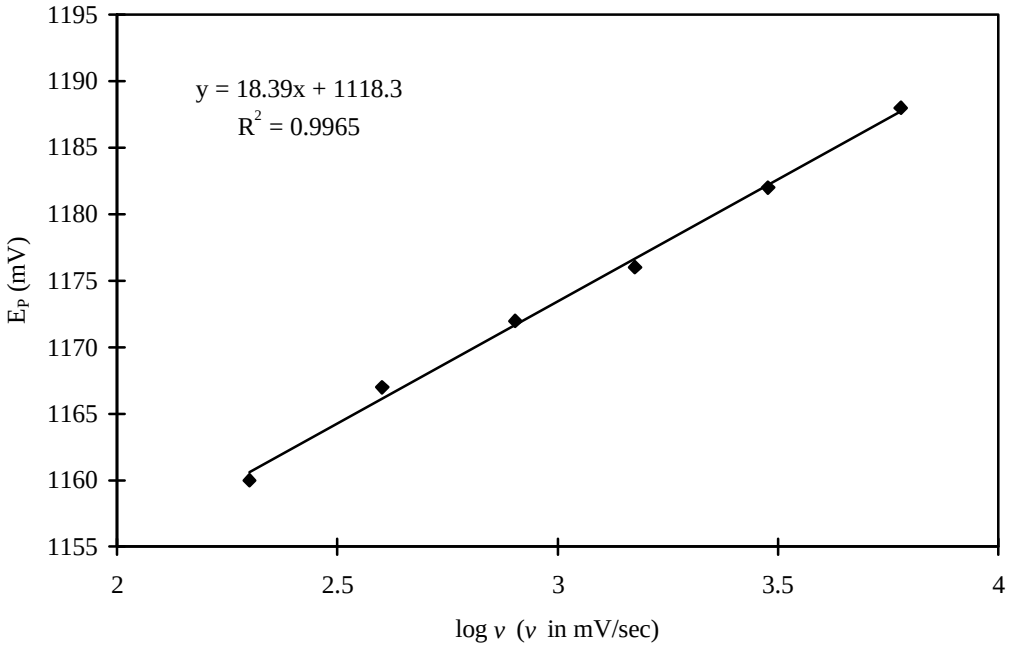

Figure 2-42. LSV analysis of **3**, $\partial E_P/\partial \log[CH_3OH]$. (0.5 M $LiBF_4$, 0.0125→0.5 M CH_3OH, 1.19×10^{-3} M **3**, v = 400 mV/sec)

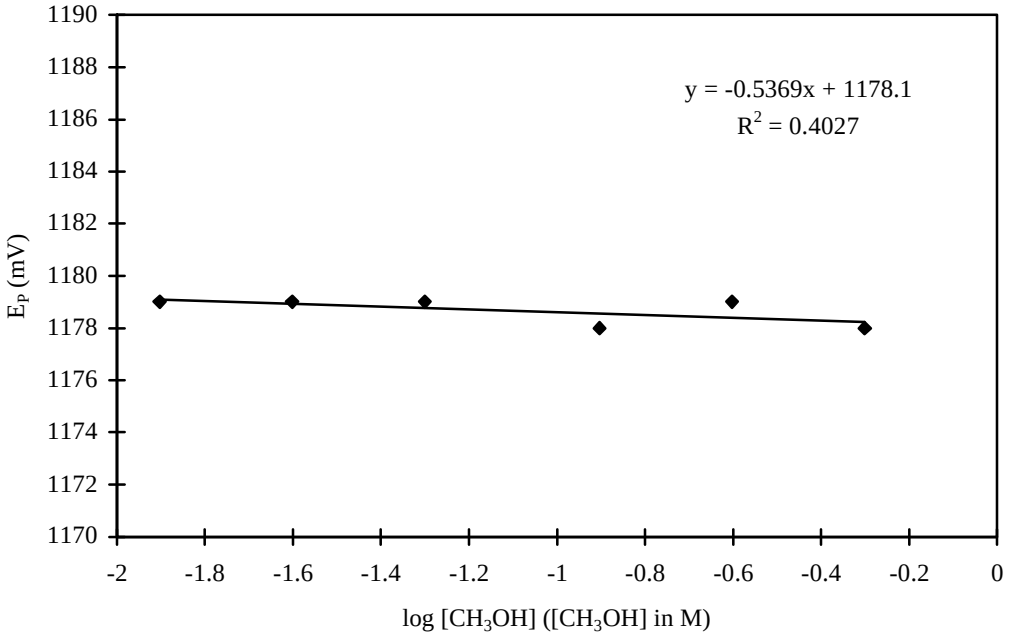

Figure 2-43. LSV analysis of **3**, $\partial E_P/\partial \log[\mathbf{3}]$. (0.5 M $LiClO_4$, 0.5 M CH_3OH, 1.19→7.14 × 10^{-3} M **3**, ν = 400 mV/sec)

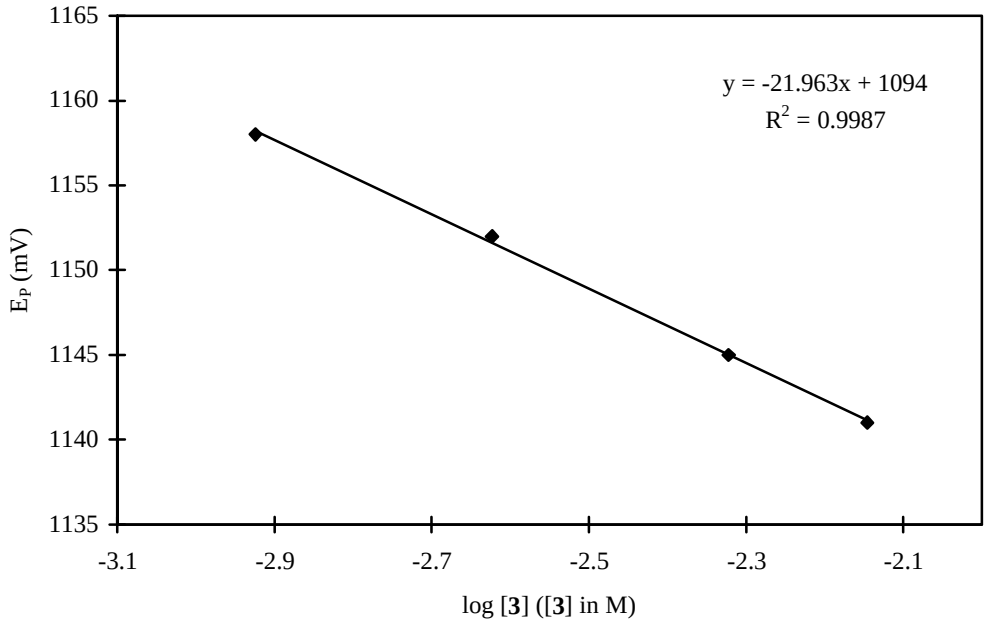

Figure 2-44. LSV analysis of **3**, $\partial E_P/\partial \log(\nu)$. (0.5 M $LiClO_4$, 0.5 M CH_3OH, 7.1 × 10^{-3} M **3**, ν = 200→3000 mV/sec)

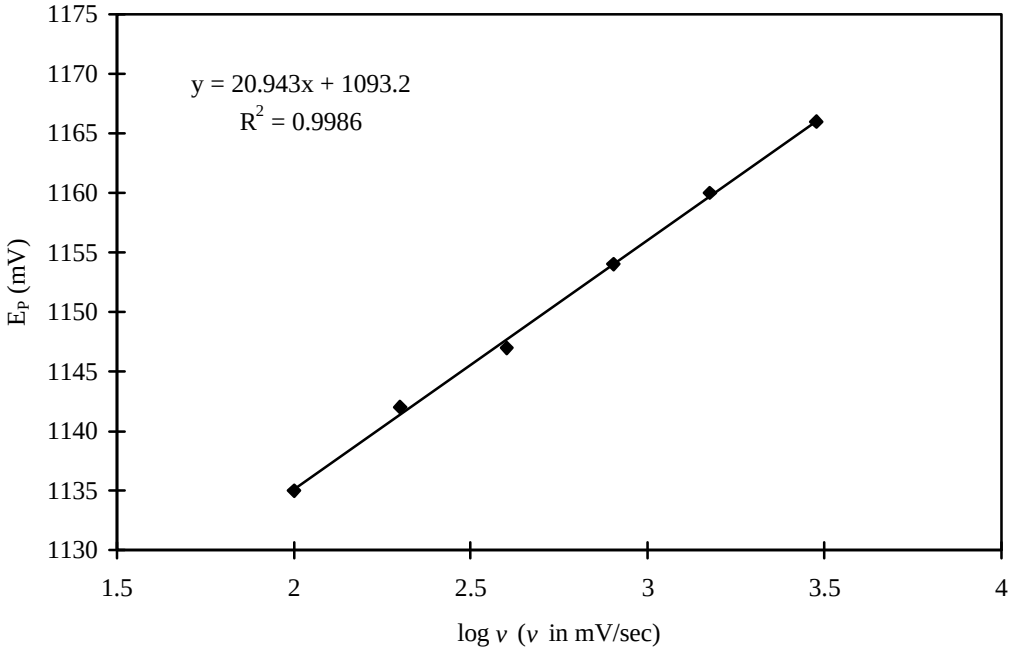

Figure 2-45. LSV analysis of **3**, $\partial E_P/\partial \log(\nu)$. (0.5 M $LiClO_4$, 0.5 M CH_3OH, 1.2×10^{-3} M **3**, ν = 200→3000 mV/sec)

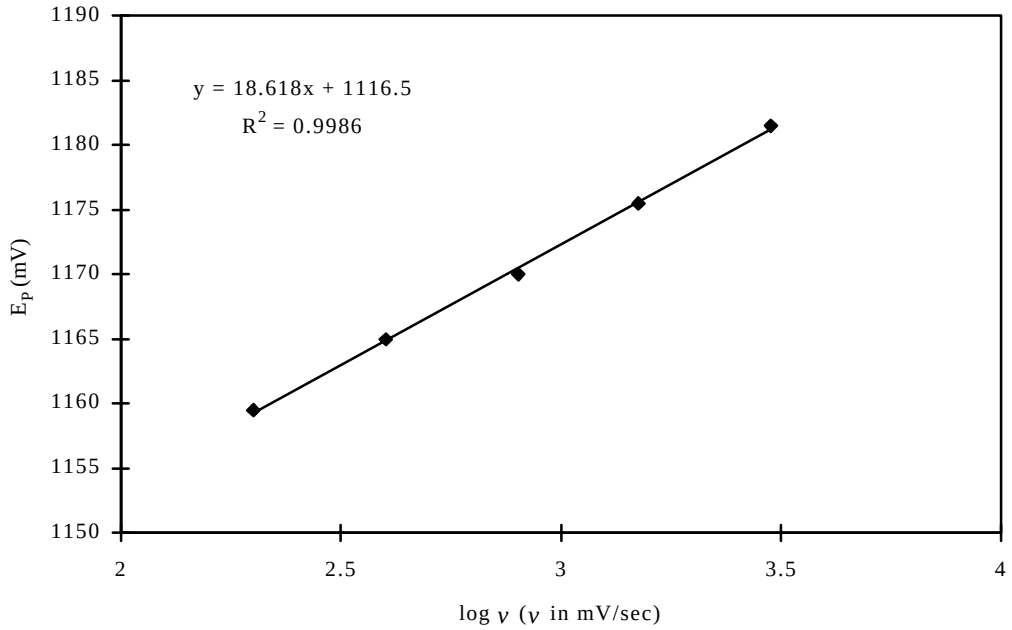

Figure 2-46. LSV analysis of **3**, $\partial E_P/\partial \log[CH_3OH]$. (0.5 M $LiClO_4$, 0.025→0.5 M CH_3OH, 1.0×10^{-3} M **3**, ν = 400 mV/sec)

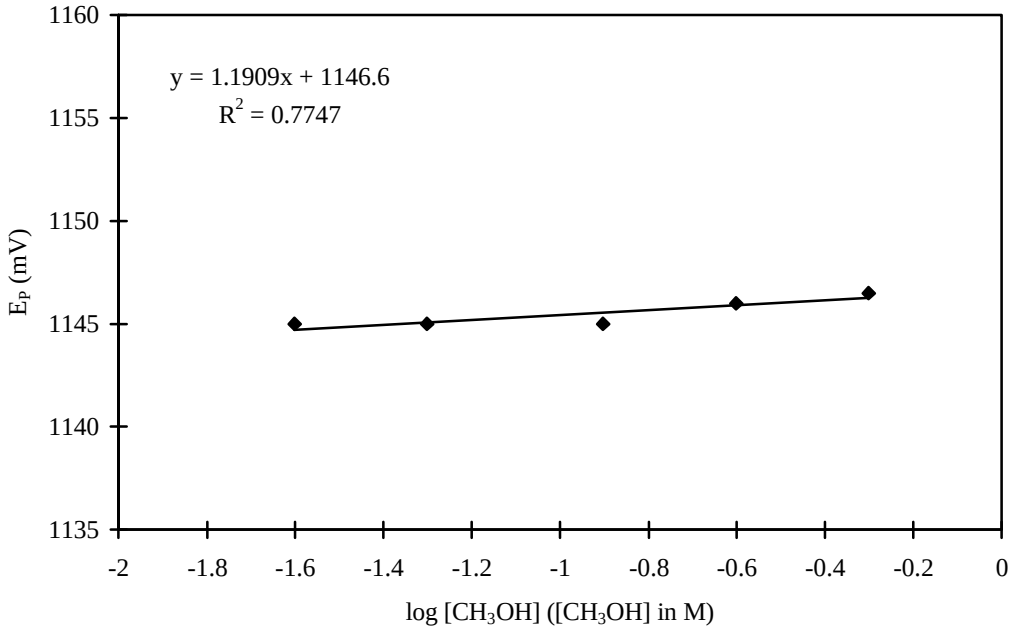

2.2.2 Product Analysis from Preparative Electrolysis

Constant current electrolyses of **1**, **2** and **3** were conducted in CH_3CN/CH_3OH with 0.1 M $LiClO_4$ as the supporting electrolyte. Ultrasound was employed to increase mass transfer efficiency during electrolysis. GC was used to monitor electrolytic progress.

1-Cyclopropylnaphthalene (1). The anodic oxidation of **1** in CH_3CN/CH_3OH mainly produces cyclopropane ring-opened products, 1-(1,3-dimethoxypropyl)-naphthalene (**4**) and dimer 4,4'-di(1,3-dimethoxypropyl)-1,1'-binaphthalene (**5**, Scheme 2-2). In a typical run, 17.4% of **4**, 26.3% of **5**, and 7.5% of **1** were recovered after the transfer of 3.5 equivalents of electrons. Minor product **6** was detected by GC/MS, but not isolated.

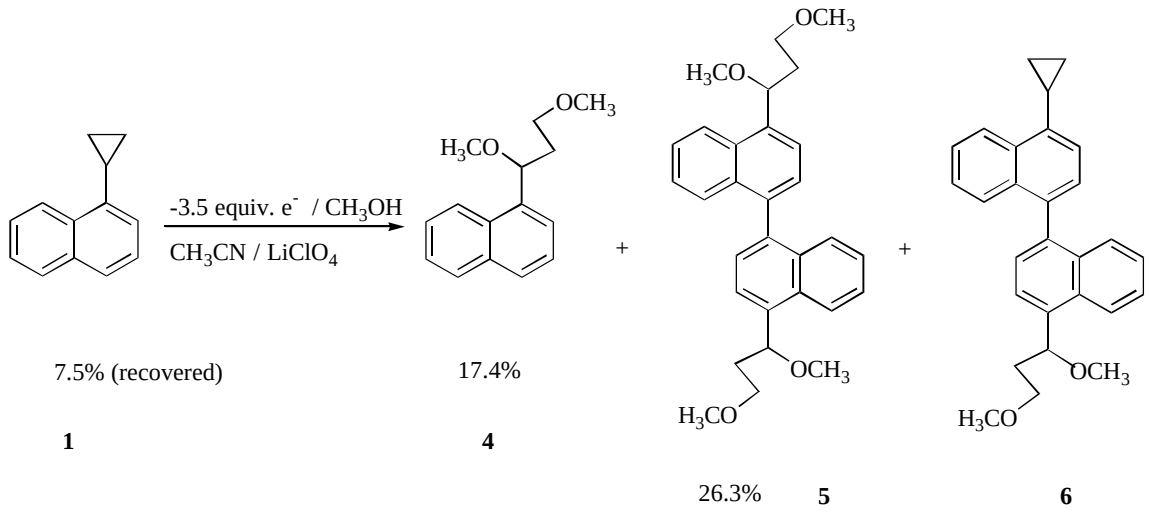

Scheme 2-2 Anodic oxidation of **1** in CH_3CN/CH_3OH

1-Bromo-4-cyclopropylnaphthalene (2). Oxidation of **2** yields exclusively cyclopropane ring-opened 1-bromo-4-(1,3-dimethoxypropyl)-naphthalene (**7**), in 80% yield after the transfer of two equivalents of electrons (Scheme 2-3). Some **2** (13.2%) was also recovered.

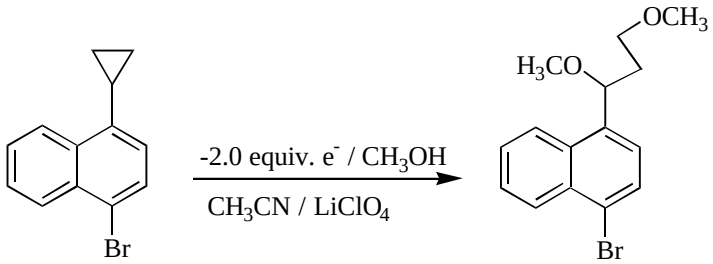

13% (recovered) 80%

2 **7**

Scheme 2-3. Anodic oxidation of **2** in CH_3CN/CH_3OH

2-Cyclopropylnaphthalene (3). The anodic oxidation of **3** in CH_3CN/CH_3OH yields, after the transfer of two equivalents of electrons, 2-(1,3-dimethoxypropyl)-naphthalene (**8**) and dimer 2, 2'-dicyclopropyl-1,1'-binaphthalene (**9**) as major products. The isolated yield of **8** and **9** was 16.2% and 17.5%, respectively (Scheme 2-4). In addition, a large amount of starting material (34.1%) was recovered.

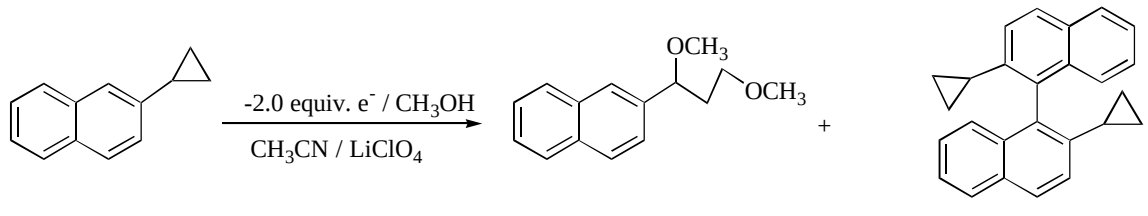

34.1% (recovered) 16.2% 17.5%

3 **8** **9**

Scheme 2-4. Anodic oxidation of **3** in CH_3CN/CH_3OH

2.2.3 Reaction Mechanism

Oxidation of 1-cyclopropylnaphthalene (1). LSV analyses for **1** reveal that decay of $\mathbf{1}^{+\cdot}$ in CH_3CN is second-order in radical cation and zero order in methanol. Preparative electrolysis of **1** produces the cyclopropane ring-opened (1,3-dimethoxypropyl) products. These results suggest that attack of methanol at the cyclopropane ring must occur after the rate determining step.

The second order rate law and appearance of dimers **5** and **6** as products are consistent with a radical cation dimerization mechanism (Scheme 2-5). Dication dimer **10**, formed by coupling (or complexing) of two monomeric radical cations ($\mathbf{1}^{+\cdot}$), is attacked by CH_3OH to produce **4** or loses two protons to form binaphthyl dimer **11**, which upon further oxidation produces **5** or **6**.

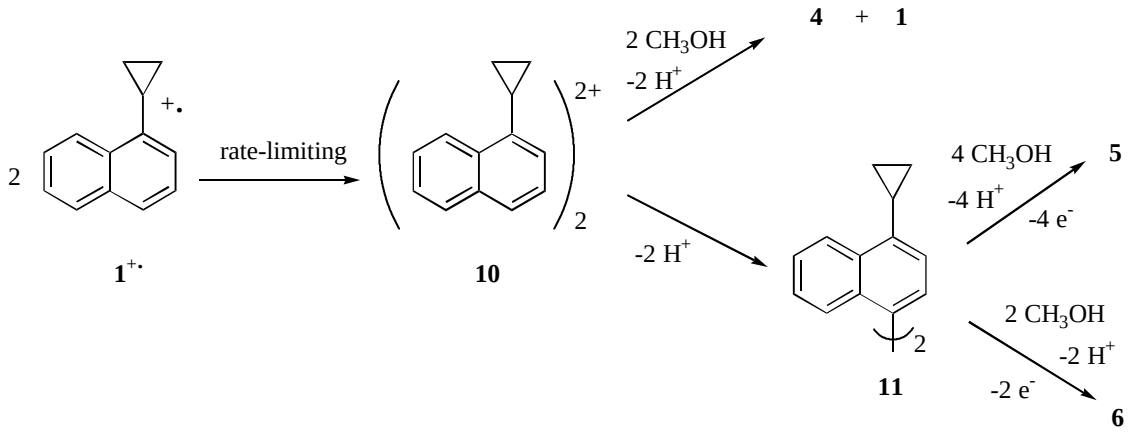

Scheme 2-5. Anodic oxidation mechanism of **1** in CH_3CN/CH_3OH (Dimerization)

Intermediate **10** may be formulated as a π-complex, or more likely as a σ-bonded dimer dication which undergoes ring opening as illustrated in Scheme 2-6. Dimer dications are proposed intermediates leading to dehydrodimers (biaryls) frequently observed in the oxidations of aromatic hydrocharbons).[87,93]

The second order rate law and appearance of products in preparative electrolysis are also consistent with a radical cation disproportionation mechanism (Scheme 2-7). It is the monomeric dication $\mathbf{1}^{++}$, formed from disproportionation of two $\mathbf{1}^{+\cdot}$, that is attacked by methanol to produce **4**. The dication $\mathbf{1}^{++}$ at same time can be captured by a neutral **1** in the cage to form dimer dication **10**, which produces **11** after losing two protons. **11** upon further oxidation produces **5** or **6**, as proposed in Scheme 2-5.

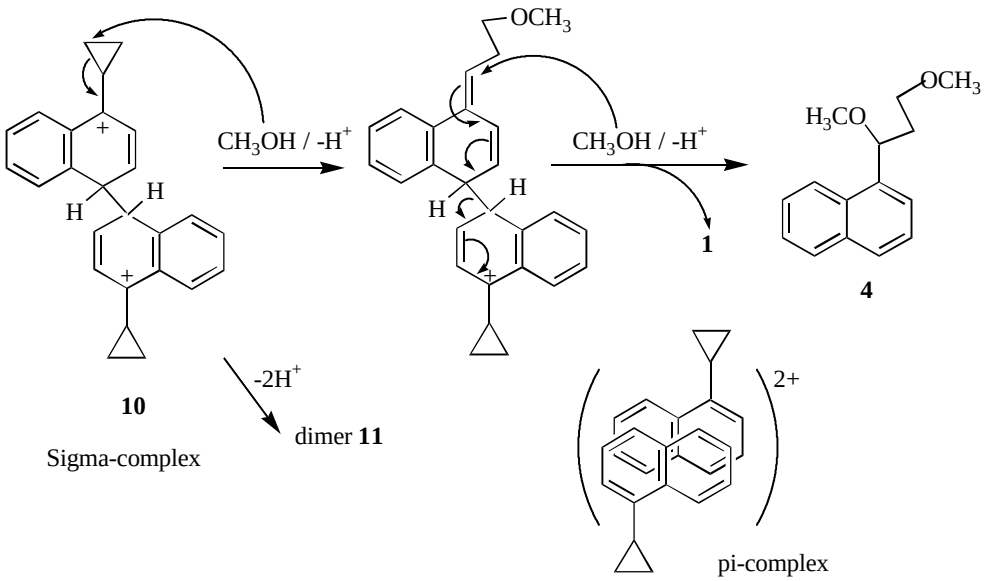

Scheme 2-6. Ring opening mechanism of dimer dication **10** in CH_3CN/CH_3OH

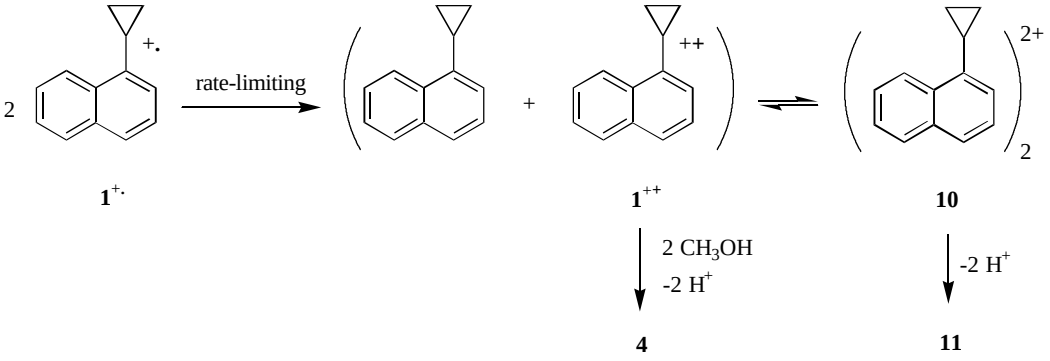

Scheme 2-7. Anodic oxidation mechanism of **1** in CH_3CN/CH_3OH (Disproportionation)

Oxidation of 1-bromo-4-cyclopropylnaphthalene (2). Both the LSV and DCV results for **2** are consistent with a rate law for decay of $\mathbf{2}^{+\cdot}$ which is second order in radical cation and zero order in methanol. Preparative electrolysis of **2** yields exclusively cyclopropane ring-opened product. These results suggest that the attack of methanol occurs after the rate-limiting step. A mechanism analogous to that proposed for decay of $\mathbf{1}^{+\cdot}$ is consistent with these results (Scheme 2-8). Intermediate dication dimer **12** reacts with methanol to produce **7** (and release **2**). Because it is not possible to lose "Br^+" under these conditions, the dimerization pathway (**12** → **11**) is effectively "turned off," and only the monomeric, cyclopropane ring-opened product is produced. The disproportionation is another likely mechanism for the decay of $\mathbf{2}^{+\cdot}$, in which the dication $\mathbf{2}^{++}$ is attacked by methanol to produce **7**.

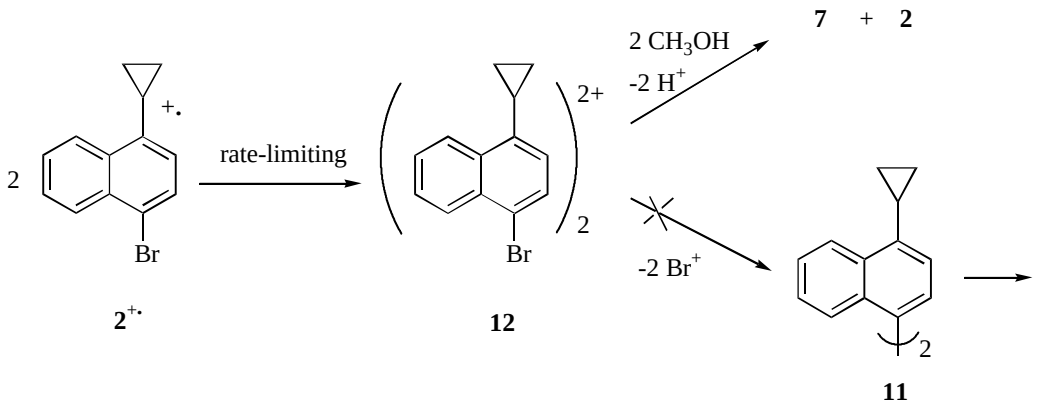

Scheme 2-8. Anodic oxidation mechanism of **2** in CH_3CN/CH_3OH

As noted earlier, $\mathbf{2}^{+\cdot}$ is longer-lived in CH_2Cl_2 compared to in CH_3CN. This observation is reasonable because CH_3CN is more polar than CH_2Cl_2. In general, oxidation potentials become more positive as the dielectric constant of the solvent decreases, attributable to variations in the solvation energy of the radical cations.[94] The reactivity of radical ions is subject to ion-pairing effects.[95] We suggest that $\mathbf{2}^{+\cdot}$ is longer lived in CH_2Cl_2 because of increased ion pairing (which decreases the rate constant for dimerization).

The rate constant for dimerization of $\mathbf{2}^{+\cdot}$, determined by fitting the DCV results to theoretical working curves generated via digital simulation is $3.9\ (\pm 0.2) \times 10^3\ M^{-1}s^{-1}$ in CH_2Cl_2. Also, the rate constant for dimerization of $\mathbf{2}^{+\cdot}$ (k_{dim}) was determined at various concentrations of CH_3CN (in CH_2Cl_2, Table 2-5). Using these data, it is possible to determine the value of k_{dim} in CH_3CN solvent via extrapolation. A plot of $\log(k_{dim})$ vs. $\log[CH_3CN]$ is linear (Figure 2-47): $\log(k_{dim}) = 4.0786 + 0.2758 \log[CH_3CN]$. Extrapolation to pure CH_3CN (19.1M) yields $k_{dim} = 3.1 \times 10^4\ M^{-1}s^{-1}$.

Figure 2-47 Variation of k_{dim} for $\mathbf{2}^{+\cdot}$ with $[CH_3CN]$ in CH_2Cl_2 solvent

Label1

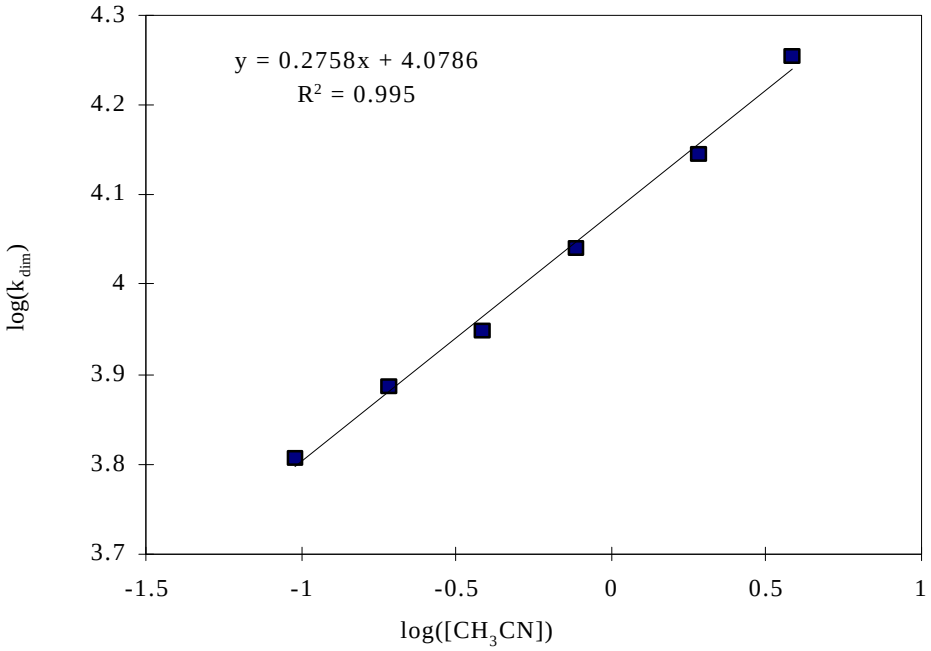

Oxidation of 2-cyclopropylnaphthalene (3). The decay of $\mathbf{3}^{+\cdot}$ is found to be second order in radical cation and zero order in methanol. A mechanism analogous to that depicted in Scheme 2-5 (involving a dimer dication intermediate **13**) is likely operative (Scheme 2-9). The alternative mechanism, disproportionation, is also consistent with second order rate law and product analysis (involving dication $\mathbf{3}^{++}$).

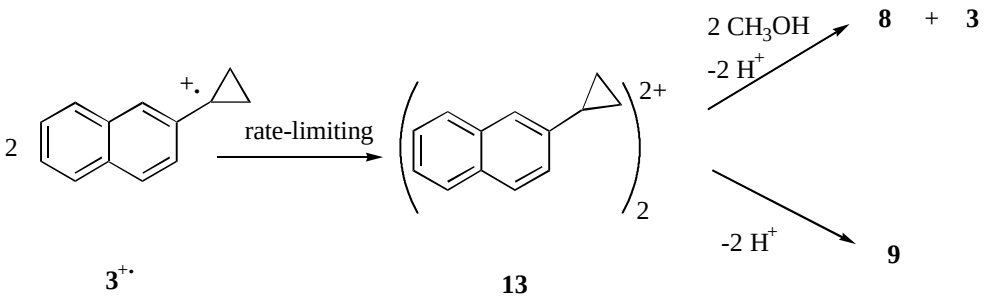

Scheme 2-9. Anodic oxidation mechanism of **3** in CH_3CN/CH_3OH

2.2.4 Stereoelectronic vs. Thermodynamic Factors

Estimated rate constant for ring opening of 1-cyclopropylnaphthalene radical cations. In the presence of methanol, oxidation of cyclopropylnaphthalenes **1**, **2**, and **3** leads mostly to cyclopropane ring-opened products, i.e., the corresponding 1,3-dimethoxypropyl derivatives. However, the radical cation of each of these substrates was found to decay via a rate law second-order in radical cation and zero-order in methanol, which means that methanol attack on the cyclopropane ring must occur after rate-limiting dimerization or disproportionation. Consistent with the observed rate law and nature of the products formed, we suggest that this second-order decay leads to formation of a dimer dication (which can be formulated as either a σ- or π-complex) or dication. The important point is that regardless of the exact nature of the dimer dication or dication, this second-order process must be occurring at a rate significantly faster than methanol-induced cyclopropane ring opening (e.g., k_{dim} [**2**$^{+\cdot}$] >> k_{MeOH} [CH_3OH], Scheme 2-10).

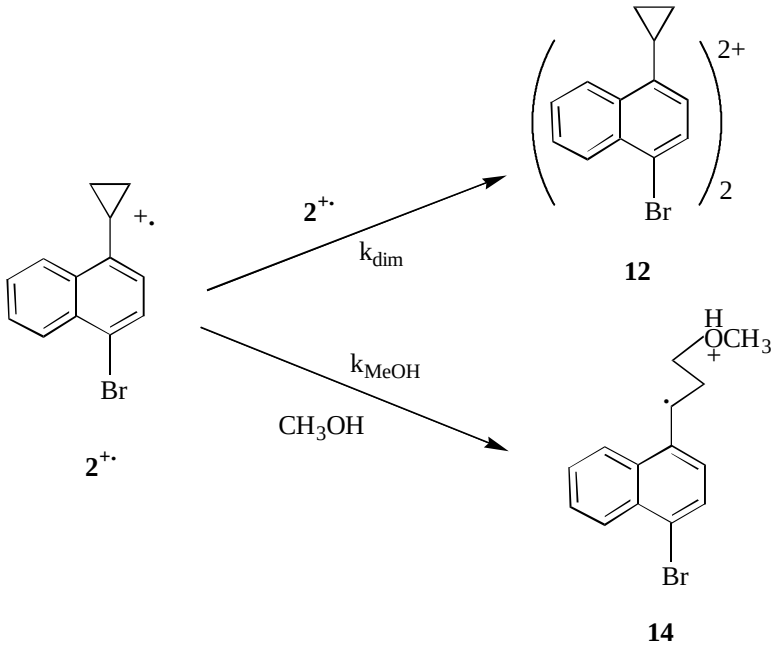

Scheme 2-10. Scheme for estimate of rate constant for CH_3OH-induced ring opening of $\mathbf{2}^{+\cdot}$

Utilizing these results, it is possible to use this dimerization process as a "clock" to estimate an upper limit for the rate constant for methanol-induced ring opening of α-cyclopropylnaphthalene radical cations (k_{MeOH}). In CH_3CN solvent, the rate law $k_{dim}[\mathbf{2}^{+\cdot}]^2$ was observed over a range of CH_3OH concentrations from 0 to 1.4 M, with $k_{dim} = 3.1 \times 10^4$ $M^{-1}s^{-1}$. The concentration of $\mathbf{2}^{+\cdot}$ never exceeds 0.01 M (the maximum concentration of substrate used in any of these experiments). Assuming that the rate of radical cation dimerization or disproportionation is at least 10 times faster than CH_3OH-induced ring opening ($k_{dim}[\mathbf{2}^{+\cdot}] \geq 10 \times k_{MeOH}[CH_3OH]$) one obtains $k_{MeOH} \leq 20$ $M^{-1}s^{-1}$.[96]

Dinnocenzo reported that the absolute rate constant for the methanol-induced ring opening of C_6H_5-*c*-$C_3H_5^{+\cdot}$ is 9.5 x 10^7 $M^{-1}s^{-1}$ in CH_3CN. Thus, the change from phenyl to 1-naphthyl results in (at least) a six order of magnitude diminution in the rate of cyclopropane ring opening.

Thermodynamic Considerations. A possible explanation for the extremely low rate of ring opening of cyclopropylnaphthalene radical cations may be related to the relative stability of naphthalene vs. benzene radical cations, i.e., because of the intrinsic stability of the naphthalenes, ring opening is thermodynamically (and thus kinetically) disfavored. Similar arguments have been advanced to explain the extremely low rate of ring opening of several cyclopropane-containing radical anions.

Using the thermodynamic cycle outlined in Scheme 2-11, it is possible to obtain an estimate of ΔG^o for CH_3OH-induced ring opening of a cyclopropylarene radical cation in CH_3CN solvent. The pertinent ΔG^o's for reactions (i) $\rightarrow$ (vi) were obtained as follows: (i) the oxidation potential of Ar-*c*-C_3H_5, (ii) the C-C bond dissociation energy of cyclopropane ($BDE_{C\text{-}C}$ = 61 kcal/mol) corrected for the radical stabilization energy (RSE) of the different aryl groups,[97] (iii) the bond dissociation energy of a 1^o R-OCH_3 bond ($BDE_{C\text{-}O}$ =82 kcal/mol),[98] (iv) the H-O bond strength of methanol ($BDE_{O\text{-}H}$ = 104 kcal/mol), (v) the standard potential of the $H^+/H^\cdot$ couple in CH_3CN (reported by Parker to be -1.88 V vs. NHE),[99] and (vi) the difference in pK_a between CH_3CN and the ether oxygen ($pK_a(CH_3CN)$ = -10.12;[100] $pK_a(CH_3CH_2OCH_2CH_3)$ = -3.59).[101]

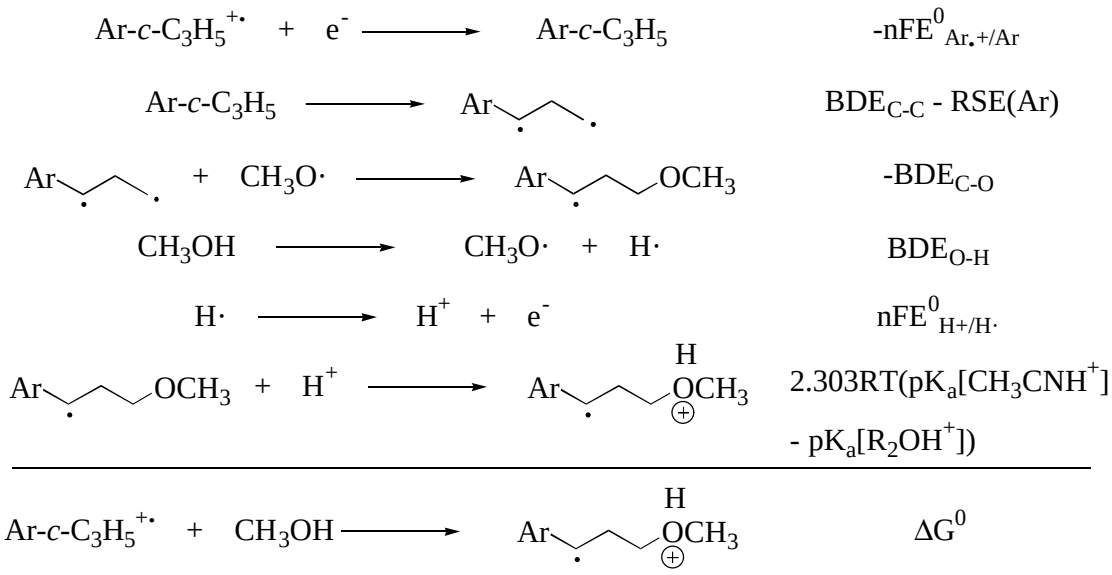

Scheme 2-11. Thermodynamic cycle for calculation of ΔG^o

The oxidation potentials (E^0) of cyclopropylarenes were estimated from ionization potentials of these compounds. Because the cyclic voltammograms for cyclopropybenzene, 1-cyclopropylnaphthalene, and 2-cyclopropylnaphthlene are all irreversible, it is not possible to measure the oxidation potentials of these substrates directly. Using SCF-MO (AM1), ionization potentials (IP's) were calculated for a series of aromatic hydrocarbons. IP's calculated via AM1 correlate well to IP's obtained experimentally via photoelectron spectroscopy[102] (Figure 2-48, $R^2 = 0.995$).

Figure 2-48. Comparison of IP's obtained via AM1 vs. those via experiment

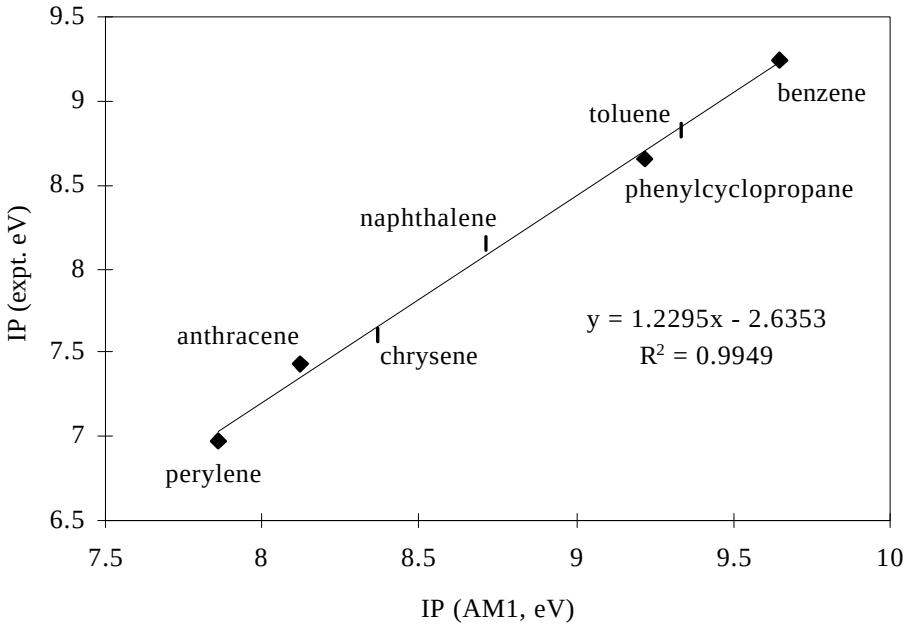

As shown in Table 2-7 and Figure 2-49, a good linear relationship also exists between the IP's obtained from AM1 and the oxidation potential of the arene (E^o),[16] E^o(V vs. NHE) = 0.9121 × IP - 5.8225. On the basis of this relationship, E^o for cyclopropylbenzene, 1-, and 2-cyclopropylnaphthalene were estimated to be 2.58, 1.99, and 2.02 V (vs. NHE in CH_3CN), respectively. These estimated E^o's appear to be quite accurate. For example, the cyclic voltammogram of 9-bromo-10-cyclopropylanthracene is reversible at high sweeprates, with E^o = 0.920 V (vs. 0.1 M Ag^+/Ag),[103] 1.498 V (vs. NHE). Using the AM1-calculated IP (8.14 eV), E^o(estimated) is 1.599V (vs. NHE).

Table 2-7. Oxidation potentials and AM1-calculated ionization potentials for several aromatic hydrocarbons

compound	IP (AM1, eV)	E^o (V vs. NHE) in CH_3CN
benzene	9.65	3.03
naphthalene	8.71	2.08
anthracene	8.12	1.61
toluene	9.33	2.61
perylene	7.86	1.3
chrysene	8.37	1.88

Figure 2-49. E^o as a function of AM1-calculated IP's

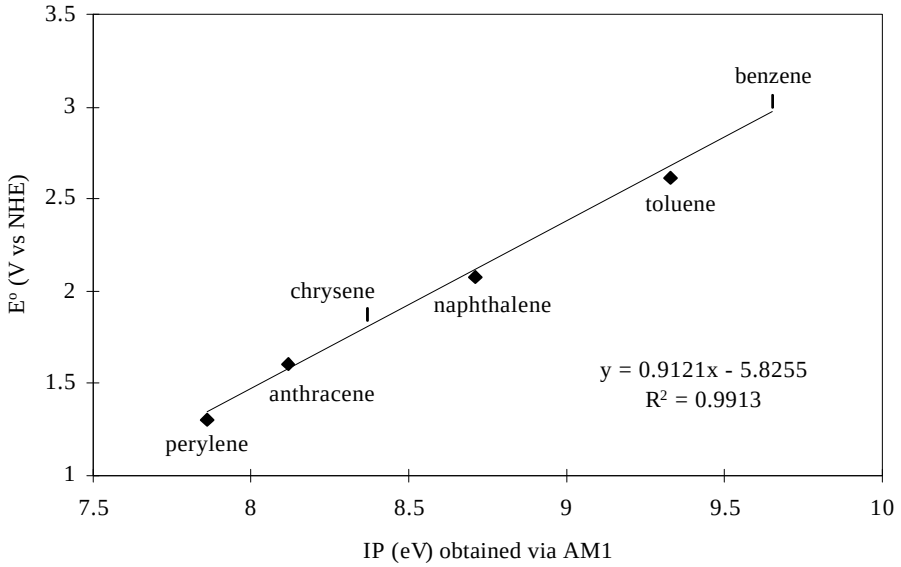

The results of this analysis are summarized in Table 2-8. The surprising fact that emerges is that regardless of the identity of aryl group, all these ring openings are substantially exothermic.

Table 2-8. ΔG^0 for the methanol-induced ring opening of cyclopropylarene radical cations in CH_3CN

Aryl group	$E^0_{Ar+./Ar}$ (V vs. NHE)	RSE (kcal/mol)	ΔG^0 (kcal/mol)[a]
phenyl	2.58	10.2	-39.1
1-naphthyl	1.99	13.1	-28.4
2-naphthyl	2.02	12.5	-28.5

[a] $\Delta G^0 = 30.7\text{-}23.1\ E^0_{Ar+./Ar}$ - RSE(Ar) in kcal/mol.

Stereoelectronic Considerations. Two conformational extremes are important for cyclopropane rings attached to a π-system, bisected ($\theta = 0^o$) and perpendicular ($\theta = 90^o$), where θ is the angle defined by the cyclopropyl methine C-H bond with respect to the atoms of the adjacent π-system. In general, the bisected conformation is preferred because overlap between the cyclopropyl HOMO and LUMO of the π-system is maximal in this conformation.[104]

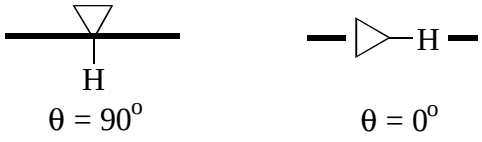

$\theta = 90^o$ $\theta = 0^o$

perpendicular bisected

The conformational preference(s) of 1-cyclopropylnaphthalene radical cation was explored using SCF-MO theory (AM1, C.I.=1). Earlier studies have found that the neutral molecule adopts a conformation midway between bisected and perpendicular ($\theta = 54^o$) because the normally preferred bisected is destabilized by steric interactions between the cyclopropyl group and the *peri*-hydrogens.[105] In contrast 1-cyclopropylnaphthalene radical cation exhibits no overwhelming conformational preference, presumably because removal of an electron increases the magnitude of the interaction between the cyclopropyl HOMO and the π-system. Structures with $\theta = 0^o$ and 54^o are degenerate (within 0.1 kcal/mol) and separated by a barrier of approximately 0.5 kcal/mol. For 2-cyclopropylnaphthalene radical cation, AM1 calculations predict the bisected conformation to be favored by 1.4 kcal/mol.

Thus for 1- or 2-cyclopropylnaphthalene radical cations, the bisected conformation is readily accessible, suggesting that stereolectronic factors are not responsible for the extraordinarily sluggish rate of ring opening.

Ring opening of cyclopropylarene radical cations. Dinnocenzo, et al. reported the effect of alkyl substituents on the rate and regiochemistry of the methanol-induced (S_N2) ring opening of cyclopropylbenzene radical cations. Generally, alkyl substituents on

the cyclopropane ring increase the rate of ring opening, with nucleophilic attack occurring at the most hindered position (C-2, Scheme 2-12).[106] These observations were explained on the basis that the alkyl group could stabilize the partial positive charge on the carbon undergoing substitution. It was further argued on the basis of the Hammond's postulate that these reactions have an early (reactant-like) transition state and that the charge distribution in the transition state was similar to the radical cations themselves.

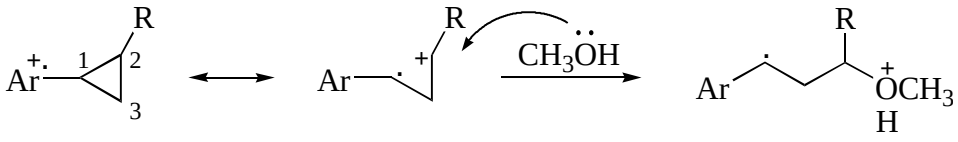

Scheme 2-12. Methanol-induced ring opening of cyclopropylarene radical cation

An early (reactant-like) transition state would imply that the rate of the reaction would be only modestly affected by changes in ΔG^o for the reaction (i.e., $\partial\Delta G^{\neq}/\partial\Delta G^o < 0.5$). Our results show that for decay of Ar-*c*-$C_3H_5^{+\cdot}$, the change from Ar = phenyl to Ar = 1-naphthyl results in at least a six order of magnitude decrease in rate, corresponding roughly to a difference in free energies of activation ($\Delta\Delta G^{\neq}$) for these two processes of at least 8.2 kcal/mol. The difference in ΔG^o for these two processes ($\Delta\Delta G^o$) is 10.7 kcal/mol. Thus $\Delta\Delta G^{\neq}/\Delta\Delta G^o \geq 0.77$, suggestive of a transition state which is more product- than reactant-like.

As the data in Table 2-8 reveals, two important factors contribute to ΔG^{o} for these ring opening reactions: The ability of the aryl group to stabilize the ring-closed radical cation (manifested by the difference in redox potentials, $\Delta E^{o}_{Ar+\cdot/Ar}$) and the ability of the aryl group to stabilize the benzylic radical formed after ring opening (ΔRSE). Of these two, the effect of the aryl group on radical cation stability is far more profound.

These observations are consistent with a transition state for ring opening in which spin density is delocalized over C-1 (the benzylic carbon) and the aromatic ring but charge is highly localized at C-2 and oxygen (e.g., **15**). As such, in the transition state, the aryl group can stabilize the radical portion of the developing distonic radical ion (presumably to a lesser degree than for the fully developed radical), but will have little effect on the positive charge (Figure 2-50). (This proposal is consistent with recent transition state calculations for ring opening of C_6H_5-*c*-$C_3H_5^{\bullet+}$ by CH_3OH which reveal that in the progression from reactant to transition state, there is an increase in positive charge at C-2 (from 0.19 to 0.40) at the expense of the phenyl group (0.68 to 0.28).

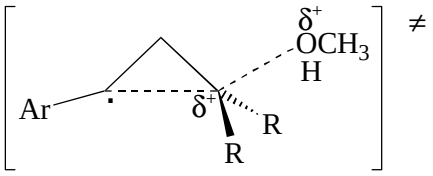

15

Figure 2-50. The proposed effect of aryl rings on the stabilities of reactants, transition states and products for CH_3OH-assisted cyclopropane ring opening

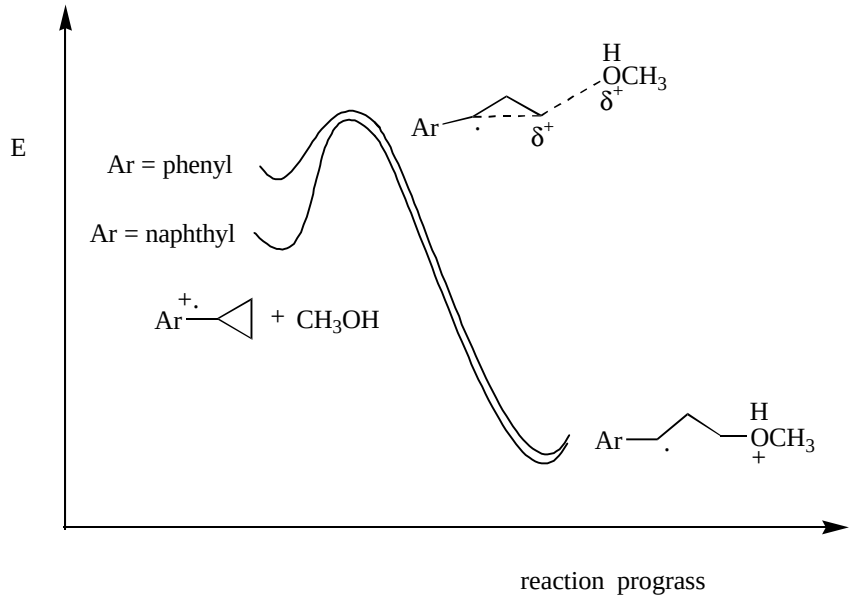

Thus nucleophile-induced ring opening of cyclopropylarene radical cations provide an intriguing exception to the Hammond's postulate in that they are overwhelmingly exothermic, yet in terms of the distribution of charge and spin, have transition states which are more product- than reactant-like. Moreover, the effect of the aromatic ring on the rate is primarily due to changes in the free energy of the reactant, with only a modest effect on the free energy of the transition state for ring opening.

Implications for the use of cyclopropane-substituted compounds as SET probes. Cyclopropane-containing substrates are frequently employed as probes for single electron transfer. The implicit assumption in such a study is that if a paramagnetic

intermediate (neutral free radical or radical ion) is produced, it will undergo ring opening. Earlier work dealing with neutral free radicals and ketyl radical anions has shown that the rate constant for ring opening is quite large when the ring-opening is thermodynamically favored. For example, ΔG^{o} for the cyclopropylcarbinyl → homoallyl radical rearrangement (Scheme 1-13) is -3.1 kcal/mol, and the rate constant is 1.2×10^{8} s^{-1}.[107] Similarly, ring opening of radical anion **16** (Scheme 2-12) is estimated to be exothermic by about 2 kcal/mol (R = phenyl or vinyl), and the rate constant is $>10^{5}$ s^{-1}.[108]

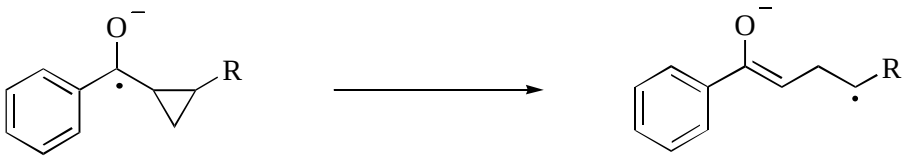

16 **17**

Scheme 2-13 Ring opening of cyclopropylphenylketyl radical anion

In the case of Ar-*c*-$C_3H_5^{+\bullet}$, despite the fact that ring opening enjoys an enormous thermodynamic driving force, the process occurs at a dramatically slower rate. Clearly, the intrinsic barrier to ring opening is greater for ring opening of these radical cations. The unique activation/driving force relationship for radical cation ring opening is likely attributable to the fact that the process is bimolecular (nucleophile-assisted). The rate of ring opening is governed by the amount of positive charge transmitted to the cyclopropane ring via resonance (Figure 2-53), and the fact that this charge becomes localized in the transition state (e.g., **15**).

For neutral radicals or ketyl anions, it is spin rather than charge which is transmitted to the cyclopropyl group upon ring opening. Because ring opening is unimolecular, spin (and charge for the radical anions) is not localized in the transition state and the intrinsic barrier to ring opening is considerably lower.

For cyclopropylarene radical cations, and presumably other systems which would undergo nucleophile-assisted ring opening, the fact that the ring opening reaction may enjoy a potent thermodynamic driving force is no guarantee that the ring opening will occur at an appreciable rate. Indeed, it is likely that many of the substrates discussed herein would fail to detect a bona fide SET process. Thus, these results reveal a new (and unexpected) complication in the design and utilization of SET probes.

2.3 SUMMARY

Radical cations generated from 1-cyclopropylnaphthalene (**1**), 1-bromo-4-cyclopropylnaphthalene (**2**), and 2-cyclopropylnaphthalene (**3**) were studied electrochemically. Oxidation of all these substrates in CH_3CN in the presence of CH_3OH leads to cyclopropane ring-opened products, i.e., the corresponding 1,3-dimethoxypropylnaphthalenes. However, the rate constant for methanol induced ring opening ($Ar\text{-}c\text{-}C_3H_5^{+\cdot} + CH_3OH \rightarrow ArCH(\bullet)CH_2CH_2O(H^+)CH_3$) is extremely small (<20 $M^{-1}s^{-1}$ for the 1-cyclopropylnaphthalenes) despite the fact that ring opening is exothermic by nearly 30 kcal/mol. These results are explained on the basis of a product-like transition

state for ring opening wherein the positive charge is localized on the cyclopropyl group, and thus unable to benefit from potential stabilization offered by the aromatic ring.

CHAPTER 3. CERIUM (IV) OXIDATION OF CYCLOPROPYLBENZENES AND CYCLOPROPYLNAPHTHALENES

3.1 INTRODUCTION

The kinetics and mechanism of the ring opening of cyclopropylarene radical cations in the presence of nucleophiles have been the subject of numerous investigations. As introduced in Chapter 1, anodic, photochemical and Ce(IV) oxidation of cyclopropylbenzenes all led to cyclopropane ring-opened products. Dinnocenzo, et al. have shown that ring opening of cyclopropylbenzene radical cation occurs via a nucleophile-assisted (i.e., S_N2) pathway, which has been well characterized in terms of its stereochemistry, kinetics, regiochemistry and kinetic isotope effects.

In Chapter 2, we have examined the follow-up chemistry of radical cations generated from cyclopropylnaphthalenes electrochemically. Although anodic oxidation of all these substrates in the presence of CH_3OH led to cyclopropropane ring opened products, the rate constant for methanol induced ring opening (if it happens) is extremely small ($< 20\ M^{-1}s^{-1}$) despite the fact that ring opening is exothermic by nearly 30 kcal/mol.

Due to the nature of the electrochemical experiment, radical cations are generated heterogeneously and in high concentration near the electrode. The dimerization or coupling of radical cations are often seen as one of the reaction pathways. The products isolated from our electrolyses of cyclopropylnaphthalenes are mainly cyclopropane ring opened monomer and dimer products, and the radical cations of cyclopropylnaphthalenes

were found to dimerize or disproportionation before cyclopropane ring opening based on the rate laws from the voltammetric analyses.

In order to confirm the product nature, we performed the homogeneous Ce(IV) oxidation of cyclopropylarenes in CH_3CN/CH_3OH. The cyclopropane-containing substrates chosen for Ce(IV) oxidation are 1-cyclopropylbenzene (**1**), 1-cyclopropyl-4-methylbenzene (**2**), 1-cyclopropylnaphthalene (**3**), 1-bromo-4-cyclopropylnaphthalene (**4**), 2-cyclopropylnaphthalene (**5**). In addition, 1-methylbenzene (toluene) and 1-methylnaphthalene were employed for comparison.

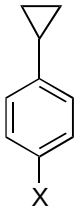

X = H, **1**
X = CH_3, **2**

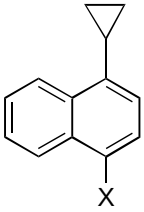

X = H, **3**
X = Br, **4**

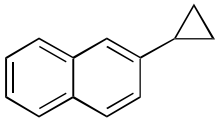

5

3.2 RESULTS AND DISCUSSION

3.2.1 Synthesis of Cyclopropylarenes

1-Cyclopropyl-4-methylbenzene (2).[109] Starting with 1-methyl-4-vinylbenzene, **2** was prepared in one step, as shown in Scheme 3-1. The cyclopropyl group was constructed from the vinyl group in the starting compound by reacting with methylene iodide and zinc-copper couple, based on Smith-Simmons's methods.

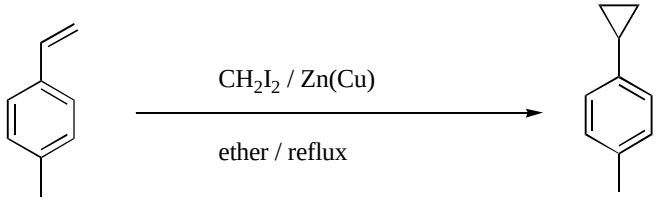

2

Scheme 3-1. Synthesis of 1-cyclopropyl-4-methylbenzene (**2**)

1-Cyclopropylnaphthalene (3), 1-Bromo-4-cyclopropylnaphthalene (4) and 2-Cyclopropylnaphthalene (5). The construction of cyclopropane ring in 2-position of naphthalene is the same as that in 1-position of naphthalene. Consequently, the methods for synthesis of **3** can be followed for synthesis of **5** by using 2-bromonaphthalene instead of 1-bromonaphthalene as starting material. **4** can be prepared by the bromination of **3**. Synthesis of **3** and **4** were shown in Scheme 3-2.

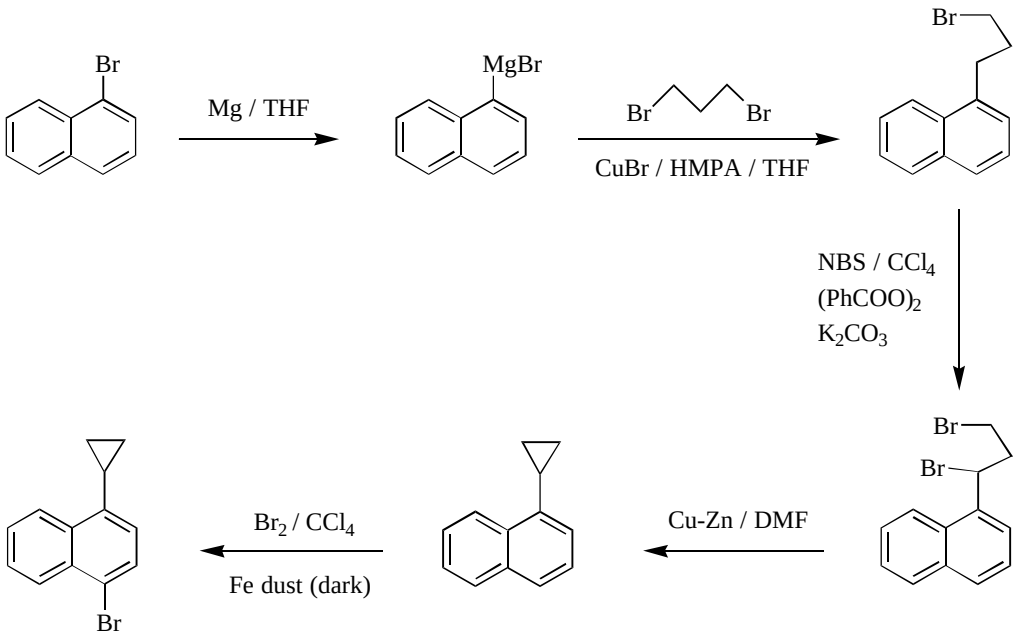

Scheme 3-2. Synthesis of 1-cyclopropylnaphthalene (**3**) and 1-bromo-4-cyclopropylnaphthalene (**4**)

3.2.2 Ce(IV) Oxidation of Cyclopropylbenzenes

1-Cyclopropylbenzene (1). Ce(IV) oxidation of **1** in CH_3CN mainly produces cyclopropane ring-opened product 1-phenylpropyl-1,3-dinitrate (**6**, 60.7%), while aromatic nitration products, 1-cyclopropy-2-nitrobenzene (**7**, 20%) and 1-cyclopropyl-4-nitrobenzene (**8**, 7.5%), are also obtained under the condition employed. The ratio of aromatic nitration products are nearly 3:1 (Scheme 3-3).

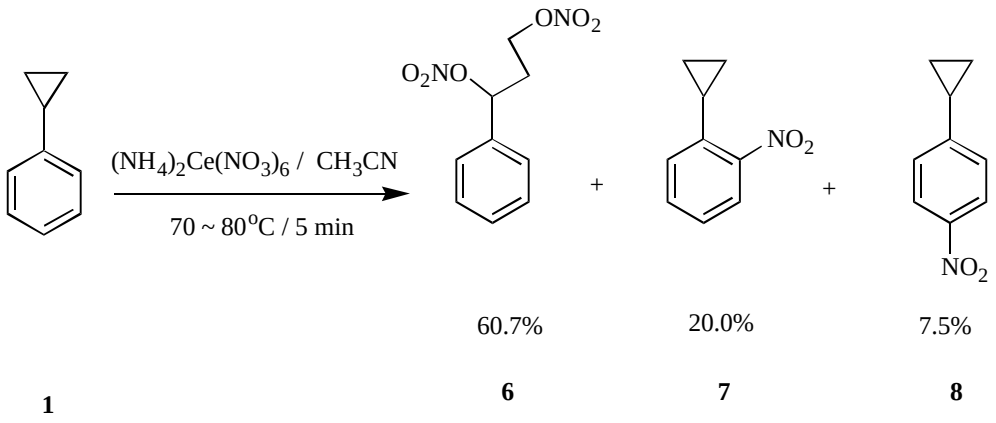

Scheme 3-3. Ce(IV) oxidation of 1-cyclopropylbenzene (**1**) in CH_3CN

1-Cyclopropyl-4-methylbenzene (2). Under the exact same condition, Ce(IV) oxidation of **2** also yields cyclopropane ring-opened product 1-(4-methylphenyl)propyl-1,3-dinitrate (**9**, 67.4%) as major product and aromatic nitration product 1-cyclopropyl-4-methyl-2-nitrobenzene (**10**, 12.8%) as minor product (Scheme 3-4).

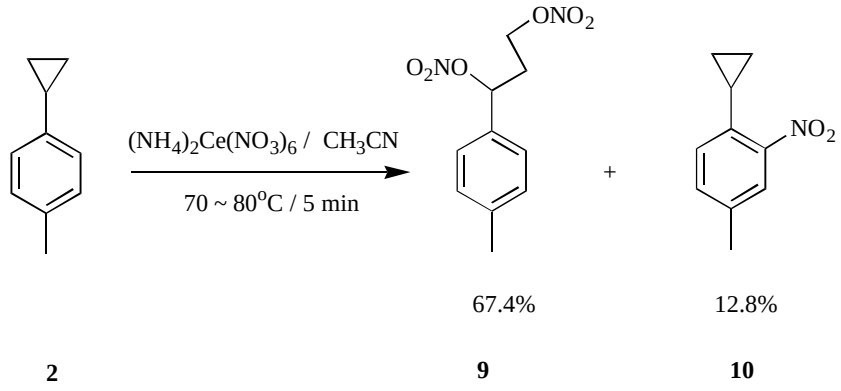

Scheme 3-4. Ce(IV) oxidation of 1-cyclopropyl-4-methylbenzene (**2**) in CH_3CN

Toluene. For toluene, Ce(IV) oxidation under same condition is so slow that 87% starting material is recovered after same period of time of reaction. Only about 1% of side-chain deprotonation product, nitrate **11**, is detected by ^{1}HNMR (Scheme 3-5).

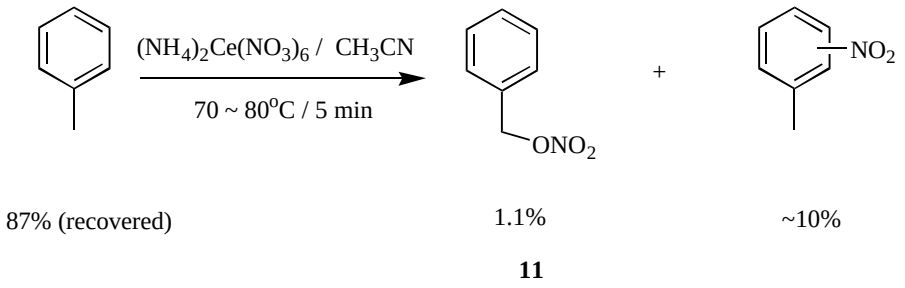

Scheme 3-5. Ce(IV) oxidation of toluene in CH_3CN

3.2.3 Ce(IV) Oxidation of Cyclopropylnaphthalenes

1-Cyclopropylnaphthalene (3). Ce(IV) oxidation of **3** in CH_3CN/CH_3OH mainly yielded cyclopropane ring-opened 1,3-disubstituted products: 20.4% of 1-(1,3-dimethoxypropyl)naphthalene **12**, 35% of 3-methoxy-3-naphthylpropylnitrate **13**, and 9.1% of 1-naphthylpropyl-1,3-dinitrate **14**. In the absence of methanol, Ce(IV) oxidation of **3** in CH_3CN gave 47.1% of **14** as major product. It was noted that 3-hydroxy-3-naphthylpropylnitrate **15** was formed from **14** during PTLC separation. The reaction is shown in the Scheme 3-6.

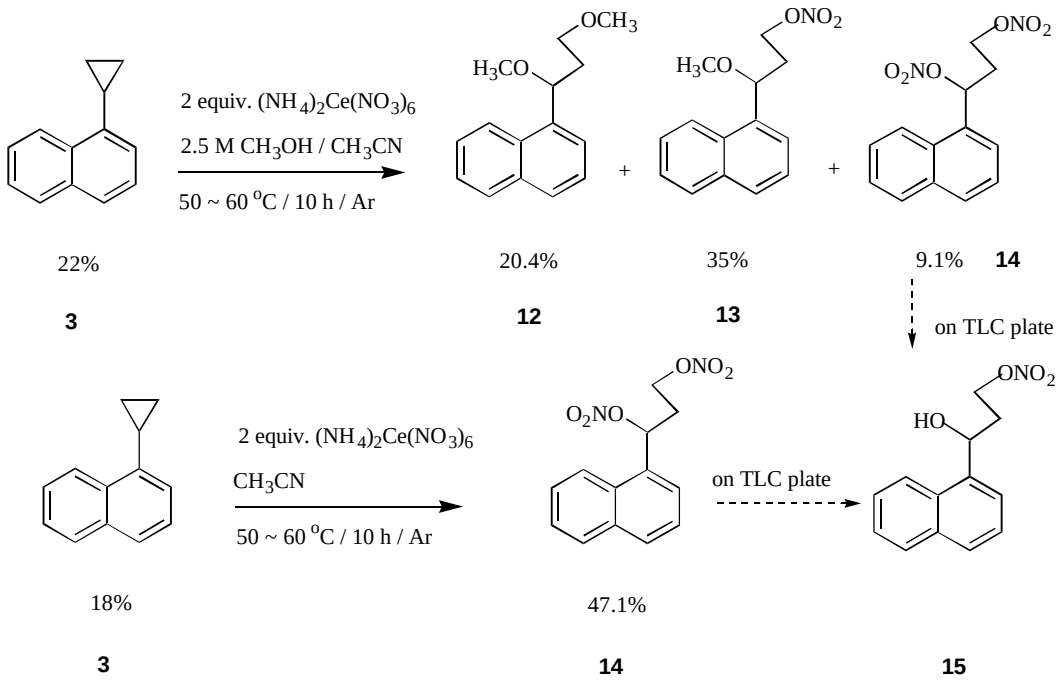

Scheme 3-6. Ce(IV) oxidation of 1-cyclopropylnaphthalene (**3**) in CH_3CN/CH_3OH

1-Br-4-cyclopropylnaphthalene (4). Like **3**, Ce(IV) oxidation of **4** in CH_3CN/CH_3OH yielded mainly cyclopropane ring-opened products, **16**, **17** and **18**, as shown in Scheme 3-7.

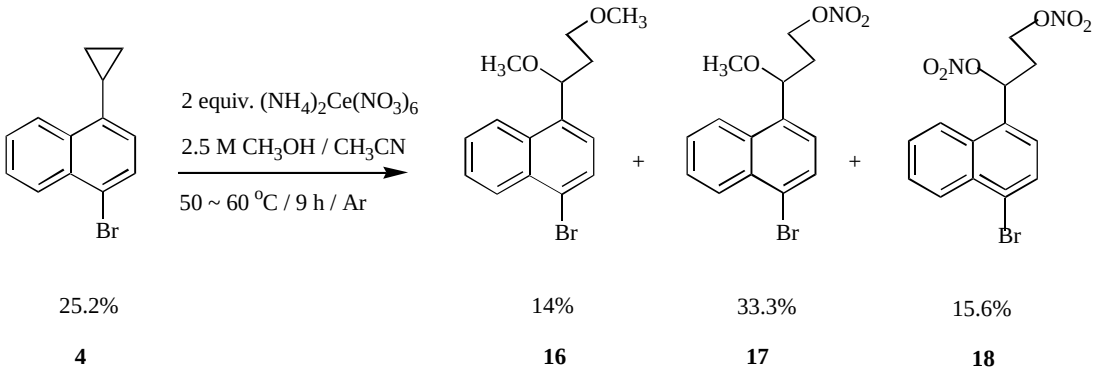

Scheme 3-7. Ce(IV) oxidation of 1-bromo-4-cyclopropylnaphthalene (**4**) in CH_3CN/CH_3OH

2-Cyclopropylnaphthalene (5). Ce(IV) oxidation of **5** in CH_3CN/CH_3OH yielded similar cyclopropyl ring opened products, **19**, **20** and **21**, as shown in Scheme 3-8. Alcohol **22** was also noted during PTLC separation.

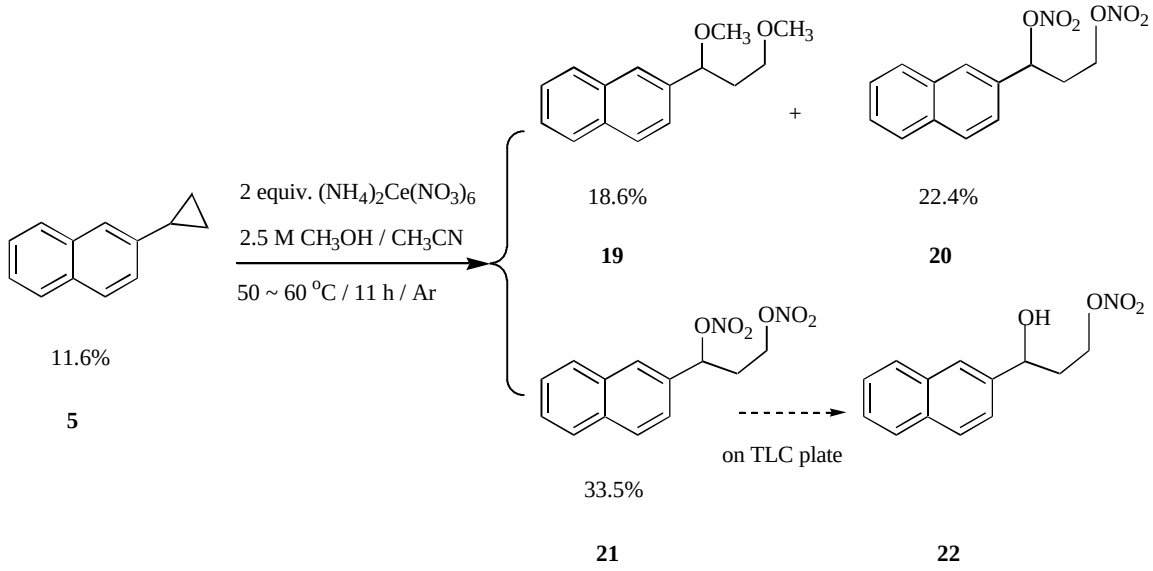

Scheme 3-8. Ce(IV) oxidation of 1-cyclopropylnaphthalene (**3**) in CH_3CN/CH_3OH

1-Methylnaphthalene. Ce(IV) oxidation of 1-methylnaphthalene in CH_3CN/CH_3OH gave mainly side-chain deprotonation products, **23**, **24** and **25**, as shown in Scheme 3-9. Without methanol, nitrate **23** was the only major product.

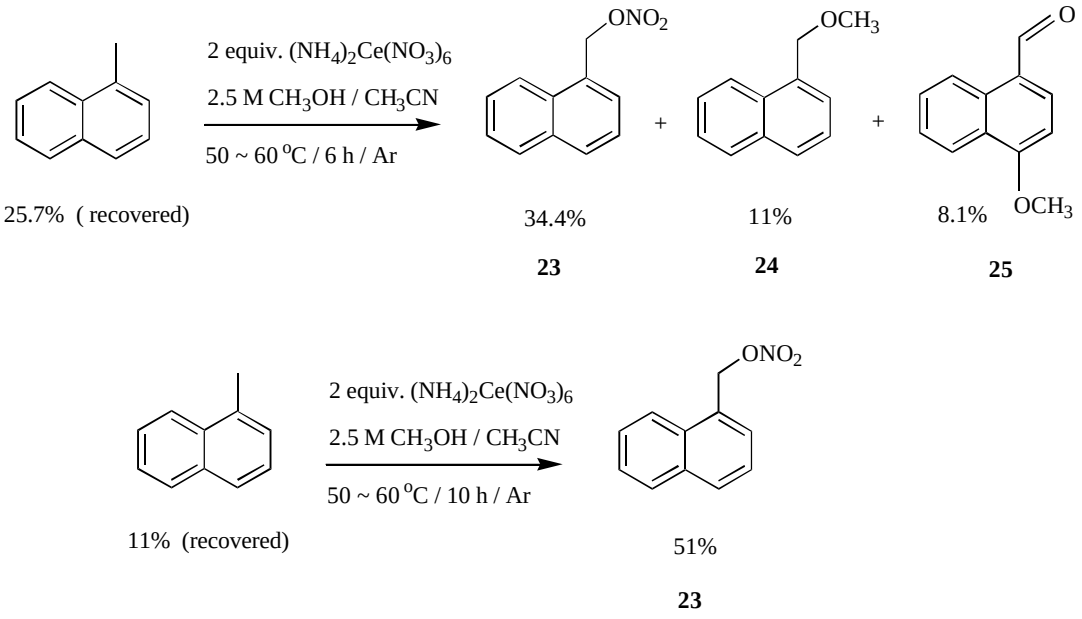

Scheme 3-9. Ce(IV) oxidation of 1-methylnaphthalene in CH_3CN/CH_3OH

3.2.4 Cyclopropane Ring Opening Mechanism

Cyclopropylbenzenes. Like **1**, Ce(IV) oxidation of **2** in CH_3CN yields mainly cyclopropane ring-opened product and no side-chain deprotonation product is detected. The results suggest that cyclopropane ring opening of $\mathbf{2}^{+\cdot}$ is much faster then deprotonation of this radical cation. Obviously, cyclopropane ring strain is the driving

force for the ring opening of cyclopropylbenzene radical cations. The mechanism of oxidation is proposed as in Scheme 3-10.

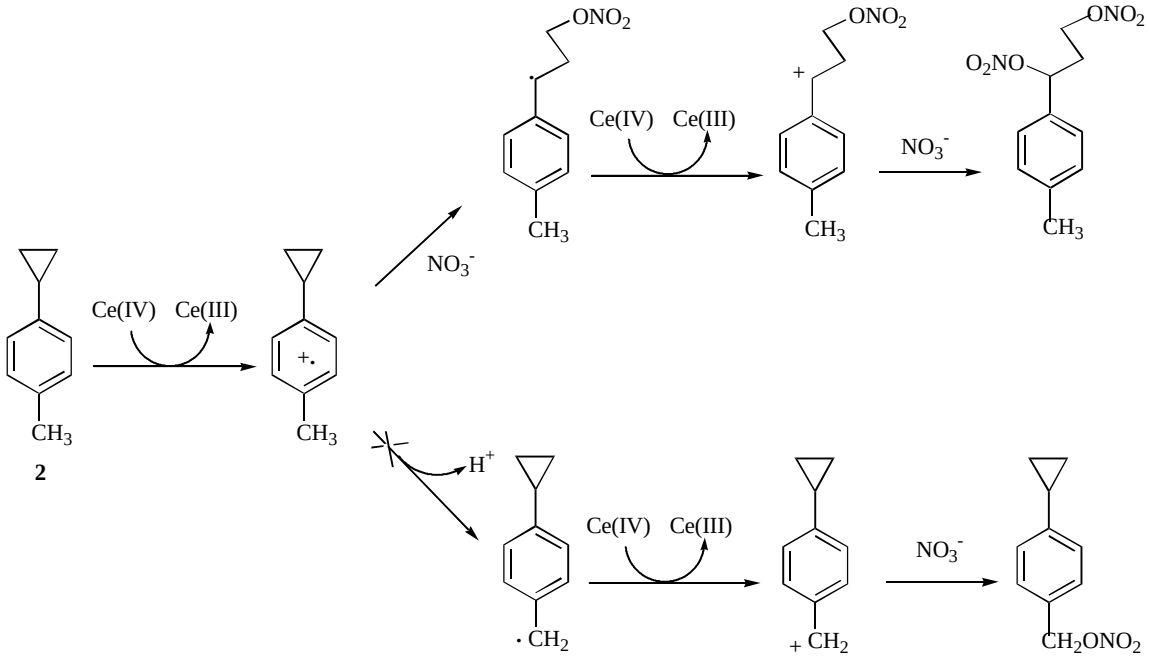

Scheme 3-10. Ce(IV) oxidation mechanism of 1-methyl-4-cyclopropylnaphthalene (**2**)

Cyclopropylnaphthalenes. The mechanism of Ce(IV) oxidation of cyclopropylnaphthalenes is assumed to be similar to that of cyclopropylbenzenes. The radical cation $\mathbf{3}^{+\cdot}$ undergoes nucleophile (e.g., ONO_3^-) assisted ring opening to form benzylic-type radical, which further is oxidized to the corresponding cation and then captured by another molecular of nucleophile to give the final product (Scheme 3-11).

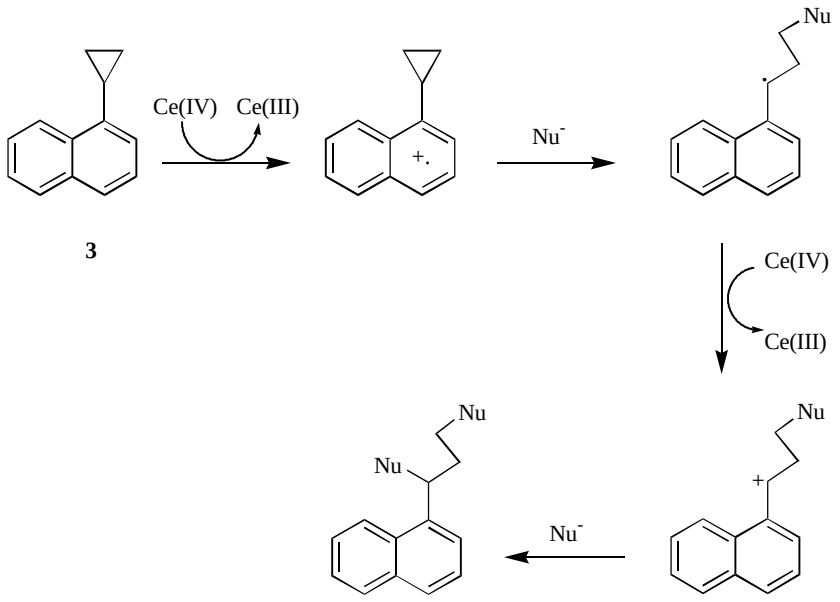

Scheme 3-11. Ce(IV) oxidation mechanism of 1-cyclopropylnaphthalene (**3**)

The alternative mechanisms follow ones proposed for anodic oxidation of cyclopropylnaphthalenes. Dimerization mechanism: Radical cation $\mathbf{3}^{+\cdot}$ dimerizes to form dimer dication, which experiences nucleophile attack to form benzylic-type cation and release neutral **3**. The cation is captured by nuclophile to give 1,3-disubstituted product. Disproportionation mechanism: Two radical cations of **3** disproportionate to a neutral **3** and dication $\mathbf{3}^{++}$, which is attacked by methanol to lead the same product. Scheme 3-12 shows the proposed mechanism for decay of $\mathbf{3}^{+\cdot}$, based on dimerization and disproportionation pathways.

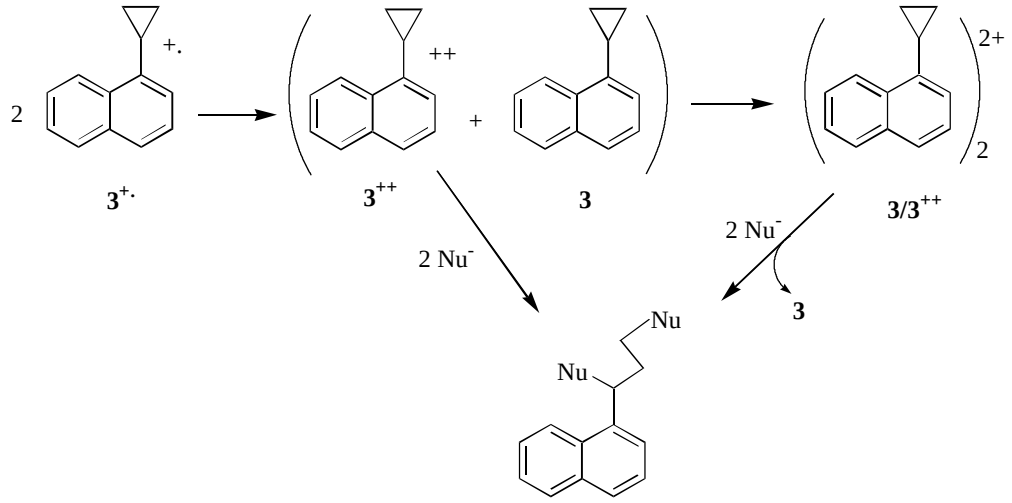

Scheme 3-12. The alternative mechanisms for oxidation of 1-cyclopropylnaphthalene (**3**)

In Chapter 2, we found that although the cyclopropyl group in neutral molecule of 1-cyclopropylnaphthalene adopts a conformation midway between bisected and perpendicular ($\theta = 54^{o}$), the radical cation of this molecule exhibits no overwhelming conformational preference and structures with $\theta = 0^{o}$ and 54^{o} are degenerate (within 0.1 kcal/mol) and separated by a barrier of approximately 0.5 kcal/mol. Thus for 1-cyclopropylnaphthalene radical cations, the bisected conformation is readily accessible, suggesting that stereoelectronic factors are not important in the reactivity of cyclopropylnaphthalene radical cations.

3.3 SUMMARY

Ce(IV) oxidation of cyclopropylbenzenes and cyclopropylnaphthalenes in the presence of nucleophiles all led to cyclopropane ring opened 1, 3-disubstitued products. For *p*-methylcyclopropylbenzene, the radical cations undergo cyclopropane ring opening rather then deprotonation. Since the bisected conformation is readily accessible for both cyclopropylbenzene and cyclopropylnaphthalene radical cations, stereolectronic factors are not important in reactivity of these radical cations.

CHAPTER 4. ANODIC OXIDATION OF CYCLOPROPYLANTHRACENES

4.1 INTRODUCTION

Since radical cations were first proven to be the primary intermediates of the anodic oxidation of anthracene and related compounds by three independent research groups in 1967,[110,111,112] the follow-up reactions of radical cations of anthracene and derivatives have been the subject of numerous investigations, most of which are attributed to Parker and co workers.[113] Radical cations in general are highly reactive species. However, the ease with which radical cations undergo reactions with nucleophiles or form dimeric products can be moderated by suitable structural modification as well as reaction medium conditions. The reaction pathways of radical cations with various nucleophiles have extensively been studied by means of electrochemical techniques.[114] Detailed studies of reactions of anthracene and substituted anthracene radical cations included hydroxylation,[115] acetoxylation,[116] methoxylation[117] and pyridination.[118,119]

As shown in Chapters 2 and 3, anodic and Ce(IV) oxidation of cyclopropylbenzenes and cyclopropylnaphthalenes all led to cyclopropane ring-opened products. However, while free radical bromination of cyclopropylbenzenes and cyclopropylnaphthalenes also gave cyclopropane ring-opened products, the free radical bromination of 9-cyclopropylanthracene and derivatives yielded exclusively hydrogen abstraction products. This variation in the chemoselectivity of bromination of cyclopropylarenes was explained as the result of stereoelectronic factors (Scheme 1-17).

The transition state for the reaction of a cyclopropylarene with a neutral free radical is isoelectronic to that of the reaction of its radical cation with a nucleophile (Ar-*c*-$C_3H_5^{+\cdot}/X^-$ *vs.* Ar-*c*-$C_3H_5/X^{\cdot}$). Consequently, it is reasonable to suspect that the same stereoelectronic factors may pertain to radical cation chemistry. In this chapter, the chemistry of radical cations generated from 9-cyclopropylanthracene (**1**) and 9-bromo-10-cyclopropylanthracene (**2**) is examined electrochemically.

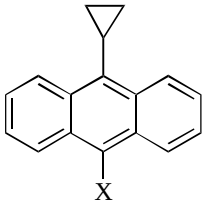

X = H, **1**
X = Br, **2**

4.2 RESULTS AND DISCUSSION

4.2.1 Kinetic Analysis from Voltammetry

The mechanism and kinetics of decay of radical cations generated from **1** and **2** were studied electrochemically. All voltammetric measurements were performed in anhydrous CH_3CN/CH_3OH with 0.5 M $LiClO_4$ as supporting electrolyte. A Pt microdisk electrode served as working electrode, and the reference electrode was 0.1 M Ag^+/Ag (0.337 V *vs.* SCE). An ultrasonic system was employed to clean electrode surface between voltammetric runs.

9-Cyclopropylanthracene (1). The cyclic voltammogram of **1** (Figure 4-1) is characterized by an initial oxidation wave ($E_P \approx +780$ mV at 500 mV/sec) and several additional oxidation waves at more positive potentials. In the presence of CH_3OH the peaks at more positive potentials are changed but the initial oxidation wave is unaffected (i.e., the peak potential and current remain the same, Figure 4-1).

Figure 4-1. Cyclic voltammogram of 9-cyclopropylanthracene (**1)** in CH_3CN (0.5 M $LiClO_4$, 5×10^{-3} M **1**, v = 500 mV/s)

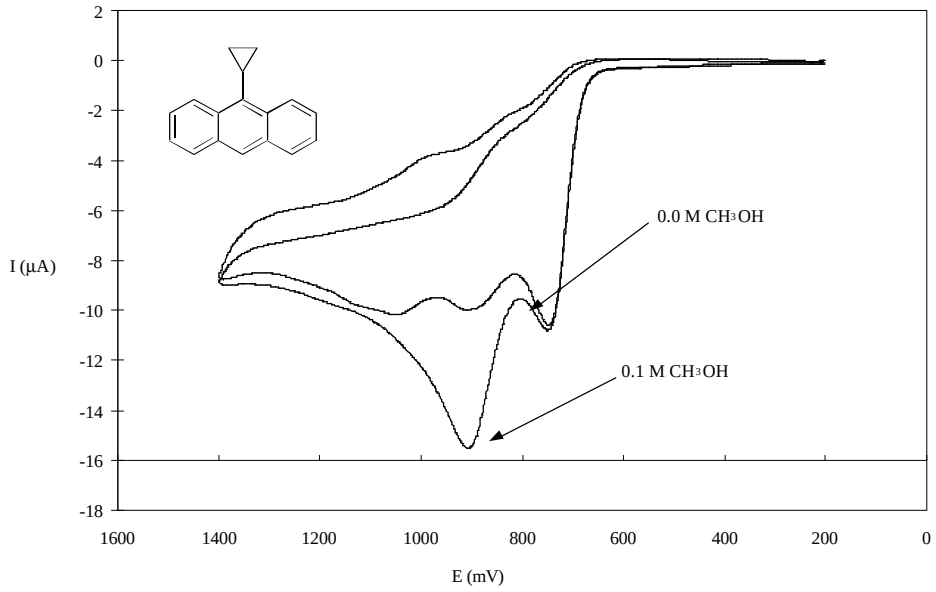

The initial oxidation wave is irreversible at all accessible sweeprates (up to 50 V/sec for our system). Consequently, LSV was an appropriate technique for studying this system. E_P was found to vary both as a function of sweeprate and substrate concentration, but was independent of the concentration of methanol. Figures 4-2 through 4-4 show typical LSV analyses for **1**, and the results of these experiments are summarized in Table 4-1. These observations are in excellent agreement with a second-order mechanism for radical cation decay (Eq. 4-1).

$$-d[\mathbf{1}^{+\cdot}]/dt = k\,[\mathbf{1}^{+\cdot}]^2 \qquad (4\text{-}1)$$

Figure 4-2. LSV analysis of **1**, $\partial E_P/\partial \log(v)$. (0.5 M $LiClO_4$, 2.5 M CH_3OH, 10×10^{-3} M **1**, v = 100→8000 mV/sec)

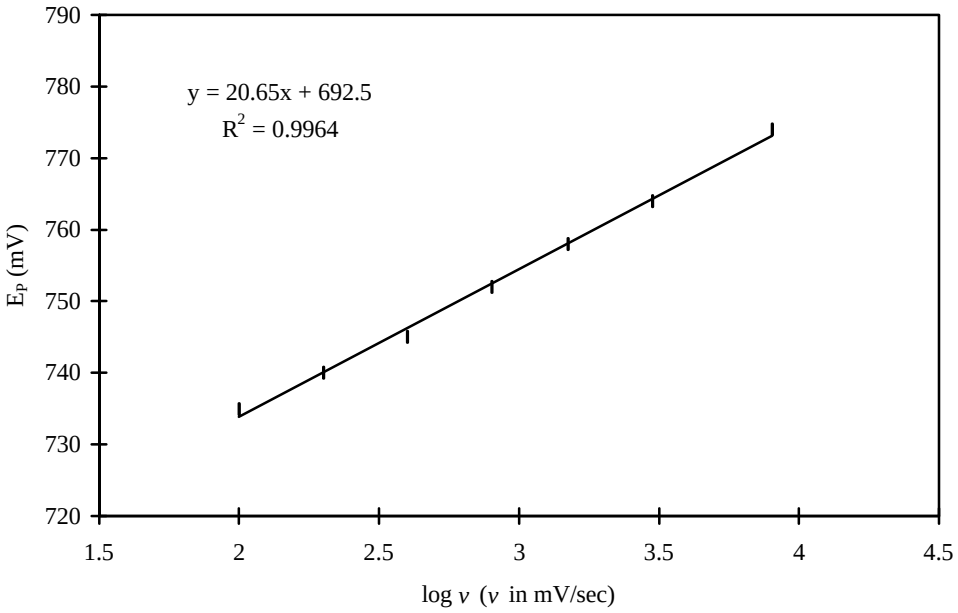

Figure 4-3. LSV analysis of **1**, $\partial E_P/\partial \log[CH_3OH]$. (0.5 M $LiClO_4$, 0.025→2.5 M CH_3OH, 10×10^{-3} M **1**, ν = 400mV/sec)

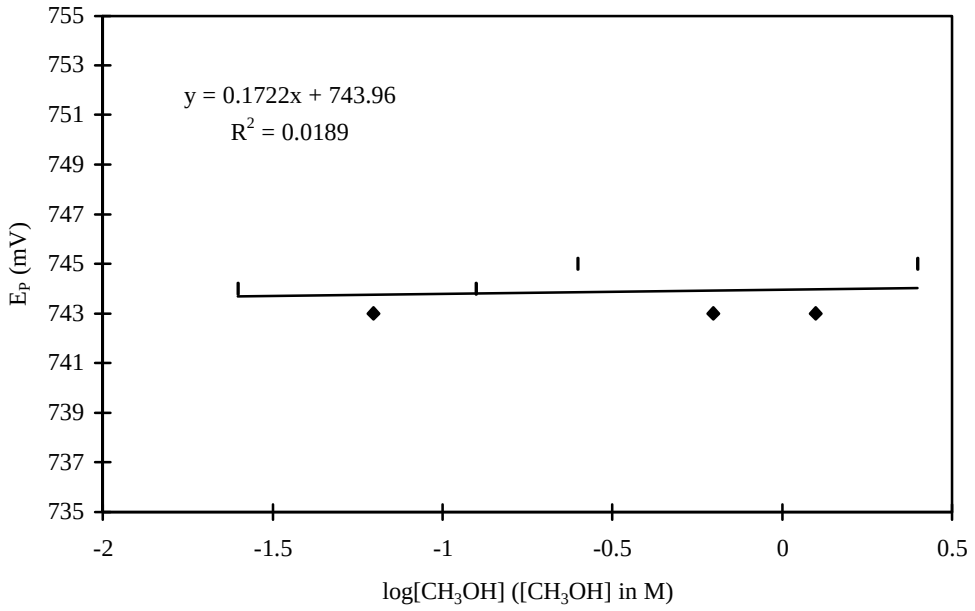

Figure 4-4. LSV analysis of **1**, $\partial E_P/\partial \log[\mathbf{1}]$. (0.5 M $LiClO_4$, 2.5 M CH_3OH, $1.79 \rightarrow 20.8 \times 10^{-3}$ M **1**, ν = 100mV/sec)

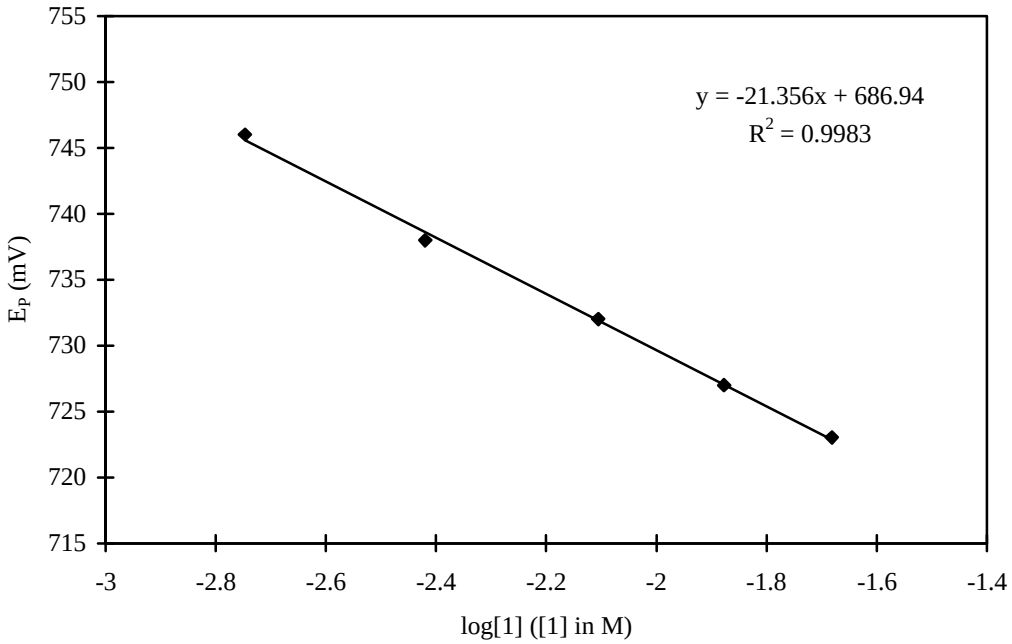

Table 4-1. LSV analysis of the electrochemical oxidation of **1**

Rate law	$\partial E_P/\partial \log(v)$	$\partial E_P/\partial \log[A]$	$\partial E_P/\partial \log[X]^a$
k [B]	29.6[b]	0[b]	0[b]
k $[B]^2$	19.7[b]	-19.7[b]	0[b]
k $[B]^2$ [X] / [A]	19.7[b]	0[b]	-19.7[b]
observed	20.7 ± 0.6	-21.4 ± 0.5	0.17 ± 0.56

[a]X = CH_3OH; [b]Theoretical responses

9-Bromo-10-cyclopropylanthracene (2). The cyclic voltammogram of **2** (Figure 4-5) reveals an initial oxidation wave ($E_P \approx +950$ mV at 2000 mV/sec) and subsequent oxidation waves at more positive potentials. However, unlike **1**, at higher sweeprates the initial oxidation wave becomes reversible (Figure 4-6).

At higher sweep rates, the DCV reaction order approach is applicable. The results of these experiments are summarized in Figures 4-7→4-8 and Table 4-2.

Figure 4-5. Cyclic Voltammogram of **2** in CH_3CN (whole view) (0.5 M $LiClO_4$, 5×10^{-3} M **2**, v = 2000 mV/sec)

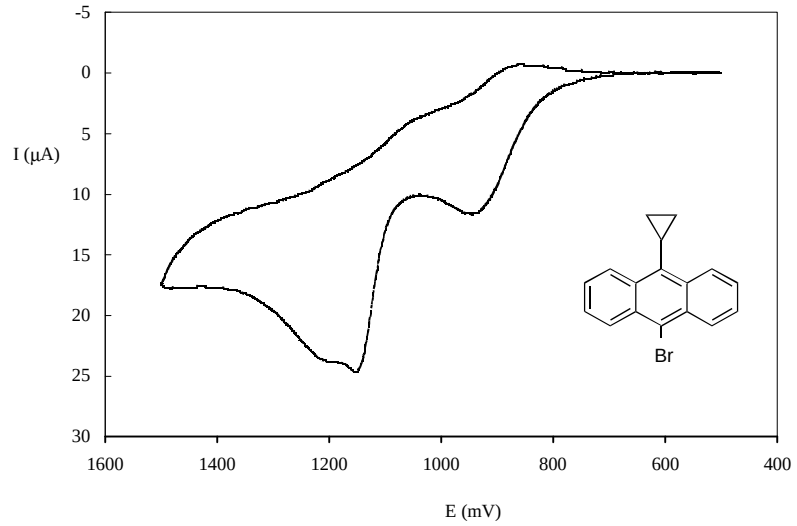

Figure 4-6. Cyclic Voltammogram of **2** in CH_3CN (partial view) (0.5 M $LICl O_4$, 5×10^{-3} M **2**, v = 8000 mV/sec)

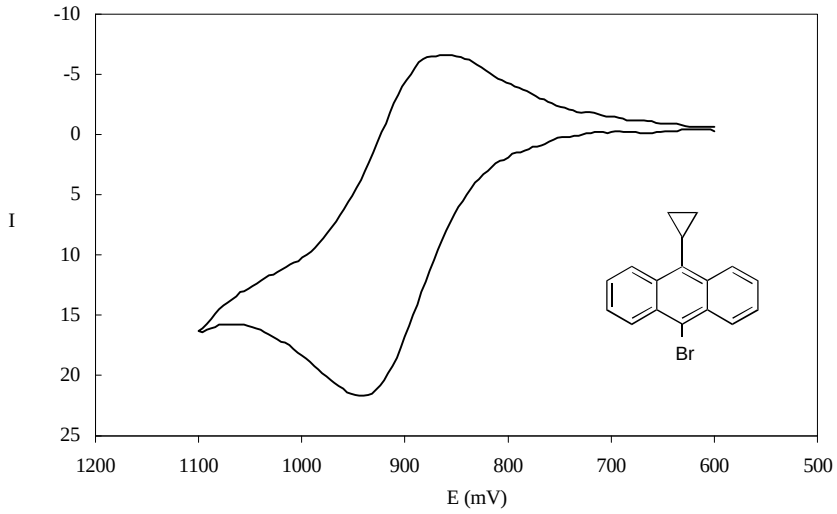

Figure. 4-7. DCV analysis of **2**, $\partial\log(v_c)/\partial\log[\mathbf{2}]$. (0.5 M $LiClO_4$, 0.5 M CH_3OH, $3.7 \rightarrow 13.9 \times 10^{-3}$ M **2**, $I'_{pc}/I'_{pa} = 0.5$)

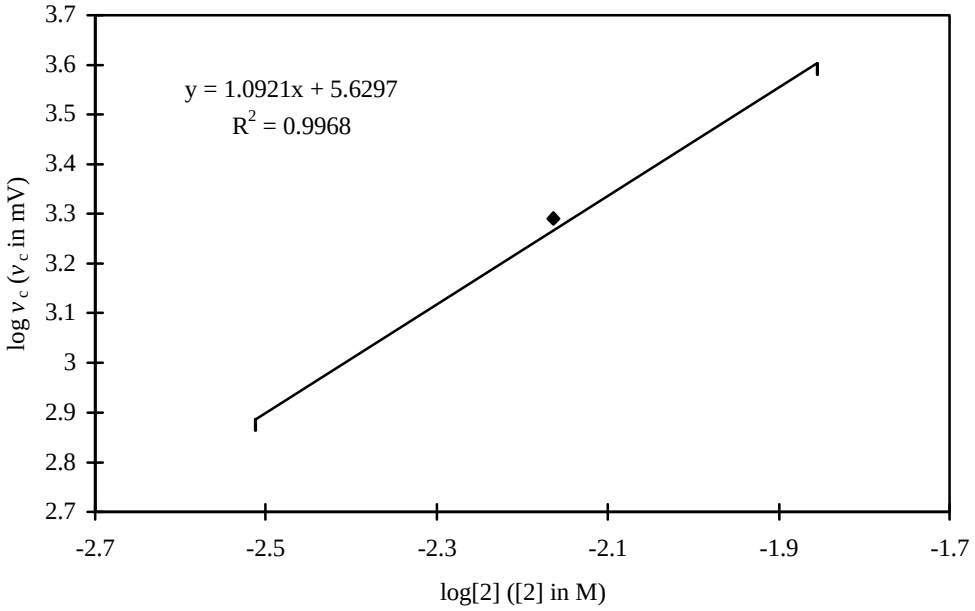

Figure. 4-8. DCV analysis of **2**, $\partial\log(v_c)/\partial\log[CH_3OH]$. (0.5 M $LiClO_4$, 0.25→5 M CH_3OH, 5.0×10^{-3} M **1**, $I'_{pc}/I'_{pa} = 0.5$)

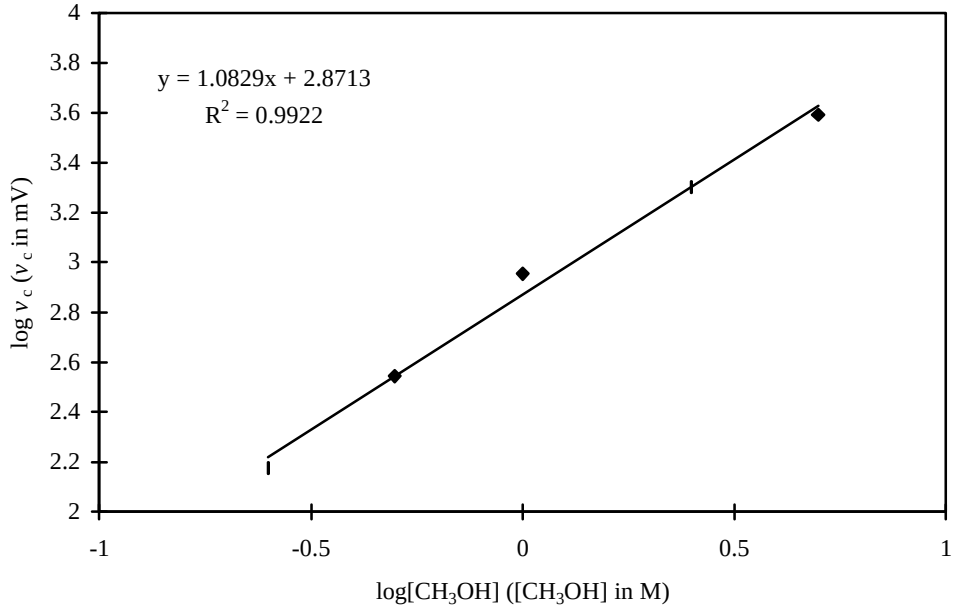

Table 4-2. DCV analysis of the electrochemical oxidation of **2**

Rate law	$\partial\log(\nu_C)/\partial\log[A]$	$\partial\log(\nu_C)/\partial\log[X]^a$	$R_{A/B}$	$R_X{}^a$
k [B] [X]	0.0[b]	1.0[b]	1	1
k $[B]^2$ [X]	1.0[b]	1.0[b]	2	1
k [A] [B] [X]	1.0[b]	1.0[b]	2	1
observed	1.1 ± 0.1	1.1 ± 0.1	2	1

[a]X = CH_3OH; [b]Theoretical responses.

Two rate laws are consistent with the observed DCV results. (DCV does not allow deconvolution of the individual reaction orders in **A** and **B)**. However, both CV and LSV permit the separation of the individual reaction orders in **A** and **B**. LSV is applicable at lower sweep rates where no reverse (cathodic) wave is observed. At low scan rates, E_P was found to vary as a function of sweep rate and both the concentrations of **2** and CH_3OH (Figure 4-9→4-11, and Table 4-3), supporting a rate law that is first-order each in $\mathbf{2}^{+\cdot}$, **2**, and CH_3OH (Eq. 4-2).

$$-d[\mathbf{2}^{+\cdot}]/dt = k\,[\mathbf{2}^{+\cdot}]\,[\mathbf{2}]\,[CH_3OH] \qquad (4\text{-}2)$$

Figure. 4-9. LSV analysis of **2**, $\partial E_P/\partial \log(\nu)$. (0.5 M $LiClO_4$, 0.5 M CH_3OH, 5×10^{-3} M **1**, ν = 50→1500mV/sec)

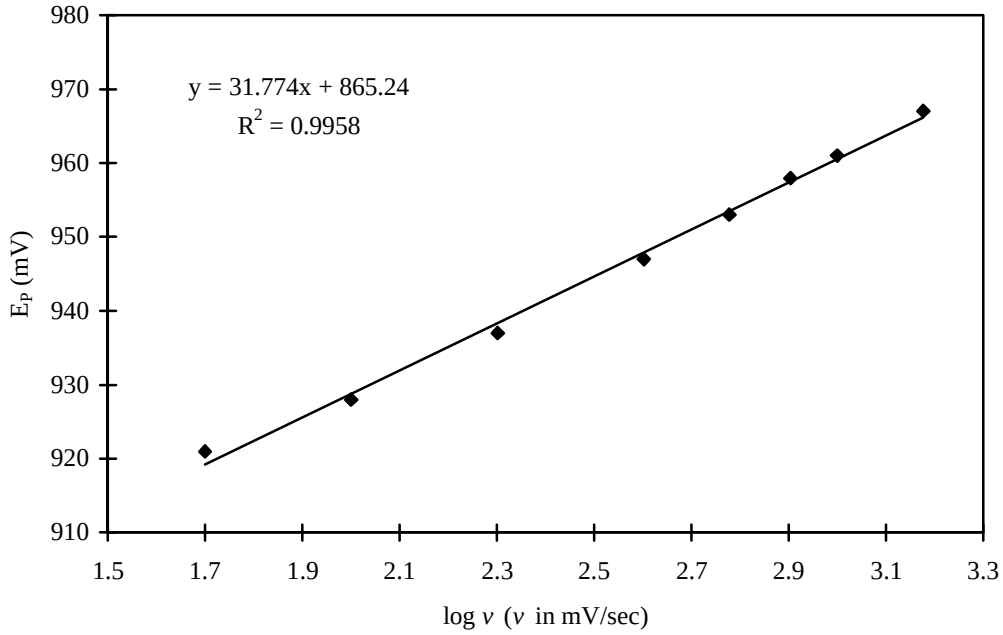

Figure. 4-10. LSV analysis of **2**, $\partial E_P/\partial \log[CH_3OH]$. (0.5 M $LiClO_4$, 0.5→5 M CH_3OH, 5.0×10^{-3} M **2**, ν = 50 mV/sec)

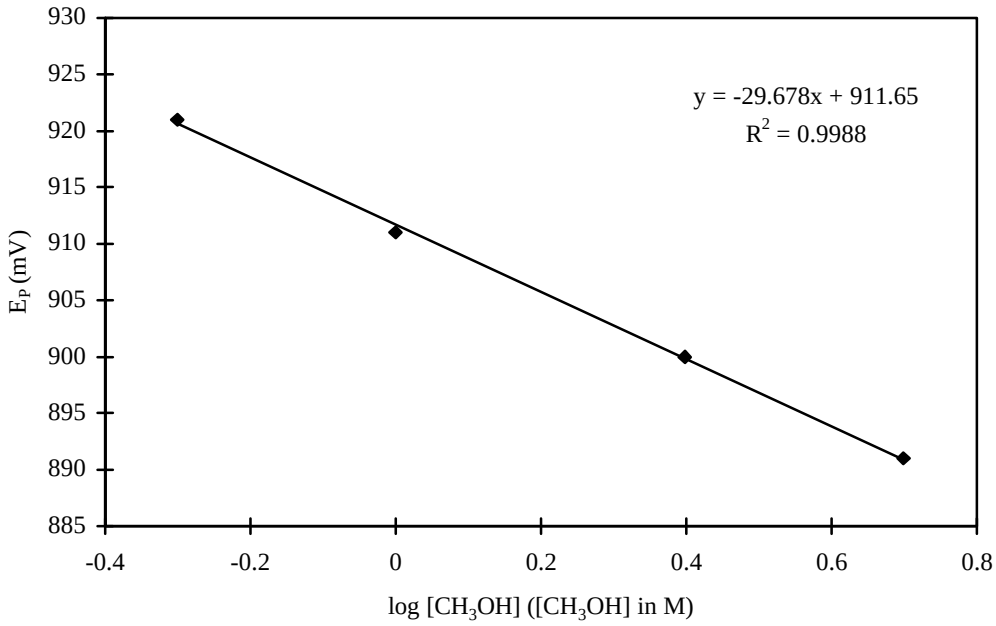

Figure. 4-l1. LSV analysis of **2**, $\partial E_P/\partial \log[\mathbf{2}]$. (0.5 M $LiClO_4$, 1.0 M CH_3OH, 2.0→12.4 × 10^{-3} M **2**, ν = 200 mV/sec)

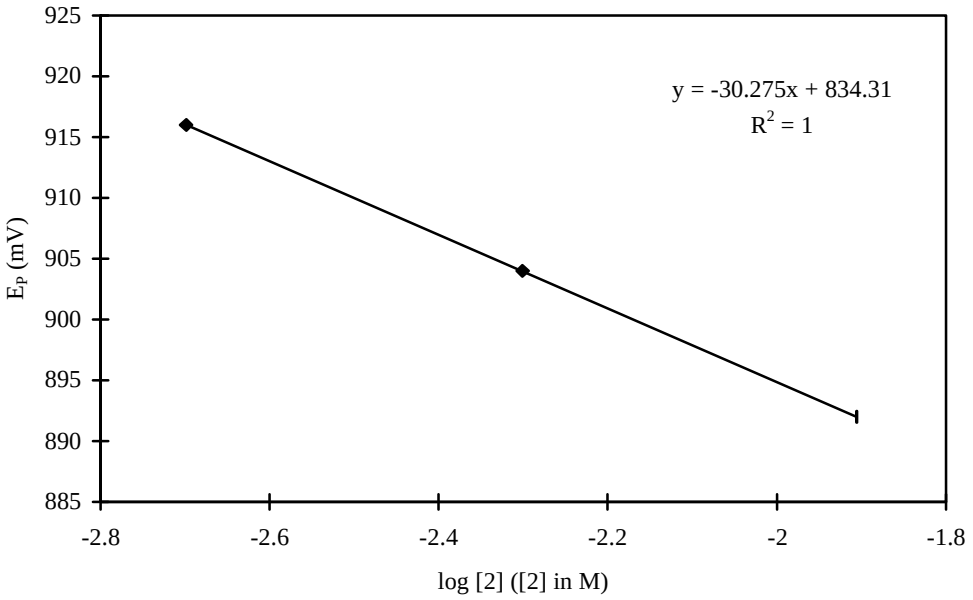

Table 4-3. LSV analysis of the electrochemical oxidation of **2**

Rate law	$\partial E_P/\partial \log(\nu)$	$\partial E_P/\partial \log[A]$	$\partial E_P/\partial \log[X]^a$
k [A] [X]	29.6[b]	0.0[b]	-29.6[b]
k [A] [B]	29.6[b]	-29.6[b]	0.0[b]
k [A] [B] [X]	29.6[b]	-29.6[b]	-29.6[b]
observed	31.8 ± 0.8	-29.7 ± 0.7	-30.3 ± 0.1

[a]X = CH_3OH; [b]Theoretical responses.

At higher sweep rates where the CV becomes partly reversible, differentiation between the rate laws k[**A**]]**B**][**X**} *vs.* k[**B**]^2[**X**] can also be achieved by examining the variation of the cathodic to anodic current ratio (I_{pc}/I_{pa}) as a function of sweep rate.[89,120] In Figures 4-12→4-15, the theoretical responses for these two rate laws and the experimental results obtained at several methanol concentration are compared. A substantially better fit to the curve corresponding to the rate law first order each in **A** and **B** is observed.[121]

Figure 4-12. Variation of the cathodic to anodic current ratio ($-I_{pc}/I_{pa}$) with sweeprate for the oxidation of **2** (0.0 M CH_3OH).

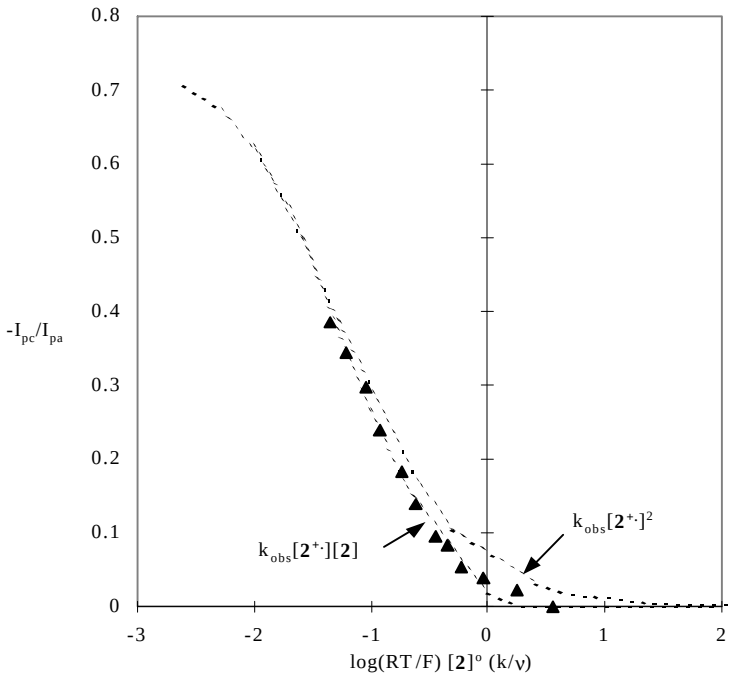

Figure 4-13. Variation of the cathodic to anodic current ratio ($-I_{pc}/I_{pa}$) with sweeprate for the oxidation of **2** (0.25 M CH_3OH).

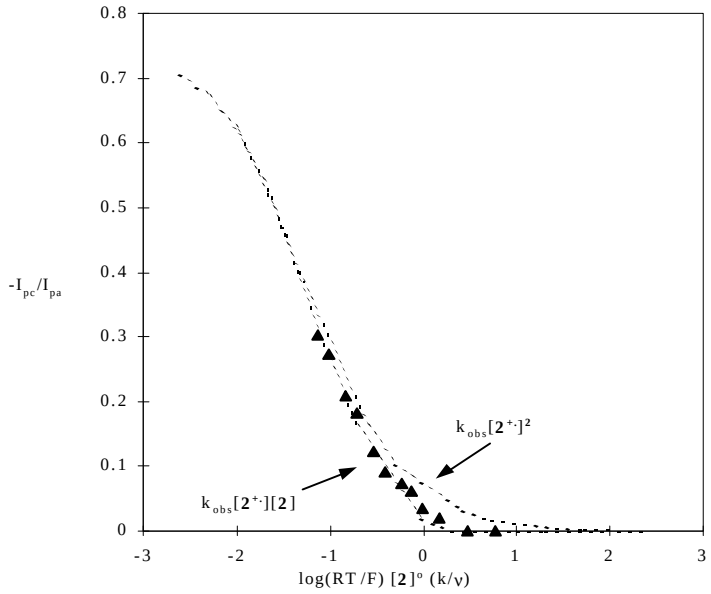

Figure 4-14. Variation of the cathodic to anodic current ratio ($-I_{pc}/I_{pa}$) with sweeprate for the oxidation of **2** (0.5 M CH_3OH).

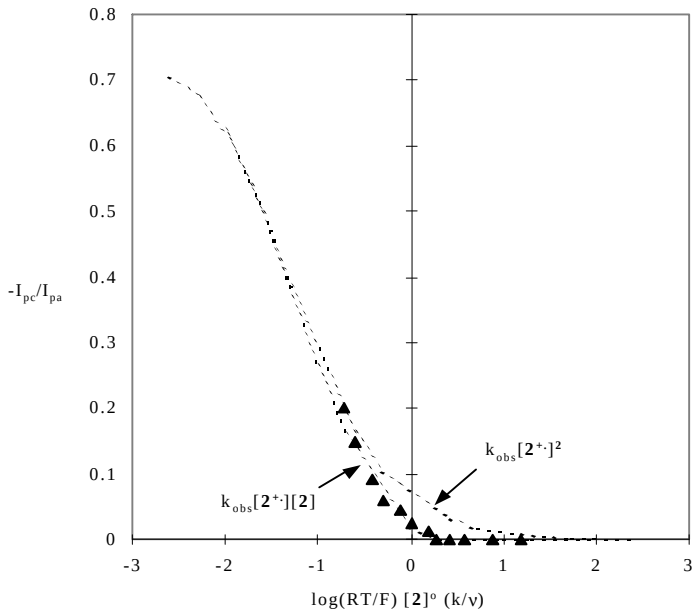

Figure 4-15. Variation of the cathodic to anodic current ratio ($-I_{pc}/I_{pa}$) with sweeprate for the oxidation of **2** (1.0 M CH_3OH).

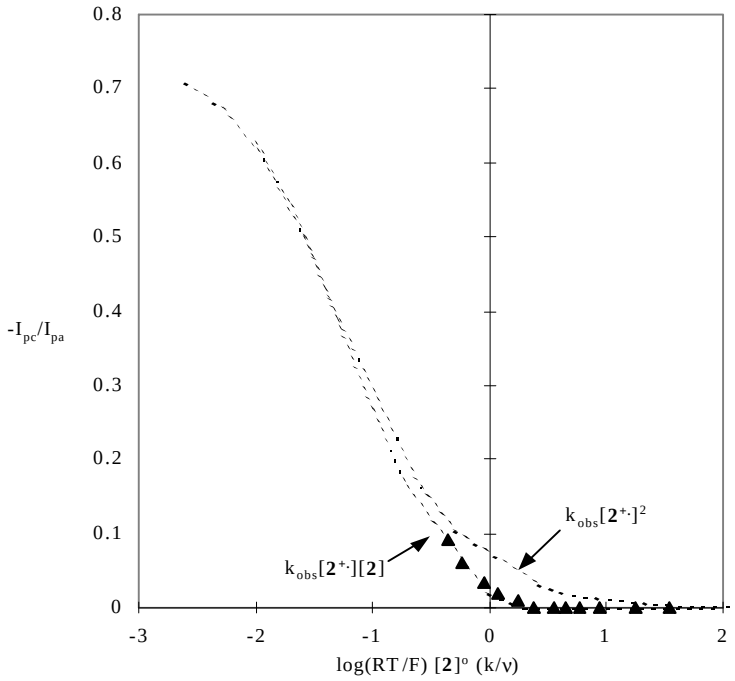

Electron Stoichiometry (n). The peak current for a CV wave reflects the total number of electrons transferred, including the initial heterogeneous electron transfer, as well as any follow-up hetero- or homogeneous electron transfer. Many examples pertaining to the oxidation of aromatic hydrocarbons show that n = 1 for the oxidation wave if the CV is reversible (i.e., the radical cation is stable within the time-frame of the experiment) and that n = 2 (or more) if the CV is irreversible (i.e., the follow-up reactions involve the transfer of additional electrons and contribute to the initial oxidation wave). Frequently two or more electrons need to be transferred in order to obtain a stable product.

In addition to constant potential electrolysis or coulometry, CV provides a qualitative means for estimating the n-value for an oxidation wave in accordance with the following equations (Eq. 4-3 and 4-4), which pertain to reversible systems:

$$| E_P - E_{P/2} | = (56.5/n) \text{ mV (at } 25^oC) \quad (4\text{-}3)$$

$$I_P = (2.69 \times 10^5) n^{3/2} A D_o^{1/2} \nu^{1/2} C_o^* \quad (4\text{-}4)$$

A plot of I_P vs. $\nu^{1/2}$ is often used to check whether any follow up reactions involve electron transfer and to estimate the number of electrons transferred.

*9-Bromo-10-cyclopropylanthracene (**2**).* At higher sweeprates, the reversible oxidation wave for **2** corresponds to n = 1 ($E_{pa} - E_{P/2}$ = 50 - 60 mV). At lower sweeprates and/or in the presence of methanol, the wave becomes irreversible because follow-up reactions involving $\mathbf{2}^{+\cdot}$ are occurring. A total of two electrons need to be transferred in order to form **3**.

A plot of I_P/C_o^* vs. $\nu^{1/2}$ for the oxidation of **2** (Figure 4-16) suggests that with methanol addition, the slope changes (corresponding to a change from n = 1 in the absence of methanol to n = 2 in the presence of methanol).

*9-Cyclopropylanthracene (**1**).* A plot of I_P/C_o^* vs. $\nu^{1/2}$ for the oxidation of **1** is presented in Figure 4-17. The slope of this line is nearly the same as that observed for 9-bromo-10-cyclopropylanthracene in the presence of methanol. Assuming that the diffusion coefficients of **1** and **2** are similar, this would suggest that the initial oxidation wave for **1** also corresponds to the transfer of two electrons.

Figure 4-16. I_P/C_o^* vs. $v^{1/2}$ plot for **2** at various concentrations of methanol (0.005 M **2**, 0.5 M $LiClO_4$ in CH_3CN)

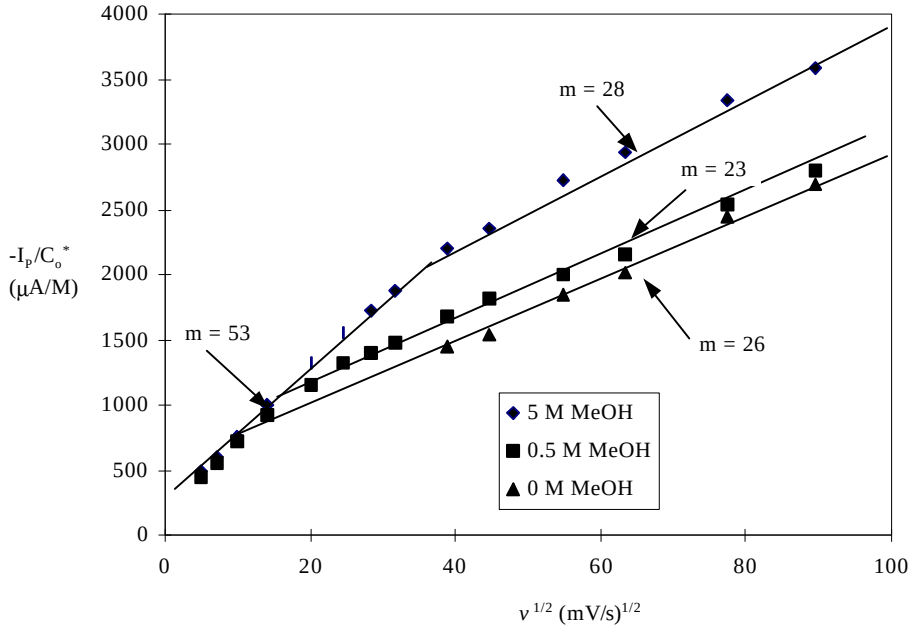

Figure 4-17. I_P/C_o^* vs. $v^{1/2}$ plot for **1** in the presence of methanol (0.004 M **1**, 0.5 M $LiClO_4$, 2.5 M CH_3OH in CH_3CN)

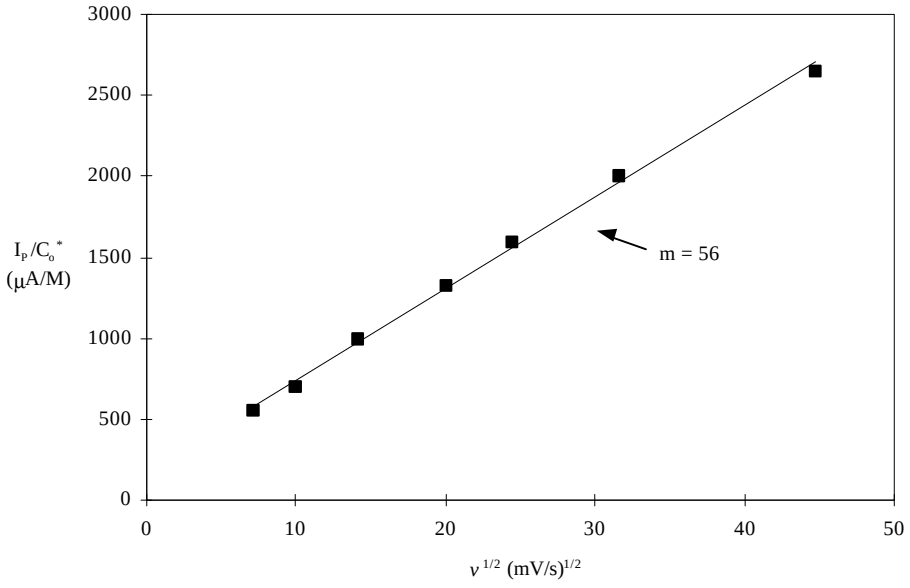

4.2.2 Product Analysis from Preparative Electrolysis

9-Bromo-10-cyclopropylanthracene (2). The preparative (constant current) electrolysis of **2** was conducted in CH_3CN/CH_3OH with 0.1 M $LiClO_4$ as the supporting electrolyte. The products isolated from this electrolysis (Scheme 4-1) varied dramatically as a function of the work-up procedure employed. Aqueous work-up (extraction with H_2O/ether) yielded exclusively 9-cyclopropyl-9-methoxyanthrone (**3**). In contrast, non-aqueous work-up (removing solvent by rotary evaporation followed by extraction with CH_2Cl_2) yielded mainly cyclopropane ring-opened products (**4**, **5**, and **6**). The yields of several representative runs are shown in Table 4-4.

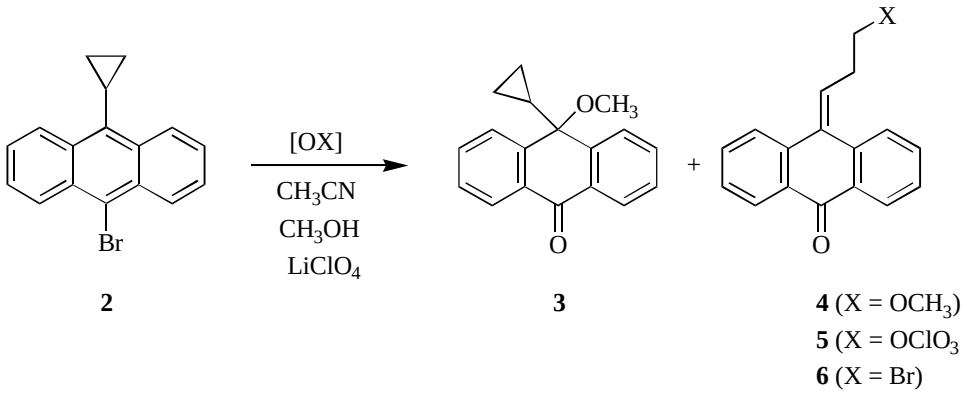

2 **3** **4** (X = OCH_3) **5** (X = $OClO_3$) **6** (X = Br)

Scheme 4-1. Anodic oxidation of **2** in CH_3CN/CH_3OH

Table 4-4. Yields of products produced in the controlled-current oxidation of **2**

[CH_3OH] (M)	electrons (equiv.)	workup method	yield (%) **3**	**4**	**5**	**6**
4.1	2.8	aqueous	62[a]	---[b]	---[b]	---[b]
2.5	2.7	aqueous	68[c]	---[b]	---[b]	---[b]
4.1	2.5	non-aqueous	0.0	7.4[a]	21.8[a]	23.2[a]
2.5	2.7	non-aqueous	0.0	9.3[c]	41.0[c]	12.3[c]
0.25	2.5	non-aqueous	0.0	5.8[c]	12.6[c]	4.3[c]

[a]Isolated yield; [b]Trace; [c]Yield determined by ^{1}HNMR.

Although substantially different products resulted, the mass balances observed for both the aqueous and non-aqueous work-up procedures were similar (60 - 70 %) leading to the suspicion that the reaction products might be interconverting during non-aqueous workup. Indeed, monitoring of the electrolysis prior to workup by either GC or TLC revealed that only **3** was produced during the electrolysis, suggesting that this compound was the precursor to **4**, **5**, and **6**.

In separate experiments this hypothesis was validated by subjecting **3** to conditions designed to emulate the conditions of the non-aqueous work-up procedure. For example,

treatment of **3** with HBr in CH_3CN led to formation of ring-opened bromide **6** in 80 % yield (unoptimized). Similarly, treatment of **3** with $HClO_4$ in CH_3CN yielded perchlorate ester **5** in 46 % yield (unoptimized). These results substantiate the contention that cyclopropane ring-opened products **4**, **5**, and **6** are produced during non-aqueous workup (Scheme 4-2).

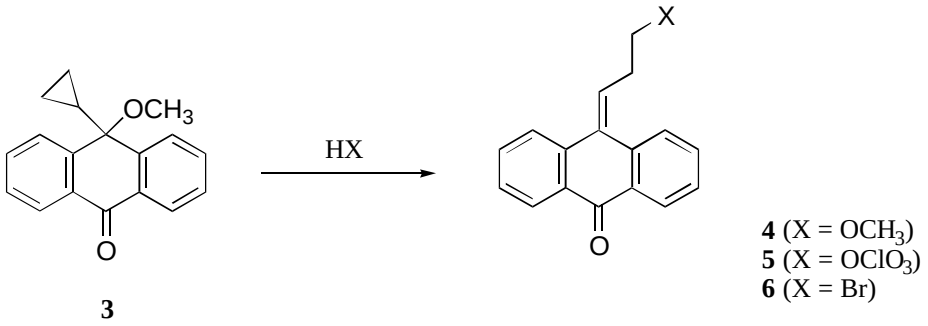

3

4 (X = OCH_3)
5 (X = $OClO_3$)
6 (X = Br)

Scheme 4-2. Conversion of product **3** to product **4**, **5**, or **6** under acidic conditions

9-Cyclopropylanthracene (1). Controlled-current electrolysis of **1** in CH_3CN/CH_3OH followed by a non-aqueous work-up resulted in the formation of cyclopropane ring-opened products (in analogy to the results observed in the oxidation of **2**). However, ring-opened products were also found when an aqueous work-up was employed (Table 4-5). Periodic monitoring of the reaction mixture during the electrolysis by TLC and GC revealed that 9-cyclopropyl-10-methoxyanthracene (**7**) was formed early in the electrolysis, but was converted to other products upon further electrolysis (The yield of **7** reached a maximum of 37 % after two equivalents of electrons were transferred). A small quantity of anthraquinone (**8**) was detected, even at the early stages

of the electrolysis. Bianthrone (**9**) was also detected in runs at low methanol concentration.

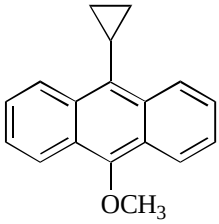

7

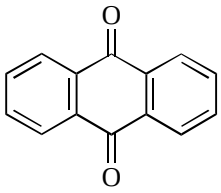

8

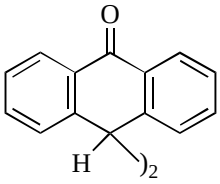

9

Table 4-5. Yields of products produced in the controlled-current oxidation of **1**

[CH_3OH](M)	Electrons (equiv.)	workup method	yield, %[a]						
			7	**3**	**4**	**5**	**8**	**9**	**1**
4.1	2.0	aqueous	37.0	19.8	1.2	0.0	13.9	---[b]	20.4
2.5	3.0	aqueous	3.6	27.6	32.0	0.0	3.6	---[b]	17.8
2.5	3.0	non-aqueous	0.0	2.8	41.4	20.4	13.0	---[b]	6.2
0.25	2.5	non-aqueous	0.0	---[b]	12.8	16.7	---[b]	8.0	---[b]

[a]Yield determined by GC or ^{1}HNMR; [b]Trace.

Characterization of Perchlorate Ester 5. Surprisingly, perchlorate ester **5** was successfully isolated and characterized despite the unstable and extremely explosive nature

of alkyl perchlorates. Recent studies have demonstrated that perchlorate ion can manifest nucleophilic properties in the presence of extraneous nucleophiles (e.g., halide ions).[122] Because of the novelty of this compound, some discussion of its characterization is warranted. The IR spectrum of **5** exhibited two peaks at 1230 and 1260 cm^{-1} (Cl-O asymmetric stretching) and a peak at 1040 cm^{-1} (Cl-O symmetric stretching), which are a characteristic of covalent organic perchlorates. The ^{1}HNMR spectrum of **5** possesses a triplet shifted unusually downfield (δ = 4.8 ppm vs. TMS) corresponding to the CH_2 α to the perchlorate group. Finally, the molecular weight (and formula) were confirmed using FAB-MS, HRMS, and elemental analysis.

4.2.3 Reaction Mechanism

Oxidation of 9-Cyclopropylanthracene (1). LSV results for **1** show that decay of $\mathbf{1}^{+\cdot}$ in CH_3CN/CH_3OH is second-order in radical cation and zero order in CH_3OH. Consequently, CH_3OH attack must occur after the rate-limiting step. Based on these results, a disproportionation mechanism for decay of the radical cation from **1** is proposed (Scheme 4-3).[123] Because the dication will invariably be more reactive toward nucleophiles than the radical cation, it is reasonable to suppose that $k_2[CH_3OH] > k_{-1}[\mathbf{1}]$ so that the overall rate law reduces to $k_1[\mathbf{1}^{+\cdot}]^2$. A nearly identical mechanism for decay of 9-alkylanthracene radical cations in CH_3CN/H_2O, studied by stopped-flow kinetics was recently reported by Fujita and Fukuzumi.[124] This mechanism is further supported by the bulk electrolysis results which reveal that **7** is the product initially produced during the oxidation. The isolation of **7** and **3** as the only detectable products provides direct

evidence that the cyclopropyl group survives both the radical cation and dication stages of oxidation.

Further oxidation of **7**[125] forms $\mathbf{7}^{+\cdot}$ which likely undergoes oxidative methyl transfer (Scheme 4-4), as proposed in Parker's studies of the anodic oxidation of dimethoxydurene,[126] to form **11**. Further oxidation yields **10** which leads to the isolated product **3** after nucleophilic attack of methanol.

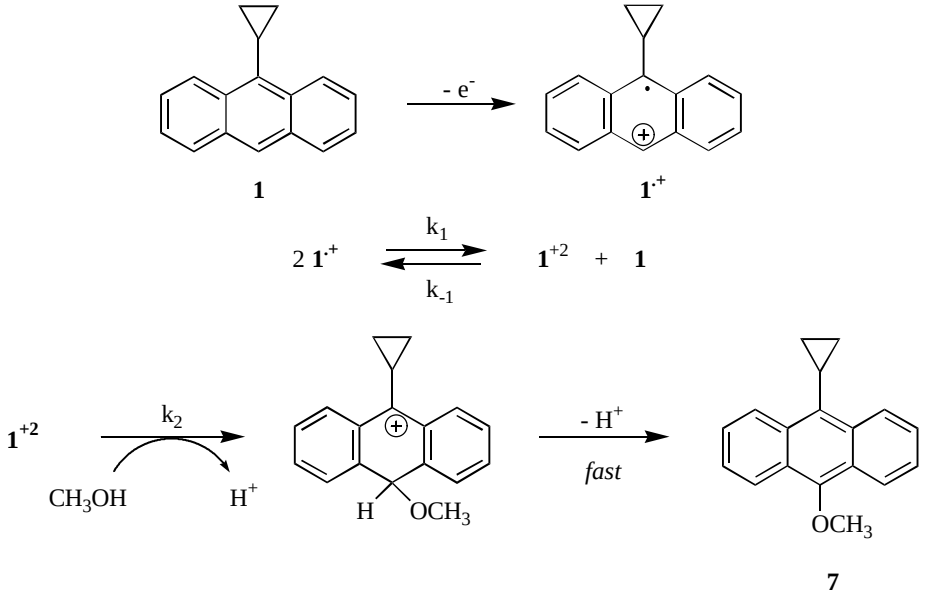

Scheme 4-3. Anodic oxidation mechanism of **1** (from **1** to **7**)

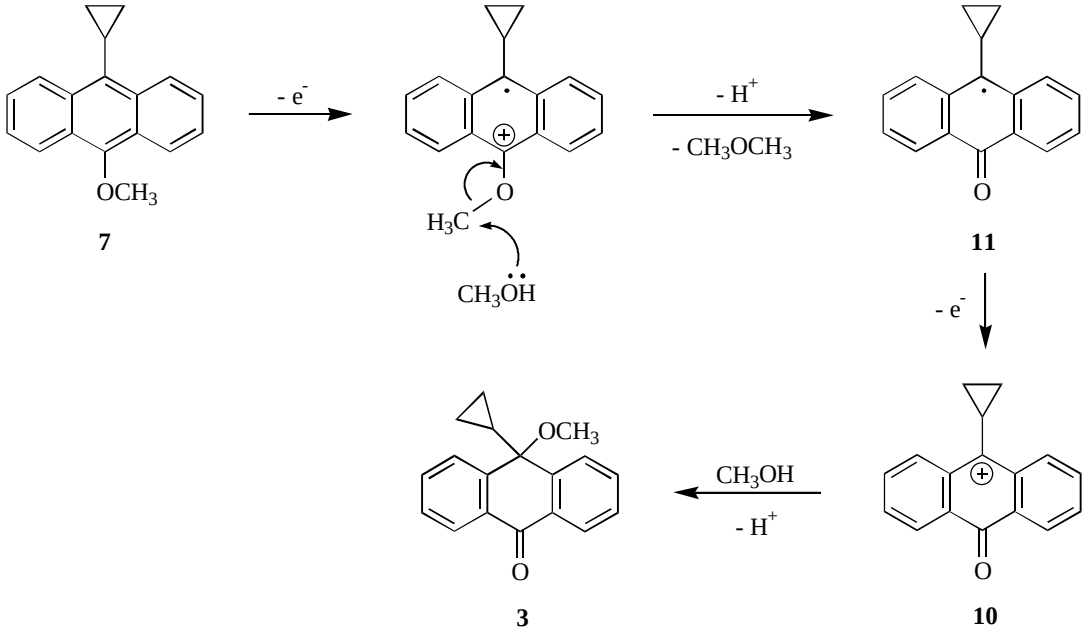

Scheme 4-4. Anodic oxidation mechanism of **1** (from **7** to **3**)

Because the anodic process produces H^+, some of **3** is converted to cyclopropane ring-opened products either during the electrolysis or upon work-up.

Oxidation of 9-Bromo-10-cyclopropylanthracene (2). CV, DCV and LSV results for **2** are all consistent with a rate law for decay of $\mathbf{2}^{+\cdot}$ which is first order each in radical cation, parent compound and methanol ($-d[\mathbf{2}^{+\cdot}]/dt = k[\mathbf{2}^{+\cdot}][\mathbf{2}][CH_3OH]$). The reason why $\mathbf{2}^{+\cdot}$ does not decay via a disproportionation mechanism (as proposed for $\mathbf{1}^{+\cdot}$) may be due to the fact that the bromine substituent deactivates the aromatic ring making the removal of a second electron from $\mathbf{2}^{+\cdot}$ energetically prohibitive. (Parker found that E^o for 9-bromoanthracene was more positive than anthracene by 90 mV).[127] As a

consequence of having the disproportionation pathway effectively "turned-off," decay of the radical cation follows a different pathway, presumably involving nucleophilic attack of CH_3OH prior to or during the rate-limiting step. However, the appearance of **2** in the rate law was somewhat unexpected.

A mechanism which accounts for the presence of **2** in the rate law involves formation of π-complex between **2** and $\mathbf{2}^{+\cdot}$ (**12**, Scheme 4-5). Radical cation/neutral molecule complexes involving aromatic radical cations have been characterized spectroscopically, and are usually formulated as a π-dimer with the two molecules oriented face to face, with charge and spin delocalized into both rings.[87]

Methanol attack on the dimer radical cation **12** in the rate determining step to form the radical catoin of a methoxy derivative, which quickly loses a HBr to produce $\mathbf{7}^{+\cdot}$. The follow-up reaction of $\mathbf{7}^{+\cdot}$ is the same as proposed in Scheme 4-4, producing the final product **3**. The total electrons from **2** to **3** is two, which is consistent with the results from CV analysis.

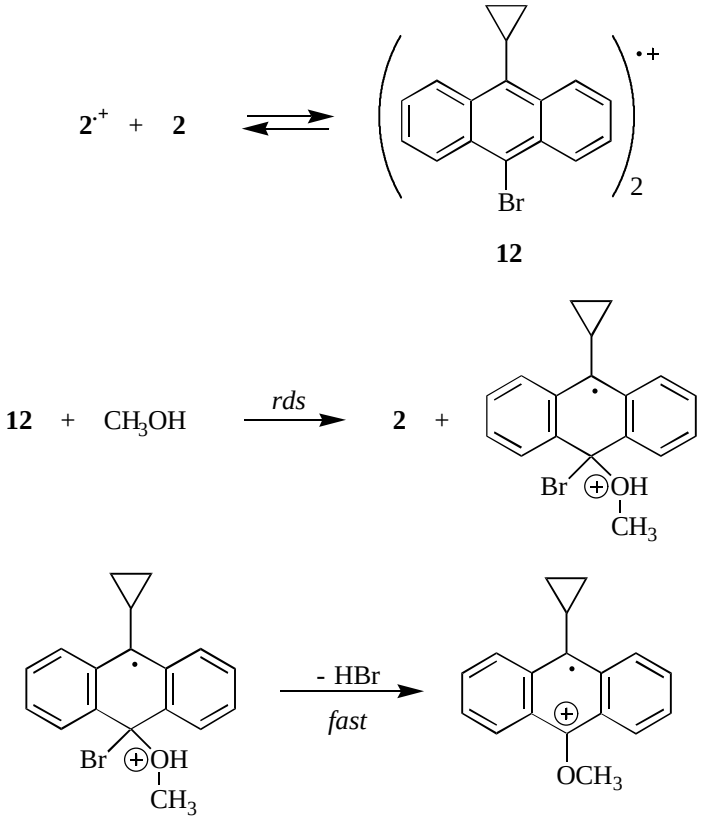

Scheme 4-5. Anodic oxidation mechanism of **2**

Ring Opening of 3 Under Acidic Conditions. As discussed earlier, cyclopropane ring-opened products (**4**, **5**, and **6**) are not the primary oxidation products of the oxidation of **1** or **2**. Indeed, these ring-opened products are produced from **3** by reaction with ClO_4^-, Br^-, or CH_3OH, facilitated by the H^+ produced during the electrolysis. Presumably, ring opening could occur via an S_N1 or S_N2' pathway (Scheme 4-6). The S_N1 pathway is unlikely, however, because we have already shown that cation **10** (an intermediate in the electrochemical oxidation) does not lead to ring-opened products

(presumably because of stereoelectronic considerations). In contrast, because of the sp^3 canter in **3**, the cyclopropyl group is essentially freely rotating and can readily achieve the conformational requirements for ring opening by the S_N2' mechanism (i.e., alignment of the C-O bond with the p-component of the vicinal C_1-C_2 or C_1-C_3 bonds).

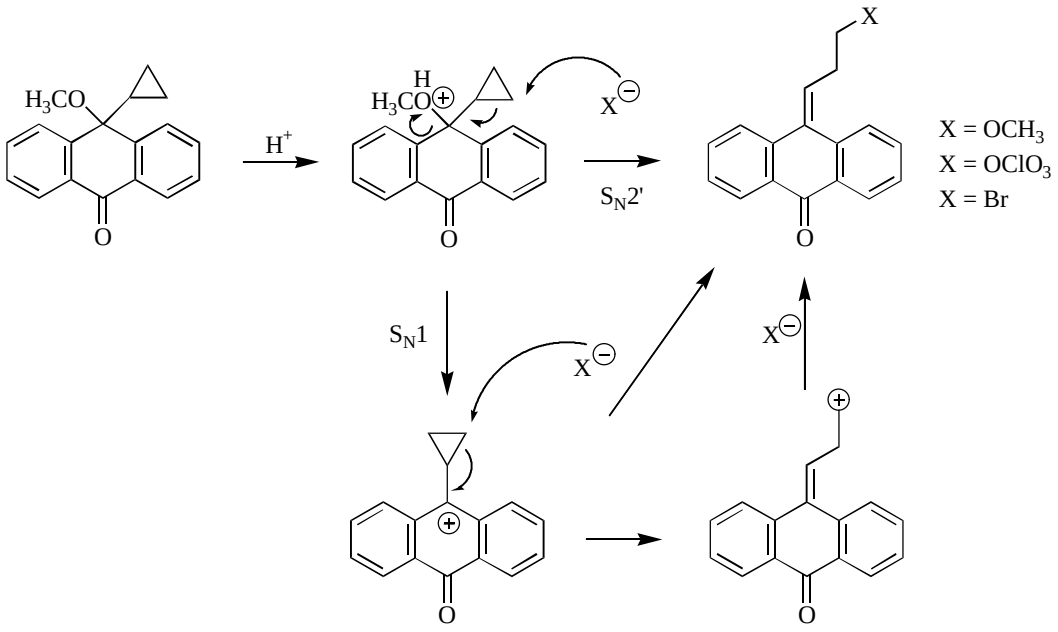

Scheme 4-6. Proposed ring opening mechanism of **3** under acidic condition

4.2.4 Stereoelectronic vs. Thermodynamic Factors

Semiempirical MO Calculations. In order to assess the role of conformation on the reaction pathway for the anodic oxidation of cyclopropylanthracenes, semiempirical MO calculations were performed on **1**, $\mathbf{1}^{+\cdot}$, and other potential intermediates generated during the oxidation of **1**. Towards this end, the AM1 approximation developed by

Dewar et al and implemented through MOPAC 6.0 was employed.[128] The keyword "C.I.=1" was used for $\mathbf{1}^{+\cdot}$ (i.e., the half-electron approximation). For comparison, analogous calculations were performed on cyclopropylbenzene, as well as its corresponding radical cation and dication. The results are summarized in Table 4-6.

Table 4-6. AM1-calculated ΔH^o for conformational interconversion (perpendicular → bisected) for the 9-cyclopropylanthracene and cyclopropylbenzene system

Species	**ΔH^o, kcal/mol**
1	6.2
$\mathbf{1}^{+\cdot}$	4.5
$\mathbf{1}^{2+}$	0.7
10	3.5
C_6H_5-*c*-C_3H_5	-0.3
C_6H_5-*c*-$C_3H_5^{+\cdot}$	-4.6
C_6H_5-*c*-$C_3H_5^{2+}$	-----[a]

[a]Although the geometry and energy of the perpendicular conformation were successfully obtained, geometry optimizations of the bisected conformation always led to a cyclopropane ring-opened structure.

For cyclopropylbenzene, the bisected conformation is found to be more stable by 0.3 kcal/mol, in reasonable agreement with the experimental value of 1.4 kcal/mol reported by Closs and Klinger.[129] The bias in favor of the bisected conformation is predicted to increase for the radical cation, although there are no experimental values available for comparison.

As was reported earlier for the neutral molecule,[105] the perpendicular conformation is predicted to be more stable than the bisected for **1**, $\mathbf{1}^{+\cdot}$, $\mathbf{1}^{2+}$ because of unfavorable steric interactions (i.e., interaction of the cyclopropyl group with the *peri*-hydrogens).

These calculations also suggest that **1**, $\mathbf{1}^{+\cdot}$, $\mathbf{1}^{2+}$, or **10** cannot achieve a true bisected conformation. For the "bisected" conformation of each of these species, the anthryl system adopts a "butterfly" geometry, and the cyclopropyl methine C-H bond is out-of-plane by as much as 20^{o} (Figure 4-18).

Figure 4-18 . AM1-predicted geometry for the "bisected" and perpendicular conformations of $\mathbf{1}^{+\cdot}$

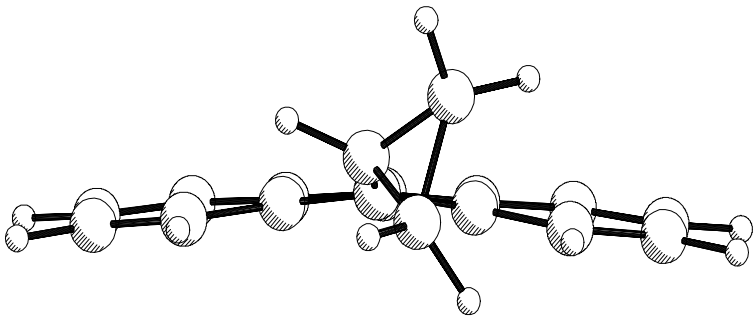

pseudo-bisected conformation

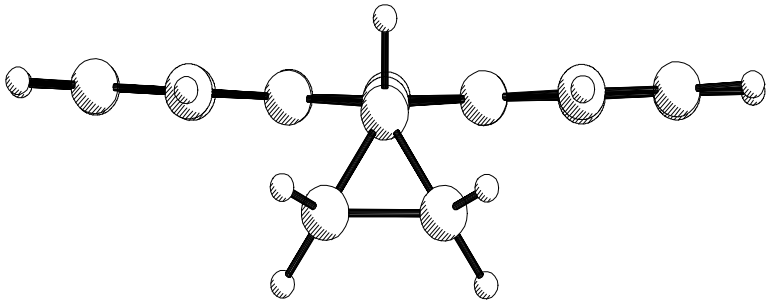

perpendicular conformation

Steroelectronic Consideration. AM1 calculations (Table 4-6) suggest that 9-cyclopropylanthracene exists primarily in the perpendicular conformation, and that the same also holds true for the other intermediates likely generated in the oxidation of **1** (**1**$^{+\cdot}$, **1**$^{2+}$, or **10**). In 1969, Bauld et al. reported the ambient temperature EPR spectrum of **1**$^{+\cdot}$ (generated from treatment of **1** with H_2SO_4).[130] The observed hyperfine coupling constant to the cyclopropyl methine hydrogen (a_H^{β}) was reported to be 4.0 G. This coupling is the result of hyperconjugation, and the magnitude of a_H^{β} depends upon both the angle (θ) between the C-H bond and the *p*-orbital containing the unpaired electron, and the spin density at (ρ) in this orbital: $a_H^{\beta} = [A + B \cos^2(\theta)]\ \rho$, where A and B are constants. (a_H^{β} is expected to be near zero for the bisected conformation since the C-H bond is orthogonal to the π-system). Assuming that ρ and B were approximately equal for both **1**$^{+\cdot}$ and 9-methylanthracene$^{+\cdot}$ (yielding $\theta_{avg} \approx 60^{o}$), the spectrum was interpreted on the basis of a freely rotating cyclopropyl group with a slight preference for the bisected conformation.

As noted above, however, AM1 calculations suggest the perpendicular conformation is lower in energy and that because of steric constraints, the bisected conformation is not truly bisected (i.e., the anthracene ring adopts a butterfly geometry with $\theta \approx 70 - 75^{o}$ rather than 90^{o}, Figure 4-18). Utilizing AM1, the calculated a_H^{β}'s for the pseudo-bisected and perpendicular conformations of $\mathbf{1}^{+\cdot}$ are 0.68 G and 7.0 G, respectively.[131] The experimentally observed value of 4.0 G falls slightly toward the upper end of this range, suggesting a) the pseudo-bisected and perpendicular conformations are both important, with the latter slightly favored, or b) that the ground state conformation of $\mathbf{1}^{+\cdot}$ is midway between these two conformations.

However, the important point is that the experimentally observed a_H^{β} appears to be too large to be attributed to $\mathbf{1}^{+\cdot}$ existing preferentially in the bisected conformation (or even the pseudo-bisected conformation). Whether the perpendicular conformation actually predominates as the calculations suggest (Table 4-6), or whether the conformation is intermediate between the pseudo-bisected and perpendicular conformations (as the combined EPR and computational results suggest), either via time-averaged equilibration or as a discrete conformation, is not resolved.

Dinnocenzo has provided convincing evidence that ring opening of cyclopropylarene radical cations is nucleophile-assisted (e.g., S_N2). However, the stereoelectronic requirements for ring opening may only be met when the cyclopropylarene is in the bisected conformation (Scheme 4-7).

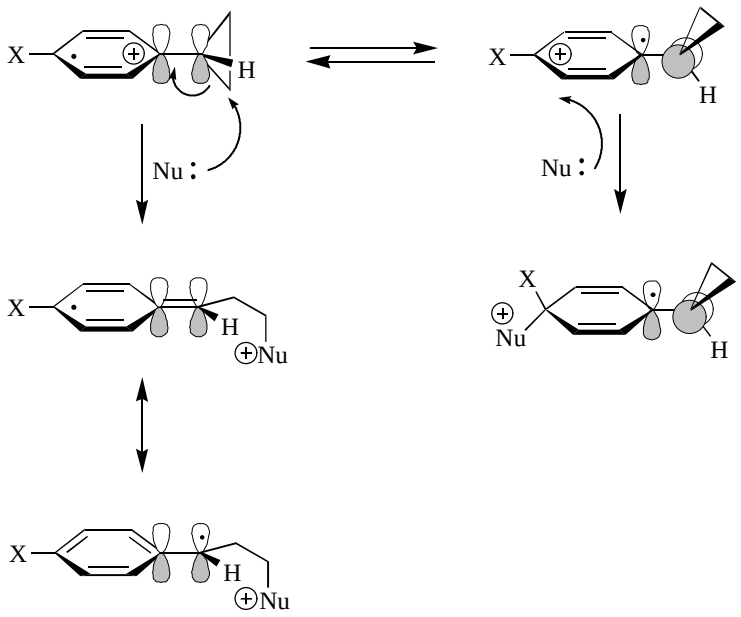

Scheme 4-7. Stereoelectronic effects on reactivity of cyclopropylarene radical cations

Thus, if the bisected conformation is not accessible to $\mathbf{1}^{+\cdot}$, the failure of the cyclopropane ring in this system to undergo ring opening may be attributed to unfavorable stereoelectronic factors. Consequently, the initial oxidation products arise primarily from nucleophilic attack on the aromatic ring (Scheme 4-7).

Thermodynamic Consideration. In its reaction with methanol, cyclopropylbenzene radical cation yields the thermodynamically-favored (ring-opened product). Although 9-cyclopropylanthracene radical cation is intrinsically more stable than Ph-*c*-$C_3H_6^{+\cdot}$ because of resonance, the same resonance stabilization is also available to both the ring-opened benzylic-type radical (formed after CH_3OH-induced ring opening) and to the cyclohexadienyl-type radical formed from addition of CH_3OH to the aromatic

ring. There is no obvious reason to expect a reversal in the stabilities of these two products. Consider the stability of the following two pairs of radicals (ΔH^o's were obtained using SCF-MO, AM1 approximation, Scheme 4-8)).

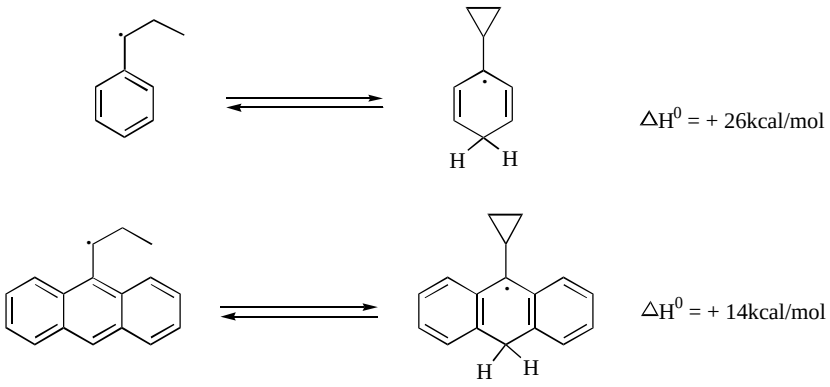

Scheme 4-8. Stability of benzylic-type radical and cyclohexadienyl-type radical

Although the difference is smaller in the anthracene system, the cyclopropane ring-opened benzyl-type radical is predicted to be substantially more stable than the cyclopropane ring-closed cyclohexadienyl-type radical for both the anthryl and phenyl systems. This prediction is reasonable in light of the relative stabilities of benzyl vs. cyclohexadienyl radicals, and the effect of cyclopropane ring strain.

Using the thermodynamic cycle, as introduced in Chapter 2 (Scheme 2-11), ΔG^o for methanol-induced ring opening of $\mathbf{1}^{+\cdot}$ in CH_3CN is estimated (Table 4-7). It was found that although ΔG^o is smaller in anthracene system, all these ring opening are substantially exothermic.

Table 4-7. ΔG^0 for the methanol-induced ring opening of cyclopropylarene radical cations in CH_3CN

Aryl group	$E^0_{Ar+./Ar}$ (V vs NHE)	RSE (kcal/mol)	ΔG^0 (kcal/mol)[a]
phenyl	2.58	10.2	-39.1
1-naphthyl	1.99	13.1	-28.4
9-anthyl	1.48	16.4	-21.1

[a] $\Delta G^0 = 30.7\text{-}23.1\ E^0_{Ar+./Ar}$ - RSE(Ar) in kcal/mol.

Thus, for both the phenyl and anthryl systems, ring opening is expected to be the thermodynamically preferred pathway. The fact that the thermodynamically least stable product is formed from cyclopropylanthracene radical cations suggests that its chemistry may be under kinetic, rather than thermodynamic control.

The Story Has Not Ended, Design of A New "Probe". Although the stereoelectronic argument above is reasonable, there is no direct experimental evidence that conformation of cyclopropylarene radical cations does affect their reactivity (i.e., cyclopropane ring opening). Moreover, the energy difference between bisected and perpendicular conformation becomes smaller and smaller from **1** to $\mathbf{1}^{+\cdot}$ to $\mathbf{1}^{++}$, although perpendicular conformation of these species are still the lowest energy conformation. For 1-cyclopropylnaphthalene radical cation (see Chapter 2), the bisected conformation is found to be readily accessible and stereoelectronic factors was suggested being not

responsible for the extremely sluggish rate of ring opening. Consequently, based on thermodynamic consideration, a transition state which is more product-like than reactant-like was proposed for methanol-induced cyclopropane ring opening of 1-cyclopropylnaphthalene radical cation (see Chapter 2). The similar considerations also pertain to 9-cyclopropylanthracene radical cation and much higher intrinsic barrier to nucleophile-induced ring opening is expected (Figure 4-19).

Figure 4-19. The proposed effect of aryl rings on the stabilities of reactants, transition states and products for CH_3OH-assisted cyclopropane ring opening

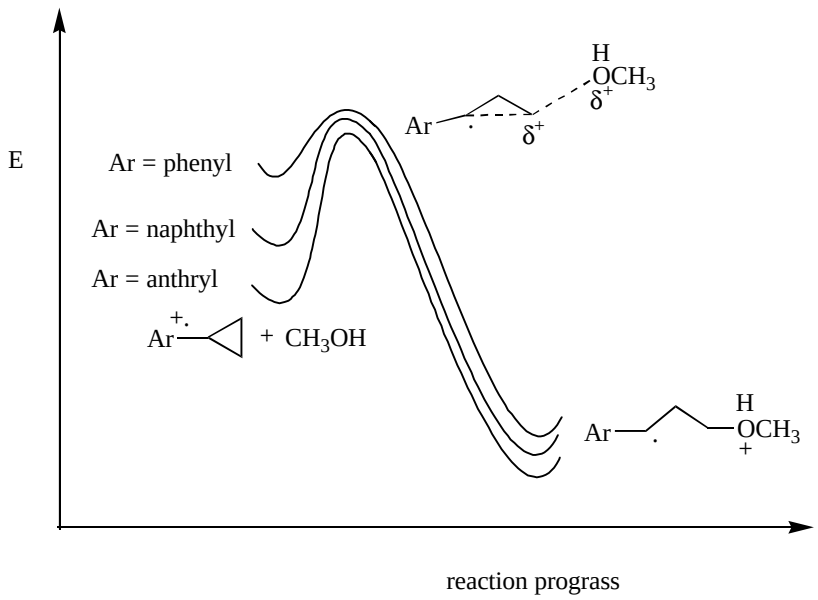

Thus, using the picture described in Figure 4-19, the fact that $\mathbf{1}^{+\cdot}$ does not undergo ring opening can be explained on a kinetic basis. Due to much higher intrinsic barrier to nucleophile-induced cyclopropane ring opening of $\mathbf{1}^{+\cdot}$, cyclopropyl group survives

oxidation, and alternatively, other process such as aromatic ring oxidation (e.g., nucleophilic attack) occurs (also see Chapter 5).

However, stereoelectronic factors can not be excluded from above consideration (Figure 4-19). Stereoelectronic factors may make a contribution to the intrinsic barrier (i.e., the barrier may be greater than predicted in Figure 4-19). Thus, a new "probe" needs to be designed to answer the question: Are streoelectronic factors important in ring opening reactions of cyclopropylarene radical cations?

It is our hypothesis that if the cyclopropane ring does not open during oxidation of an anthracene substrate in which the cyclopropyl group is locked in the bisected conformation, stereoelectronic factors can be discounted, and the failure of these species for ring opening can be wholly attributed to a product-like transition state when the positive charge is highly localized (in analogy to cyclopropylnaphthalenes). In the light of this consideration, a new "probe", 1-spiroaceanthracene and derivatives (**13, 14, 15**), will be synthesized to test this hypothesis.

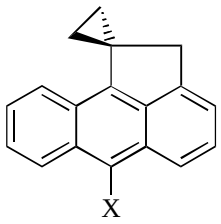

X = H, 13
X = Br, 14
X = Me, 15

4.3 SUMMARY

Reactions of radical cations generated from 9-cyclopropylanthracene (**1**) and 9-bromo-10-cyclopropylanthracene (**2**) in the presence of methanol have been investigated electrochemically. The major products arising from oxidation of both substrates are attributable to CH_3OH attack at the aromatic ring (occurring at the radical cation stage for **2** and the dication stage for **1**) rather than CH_3OH-induced cyclopropane ring opening. The cyclopropyl group in these anthryl systems adopts a perpendicular conformation which may not meet the stereoelectronic requirements for cyclopropane ring opening at either the radical cation or dication stage. However, an alternative interpretation for the survival of cyclopropyl group during oxidation of **1** and **2** based on thermodynamic and kinetic consideration also contributes to the barrier for ring opening. A transition state which is more product-like than reactant-like is proposed and it demonstrates that aromatic ring oxidation occurs due to higher intrinsic barrier to nucleophile-induced cyclopropane ring opening.

CHAPTER 5. CERIUM (IV) OXIDATION OF CYCLOPROPYLANTHRACENES AND 9,10-DIMETHYLANTHRACENE

5.1 INTRODUCTION

5.1.1 Initiation of The Project

In Chapter 4, we observed that anodic oxidation of 9-cyclopropylanthracene and 9-bromo-10-cyclopropylanthracene led to aromatic ring oxidation products. Unlike cyclopropylbenzene, the cyclopropyl group in these two anthryl substrates survived the oxidation processes. The higher barrier to ring opening of these radical cations is attributable to stereoelectronic factors and/or to the fact that positive charge is highly localized in the transition state for ring opening, and is thus unable to be stabilized by the anthryl system. A detailed analysis of these two considerations was presented in Chapters 2 and 4. Because the cyclopropane ring in the anthryl system does not open during the oxidation process, it is difficult to separate the relative importance of these two factors on the methanol-induced ring opening of cyclopropylanthracene radical cations.

The ring opening of cyclopropylarene radical cation is similar to the deprotonation of corresponding alkylarene radical cation (Eq. 5-1 and Eq. 5-2).

$$Ar^{+\cdot}\text{-}c\text{-}C_3H_5 + B\text{:} \rightarrow Ar\text{-}CH_2(\bullet)CH_2CH_2B^+ \qquad (5\text{-}1)$$

$$Ar^{+\cdot}\text{-}CH_3 + B\text{:} \rightarrow Ar\text{-}CH_2(\bullet) + BH^+ \qquad (5\text{-}2)$$

It was expected that an intramolecular competition experiment might confirm or rule out the role of stereoelectronic factors in the cyclopropane ring opening reaction. The

substrates designed for this experiment are *p*-methylcyclopropylarenes. In Chapter 3, we reported that Ce(IV) oxidation of 1-cyclopropyl-4-methylbenzene produced solely ring-opened products (no side-chain deprotonation products were observed. If the deprotonation products were obtained from oxidation of 9-cyclopropyl-10-methylanthracene under same condition, it would have given us a clue about existence of stereoelectronic factors. Because cyclopropyl group in 9-cyclopropyl-10-methylanthracene adopts a perpendicular conformation while in 1-cyclopropyl-4-methylbenzene it prefers to adopt a bisected conformation, the product ratio (or nature) of cyclopropane ring opening vs. side-chain deprotonation may reflect the role of stereoelectronic effects on these reactions.

Tolbert's work[68,69] on Fe(III) oxidation of 9,10-dimethylanthracene (DMA) gave us the basis to test our hypothesis. Indeed, we obtained deprotonation products (e.g. 9-cyclopropyl-10-methoxymethylanthracene) from Ce(IV) oxidation of 9-cyclopropyl-10-methylanthracene at room temperature in CH_3CN/CH_3OH. However, when reaction temperature was lowered to 0^oC, ring oxidation products were produced exclusively. This surprising result suggests that the radical cation of 9-cyclopropyl-10-methylanthracene undergoes neither cyclopropane ring opening nor deprotonation. Instead, nucleophilic addition to the aromatic ring is probably the initial reaction of anthryl system. Consequently, the attempt to evaluate stereoelectronic factors by using competition experiments (ring opening vs. deprotonation) was destined to fail because the assumption on which these experiments were based (9-methylanthracene radical cations deprotonate) is likely invalid. This result brought into question a number literature results which claimed that alkylanthracene radical cations quickly deprotonate. Thus, experiments were

designed to ascertain whether or not alkylanthracene radical cations do undergo deprotonation. The substrates chosen for this study are 9-cyclopropylanthracene (**1**), 9-bromo-10-cyclopropylanthracene (**2**), 9-cyclopropyl-10-methylanthracene (**3**) and 9,10-dimethylanthracene (**4**).

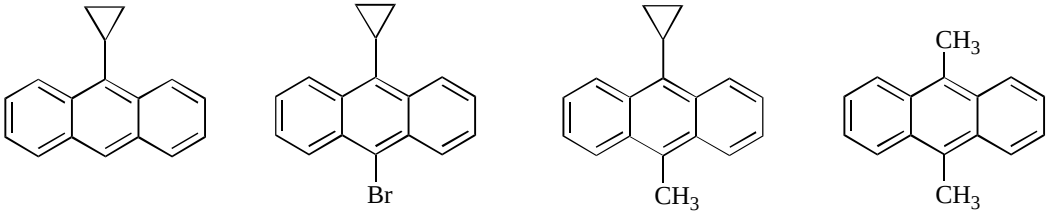

1 **2** **3** **4**

5.1.2 Literature Review

The cyclopropane ring opening and alkyl deprotonation of radical cations generated from benzene derivatives has been reviewed in detail in Chapter 1. The following highlights literature pertaining to the oxidation of alkylanthracenes. There are basically three groups who have done most of significant work on this area.

Parker's Group. The reactions of the radical cations of anthracene and its 9-mono- and 9,10-disubstitued methyl, phenyl, methoxy and halogen derivatives have been studied by Parker using electrochemical methods.[132] These studies mainly revealed products derived from nucleophilic addition of solvent (water, acetic acid or alcohol) to the radical cations, except for 10-methoxy-9-methylanthracene.[133] Proton loss from methyl-substituted anthracene radical cations was not observed. Anodic

acetoxylation[132,134] and methoxylation[132] of anthracene, 9-methylanthracene and 9,10-dimethylanthracene (DMA, **4**) produce 9,10-disubstituted derivatives (Scheme 5-1).

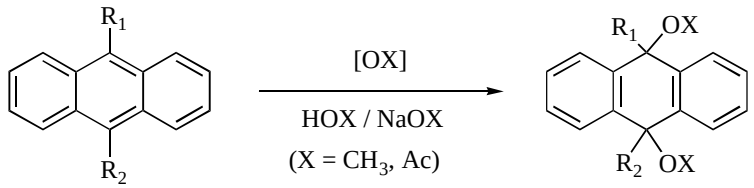

R_1 = H, CH_3
R_2 = H, CH_3

Scheme 5-1. Anodic oxidation of anthracene and substituted anthracenes

Lead tetraacetate oxidation of anthracene in benzene[135] was reported to give 9,10-diacetate-9,10-dihydroanthracene,[132] but lead tetraacetate oxidation of DMA was reported to yield side-chain substituted diacetate (Scheme 5-2).[136] The mechanism for this reaction was suggested to involve the initial formation of 9,10-diacetate-9,10-dimethylanthracene **A**, followed by elimination of acetic acid to give **B**, and rearrangement of **B** to give **C** as an intermediate (Scheme 5-2).[137] Heating **A** in acetic acid resulted in the formation of **C** in quantitative yield,[132] which supported this mechanism.

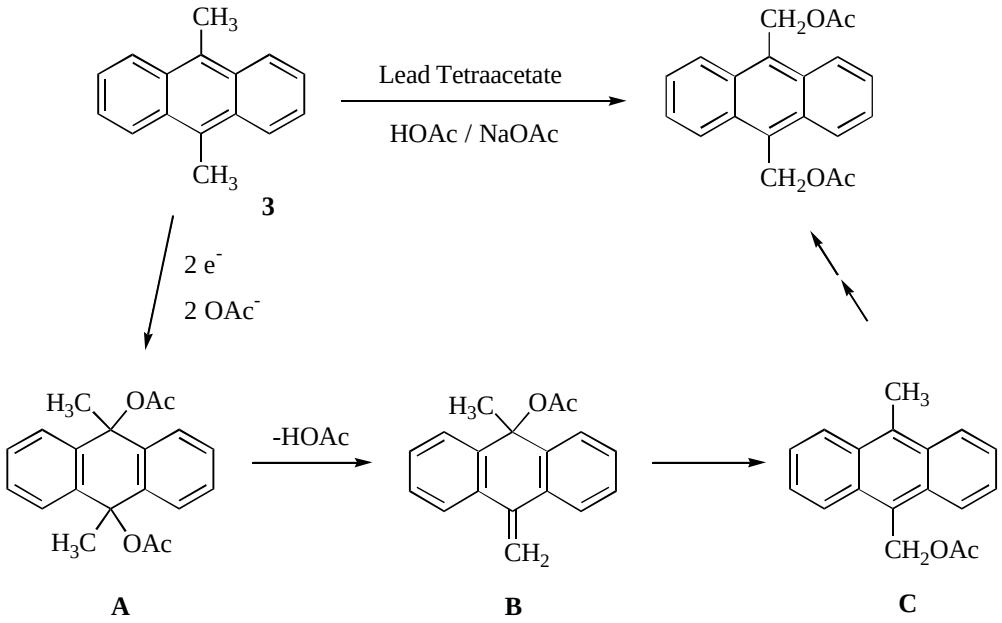

Scheme 5-2. Lead tetraacetate oxidation of DMA and proposed mechanism

Tolbert's Group. Tolbert and coworkers studied chemical and biomimetic oxidation of 9,10-dialkylanthracenes in CH_3CN/H_2O in 1990's (see Chapter 1.2). They found that when a methyl group is present, rapid deprotonation of these radical cations occurs. For example, *meso*-methylanthracenes were oxidized by one-electron oxidant (e.g., Fe(III)) to hydroxymethyl derivatives (Scheme 5-3).[68] No significant ring oxidation products were observed. On the other hand, they observed that when an ethyl group is present, stereoelectronic effects inhibit deprotonation of the radical cation. *Meso*-ethylanthracenes was found to undergo a facile chemical or biochemical oxidative elimination of ethylene to yield an anthrone rather than deprotonation product (Scheme 5-3).[69]

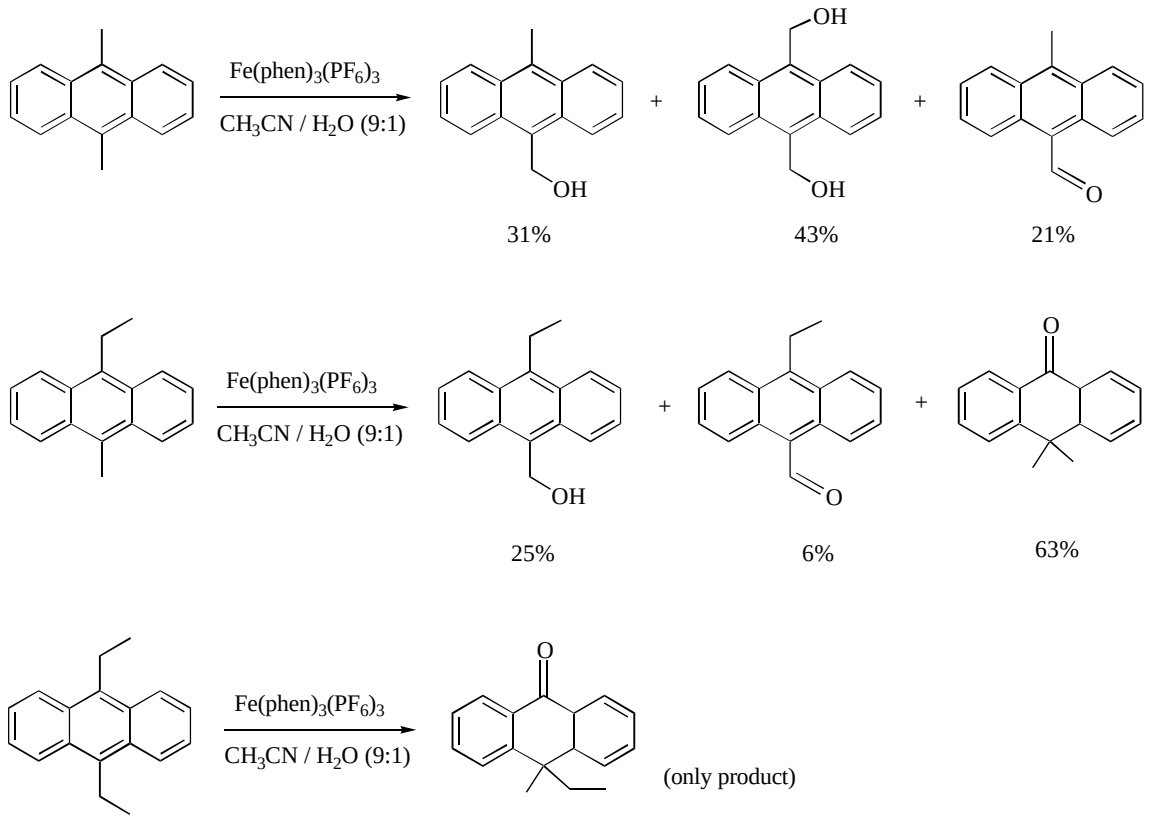

Scheme 3-3. Fe(III) oxidation of 9,10-dialkylanthracenes in CH_3CN/H_2O

More recently, iodine,[138,139] Ce(IV)[140] and biochemical oxidation[71] of 9-mono-, and 9,10-disubstituted-anthracenes were reported. Oxidation of 9-alkylanthracenes by I_2 in $CHCl_3$/pyridine led to nuclear oxidation product. In contrast, oxidation of 9-alkyl-10-methylanthracenes gave side-chain oxidation products (Scheme 5-4).

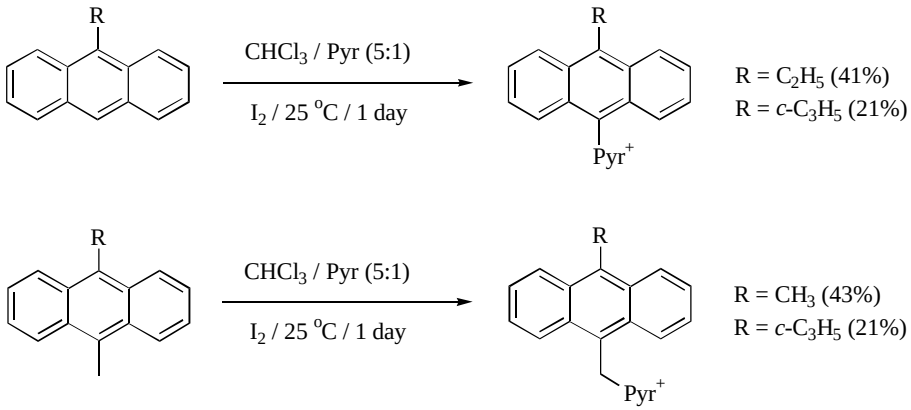

Scheme 5-4. Iodine oxidation of 9-alkyl-, and 9-alkyl-10-methyl-anthracenes

For aceanthracene and 9-methylaceanthracene, oxidation under same conditions led to predominantly side-chain oxidation products (Scheme 5-5).

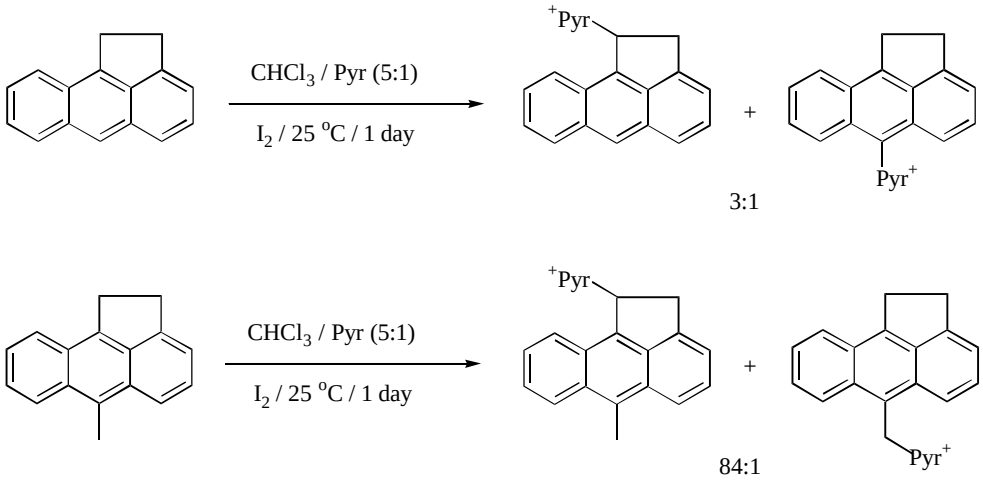

Scheme 5-5. Iodine oxidation of aceanthracene and 9-methylaceanthracene

Ce(IV) oxidation of 9-alkylanthracene and 9,10-dialkylanthracene in CH_3CN/H_2O was also reported. When R was methyl, ethyl and cyclopropyl, nuclear oxidation products were obtained. The rate of loss of alkyl or hydrogen was H > CH_3 > C_2H_5. However,

oxidation of aceanthracene mainly produced side-chain oxidation product. The product distribution of these reactions is shown in Scheme 5-6, in which the number below each product is the area percent obtained from GC (not yields).

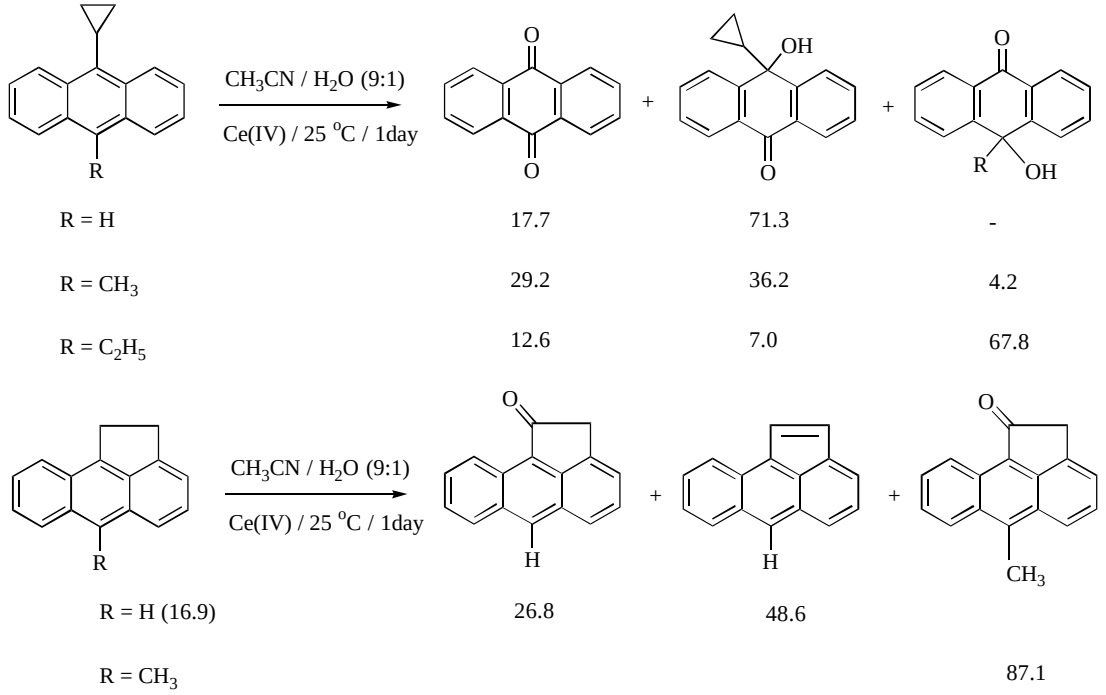

Scheme 5-6. Ce(IV) oxidation of alkylanthracenes in CH_3CN/H_2O

The results obtained from Tolbert's group obviously conflict with those from Parker's group in terms of initial oxidation products. Thus, the decay mechanism of alkylanthracene radical cations, namely side-chain vs. nuclear oxidation, is unclear.

Camaioni's Group. Cu(II)-catalyzed peroxydisufate oxidation of anthracene and alkylanthracenes in CH_3CN in the presence of water or acetic acid was extensively studied by Camaioni and coworkers.[141,142,143] For 9-methylanthracene,[72,73] side-chain and nuclear

oxidation products and the dimeric compound, lepidopterene, were produced. The product nature is depended on solvent system being used. In CH_3CN/H_2O, the ring oxidation products, 9-hydroxy-9-methylanthrone and its dehydronation product 9-methyleneanthracene, are predominant, while in $CH_3CN/HOAc$, the side-chain oxidation products like 9-anthracenylmethyl acetate is mainly produced (Scheme 5-7).

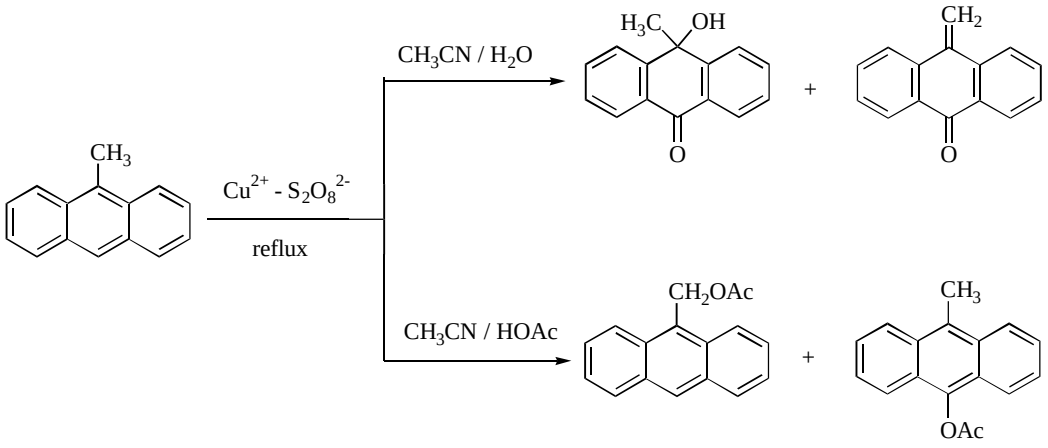

Scheme 5-7. Cu^{2+}-$S_2O_8^{2-}$ oxidation of 9-methylanthracene

Similar oxidations were also performed for the other related substrates such as 9-phenylethylanthracene and DMA, and the products are similar to those obtained from oxidation of 9-methylanthracene (Scheme 5-8).

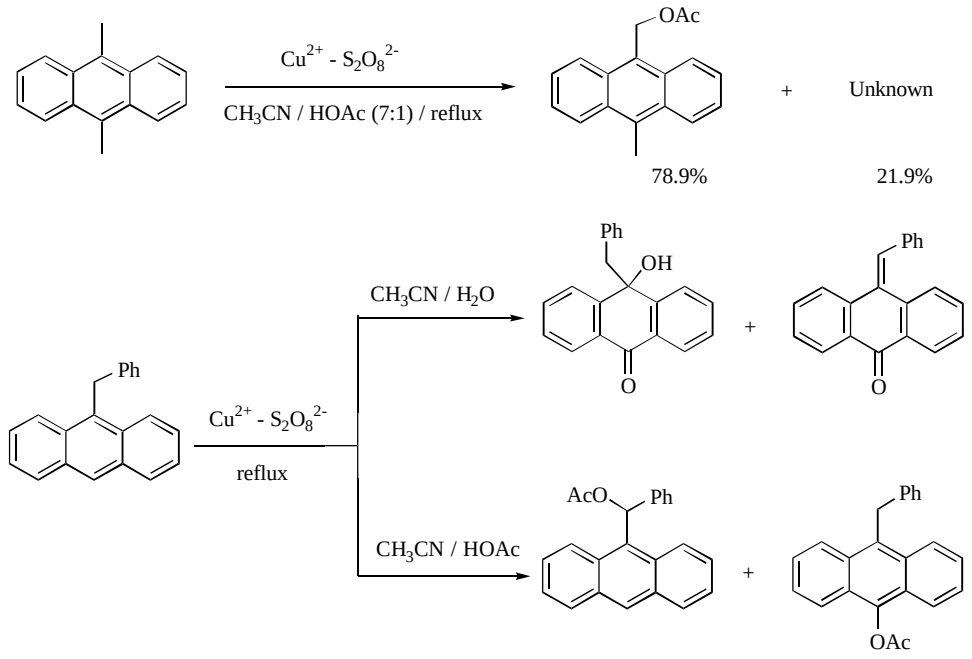

Scheme 5-8. Cu^{2+}-$S_2O_8^{2-}$ oxidation of DMA and 9-phenylethylanthracene

A mechanism was proposed where the initially formed radical cation underwent competing proton loss and reversible nucleophile addition reactions. The preferred reaction pathway was observed to be structure and medium dependent. It was also noted that acidity of medium might play a role in the product nature of the oxidation. However, the detailed mechanism for the formation of side-chain oxidation product was still unsolved.

Other Groups. Sugiyama[144] in 1987 reported direct alkoxylation of anthracene with some lower alcohols and ethylene glycol monoalkyl ethers, or monoacetate in the presence of cerium(IV)tetrakis(trifluoro acetate), and the expected alkoxylated anthracene derivatives were obtained (Scheme 5-9). Fujita and Fukuzumi[145] in 1993 found that

Fe(III) oxidation of 9-benzylanthracene in CH_3CN led to nuclear oxidation product, 9-benzyl-9-hydroxyanthrone (Scheme 5-9). The decay kinetics of 9-benzylanthracene radical cation in CH_3CN was studied by using a stopped flow spectrophotometer. In 1991, Oyama, M., et al.[146] studied substituent effects on the reaction kinetics of electrogenerated 9-substituted 10-phenylanthracene radical cation with water and methanol. While the products of the reactions of 9,10-diphenylanthracene radical cation with methanol were 9,10-dialkoxy-9,10-diphenylanthracene,[147] the isolated product was 9-methoxy-9-phenylanthrone in all reaction of other 9-substituted-10-phenylanthracene radical cation with methanol (Scheme 5-9). In the reactions with water, the product was hydroxy form instead of the methoxy one. The reaction kinetics and mechanism of these radical cations were studied in detail by pulse-electrolysis stopped-flow method.

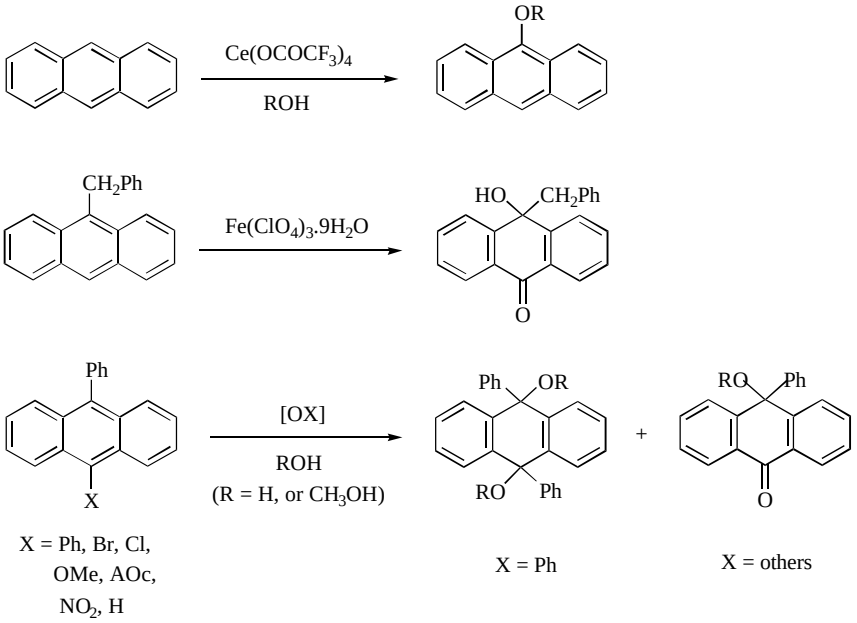

Scheme 5-9. Oxidation of anthracenes and substituted anthracenes

5.2 RESULTS AND DISCUSSION

5.2.1 9-Cyclopropylanthracene and 9-Bromo-10-cyclopropylanthracene

In Chapter 4, the follow-up chemistry of radical cations generated from 9-cyclopropylanthracene (**1**) and 9-bromo-10-cyclopropylanthracene (**2**) in the presence of methanol were examined electrochemically. It is found that these radical cations do not undergo unimolecular or methanol-induced cyclopropane ring opening and products isolated are attributable to methanol addition to aromatic ring. In an extension of this work, we began an examination of ceric (IV) ammonium nitrate (CAN) oxidation of **1** and **2** in CH_3CN/CH_3OH, based on the fact that Ce(IV) is a typical one-electron oxidant.

9-Cyclopropylanthracene (1). Ce(IV) Oxidation of **1** in 9:1 (v/v) CH_3CN/CH_3OH at room temperature mainly produces 9-cyclopropyl-10-methoxyanthracene (**5**) and 9-cyclopropyl-9-methoxyanthrone (**6**). Some anthraquinone (**7**) and 9,10-dimethoxy derivative (**8**) were also formed (Scheme 5-10). The results are summarized in Table 5-1. The nature of the reaction products is consistent with the literature and is also consistent with the results from our electrochemical oxidation (see Chapter 4).

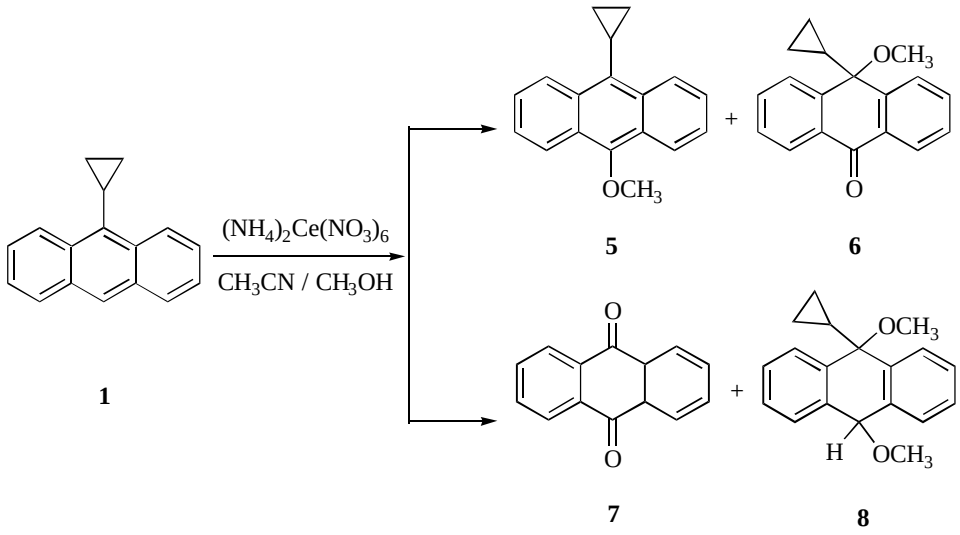

Scheme 5-10. Ce(IV) oxidation of **1** in CH_3CN/H_2O

Table 5-1. Product yields of Ce(IV) oxidation of **1** in CH_3CN/CH_3OH

Substrate (mmol)	Mole Ratio (Ce(IV)/**1**)	Product Yields (%)[a]				
		1	**5**	**6**	**7**	**8**
0.225	2	10	29	17	9	9
0.122	4	0	22	48	21	2

[a] Isolated yields.

Since Ce(IV) is known to be a one-electron oxidant, the mole ratio of two reactants (Ce(IV)/substrate) reflects the number of electrons transferred in an oxidation

reaction. Table 5-2 showed the effect of mole ratio of **1** to Ce(IV) on product yield distribution. Obviously, **5** is a two-electron oxidation product, which is initially produced and than further oxidized to a four-electron product **6**.

Table 5-2. Product distribution of Ce(IV) oxidation of **1** in different mole ratios of Ce(IV):**1**

Substrate (mmol)	Mole Ratio (Ce(IV)/**1**)	Product Yields (%)[a]		
		1	**5**	**6**
0.025	1	61	8	2
0.025	2	29	38	10
0.025	3	0	31	22
0.025	4	0	21	43

[a] GC/HPLC yields, only **1**, **5**, **6** were analyzed.

9-Bromo-10-cyclopropylanthracene (2). For **2** under similar condition, only **6** is produced as major product (Scheme 5-11). Some anthraquinone (**7**) is also formed during oxidation, which is attributable to trace water present in the solvent. The results are shown in table 5-3.

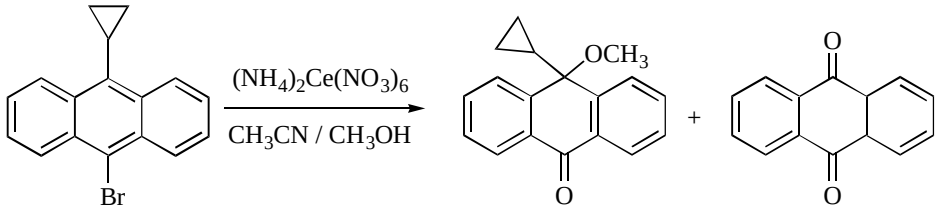

2 **6** **7**

Scheme 5-11. Ce(IV) oxidation of **2** in CH_3CN/CH_3OH

Table 5-3. Product yields of Ce(IV) oxidation of **2** in CH_3CN/CH_3OH

Substrate (mmol)	Mole Ratio (Ce(IV)/**2**)	Product Yields (%) **6**	**7**
0.143	2.1	60[a]	9[a]
0.021	2.1	76[b]	8[b]

[a] Isolated yields; [b] HPLC yields.

For the oxidation of **2**, two moles of electrons are needed to form product **6**. It is noted that **5** was not formed during oxidation of **2** and HBr was produced in the solution. The product nature and yields are similar to those observed in our electrochemical studies (see Chapter 4).

Oxidation Mechanism of 1 and 2. The oxidation mechanism for **1** and **2** is proposed in Scheme 5-12. Radical cation $\mathbf{1}^{+\cdot}$ can be either attacked by CH_3OH followed by oxidation or disproportionated to a dication followed by CH_3OH attack to form methoxy substituted cation. Our electrochemical results and results from Fujita and Fukuzumi's Fe(III) oxidation of 9-benzylanthracene revealed that the 9-substituted anthracene radical cation undergoes disproportionation[145] to give the corresponding dication, which is caught by methanol to form the methoxy substituted cation followed by rapid proton loss to produce **5**. From **1** to **5**, two electrons must be transferred. Radical cation $\mathbf{5}^{+\cdot}$ demethylates to a ketyl radical which experiences further oxidation to the corresponding cation, followed by methanol attack to form **6**. From **5** to **6**, two more electron transfers must be transferred. For **2**, it is radical cation or dimer radical cation (complex) that is attacked by methanol based on our electrochemical results. Since HBr was produced and no **5** was detected, the mechanism is better proposed as in Scheme 5-12. However, loss of HBr was questioned by Oyama, et al..[146] From **2** to **6**, a two electron transfer is needed. The final product **6** is similar to those obtained from oxidation of 9-phenylanthracene and 9-bromo-10-phenylanthracene.[146]

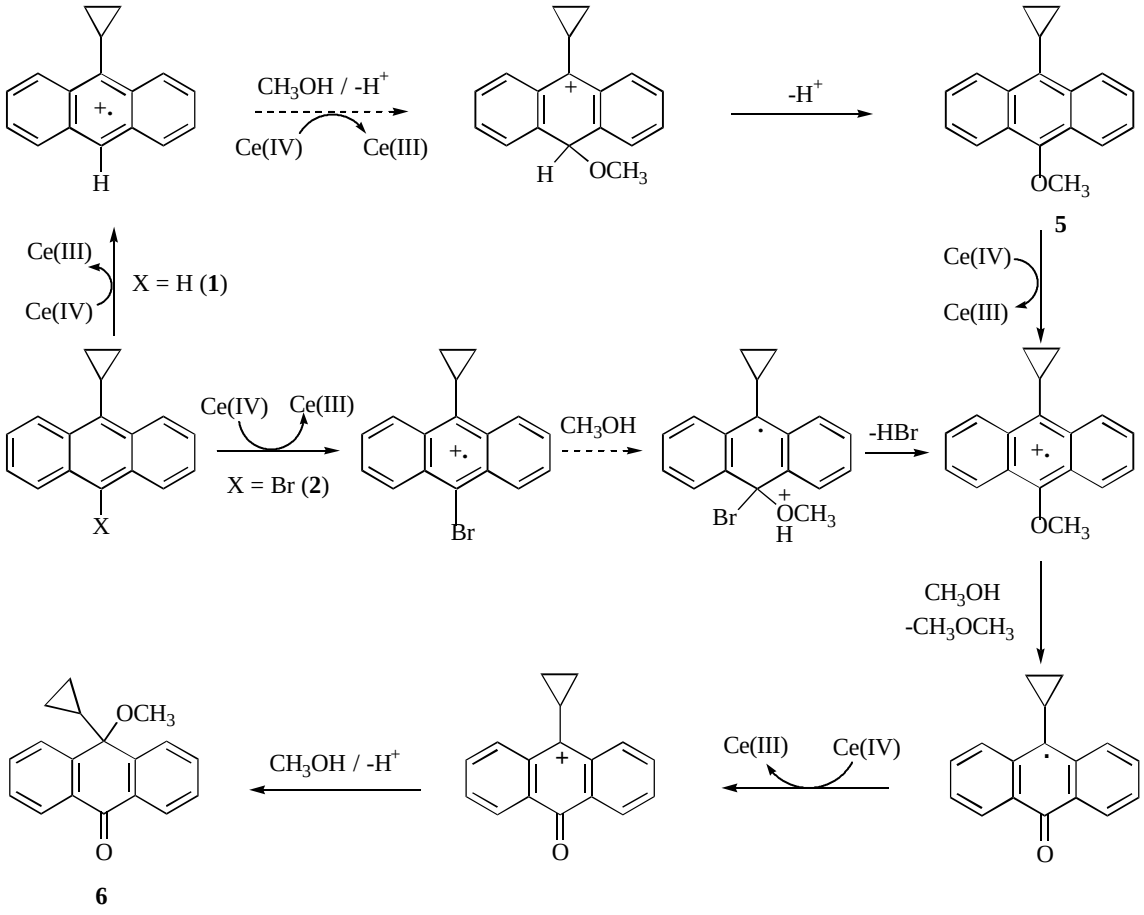

Scheme 5-12. Proposed mechanism of Ce(IV) oxidation of **1** and **2**

Unlike cyclopropylbenzenes, radical cations generated from **1** and **2** do not experience methanol-induced ring opening but rather methanol attack to aromatic ring. The possible reasons for the lack of reactivity of the cyclopropyl group were discussed earlier. However, regardless of the interpretation, the survival of cyclopropyl group in **1** and **2** during oxidation processes makes a case that the assumption (that cyclopropane ring opened products will be obtained if the radical cation is an important reaction

intermediate) being used is misleading, and suggest that caution should be exercised in the use of cyclopropane-containing systems as radical cation probes.

5.2.2 9-Cyclopropyl-10-methylanthracene and 9,10-Dimethylanthracene

9-Cyclopropyl-10-methylanthracene (3). Results for the Ce(IV) oxidation of **3** in CH_3CN/CH_3OH under two conditions are summarized in Scheme 5-13 and Table 5-4. The two-electron oxidation products **9** and **10** were obtained. At 0 ^oC, only the nuclear oxidation product, 9-cyclopropyl-10-methyl-9,10-dimethoxyanthracene (**10**), was produced in a 90.5% yield. When reaction temperature is increased to 45 ^oC, side-chain oxidation product, 9-cyclopropyl-10-methoxymethylanthracene (**9**), along with **10** was also obtained. The cyclopropyl group survived during the oxidation processes and behaved just like any other alkyl substituent. The reaction proceeded quantitatively and mass balance is greater than 95%. The product yields were determined by ^1H NMR with $(CH_3)_3SiOSi(CH_3)_3$ as an internal standard.

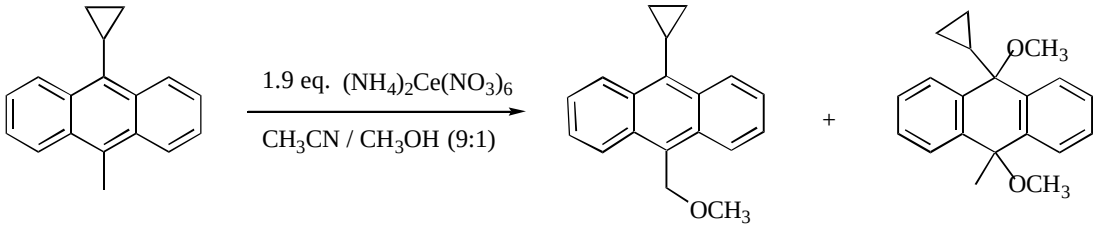

3 **9** **10**

Scheme 5-13. Ce(IV) oxidation of **3** in CH_3CN/CH_3OH

Table 5-4. Product yields of Ce(IV) oxidation of **3** in two reaction conditions

Run	Reaction Conditions	Product Yields (%)[a]	
		9	**10**
1	0 ^{o}C / 30 min	0.0	90.5
2	45 ^{o}C / 30 min	37.3	57.4

[a] ^{1}HNMR yields.

9,10-Dimethylanthracene (4). Results for the Ce(IV) oxidation of **4** under CH_3CN/CH_3OH in different conditions are summarized in Scheme 5-14 and Table 5-5. The two-electron oxidation products, 9,10-dimethoxy-9,10-dimethylanthracene (**12**) and 9-methoxymethyl-10-methylanthracene (**11**) were obtained. As found for the oxidation of **3**, at 0 ^{o}C, nuclear oxidation product **12** is sole product detected, while at 45 ^{o}C both nuclear and side-chain oxidation products **11** and **12** were formed. The product yields and mass balance are very good. To answer the question as to whether or not product **11** is derived from **12**, a control experiment (run 3 in Table 5-5) was performed in the following manner: Oxidation of **4** in CH_3CN/CH_3OH was run at 0 ^{o}C for 30 min, then the reaction solution was divided into two portions. Portion one was directly worked up and analyzed by ^{1}HNMR. Portion two was heated to 45 ^{o}C for another 30 min and then worked up and analyzed. The product nature and yields were the same as those in two other independent experiments (run 1 and run 2). From these results, it is obvious that the side-chain oxidation product **11** comes from nuclear oxidation product **12** at higher temperature.

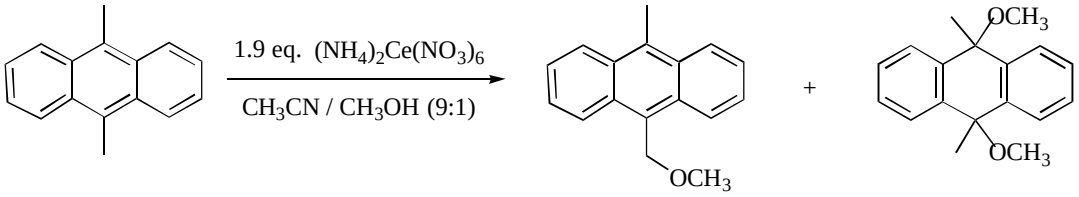

4 **11** **12**

Scheme 5-14. Ce(IV) oxidation of **4** in CH_3CN/CH_3OH

Table 5-5. Product yields of Ce(IV) oxidation of **4** in different conditions

Run	Reaction Conditions	Product Yields (%)[a]	
		11	**12**
1	0 °C / 30 min	0.0	98.3
2	45 °C / 30 min	40.8	53.0
3 portion 1	0 °C / 30 min	0.0	94.3
portion 2	0 °C / 30 min, then 45 °C /30 min	43.0	49.0

[a] ^1H NMR yields.

Ce(IV) oxidation of **4** in CH_3CN in the absence of methanol at 0 °C gave side-chain oxidation product **14**, which was thought to be converted from intermediate compound **13** during workup (Scheme 5-15). Since **13** is extremely unstable, its isolation is difficult. On the other hand, conversion from **13** to **14** is expected to be much easier,

even at lower temperature. One experiment was designed to confirm that side-chain oxidation product is not initial oxidation product in the following manner: The oxidation was conducted in the CD_3CN at 0 ^oC and the reaction mixture was directly analyzed by ^{1}HNMR before workup and after workup. Figure 5-1 shows the ^{1}HNMR of starting material **4** (**a**), and the reaction mixture before workup (**b**) and after workup (**c**). Obviously, after reaction and before workup (**b**), almost all of **4** is consumed and no signal attributable to side-chain oxidation product **14** was detected (no $\delta = 6.5$ singlet in ^{1}HNMR, which corresponds to methylene protons attached to nitrate group). This experiment revealed that initial oxidation product(s) was anthryl ring oxidation product (**13**?, which is unstable and easy to be converted) rather than side-chain oxidaton product (**14**).

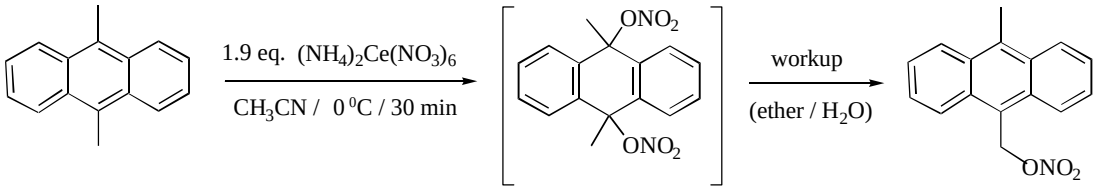

4 **13** **14**

82% (run 1)
85% (run 2)

Scheme 5-15. Ce(IV) oxidation of **4** in CH_3CN

Figure 5-1. ^{1}HNMR of **4** (**a**), reaction mixtures before workup (**b**) and after workup (**c**)

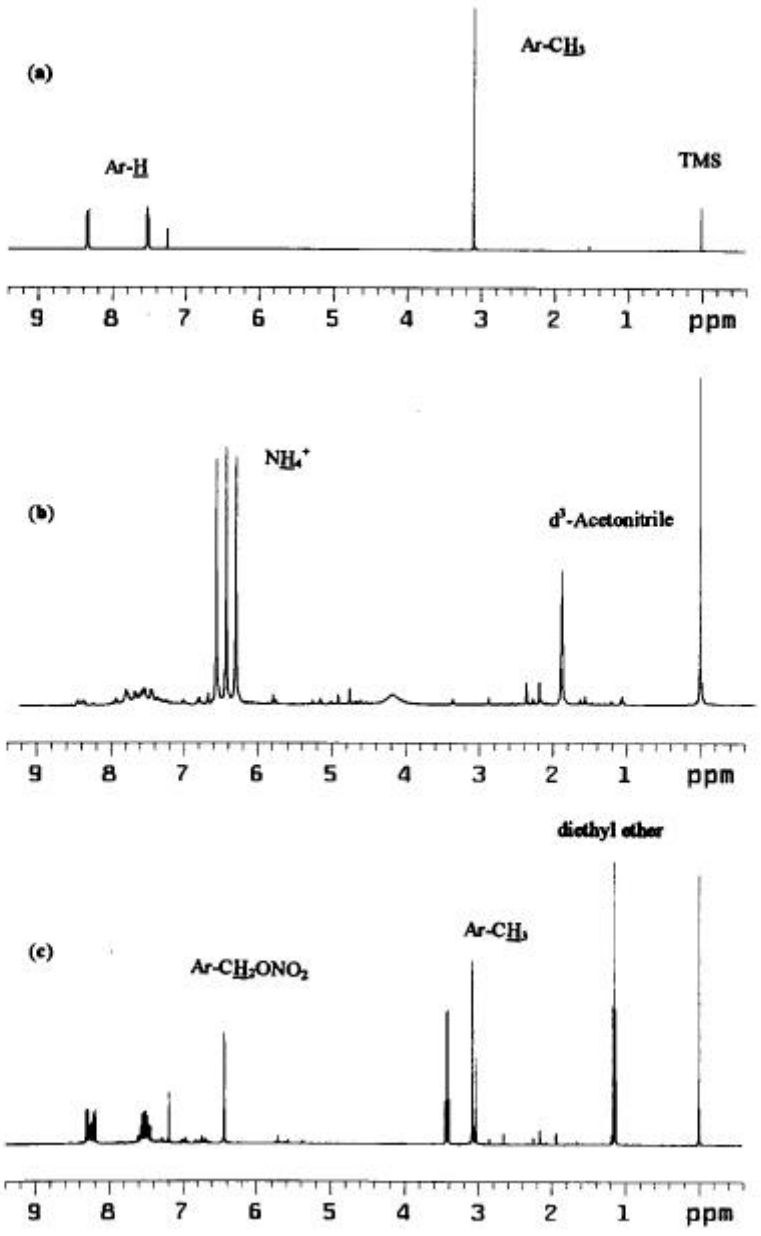

Control Experiment. In order to confirm that the observed side-chain oxidation products are formed from nuclear oxidation products, the following control experiments were run (Scheme 5-16). Compound **10** was heated in $CDCl_3$ at 50 ^oC for one hour and no reaction occurred. However, when two drops of H_3PO_4 were added, the product **9** was produced. It was noted that protons present in the solution catalyze the conversion of **10** to **9**. Because under conditions of Ce(IV) oxidation protons were produced from CH_3OH (formation of one mole of oxidation product **10** can introduce two moles of protons), side-chain oxidation products are formed from nuclear oxidation products.

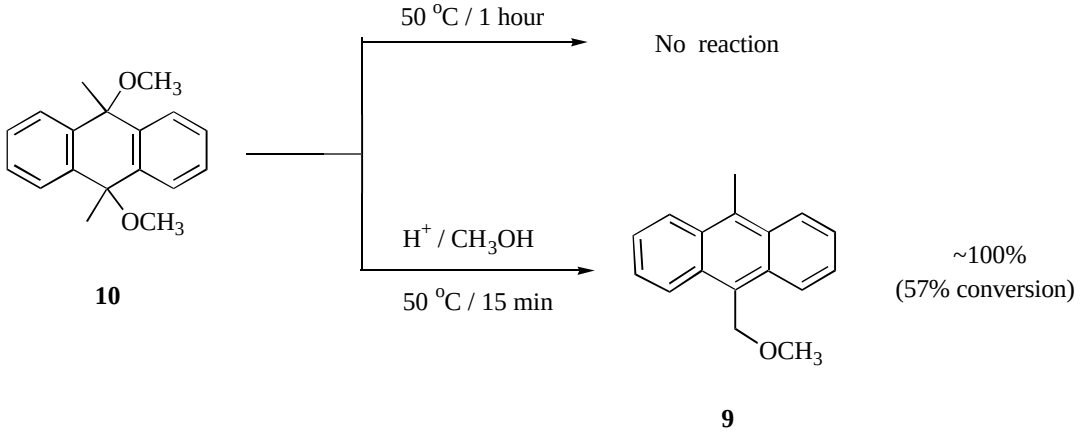

Scheme 5-16. Control experiment to test whether **10** can be converted into "deprotonation" product **9** under conditions of Ce(IV) oxidation

5.2.3 Nuclear vs. Side-Chain Oxidation

Our results from Ce(IV) oxidation of **3** and **4** in CH_3CN/CH_3OH reveal that the initial oxidition products are nuclear oxidation products rather than side-chain oxidation products. The latter are formed from the former under acidic conditions at higher temperatures. There are two questions will be discussed in this section: Why do the radical cations of alkylanthracene undergo nucleophilic addition rather than deprotonation? Where do the side-chain products come from and how are they formed?

Oxidation Mechanism of 4. The mechanism for the Ce(IV)-induced oxidation of **4** is shown in Scheme 5-17, and is similar to those proposed for 9,10-dialkylanthracenes. One electron oxidation of **4** by Ce(IV) generates $\mathbf{4}^{+\cdot}$. CH_3OH attack on $\mathbf{4}^{+\cdot}$ forms 9-methoxy-9,10-dimethylanthracene radical, which upon removal of another electron by Ce(IV) produces the corresponding cation. The cation is captured by a molecule of methanol to form the addition product **10**.

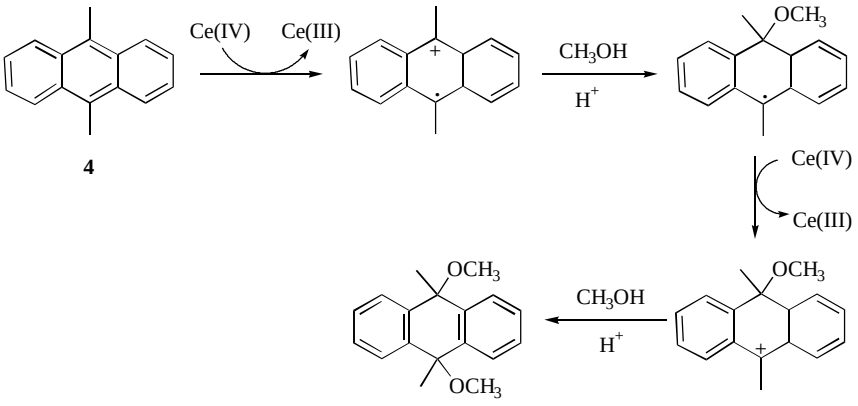

4 **10**

Scheme 5-17. Oxidation mechanism of **4** in CH_3CN/CH_3OH

Decay Pathway of Alkylarene Radical Cations. The fact that radical cations generated from alkylbenzenes (e.g., toluene and polymethylbenzenes) undergo "fast deprotonation" has been accepted as a typical reaction pathway of alkyl aromatic compounds (Chapter 1). The pK_a of toluene radical cation is negative (-13 in CH_3CN, -20 in DMSO[148]), which seems to be consistent with this conclusion because deprotonation of toluene radical cation is exothermic (suppose that CH_3OH is the base in the reaction, the pK_a of its conjugated acid is -2 → -4). However, this rationale is questioned based on the fact that alkylanthracene radical cations do not undergo deprotonation even if deprotonation of these anthryl radical cations is also exothermic although less so than for toluene radical cations (the pK_a of 9-methylanthracene radical cation is also around -6.4[149]). This situation is analogous to the methanol-induced cyclopropane ring opening of cyclopropylanthracene radical cation which is disfavored due to a higher intrinsic barrier because of the localized positive charge in the transition state. Instead, nucleophilic addition of methanol to alkylanthracene radical cations become predominant. Since the mechanism of deprotonation of an alkylarene radical cation is similar to that of ring opening of a cyclopropylarene radical cation, we suggest that an analogous transition state picture can be applied for deprotonation process of alkylarene radical cations (Figure 5-2).

In Figure 5-2, a product-like transition state for deprotonation was proposed, in which spin density is delocalized over the benzylic carbon and the aromatic ring, but charge is highly localized at methyl-hydrogen and methanol-oxygen. As such, in the transition state, the aryl group can stabilize the radical portion of the radical ion, but will

have little effect on the positive charge. The effect of the aromatic ring on the rate of deprotonation is primarily due to changes in the free energy of the reactant, with only a modest effect on the free energy of the transition state for deprotonation.

Figure 5-2. Proposed effect of different aryl groups on the stabilities of reactants, transition states, and products for deprotonation of $ArCH_3^{+\cdot}$

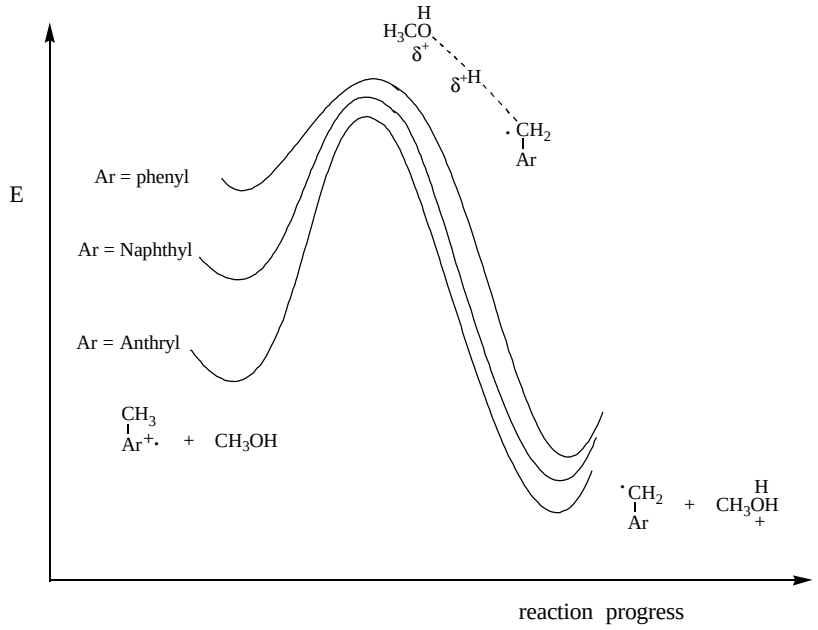

Thus, for alkylanthracene radical cations, due to higher intrinsic energy barrier, deprotonation process is basically “turn off” and nucleophilc addition to aromatic ring becomes kinetically favored.

Sehested and Holcman[150] studied reactions of the radical cations of methylated benzene derivatives in aqueous solution and measured the rate constants for proton loss reaction and nucleophilic addition reaction of these radical cations. They found that nucleophilic addition is faster than proton loss but is highly reversible (Scheme 5-18). The

deprotonation product is the isolated product since proton loss of radical cation is irreversible.

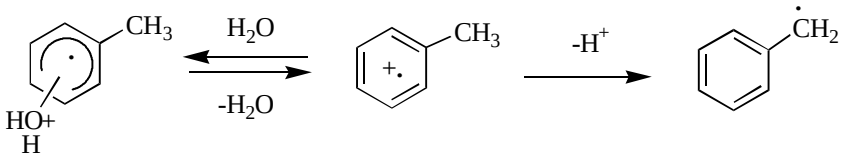

Scheme 5-18. Nucleophilic addition vs. deprotonation of toluene radical cation

For alkylbenzene radical cations, Scheme 5-18 describing two two competing decay pathways can be pictured in the reaction energy diagram shown in Figure 5-3. Nucleophilic addition to toluene radical cation is the kinetically favored process and deprotonation of this radical cation is thermodynamically favored process. Since the intrinsic energy barrier is lower for deprotonation process of toluene radical cation (compared to 9-methylanthracene radical cation, see Figure 5-2), the deprotonation is the observed pathway under certain conditions (e.g., relatively long reaction time or higher temperature).

Figure 5-3. Proposed reaction energy diagram of toluene radical cation

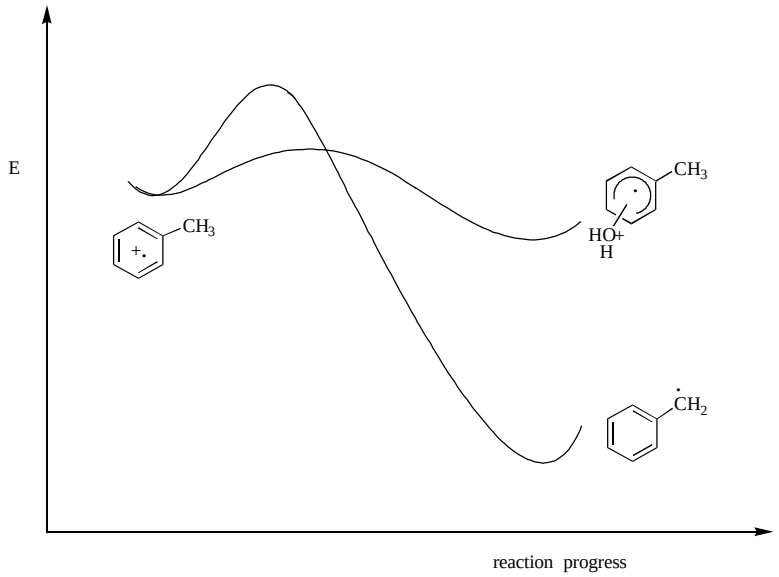

It was also noted by Sehested and Holcman[150] that the rate constants for deprotonation of methylated benzene radical cations decreases by three orders of magnitude as the number of methyl groups increases from one to five. This means that more stable radical cation is less likely to deprotonate because the intrinsic barrier for deprotonation is higher and thus it is kinetically disfavored (Figure 5-2).

For alkylanthracene radical cation, as shown in Figure 5-2, the intrinsic barrier is so high for deprotonation process that no deprotonation product is produced (Figure 5-4). Instead, nucleophilic addition predominates.

Figure 5-4. Proposed reaction energy diagram for 9-methylanthracene radical cation

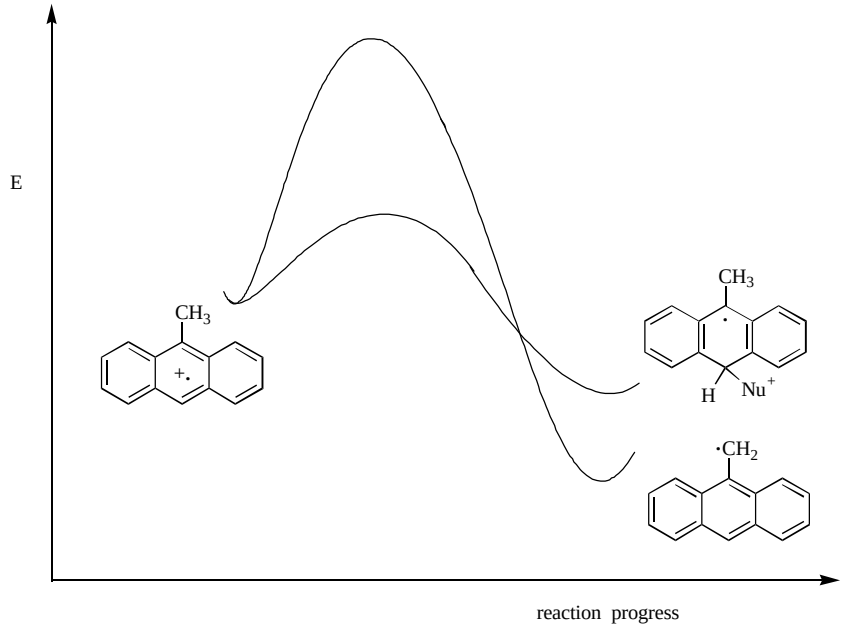

Conversion Mechanism of Product 10 to 9. A likely mechanism for the conversion of **10** to **9** is shown in Scheme 5-19.

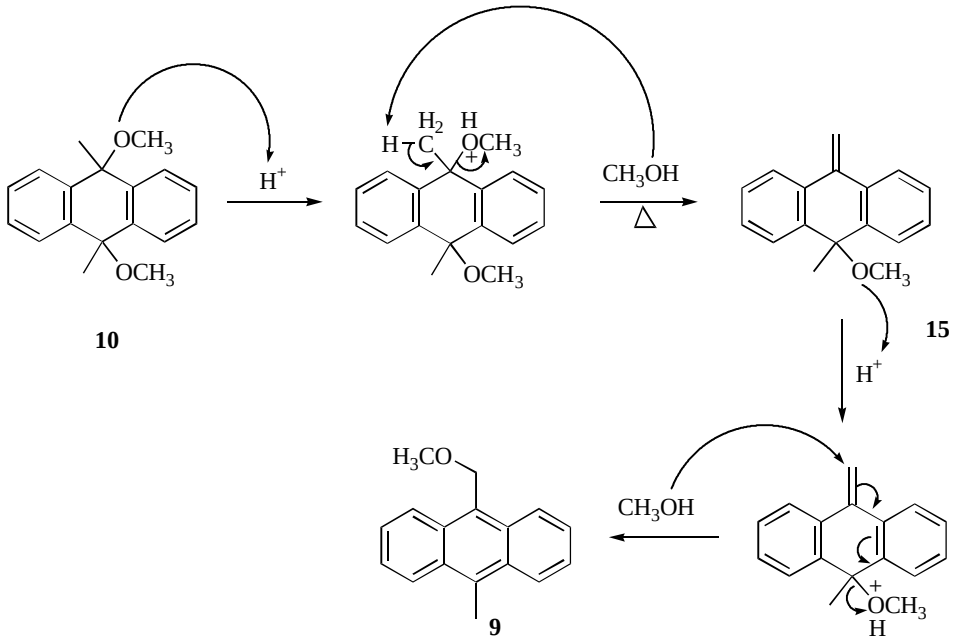

Scheme 5-19. Mechanism for the conversion (**10** → **9**) under acidic conditions

The methoxy group in **10** is protonated under acidic conditions, and methanol is eliminated at higher temperature. The resulting 9-methoxy-9-methyl-10-methyleneanthracene (**15**) is then converted into **9**. This mechanism is further conformed by isolating **15** as an intermediate product.

Elimination of a molecule of nucleophile (e.g., H_2O or CH_3CO_2H) from addition products to form 9-methyleneanthracene derivatives under acidic conditions was also reported by Camaioni[143] in his studies (e.g., Scheme 5-8). A similar mechanism for product interconversion was proposed by Camaioni[143] for solvolysis of 9,10-diethyl-9,10-dihydroxyanthracene catalyzed by perchloric acid in CH_3CN/H_2O (Scheme 5-20). The "deprotonation" product is formed from the addition product under acidic condition.

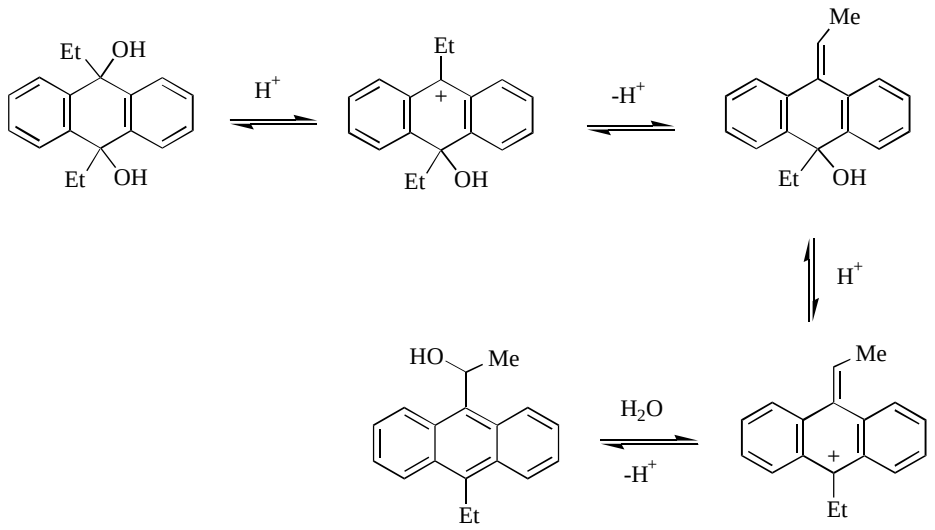

Scheme 5-20. Mechanism of solvolysis of 9,10-diethyl-9,10-dihydroxyanthracene in H^+/H_2O

Stereoelectronic vs. Thermodynamic Factors. Stereoelectronic effects on deprotonation of alkylanthracene radical cations have been reported by Tolbert, et al..[69] If the alkylanthracene radical cation does not undergo deprotonation, stereoelectronic factors can not be evaluated. Stereoelectronic factors if any may increase the intrinsic barrier to deprotonation as shown in Figure 5-1.

A very good question arose here: Does the radical cation of 9-cyclopropyl-10-methylanthracene (**3**) deprotonate at higher temperature? If it does this result might argue for the existence of stereoelectronic factors. In chapter 3, it was found that the radical cation of 1-cyclopropyl-4-methylbenzene undergoes cyclopropane ring opening rather than deprotonation. However, the cyclopropyl group in **3** survives a similar oxidation

process. The reversal of product nature might reflect the stereoelectronic effects on cyclopropane ring opening of these radical cations. On the other hand, if it does not then the intrinsic barrier for deprotonation as well as cyclopropane ring opening are both high and stereoelectronic factors (if any) can not be evaluated. The possible decay pathways of $\mathbf{3}^{+\cdot}$ was shown in Scheme 5-21.

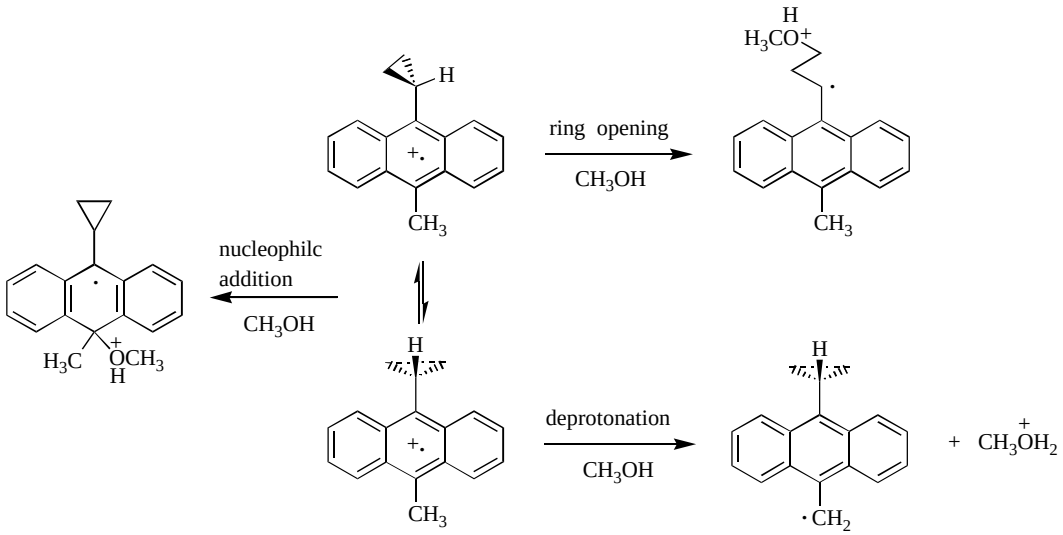

Scheme 5-21. Possible decay pathways of 9-cyclopropyl-10-methylanthracene radical cation

A Note on Reaction Conditions and Product Identification. The reaction conditions for Ce(IV) oxidation of alkylanthracenes are very important in evaluating product nature and distribution. The reaction produces protons from either solvent or added nucleophiles (e.g., H_2O, CH_3OH or CH_3CO_2H). These protons present in the solution can catalyze the interconversion of the products and proper temperature will

realize or speed up this process. It is dangerous to propose a mechanism only based on the nature of the products isolated without considering the effects of reaction conditions (e.g., temperature) on product distribution. Put more succinctly, these results suggest that in several literature studies, products attributed to the deprotonation of a radical cation may have been formed by a different pathway.

It was also found in our Ce(IV) oxidation of 9,10-dialkylanthracenes that the parent ions of nuclear oxidation products (e.g., **10**, **12**) were hard to detect by mass spectrometry, and the side-chain products (e.g., **9**, **11**) do not go through the GC (they decompose or interconvert in our GC temperature). As a result, ^{1}HNMR was employed to analyze our products.

These experimental notes can partially explain the conflicting results reported from the literature. For example, the product yields and distribution have been analyzed by GC or GC-MS in some groups. Also, It is difficult to compare the product nature and distribution in a set of reactions when the reaction conditions (e.g., temperature) are different.

5.3 SUMMARY

Ce(IV) oxidation of 9-cyclopropylanthracenes and 9,10-dimethylanthracene in CH_3CN/CH_3OH all led to aromatic nuclear oxidation products. The radical cations generated from these substrates undergo neither cyclopropane ring opening nor deprotonation but nucleophilic addition. Side-chain oxidation products from Ce(IV)

oxidation of methylated anthracenes were formed from nuclear oxidation products under acidic and higher temperature conditions. A reaction energy diagram describing the reactions of arene radical cations was proposed based on thermodynamic consideration. The results demonstrate that side-chain oxidation products formed from the oxidation of alkylanthracenes cannot be attributed solely (if at all) to the deprotonation of radical cations.

CHAPTER 6. CONCLUSIONS

The studies presented in the previous chapters detail the rich chemistry of cyclopropylarene radical cations. Anodic and Ce(IV) oxidation of both cyclopropylbenzenes and cyclopropylnaphthalenes (e.g., 1-cyclopropylbenzene, 1-cyclopropyl-4-methylbenzene, 1-cyclopropylnaphthalene, 1-bromo-4-cyclopropylnaphthalene and 2-cyclopropylnaphthalene) in CH_3CN/CH_3OH leads to cyclopropane ring-opened products (i.e., corresponding 1,3-dimethoxypropylarenes). Utilizing cyclic, derivative cyclic and linear sweep voltammetry, it was found that decay of radical cations generated from cyclopropylnaphthalenes (e.g., 1-cyclopropylnaphthalene, 1-bromo-4-cyclopropylnaphthalene, and 2-cyclopropylnaphthalene) in CH_3CN/CH_3OH is second order in radical cation and zero order in methanol. The radical cations generated from these naphthyl substrates are shown to disproportionate or dimerize before undergoing ring opening.

Dinnocenzo, et al. have reported that ring opening of 1-cyclopropylbenzene radical cation occurs via a nucleophile-induced (i.e., S_N2) pathway and the absolute rate constant for the methanol-induced ring opening is 9.5×10^7 $s^{-1}M^{-1}$. The rate constant estimated for methanol-induced ring opening ($Ar\text{-}c\text{-}C_3H_5^{+\cdot} + CH_3OH \rightarrow ArCH(\bullet)CH_2CH_2O(H^+)CH_3$) of cyclopropylnaphthalene radical cations is extremely small (<20 s^{-1} M^{-1} for 1-cyclopropylnaphthalenes). Thus, the change from phenyl to 1-naphthyl results in (at least) a six order of magnitude diminution in the rate of cyclopropane ring opening despite the

fact that ring opening for both aryl systems is exothermic (by nearly 40 kcal/mol for phenyl and 30 kcal/mol for 1-naphthyl).

AM1 calculations have shown that 1-cyclopropylnaphthalene radical cation exhibits no overwhelming conformational preference (earlier studies have found that the neutral molecule adopts a conformation midway between bisected and perpendicular). Thus for both 1- or 2-cyclopropylnaphthalene radical cations, the bisected conformation is readily accessible, suggesting that stereoelectronic factors are not responsible for the extraordinarily sluggish rate of ring opening.

Based on these results, a product-like transition state for ring opening of cyclopropylarene radical cations was proposed, in which spin density is delocalized over C-1 (the benzylic carbon) and the aromatic ring, but charge is highly localized at C-2 and oxygen. As such, in the transition state, the aryl group can only stabilize the radical portion of the developing distonic radical ion (presumably to a lesser degree than for the fully developed radical), but will have little effect on the positive charge (Figure 6-1). Consequently, the effect of the aromatic ring on the rate is primarily due to changes in the free energy of the reactant, with only a modest effect on the free energy of the transition state for ring opening.

Figure 6-1. The proposed effects of aryl rings on the stabilities of reactants, transition states and products for methanol-induced cyclopropane ring opening

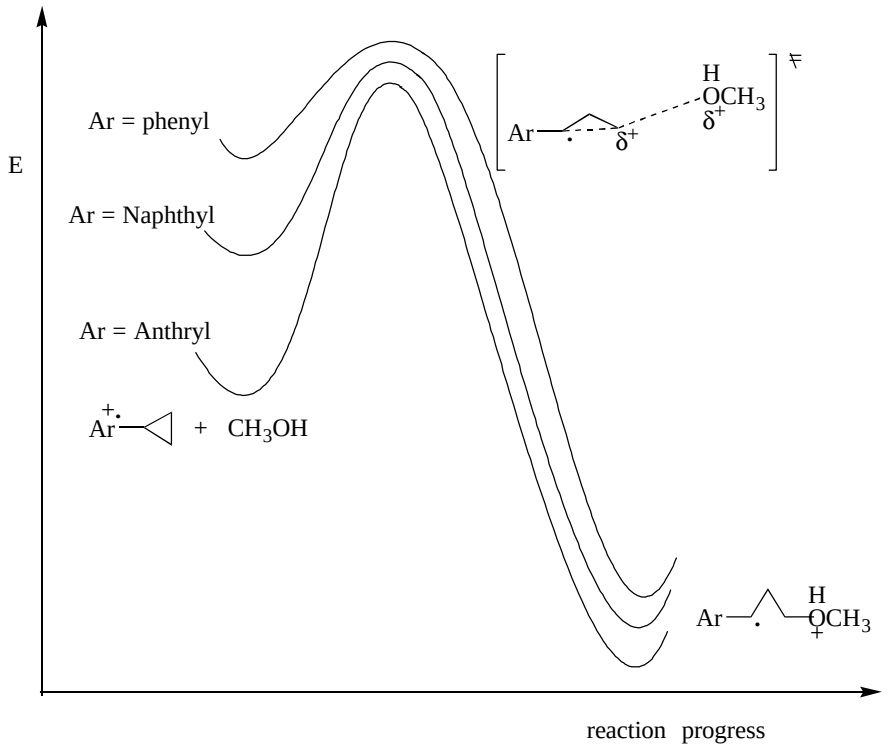

While cyclopropylbenzene radical cations undergo rapid methanol-induced ring opening and cyclopropylnaphthalene radical cations disproportionate or dimerize before undergoing slow ring opening, the radical cations generated from 9-cyclopropylanthracenes were found not to undergo cyclopropane ring opening at all. The major products arising from both electrochemical and Ce(IV) oxidation of 9-cyclopropylanthracene and 9-bromo-10-cyclopropylanthracene in CH_3CN/CH_3CN are attributable to CH_3OH attack at the aromatic ring rather than CH_3OH-induced

cyclopropane ring opening (e.g., 9-cyclopropyl-9-methoxyanthrone was produced). An analogous (more product-like) transition state picture (Scheme 6-1) can be applied for cyclopropane ring opening of these anthryl radical cations, based on similar thermodynamic and kinetic consideration. Because of higher intrinsic barrier to nucleophile-induced cyclopropane ring openong of these anthryl radical cations, nucleophilic addition occurs predominantly. The stereoelectronic effects may be another additional factor to this intrinsic barrier because the cyclopropyl group in these anthryl systems adopts a perpendicular conformation which may not meet the stereoelectronic requirements for cyclopropane ring opening at either the radical cation or dication stage.

To our surprise, Ce(IV) oxidation of 9-cyclopropyl-10-methylanthracene and 9,10-dimethylanthracene in CH_3CN/CH_3OH also leads to nuclear (aromatic ring) oxidation products. The radical cations generated from these anthryl substrates were shown to undergo neither cyclopropane ring opening nor side-chain deprotonation but nucleophilic addition to aromatic ring (e.g., Scheme 6-1). Side-chain oxidation products from Ce(IV) oxidation of these methylated anthracenes were found to be converted from nuclear oxidation products under acidic and higher temperature conditions.

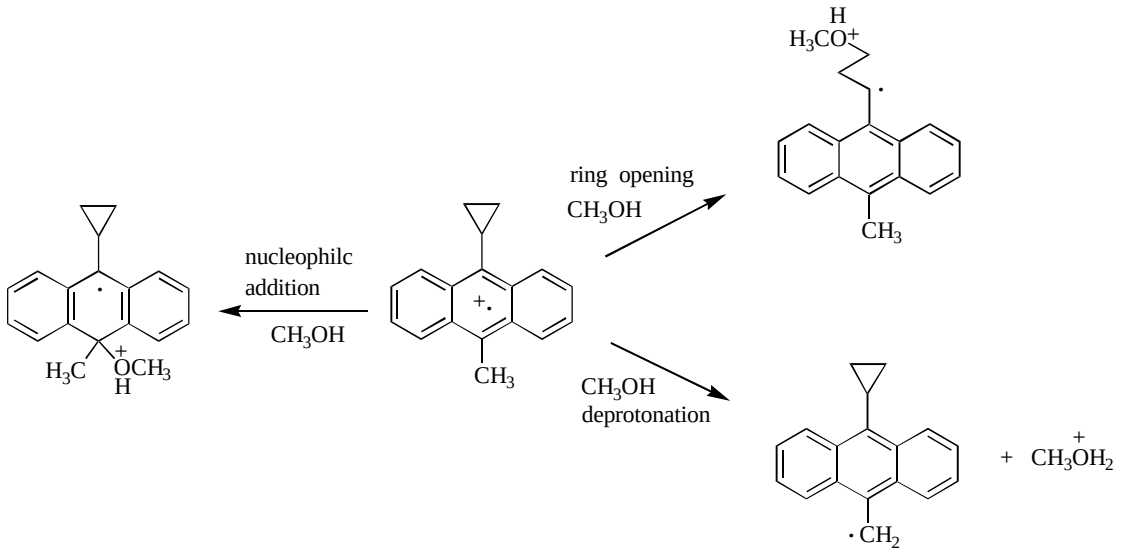

Scheme 6-1. Decay pathways of 9-cyclopropyl-10-methylanthracene radical cation in CH_3CN/CH_3OH

Because the mechanism of side-chain deprotonation of an alkylarene radical cation is similar to that of ring opening of a cyclopropylarene radical cation (Scheme 6-1), a similar transition state picture is also proposed for deprotonation reactions of alkylarene radical cations. Thus, for alkylanthracene radical cations, due to higher intrinsic energy barrier, deprotonation process is basically "turned off" and nucleophilic addition to aromatic ring becomes kinetically favored.

Cyclopropane-containing substrates are frequently employed as probes for single electron transfer. The implicit assumption in such a study is that if a paramagnetic intermediate (neutral free radical or radical ion) is produced, it will undergo ring opening. Earlier work dealing with neutral free radicals and ketyl radical anions has shown that the

rate constant for ring opening is quite large when the ring-opening is thermodynamically favored.

In the case of cyclopropylarene radical cations, despite the fact that ring opening enjoys an enormous thermodynamic driving force, the process occurs at a dramatically slower rate (for naphthyl system) or not at all (for anthryl system). Clearly, the intrinsic barrier to ring opening is greater for ring opening of these radical cations. The unique activation/driving force relationship for radical cation ring opening is likely attributable to the fact that the process is bimolecular (nucleophile-assisted). The rate of ring opening is governed by the amount of positive charge transmitted to the cyclopropane ring via resonance, and the fact that this charge becomes localized in the transition state (Figure 6-1). For neutral radicals or ketyl anions, it is spin rather than charge which is transmitted to the cyclopropyl group upon ring opening. Because ring opening is unimolecular, spin (and charge for the radical anions) is not localized in the transition state and the intrinsic barrier to ring opening is considerably lower. For cyclopropylarene radical cations, and presumably other systems which would undergo nucleophile-assisted ring opening, the fact that the ring opening reaction may enjoy a potent thermodynamic driving force is no guarantee that the ring opening will occur at an appreciable rate. Indeed, it is likely that many of the substrates discussed herein would fail to detect a bona fide SET process. Thus, these results reveal a new (and unexpected) complication in the design and utilization of SET probes.

CHAPTER 7. EXPERIMENTAL

7.1 GENERAL

7.1.1 Instrumentation Description

Melting points were determined on a Thomas Hoover capillary melting point apparatus and were uncorrected. Nuclear magnetic resonance spectra (^{1}H , ^{13}C, 2D) were obtained on either a 270 MHz Bruker or a 400 MHz Varian FT NMR spectrometer. All chemical shifts are reported in δ units relative to TMS (δ 0.00 ppm) for qualitative analysis and $(CH_3)_3SiOSi(CH_3)_3$ (δ 0.00 ppm) for quantitative analysis in $CDCl_3$. Infrared spectra were recorded on a Nicolet Impact 400 FT-IR spectrometer with Omnic software package. IR band were reported with *v* in units of cm^{-1}. Ultraviolet spectra were obtained on a Hewlett Packard HP 8452A diode array spectrophotometer and reported with λ in units of nm and ε in units of $M^{-1}cm^{-1}$. Low resolution mass spectra data were obtained from a Fisons VG Quattro triple quadrupole mass spectrometer. Electron impact ionization, chemical ionization and fast atom brombardant were employed for MS analysis. GC/MS was performed on Fisons 8060 GC with VG Quattro MS or on a Hewlett Packard model 5890 gas chromatograph with an HP methylsilicone capillary column interfaced with an HP 5097B EI mass spectrometer and an HP series computer. Gas chromatographic analyses were routinely performed on a Hewlett Parkard HP 5890A instrument equipped with FID detector, and an HP 3393A reporting integrator. Analyses were accomplished on an Alltech Econo-CAP SE-54 capillary column (30 × 0.25mm).

Analytical and preparative HPLC separations were accomplished on a Beckman instrument using a Microsorb C-18 reverse phase column (anal. 5um, 4.6mm ID × 25cm; prep. 5um, 21.4mm ID × 25cm) with acetonitrile/water solvent mixtures. Flash chromatography[151] (Merck, grade 9385 silica gel, 230 - 400 mesh, 60Å) and thin layer chromatography (anal.: Whatman, silica gel plates, 250 μm layer, UV_{254}; prep.: Analtech, Silica Gel G & GF Preparative UNIPLATES, 20 × 20 cm, 500 microns) were performed using the solvent systems specified in the specific experiments.

7.1.2 Electrochemical Experiments

Electrochemical measurements were performed on an EG & G Princeton Applied Research (EG & G / PAR) model 273 potentiostat/galvanostat interfaced to an MS-DOS computer. The detailed instrumentation employed for cyclic and linear sweep voltammetry has been described early.[79,152]

Voltammetry. Voltammetric measurements were performed on solutions which contained 0.5 M $LiClO_4$ in CH_3CN (in the presence or absence of methanol, as required). The solutions were prepared by weighing 0.532 g $LiClO_4$ (or other electrolyte) into an oven-dried 10 mL volumetric flask then placing the volumetric flask, together with all voltammetry cell pieces, in a Baxter DP-22 vacuum drying oven under vacuum (30-40 mmHg) at 40 ^oC for at least 8 hours. Purified and dried CH_3CN or/and CH_3OH were added to the septum-sealed volumetric flask with an oven and vacuum-dried syringe(s). The resulting solution was transferred to the argon-purged voltammetry cell. The electroactive substance was added and the solution continued to be purged with argon.

A three-electrode voltammetry cell was utilized. The Pt microdisk working electrode (0.32 mm in diameter) was prepared for use by polishing with alumna slurry as outlined in the BAS electrode polishing kit (part NO. MF-2056). The Ag/Ag^+ (0.10 M in CH_3CN, 0.337 V vs. SCE) reference electrode was made as described early.[152] A Pt wire (2 cm in length, 2 mm in diameter) was used as auxiliary electrode. The voltammetry cell was placed in a Fisher FS-14 solid state/ultrasonic tank filled with water. Between voltammetry runs the ultrasonic system was activated for 30 seconds to clean the working electrode surface. Positive-feedback iR compensation was set by monitoring the current response. The iR compensation was increased until oscillation and then backed off to 90% of that value. The reading error of peak potential from a cyclic voltammogram is within 1-2 mV. All experiments were performed at ambient temperature (23 ^oC).

Bulk Electrolysis. Preparative electrolysis was performed on solutions which contained 0.1 M $LiClO_4$ in CH_3CN containing CH_3OH. The blank solutions were prepared similarly as in voltammetry. A conventional H-cell, with two compartments separated by a medium glass frit (22 mm in diameter), was utilized. 60 mL of the electrolyte solution was partitioned equally between the two compartments of an oven then vacuum-dried, fully assembled H-cell under argon. The electro-active substrate was added to the anodic compartment, and both anodic and cathodic compartments were purged for at least 10 minutes with argon before electrolysis.

The working electrode was built from a Pt gauze (45 mesh, 30 mm $\times$ 20 mm). A 0.5 mm diameter by 4 cm piece of Pt wire was soldered to a 0.5 mm diameter piece of Ag wire. The Pt wire was sealed in an OD Pyrex tube and leaving the Pt partly outside and

the Ag inside the tube. The Pt mesh was then spot welded the Pt wire. The Pt gauze was shaped to conform to the electrolysis cell. the auxiliary electrode was made with copper wire (2 mm in diameter). The one end of copper wire was fabricated in shape of cycles with a diameter of 2 cm. A Ag/Ag^+ (0.10 M in CH_3CN) electrode was used for reference.

All electrolysis experiments were performed at ambient temperature (23 ^oC). Constant current electrolysis were performed at a current range from -25 to -40 mA. Both anodic and cathodic compartments purged with Argon, and set in ultrasonic system through electrolysis. GC and TLC were employed to monitor electrolysis progress. GC samples were taken, after every 0.5 equivalent of electron was consumed, from the anodic compartment by 10 μL syringe. TLC was run in solvent systems as indicated. After allowed time was reached, the electrolysis was stopped, and the anodic solution was then transferred into a suitable flask for work-up. The products were separated by flash column chromatography (or preparative TLC) and characterized by NMR, IR, MS and other methods.

7.1.3 Materials and Purification[153]

$LiClO_4$, $LiBF_4$ and $^nBu_4NPF_6$ were purchased from Aldrich and were dried under vacuum before use. $(NH_4)_2Ce(NO_3)_6$ (Aldrich) was dried under vacuum before use. CH_3CN (Mallinckrodt, HPLC grade, 99+ %) was stirred over calcium hydride (Aldrich) until the cessation of gas evolution, refluxed over calcium hydride at least one hour, then distilled slowly, discarding the first 5 and last 10 % of distillate. CH_3OH (Baker Analyzed HPLC) was dried by stirring over calcium hydride, followed by distillation before use.

CH_2Cl_2 was refluxed with P_2O_5 and distilled before use. Argon was dried and purified according to reference. THF was distilled from $LiAlH_4$ before use.

The following reagents for synthesis and reactions were purchased and used without purification: cyclopropylbenzene, toluene, 1-methylnaphthalene, 9,10-dimethylanthracene, anthrone, Mg, cyclopropylbromide, NBS, Br_2, CH_3Li, CH_3I, 1-bromo-4-methylnaphthalene, acetaldehyde, ethyl iodide, methylene iodide, and other common solvents and inorganic reagents.

7.2 SYNTHESIS OF STARTING MATERIALS

7.2.1 Cyclopropylanthracenes

9-Cyclopropylanthracene.[130] Cyclopropylmagnesium bromide was prepared by mixing cyclopropylbromide (6.5 mL, 80 mmol) with magnesium turnings (3.0 g, 124 mmol) in 100 mL diethyl ether in the presence of small amount of iodine. A weighed amount of anthrone (14.0 g, 70 mmol) was dissolved in 200 mL THF and the solution was added dropwise to the Grignard reagent. The reaction mixture was refluxed for 3 hours. After cooling to room temperature and chilling in an ice-bath for 10 min, the resulting solution was gradually acidified with concentrated HCl and extracted with CH_2Cl_2/H_2O. The combined extracts were washed with saturated solution of sodium bisulfate and dried over anhydrous sodium sulfate. Crude product was obtained by percolating the product through a column of neutral alumina with hexane-dichloromathane (95:5, v/v). After a second column separation, 4.91g 9-cyclopropylanthracene was obtained and large amount

of anthrone was recovered. The yield of product was not calculated. Pure product was obtained by recrystallization from ethanol. Melting point of the product is 133→135 ^{o}C (literature 133→135 ^{o}C).[154]

9-Bromo-10-cyclopropylanthracene.[154] A 200 mL carbon tetrachloride solution of bromine (0.53 mL, 10.3 mmol) was added dropwise using an addition funnel to a mixture of 9-cyclopropylanthracene (4.5 g, 10.3 mmol) and NBS (1.76 g, 10.3 mmol) in a 500-mL round bottom flask wrapped with aluminum foil and equipped with a magnetic stirring bar. The reaction mixture was maintained at 15 ^{o}C in a water bath. After 1 hour, 200 mL aqueous solution of sodium bisulfite was added to quench the reaction. The organic layer was isolated, dried over anhydrous sodium sulfate, filtered and evaporated to dryness. The resulting residue was dissolved in 40 mL of hexane, chilled in an ice-bath and filtered to further remove any unreacted NBS and the corresponding succinimide that formed. After column chromatography, using neutral alumina soaked in hexane as a stationary phase and dual-solvent benzene-hexane (1:30, v/v) as a mobile phase, 9-bromo-10-cyclopropylanthracene was isolated. Recrystallization from ethanol afforded 3.26 g yellow crystal of 9-bromo-10-cyclopropylanthracene. The melting point of product was 112→113^{o}C (literature 113→114^{o}C).[154]

9-Cyclopropyl-10-methylanthracene. 1.0 g (3.4 mmol) of 9-bromo-10-cyclopropylanthracene (vacuum-dried) was added to flame-dried 250 mL round-bottomed flask fitted with stirrer and under nitrogen. 50 mL THF was then introduced into flask. 3 mL 1.4 M CH_3Li solution (4.2 mmol CH_3Li) was added via syringe dropwise to the

solution. The color of solution turned into dark yellow green immediately. 1 mL CH_3I was added to complete the reaction. The reaction mixture was stirred for one hour and then poured into water. The organic compounds were extracted with diethyl ether from water, dried over anhydrous $MgSO_4$ and concentrated. Recrystallization in ethanol yielded 0.6 g (76%) solid 9-cyclopropyl-10-methylanthracene.

9-Cyclopropyl-10-methylanthracene **^{1}H NMR** δ 0.79(2H, m), 1.46(2H, m), 2.49(1H, m), 3.11(3H, s), 7.52(4H, m), 8.32(2H, d), 8.81(2H, d); **^{13}C NMR** δ 9.7(CH_2), 10.6(CH_3), 14.1(CH), 124.4(CH, aromatic), 124.7(CH, aromatic), 125.1(CH, aromatic), 126.6(CH, aromatic), 129.6(C, aromatic), 129.9(C, aromatic), 131.4(C, aromatic), 133.2(C, aromatic); **IR** ($CHCl_3$) *v* 3085, 3002, 1461(s), 1026(s), 875; **MS(EI)** *m/e* 232($M^{+\cdot}$, 80), 217(M-CH_3, 100); HRMS(EI) for $C_{18}H_{16}$, expt'l 232.1262, calc. 232.1252, error 4.4 ppm.

7.2.2 Cyclopropylnaphthalenes

1-Cyclopropylnaphthalene.[155] The synthesis of 1-cyclopropylnaphthalene from 1-bromonephthalene was accomplished under literature's procedures.[155]

1-Bromo-3-naphthylpropane. A Grignard reagent was prepared by mixing 1-bromonaphthalene (13 mL) and Mg turnings (4.12 g) in 100 mL THF in the presence of 1,2-dibromoethane (initiator). Into a 500mL three-neck flask was added 0.35 g pre-dried CuBr, 9.5 mL HMPA, 10 mL 1,3-dibromopropane and 20 mL THF. The reaction mixture was heated to reflux, and the Grignard reagent was then added dropwise. After all Grignard reagent was added, the solution was kept to reflux for three hours. When reaction was completed, the reaction mixture was poured into a 100 mL ice-HCl solution

and extracted with benzene/H_2O. The extracts was washed with H_2O, NaOH (10%) solution and H_2O again, dried over Mg_2SO_4 and evaporated to dryness.

The dark green oily liquid obtained from above was subject to Kuaelrohr distillation. The second portion of distillate (8.3 g, boiling point range: 115→195^oC at 2→3 mmHg) was collected. ^1H NMR and GC showed impurities like 1,3-dibromopropane, HMPA and dimers existed and only ~50% of 1-bromo-3-naphthylpropane was in distillate. Short-path distillation was needed to further separate the product. The distillate in the temperature range of 145→150 ^oC (0→1 mmHg) was collected and 3.4 g (80% purity) of 1-bromo-3-naphthylpropane was obtained.

1,3-Dibromo-3-naphthylpropane. A mixture of 2.7 g (10.8mmol) 1-bromo-3-naphthylpropane, 3.36 g(13.6 mmol) NBS, 0.15 g $(PhCO_2)_2$ and 50 mL CCl_4 was reluxed in a dry 250 mL three-neck flask fitted with water condenser circulated with nitrogen. GC was employed to monitor reaction progress (monitoring appearance of starting material). More NBS was added if reaction was not complete. After all starting material was consumed, the reaction mixture was cooled to room temperature, filtered, and concentrated. The resulting dark brown oil contained 1,3-dibromo-3-naphthylpropane as only major product.

1-Cyclopropylnaphthalene. Preparation of zinc-copper couple was described elsewhere.[156] Zn-Cu couple (3.0 g) was transferred into 250 mL flask with 50 mL THF. A 30 mL of 1,3-dibromo-3-naphthylpropane THF solution was added to the flask with stirring at 0 ^oC. After addition the reaction mixture was heated to 40 ^oC and GC was used to monitor the reaction progress. After all starting material was consumed, the solution was filtered and extracted with ether/H_2O for several times. The ether layer was dried

over $MgSO_4$ and evaporated. The resulting yellow brown liquid was subject to short-path distillation, which yielded 1.0 g (85% purity) of 1-cyclopropylnaphthalene. Further purification was completed by column chromatography.

1-Bromo-4-cyclopropylnaphthalene. A mixture of 1-cyclopropylnaphthalene (0.85 g, 5 mmol), K_2CO_3 (0.85 g), Fe dust (0.2 g) and 100 mL CCl_4 was stirred in 250 mL three-neck flask. A solution of Br_2 (0.85 g, 0.28 mmol) and 50 mL CCl_4 was added dropwise. The reaction mixture was stirred under dark (covered with Aluminum foil). More Br_2 was added if reaction was not complete based on GC monitoring. After all starting material was converted, the solution was worked up with H_2O. The CCl_4 layers were combined, dried over $MgSO_4$ and concentrated. The resulting green dark oil contained 86% 1-Bromo-4-cyclopropylnaphthalene. Column chromatography using hexane as eluting solvent gave 1.2 g (~93% purity) 1-bromo-4-cyclopropylnaphthalene.

2-Cyclopropylnaphthalene.[155] Synthesis of 2-cyclopropylanthracene followed the procedures by which 1-cyclopropylnaphthalene was synthesized.

1-Cyclopropyl-4-methylnaphthalene.

1-(4-methylnaphthyl)ethanol. In a 500 mL three-necked round-bottomed flask fitted with magnetic stirrer and water condenser and circulated with nitrogen was added 4.32 g magnesium (180 mmol). 150 mL THF was added to flask via syringe. The solution was stirred and warmed (~30 ^oC). 14.2 g (60 mmol) 1-bromo-4-methylnaphthalene was then added gradually through syringe. Reaction was observed and

controlled by adjusting temperature (30→40 ^{o}C) or addition rate of 1-bromo-4-methylnaphthalene. After all reagent was added, the reaction mixture was heated under reflux for one additional hour and then cooled to room temperature.

Into the flask of Grignard reagent prepared above was added gradually 5 mL (3.94 g, 90 mmol) acetaldehyde (caution: reaction occurs rapidly and releases heat). The mixture was stirred at room temperature for about one hour. The resulting solution was poured into 20% H_2SO_4 aqueous solution. A 100 mL diethyl ether was added, and the ether layer was separated, washed with water, 10% NaOH solution and water again, dried over anhydrous $MgSO_4$, filtered and concentrated. The crude 1-(4-methylnaphthyl)ethanol was kept in refrigerator overnight. The alcohol crystal thus formed was filtered and washed with hexane. The filtrate was concentrated and the remained alcohol was separated by column (silica gel) with dichloromethane as eluting solvent. The total 1-(4-methylnaphthyl)ethanol (solid) separated weighted 12.7g (95%). **TLC** (CH_2Cl_2) R_f = 0.24; **^{1}H NMR** δ 1.55(3H, d), 2.38(1H, s), 2.60(3H, s), 5.49(1H, q), 7.21(1H, d), 7.47(3H, m), 7.98(2H, m).

1-Methyl-4-vinylnaphthalene. Into a 250mL round-bottomed flask fitted with magnetic stirrer and nitrogen flowing adapter was added 10.0 g (54 mmol) 1-(4-methylnaphthyl)ethanol. The flask was stirred and heated under nitrogen flow. After solid alcohol was melted, the flask was kept at a temperature of 60→70 ^{o}C for about 10 minutes. Tiny water drops was observed formed on the surface of the flask. The reaction was stopped by removing heater, based on reaction progress monitored by GC. Besides the desired product 1-methyl-4-vinylnaphthalene, a huge amount of polymer was formed and some starting material left unreacted. The resulting reaction mixture was worked up

with diethyl ether and water. The organic layer was separated, dried over anhydrous $MgSO_4$, filtered and concentrated. Column separation with hexane as eluting solvent yielded 1.92 g (23.2%) liquid1-methyl-4-vinylnaphthalene. **TLC** (hexane) R_f = 0.46; **^{1}H NMR** δ 2.67(3H, s), 5.41(1H, d), 5.73(1H, d), 7.27(1H, d), 7.44(1H, q), 7.50(3H, m), 7.99(1H, m), 8.11(1H, m); **^{13}C NMR** δ 19.6(**C**H_3), 116.4(=**C**H_2), 123.4(**C**H, aromatic), 124.3(**C**H, aromatic), 124.6(**C**H, aromatic), 125.6(**C**H, aromatic), 125.7(**C**H, aromatic), 126.5(**C**H, aromatic), 131.2(**C**, aromatic), 132.6(**C**, aromatic), 134.1(**C**, aromatic), 134.4(**C**, aromatic), 134.6(=**C**H-); **GC-MS(EI)** *m/e* 169(M+1, 7), 168(M, 49), 153(M-CH_3, 100).

1-Cyclopropyl-4-methylnaphthalene. 100 mL stock solution of ethylzinc iodide was prepared in the following procedure: Ethyl iodide (17.3 g, 0.11 mol) was allowed to react with zinc-copper couple II (7.5 g, 0.11 mol), which was prepared previously, and the mixture was stirred at room temperature overnight. The supernatant liquid was withdrawn free from sludge and stored in a stoppered flask carrying a drying tube. After storage at room temperature for one week no precipitate was formed, and the activity of the solution remained unchanged.

Methylene diiodide (3.5 g, 0.013 mol) was added to an aliquot of the stock solution (25 mL) containing about 0.5 equivalents of ethylzinc iodide and the mixture was stirred at reflux (30 ^{o}C) for one hour (the reaction releases heat when adding methylene iodide to ethylzinc iodide solution). To the chilled solution, 1.9 g (0.0113 mol) 1-methyl-4-vinylnaphthalene was added, and the mixture was stirred and heated under reflux (30→40 ^{o}C). After 15 hours, starting 1-methyl-4-vinylnaphthalene was all consumed and 1-cyclopropyl-4-methylnaphthalene was produced, monitored by GC. The reaction

mixture was quenched with water and dilute HCl (10%), extracted with water and diethyl ether, and the ether layer was washed with water, NH_4NO_3 aqueous solution and again water, dried over anhydrous $MgSO_4$ and concentrated. The crude product (liquid) was subjected to column separation with hexane as eluting solvent, which yielded 2.0 g (97%) 1-cyclopropyl-4-methylnaphthalene.

1-Cyclopropyl-4-methylnaphthalene **TLC** (hexane) $R_f = 0.43$; **^{1}H NMR** δ 0.84(2H, m), 1.12(2H, m), 2.38(1H, m), 2.75(3H, s), 7.26(1H, d), 7.30(1H, d), 7.64(2H, m), 8.10(1H, d), 8.54(1H, d); **^{13}C NMR** δ 6.4(CH_2), 13.4(CH), 19.5(CH_3), 123.8(**C**H, aromatic), 124.7(**C**H, aromatic), 125.1(**C**H, aromatic), 125.4(**C**H, aromatic), 125.5(**C**H, aromatic), 126.3(**C**H, aromatic), 132.6(**C**, aromatic), 132.7(**C**, aromatic), 133.6(**C**, aromatic), 137.3(**C**, aromatic); **IR**($CHCl_3$) *v* 3071, 3006, 1597, 1512, 1217, 1112, 1023, 907; **MS**(EI) *m/e* 183(M+1, 3.5), 182(M^+, 27), 167(M-15, 100), 152(49), 141(11); **HRMS**(EI) $C_{14}H_{14}$, calc. 182.1096, expt'l. 182.1100, error 2.7 ppm.

7.2.3 1-Cyclopropyl-4-methylbenzene

Zinc-Copper Couple.[156] In a 500 mL Erlenmeyer flask fitted with a magnetic stirrer was placed zinc powder (49.2 g, 0.75 mol) and 40 ml of 3% hydrochloric acid. The mixture is stirred rapidly for 1 minute, then the supernatant liquid is decanted. In a similar manner the zinc power is washed successively with three additional 40 mL portions of 3% hydrochloric acid, five 100 mL portions of distilled water, two 75 mL portions of 2% aqueous copper sulfate solution, five 100 mL portions of distilled water, four 100 mL portions of absolute ethanol, and five 100 mL portions of absolute ether. The couple is finally transferred to a Buchner funnel, washed with additional anhydrous ether, covered

tightly with a rubber dram, and suction-dried until it reaches room temperature. The zinc-copper couple is vacuum-dried at 40 ^{o}C for overnight and is then ready for use.

1-Cyclopropyl-4-methylbenzene. In a 250 mL round-bottomed flask fitted with magnetic stirrer and water condenser protected by nitrogen adapter are placed 3.1 g Zn-Cu couple and 25 mL diethyl ether. A 5mL mixture of 1-methyl-4-vinylbenzene (3.54 g, 30 mmol) and diiodomathane (8.8 g, 33 mmol) in diethyl ether is then added gradually. The reaction mixture is stirred and heated under reflux. GC was employed to monitor reaction progress and after 27 hours, reaction is stopped. The resulting mixture is poured into 30 mL saturated ammonium chloride aqueous solution. The organic layer is separated, washed with saturated $NaHCO_3$ solution then distilled water for several times, dried over anhydrous $MgSO_4$, and concentrated. Fraction distillation under vacuum (43→49 ^{o}C, ~3 mmHg) affords1.8 g (45%) liquid1-cyclopropyl-4-methylbenzene (91% purity). **^{1}H NMR** δ 0.60(2H, m), 0.85(2H, m), 1.80(1H, m), 2.24(3H, s), 6.90(2H, d), 7.00(2H, d); **^{13}C NMR** δ 8.9(**C**H_2), 15.0(**C**H), 21.0(**C**H_3), 125.6(**C**H, aromatic), 128.5(**C**H, aromatic), 134.8(**C**, aromatic), 140.8(**C**, aromatic).

7.3 ELECTROLYSIS OF CYCLOPROPYLARENES

7.3.1 Cyclopropylanthracenes

9-Bromo-10-cyclopropylanthracene. 56.0 mg (0.189 mmol) of 9-bromo-10-cyclopropylanthracene in CH_3CN containing 2.5 M methanol was electrolyzed at -30 mA for 27 min (2.7 equiv. e^{-}'s). The anodic solution (30 mL) was divided into two portions

and two work-up procedures were employed. Analogous procedures were followed for electrolyses in the presence of 4.1 and 0.25 M CH_3OH. The results are summarized in Table 4-4.

Aqueous Workup. One portion of electrolytic solution was extracted with H_2O/ether 3x. The ether layers were combined, dried with $MgSO_4$ (Mallinckrodt), and evaporated. $CDCl_3$ was then added to the flask to dissolve the residue. The $CDCl_3$ solution was filtered and transferred to an NMR tube. After addition of an internal standard [$(CH_3)_3SiOSi(CH_3)_3$], ^{1}H NMR was used to determine the yield of 9-cyclopropyl-9-methopxyanthrone. An analytical sample of 9-cyclopropyl-9-methopxyanthrone was obtained for characterization via flash column chromatography with CH_2Cl_2 as solvent:

9-Cyclopropyl-9-methopxyanthrone **TLC** R_f = 0.42 (CH_2Cl_2); **^{1}H NMR** δ 0.304(m, 2H, *trans*-cyclopropylmethene), 0.334(m, 2H, *cis*-cyclopropylmethylene), 1.20(m, 1H, cyclopropylmethine), 2.99(s, 3H, methyl), 7.94(t, 2H, aromatic), 7.67(t, 2H, aromatic), 7.76(d, 2H, aromatic), 8.29(d, 2H, aromatic); **^{13}C NMR** δ 2.44(t, **C**H_2), 28.1(d, **C**H), 52.3(q, O**C**H_3), 77.6(s), 126.7(d, aromatic), 127.3(d, aromatic), 127.9(d, aromatic), 132.1(s, aromatic), 133.1(s, aromatic), 144.2(s, aromatic), 183.4(s, **C**=O); IR *v* 1665(s, C=O), 1601(s), 1458(m), 1319(s), 1272(s), 1072, 911, 819, 738, 652; **MS**(EI) *m/e* 265(M+1, 3.38), 264(M^+, 18.7), 249(3), 236(M-28, 92), 223(M-cyclopropyl, 100), 215(17.8), 208(15.3), 202(20), 193(33.8), 165(84.6), 152(48.8); **HRMS**(EI) for $C_{18}H_{16}O_2$, cacl. 264.1150, expt'l 264.1158, error 2.9 ppm.

Non-aqueous Workup. The second portion of the electrolytic solution was transferred into a 50 mL flask and evaporated. CH_2Cl_2 was added to extract the organic materials, and the resulting solution filtered to remove $LiClO_4$. Yields of products were determined by ^{1}H NMR analysis. Analytical samples of these compounds were obtained as follows: Flash column chromatography of the non-aqueous work-up solution with CH_2Cl_2 as eluting solvent gave pure ring opened product methoxy ether , and a mixture of ring opened perchlorate ester and bromide, which were subsequently separated via flash chromatography using a solvent gradient 5 → 20% EtOAc/hexane.

Methoxy Ether **TLC**: R_f = 0.14 (CH_2Cl_2), 0.15 (hexane/CH_2Cl_2/EtOAc = 14:5:1); **^{1}H NMR** δ 2.95(q, 2H, J=6.5Hz), 3.38(s, 3H, OCH_3), 3.59(t, 2H, J=6.3Hz), 6.62(t, 1H, J=7.08Hz), 7.26~7.50(m, 2H), 7.53~7.64(m, 2H), 7.76~7.85(q, 2H), 8.21~8.32(q, 2H); **^{13}C NMR** δ 31.7(t, **C**H_2), 58.8(q, O**C**H_3), 71.9(t, **C**H_2OCH_3), 123.5(d), 126.8(d), 127.3(d), 127.4(d), 127.7(d), 127.8(d), 130.3(s), 131.7(d), 132.1(s), 132.2(s), 132.8(d), 133(d, **C**H), 136.8(s), 141.1(s), 184.8(s, **C**=O); **IR** *v* 1665(s, C=O), 1598(s), 1320(s), 1122, 912.5, 939; **MS**(EI) *m/e* 265(M+1, 7), 264(M^+, 32.7), 249(M-CH_3, 5.4), 231(19), 230(37), 219(M-CH_2OCH_3, 100), 202(32), 189(38), 165(24.6), 45($CH_2OCH_3^+$, 91), 15(CH_3^+, 9); **HRMS** (EI) for $C_{18}H_{16}O_2$, calc. 264.1150, expt'l 264.1146, error -1.6 ppm.

Perchlorate Ester: **M.P.**: 98 - 99 °C; **TLC** R_f = 0.34 (CH_2Cl_2), 0.15 (hexane/EtOAc = 4:1), 0.15 (hexane/CH_2Cl_2/EtOAc = 14:5:1); **^{1}H NMR** δ 3.20 (q, 2H, J = 7 Hz), 4.73 (t, 2H, J = 7 Hz), 6.42 (t, 1H, J = 7 Hz), 7.50 - 7.66 (m, 5H), 7.80 (d, 1H), 8.28 (q, 2H); **^{13}C NMR** δ 29.2 (t, **C**H_2), 74.4 (t, **C**H_2OClO_3), 123.4 (d), 127.0 (d), 127.3

(d, **C**H), 127.7 (d), 128.1 (d), 128.5 (d), 130.5 (s), 131.9 (d), 132.3 (s), 133.1 (d), 134.6 (s), 136.1 (s), 140.4 (s), 184.5 (s, **C**=O); **IR** *v* 1664 (s, C=O), 1598 (s), 1474, 1382, 1317, 1289, 1269 (s, $\nu_s ClO_3$), 1235 (s, $\nu_s ClO_3$), 1098, 1037 (s, $\nu_s ClO_3$); **MS**(CI) *m/e* 287 ($MH^+ + 2 - O_3$, 0.5), 285 ($MH^+ - O_3$, 1.5), 251 ($MH^+ + 2 - ClO_3$, 7.5), 249 ($MH^+ - ClO_3$, 5.4), 233 ($MH^+ - ClO_4$, 22.8), 231 (33.6), 221 (17.4), 209 (24), 195 (100), 194 (96.6), 165 (19.5); **MS**(FAB) *m/e* 335 ($MH^+ + 2$, 17.4), 333 (MH^+, 48.6), 273 (13.2), 251 ($MH^+ + 2 - ClO_3$, 16.5), 233 ($MH^+ - ClO_4$, 19.8), 231 (22.2), 220 (48.6), 219 (40.8), 83 (ClO_3^+, 34.2), 73 (65.4), 69 ($HClO_2^+$, 56.4), 55 (100); **HRMS** (CI) for $C_{17}H_{14}O_5Cl$ (MH^+), calc. 333.0529, expt'l 333.0512, error -5.0 ppm; **Elemental Analysis** (Atlantic Microlab, Inc.) for $C_{17}H_{13}O_5Cl$, calc. C 61.44, H 3.95, expt'l C 60.63, H 4.21.

<u>Bromide</u>: **TLC** R_f = 0.34 (CH_2Cl_2), 0.24(hexane/EtOAc = 4:1); **^{1}H NMR** δ 3.26 (q, 2H, J = 7 Hz), 3.57 (t, 2H, J = 7 Hz), 6.54 (t, 1H, J = 7 Hz), 7.45 - 7.56 (m, 2H), 7.59 - 7.68 (m, 3H), 7.83 (d, 1H), 8.28 (q, 2H); **^{13}C NMR** δ 31.9 (t, **C**H_2), 33.95 (t, **C**H_2Br), 126.9 (d), 127.4 (d), 127.5 (d), 127.7 (d), 128.2 (d), 133.0 (s), 130.4 (s), 131.8 (d), 132.2 (s), 132.24 (d, **C**H), 132.5 (d), 132.9 (d), 136.6 (s), 140.7 (s), 184.6 (s, **C**=O); **IR** *v* 1662 (s, C=O), 1598 (s), 1474 (s), 1383, 1315, 1287, 1098; **MS**(EI) *m/e* 314 (M + 2, 16.8), 312 (M^+, 16.5), 233 (40.8), 231 (25.8), 219 (45.6), 215 (100), 202 (39), 189 (39.6), 165 (20.4); **MS**(CI) *m/e* 343 (M + 2 + $C_2H_5^+$, 7.5), 341 (M + $C_2H_5^+$, 6.3), 315 ($MH^+ + 2$, 40.8), 313 (MH^+, 26.4), 261 (7.8), 263 (13.2), 235 (63), 233 (100); **HRMS** (EI) for $C_{17}H_{13}BrO$, calc. 312.0150, expt'l 312.0139, error -3.4 ppm.

9-Cyclopropylanthracene. 47.6 mg (0.218 mmol) of 9-cyclopropylanthracene in CH_3CN containing 2.5 M CH_3OH was electrolyzed at -30 mA for 35 min (3.0 equiv. e^-

's). Portions of the reaction mixture were subjected to aqueous and non-aqueous workup (vide supra) and quantitative ^{1}H NMR analysis. The results of this and other analogous runs are summarized in Table 4-5.

50.5 mg (0.232 mmol) of 9-cyclopropylanthracene was electrolyzed at -30 mA for 25 min. (2.0 equiv. e^-'s). The progress of the electrolysis was monitored by GC and TLC (3 : 1 hexane : CH_2Cl_2) so as to stop the electrolysis when the yield of 9-cyclopropyl-10-methoxyanthracene was maximal. The anodic solution (30ml) was extracted with ether and water several times, dried ($MgSO_4$), and evaporated. Yields (based upon ^{1}HNMR analysis are summarized in Table 4-5. Flash column chromatography with a solvent gradient starting at 0% and finishing at 25% CH_2Cl_2/hexane yielded 18% (10.4 mg) of 9-cyclopropyl-10-methoxyanthracene.

9-Cyclopropyl-10-methoxyanthracene **^{1}H NMR** δ (assignments with aid of 2D NMR), 0.80 (m, 2H, cis-cyclopropyl methylene hydrogens), 1.44 (m, 2H, trans-cyclopropyl methylene hydrogens), 2.43(m, 1H, cyclopropyl methine hydrogen), 4.14 (s, 3H, CH_3O), 7.46 - 7.55 (m, 4H, 2-, 3-, 6-, and 7-anthryl hydrogens), 8.34 (m, 2H, 1- and 8-anthryl hydrogens), 8.77 (m, 2H, 2- and 4-anthryl hydrogens). **^{13}C NMR** δ (adept assignment) 9.3 (t, **C**H_2), 10.2 (d, **C**H), 63.2 (q, O**C**H_3), 122.6 (d), 124.2 (s), 124.7 (d), 125.1 (d), 126.3 (d), 130.7 (s), 132.3 (s), 151.7 (s). **IR** *v* 1664, 1620, 1652, 1452, 1390(s), 1330(s), 1282, 1116, 1088, 1027, 971. **MS**(EI) *m/e* 249 (M + 1, 8.5), 248 (M^+, 49), 247 (30), 233 (M - CH_3, 47), 217 (M - OCH_3, 100), 215 (89), 202 (49), 189 (39); **HRMS** (EI) for $C_{18}H_{16}O$, calc. 248.1201, expt'l 248.1202, error 0.3 ppm.

Control Experiments. A 30 mL CH_3CN solution of 9-cyclopropyl-9-methopxyanthrone (27.7mg) was divided into 3 portions: 1ml CH_3OH (2.5M) and 0.1g (0.1M) $LiClO_4$ was added to the first portion and the reaction was subsequently subjected to non-aqueous workup. TLC and GC of the resulting solution revealed only unreacted 9-cyclopropyl-9-methopxyanthrone. To the second portion was added 0.1 g $LiClO_4$ and 1 drop HBr (32%). The reaction mixture was subjected to non-aqueous workup. TLC and GC of resulting solution showed the complete conversion of 9-cyclopropyl-9-methopxyanthrone → bromide. The yield of bromide based on ^{1}HNMR analysis was 80%. To the third portion was added 0.1 g $LiClO_4$ and 1 drop of $HClO_4$ (60-70%). Non-aqueous workup yielded 46% of perchlorate ester based upon ^{1}H NMR analysis.

7.3.2 Cyclopropylnaphthalenes

1-Cyclopropylnaphthalene

Run 1. 1-Cyclopropylnaphthalene (44 mg, 0.262mmol) in the presence of 2.5 M CH_3OH was electrolyzed at -30 mA for 42 min passing 3.0 equivalents of electrons. The electrolytic solution was worked up with H_2O/diethyl ether. The PTLC of the work-up solution with solvent system of hexane and ethyl acetate (3:1) yielded the following compounds:

1-(1,3-Dimethoxypropyl)naphthalene **TLC** (hexane : ethyl acetate = 3 : 1) R_f =0.40; **^{1}H NMR** ($CDCl_3$) δ 2.13(m, 2H, -C**H**$_2$-), 3.21(s, 3H, -OC**H**$_3$), 3.35(s, 3H, -OC**H**$_3$), 3.38(m, 1H, -C**H**$_2$-OCH_3), 3.60(m, 1H, -C**H**$_2$-OCH_3), 5.07(t, 1H, >C**H**-OCH_3), ~7.50(m, 3H, aromatic), 7.55(d, 1H, aromatic), 7.78(d, 1H, aromatic), 7.87(m, 1H, aromatic), 8.22(d, 1H, aromatic); **^{13}C NMR** ($CDCl_3$) δ 37.82(t, -**C**H_2-), 56.96(q, -

O**C**H_3), 58.71(q, -O**C**H_3), 69.42(t, -**C**H_2-OCH_3), 78.41(d, >**C**H-OCH_3), 123.44(d, aromatic), 123.82(d, aromatic), 125.45(d, aromatic), 125.48(d, aromatic),125.89(d, aromatic), 127.89(d, aromatic), 128.80(d, aromatic), 131.15(s, aromatic), 133.90(s, aromatic), 137.70(s, aromatic); **IR** *v* 3157, 3062, 2985, 2899, 2827, 1600, 1518, 1475, 1394, 1116(s), 809(s), 785(s); **MS**(EI) *m/e* 231(1.52, M+1), 230(7.92, $M^{+\cdot}$), 172(13.2, M+1 - -$CH_2CH_2OCH_3$), 171(100, M - -$CH_2CH_2OCH_3$), 165(15.2), 128(19.2); **HRMS**(EI) $C_{15}H_{18}O_2$, expt'l 230.1301, cacl 230.1307, error -2.7 ppm.

4, 4'-Di(1, 3-dimethoxypropyl)-1, 1'-binaphthalene **TLC** (hexane : ethyl acetate = 3 : 1) R_f =0.21; **^{1}H NMR** ($CDCl_3$) δ 2.23(m, 2H, -C**H**$_2$-), 3.40(s, 3H, -OC**H**$_3$), 3.41(s, 3H, -OC**H**$_3$), 3.46(m, 1H, -C**H**$_2$-OCH_3), 3.70(m, 1H, -C**H**$_2$-OCH_3), 5.18(m, 1H, >C**H**-OCH_3), 7.29(t, 1H, aromatic), 7.44(d, 1H, aromatic), 7.50(t, 2H, aromatic), 7.67(d, 1H, aromatic), 8.31 (d, 1H, aromatic); **^{13}C NMR** ($CDCl_3$) δ 37.91(t, -**C**H_2-), 57.15(q, -O**C**H_3), 58.76(q, -O**C**H_3), 69.49(t, -**C**H_2-OCH_3), 78.43(d, >**C**H-OCH_3), 123.27(d, aromatic), 123.52(d, aromatic), 125.50(d, aromatic), 125.75(d, aromatic), 127.46(d, aromatic), 127.55(d, aromatic), 131.15(s, aromatic), 133.28(s, aromatic), 137.50(s, aromatic), 138.25(s, aromatic); **IR** *v* 3081, 3047, 2988, 2939, 2904, 2831,1733, 1670, 1601, 1523, 1474, 1454, 1391, 1303, 1258, 1214, 1175, 1121(s), 857, 778(s); **MS**(EI) *m/e* 460(2, M+2), 459(10, M+1), 458(44, $M^{+\cdot}$), 427(3, M- -OCH_3), 401(3.6, M+2 - -$CH_2CH_2OCH_3$), 400(23.2, M+1- -$CH_2CH_2OCH_3$), 399(100, M- -$CH_2CH_2OCH_3$), 427(5), 325(22.4), 252(17.6), 170(8.6); **HRMS**(EI) $C_{30}H_{34}O_4$, expt'l 458.2445, cacl 458.2457, error -2.6 ppm.

Run 2. 1-Cyclopropylnaphthalene (41.1 mg, 0.245 mmol) in the presence of 2.5 M CH_3OH was electrolyzed at –40 mA for 35 min passing 3.5 equivalents of electrons.

The electrolytic solution was worked up with H_2O / diethyl ether. The work-up solution was subject to HPLC analysis, which yielded 2.94 mg (7.45%) of starting material, 9.42 mg (17.43%) of 1-(1,3-dimethoxypropyl)naphthalene, and 14.13 mg (26.27%) of 4, 4'-di(1, 3-dimethoxy

propyl)-1, 1'-binaphthalene (HPLC condition: CH_3CN : H_2O = 90% : 10%; flow rate = 1mL/min; λ = 224nm; C_{18} column).

1-Bromo-4-cyclopropylnaphthalene

Run 1. 1-bromo-4-cyclopropylnaphthalene (64.6 mg, 0.263 mmol) in the presence of 2.5 M CH_3OH was electrolyzed at -40 mA for 33 min passing 3.0 equivalents of electrons. The electrolytic solution was worked up with H_2O/diethyl ether. The PTLC of the work-up solution with CH_2Cl_2 as solvent yielded:

1-Bromo-4-(1, 3-dimethoxypropyl)naphthalene 40.8 mg (50.4%), **TLC** (CH_2Cl_2), R_f = 0.44; **^{1}H NMR** ($CDCl_3$) δ 2.09(q, 2H, -C**H**$_2$-), 3.29(s, 3H, -OC**H**$_3$), 3.34(m, 1H, -C**H**$_2$-OCH_3), 3.35(s, 3H, -OC**H**$_3$), 3.61(m, 1H, -C**H**$_2$-OCH_3), 5.05(t, 1H, >C**H**-OCH_3), 7.42(d, 1H, aromatic), 7.58(m, 2H, aromatic), 7.79(d, 1H, aromatic), 8.22(d, 1H, aromatic), 8.31(d, 1H, aromatic); **^{13}C NMR** ($CDCl_3$) δ 37.89(t, -**C**H_2-), 57.06(q, -O**C**H_3), 58.74(q, -O**C**H_3), 69.20(t, -**C**H_2-OCH_3), 78.02(d, >**C**H-OCH_3), 122.46(s, aromatic **C**-Br), 123.75(d, aromatic), 124.28(d, aromatic), 126.72(d, aromatic), 126.94(d, aromatic), 127.98(d, aromatic), 129.64(d, aromatic), 132.06(s, aromatic), 132.38(s, aromatic), 138.01(s, aromatic); **IR** *v* 3079, 3045, 2990, 2929, 2892, 2831, 1595, 1571, 1510, 1473, 1448, 1387, 1314, 1257, 1203, 1161, 1118(s), 1014; **MS**(EI) *m/e* 310(6.8, M+2), 308(8, $M^{+\cdot}$), 252(10), 251(100, M+2 - -$CH_2CH_2OCH_3$), 249(97.6, M-

-$CH_2CH_2OCH_3$), 165(14.8), 153(20,8), 152(38.4), 127(21.2), 126(26), 45(78.4); **HRMS** (EI) $C_{15}H_{17}O_2Br$, expt'l 308.0410, cacl. 308.0412, error -0.6 ppm.

Rum 2. 1-Bromo-4-cyclopropylnaphthalene (56.6 mg, 0.230 mmol) in the presence of 2.5 M CH_3OH was electrolyzed at -40 mA for 17.2 min passing 2.0 equivalents of electrons. The electrolytic solution was worked up with H_2O / diethyl ether. The ^{1}HNMR analysis of the work-up solution yielded 56.7 mg (80%) of 1-bromo-4-(1, 3-dimethoxypropyl)naphthalene, and GC analysis showed 7.5 mg (13.2%) of starting material left unereacted.

2-Cyclopropylnaphthalene. 2-Cyclopropylnaphthalene (82.2 mg, 0.49 mmol) in the presence of 5.0 M CH_3OH was electrolyzed at -60 mA for 27 min passing 2.0 equivalents of electrons. The electrolytic solution was worked up with H_2O/diethyl ether. The PTLC of the work-up solution with hexane : ethyl acetate = 3:1 as solvent system yielded 18.2 mg (16.2%) 2-(1, 3-dimethoxypropyl) naphthalene**,** and a mixture of 2, 2'-dicyclopropyl-1, 1'-binaphthalene and starting material. Second PTLC of the mixture with hexane as the solvent gave 14.3 mg (17.5%) of 2, 2'-dicyclopropyl-1, 1'-binaphthalene. Unreacted starting material was estimated from GC analysis was 28 mg (34.1%).

<u>2-(1, 3-Dimethoxypropyl)naphthalene</u> TLC (hexane : ethyl acetate = 3:1) R_f = 0.41; **^{1}H NMR** ($CDCl_3$) δ 1.95(hexalet, 1H, -C**H**$_2$-), 2.17(hexalet, 1H, -C**H**$_2$-), 3.25(s, 3H, -OC**H**$_3$), 3.33(m, 1H, -C**H**$_2$-OCH_3), 3.34(s, 3H, -OC**H**$_3$), 3.51(m, 1H, -C**H**$_2$-OCH_3), 4.46(t, 1H, >C**H**-CH_3), ~7.47(m, 3H, aromatic), 7.74(s, 1H, aromatic), ~7.85(m, 3H, aromatic); **^{13}C NMR** ($CDCl_3$) δ 38.01(t, -**C**H_2-), 56.75(q, -O**C**H_3), 58.65(q, -O**C**H_3),

69.15(t, -**C**H_2-OCH_3), 80.81(d, >**C**H-OCH_3), 124.36(d, aromatic), 125.79(d, aromatic), 125.86(d, aromatic), 125.86(d, aromatic), 126.08(d, aromatic), 127.70(d, aromatic), 127.83(d, aromatic), 128.36(d, aromatic), 133.10(s, aromatic), 133.23(s, aromatic), 139.38(s, aromatic); **IR** *v* 3156, 3064, 2984, 2935, 2897, 2825, 1473, 1387, 1112(s), 824, 760; **MS**(EI) *m/e* 231(3, M+1), 230(15, $M^{+\cdot}$), 215(1.5, M-15), 171(100, M-59), 155(20), 141(15); **HRMS** (EI) $C_{15}H_{18}O_2$, expt'l 230.1300, cacl. 230.1307, error -2.8 ppm.

2, 2'-Dicyclopropyl-1, 1'-binaphthalene **TLC** (hexane) R_f =0.36; **^{1}H NMR**($CDCl_3$) δ ~0.60(m, 1H, cyclopropyl-C**H_2**), ~0.74(m, 3H, cyclopropyl-C**H_2**), 1.53(m, 1H, cyclopropyl-C**H**), ~7.10(m, 2H, aromatic), ~7.21(m, 1H, aromatic), ~7.38(m, 1H aromatoc), ~7.87(m, 2H, aromatic); **^{13}C NMR** ($CDCl_3$) δ 8.46(t, cyclopropyl-**C**H_2), 9.07(t, cyclopropyl-**C**H_2), 13.38(d, cyclopropyl-**C**H), 121.43(d, aromatic), 124.76(d, aromatic), 126.04(d, aromatic), 126.06(d, aromatic), 127.71(d, aromatic), 127.85(d, aromatic), 131.81(s, aromatic), 133.02(s, aromatic), 135.01(s, aromatic), 139.85(s, aromatic); **IR** *v* 3156, 3082, 3058, 3008, 2954, 2923, 2856, 1626, 1595, 1510, 1467, 1381, 1332, 1100, 1045; **MS**(EI) *m/e* 335(30, M-1), 334(100, M), 319(20), 305(40), 289(30), 278(40), 277(40), 276(50), 265(30), 263(25); **HRMS** (EI) $C_{26}H_{22}$, expt'l 334.1719, cacl. 334.1722, error -0.6 ppm.

7.4 CAN OXIDATION OF CYCLOPROPYLARENES

7.4.1 Cyclopropylbenzenes

Into 3 vials were introduced 100 uL 1-cyclopropyl-4-methylbenzene (80 mg, 0.6 mmol), cyclopropylbenzene (94 mg, 0.8 mmol) and toluene (86 mg, 0.94 mmol), respectively. 5 mL CH_3CN was then added to each vial fitted with stirrer. To each solution, two equiv. of CAN was introduced (660 mg, 877 mg and 1030 mg, respectively). The three vials were put in the electrical plate and heated at a temperature of $75 \rightarrow 80\ ^{o}C$ for 5 minutes with stirring. For cyclopropane derivatives, the white solid (Ce(III) salt) was gradually formed, but for toluene, no obvious reaction occurred (orange color was not changed).

The reaction mixture was poured into a 30 mL diethyl ether and worked up with water for four times, then the organic layer was dried over $MgSO_4$, filtered and concentrated. 1 mL $CDCl_3$ was added to rinse the products. After addition of certain amount of internal standard, $(CH_3)_3OSiO(CH_3)_3$, ^1H NMR was run to determine the yields of products.

The product mixture was then separated via preparative thin layer chromatography. For cyclopropylbenzene, PTLC using hexane/ethyl acetate (10:1) as solvent gave pure 1-phenylpropyl-1,3-dinitrate and a mixture of 1-cyclopropy-2-nitrobenzene and 1-cyclopropyl-4-nitrobenzene, which was in turn separated with PTLC using hexane/$CHCl_3$ (2:1) as solvents. For 1-cyclopropyl-4-methylbenzene, PTLC using hexane/ethyl acetate (10:1) as solvent gave 1-(4-methylphenyl)propyl-1,3-dinitrate and 1-cyclopropyl-2-nitro-4-methylbenzene. It was noted that 1,3-dinitrates can be converted to 1-(4-methylphenyl)-1-hydroxypropylnitrate if left on the PLC plate for a long time.

The products were characterized as the following:

1-Phenylpropyl-1,3-dinitrate (60.7%) **^{1}H NMR** δ 2.24(1H, m), 2.43(1H, m), 4.42(1H, m), 4.58(1H, m), 5.9(1H, t), 7.40(5H, m); **^{13}C NMR** δ 31.9(CH_2), 68.4(CH_2), 81.3(CH), 126.3(CH, aromatic), 129.1(CH, aromatic), 129.5(CH, aromatic), 136.4(C, aromatic); **IR** *v* (cm^{-1}) 1637(s), 1278(s), 852(s); **MS**(EI) *m/e* 242(M^+, 2.6), 180(M-ONO_2, 15.2), 152(14.3), 150(25), 117(32), 105(100); **HRMS**(EI) $C_9H_{10}O_6N_2$, calc. 242.0539, expt'l 242.0537, error -0.9 ppm.

1-Cyclopropyl-2-nitrobenzene (20%) **^{1}H NMR** δ 0.71(2H, m), 1.05(2H, m), 2.39(1H, m), 7.15(1H, d), 7.28(1H, t), 7.47(1H, t), 7.79(1H, d); **^{13}C NMR** δ 8.0(CH_2), 12.4(CH), 124.0(CH, aromatic), 126.3(CH, aromatic), 127.9(CH, aromatic), 132.5(CH, aromatic), 138.0(C, aromatic); **IR** *v* (cm^{-1}) 1524(s), 1350(s); **MS**(CI) *m/e* 164(MH^+, 30), 134(77), 83(100).

1-Cyclopropyl-4-nitrobenzene (7.5%) **^{1}HN MR** δ 0.82(2H, m), 1.13(2H, m), 1.99(1H, m), 7.15(2H, d), 8.11(2H, d); **^{13}C NMR** δ 11.0(CH_2), 15.8(CH), 123.6(CH, aromatic), 125.9(CH, aromatic), 152.6(C, aromatic); **IR** *v* 1637, 1602, 1519(s), 1340(s); **MS**(CI) *m/e* 164(MH^+, 11.3); MS(EI) 163(M^+, 23), 115(100); **HRMS**(CI) $C_9H_{10}O_2N_1$, calc. 164.0712, expt'l 164.0715, error 2.0 ppm.

1-(4-Methylphenyl)propyl-1,3-dinitrate (67.4%) **^{1}H NMR** δ 2.21(1H, m), 2.37(3H, s), 2.41(1H, m), 4.41(1H, m), 4.56(1H, m), 5.88(1H, t), 7.23(4H, dd); **^{13}C NMR** δ 21.2(CH_3), 31.8(CH_2), 68.5(CH_2), 81.4(CH), 126.4(CH, aromatic), 129.8(CH, aromatic), 133.3(C, aromatic), 139.6(C, aromatic); **IR**($CHCl_3$) *v* 1641(s), 1281(s), 1216, 908, 849; **MS**(EI) *m/e* 256(M^+, 2.6), 194(M^+-ONO_2, 1.3), 164(7.8), 119(100); **HRMS**(EI) $C_{10}H_{12}O_6N_2$, calc. 256.0695, expt'l 256.0705, error 3.7 ppm.

1-Cyclopropyl-2-methyl-4-nitrobenzene (12.8%) **^{1}H NMR** δ 0.65(2H, m), 1.00(2H, m), 2.34(1H, m), 2.36(3H, s), 7.04(1H, d), 7.27(1H, d), 7.61(1H, s); **^{13}C NMR** δ 7.7(CH_2), 12.2(CH), 20.6(CH_3), 124.3(CH, aromatic), 127.9(CH, aromatic), 133.3(CH, aromatic), 134.9(C, aromatic), 136.6(C, aromatic); **IR** *v* 1530(s), 1350(s); **MS**(CI) *m/e* 178(MH^+, 37); MS(EI) 177(M^+, 2.6), 149(37), 128(47), 115(93); **HRMS**(CI) $C_{10}H_{12}O_2N_1$, calc. 178.0868, expt'l 178.0874 error 3.1 ppm.

7.4.2 Cyclopropylnaphthalenes

1-Cyclopropylnaphthalene. Into a 50 mL round-bottomed flask was added 33.6 mg (0.2 mmol) of 1-cyclopropylnaphthalene and 10 mL CH_3CN/CH_3OH (9:1, v/v). 219.2 mg(0.4 mmol) of CAN was than introduced into flask which was fitted with stirrer, circulated with N_2 and set in oil-bath. The reaction mixture was refluxed at a temperature of 55 ^{o}C for 10 hours and then poured into diethyl ether and water for workup. The combined ether layers was dried over anhydrous $MgSO_4$, filtered and concentrated. First PTLC using 7:1 (v/v) hexane/EtOAc as solvents gave 7.4 mg (22%) of starting material 1-cyclopropylnaphthalene, 18.3 mg (35%) 3-methoxy-3-naphthylpropylnitrate and a mixture of 1-naphthylpropyl-1,3-dinitrate, 3-hydroxy-3-naphthylpropylnitrate and 1- naphthyl-1,3-dimethoxypropane. Second PTLC with $CHCl_3$ as solvent yielded 9.4 mg (20.4%) of 1-naphthyl-1,3-dimethoxypropane, 2.75 mg (4.7%) 1-naphthylpropyl-1,3-dinitrate and 2.15 mg (4.4%) of 3-hydroxy-3-naphthylpropylnitrate. It was noted that 3-hydroxy-3-naphthylpropylnitrate was produced in PTLC from 1-naphthylpropyl-1,3-dinitrate.

3-Methoxy-3-(1-naphthyl)propylnitrate **^{1}H NMR** δ 2.27(2H, m), 3.31(3H, s), 4.55(1H, m), 4.74(1H, m), 5.04(1H, t), 7.53(3H, m), 7.82(1H, d), 7.91(1H, d), 8.13(1H, d); **^{13}C NMR** δ 34.7(CH_2), 57.0(CH_3O), 70.4(CH_2), 77.7(CH), 122.8(CH, aromatic), 123.9(CH, aromatic), 125.4(CH, aromatic), 125.7(CH, aromatic), 126.3(CH, aromatic), 128.4(CH, aromatic), 129.1(CH, aromatic), 130.8(C, aromatic), 134.0(C, aromatic), 136.1(C, aromatic); **IR** *v* 1633(s, O-N asymmetric stretching), 1281(s, O-N symmetric stretching), 1113, 862(p bond N-O linkage); **MS**(EI) *m/e* 262(M+1, 1.3), 261(M^+, 11), 171(M-$CH_2CH_2ONO_2$, 100), 153(54), 127(29); **HRMS**(EI) $C_{14}H_{15}O_4N$, expt'l 261.0994, calc. 261.1001, error -2.5 ppm.

1-Naphthylpropyl-1,3-dinitrate **^{1}H NMR** δ 2.48(2H, m), 4.48(1H, m), 4.66(1H, m), 6.71(1H, t), 7.56(3H, m), 7.9(2H, m), 8.06(1H, d); **^{13}C NMR** δ 31.9(CH_2), 68.6(CH_2), 78.4(CH), 121.9(CH, aromatic), 123.5(CH, aromatic), 125.4(CH, aromatic), 126.3(CH, aromatic), 127.2(CH, aromatic), 129.3(CH, aromatic), 129.8(C, aromatic), 129.9(CH, aromatic), 132.6(C, aromatic), 133.7(C, aromatic); **IR**($CHCl_3$) *v* 3021, 1647(s), 1281, 1215(s); **MS**(EI) *m/e* 292(15.7), 127(100); **HRMS**(EI) $C_{13}H_{12}O_6N_2$, calc. 292.0695, expt'l 292.0688, error -2.5 ppm.

3-Hydroxy-3-(1-naphthyl)propylnitrate **^{1}H NMR** δ 2.07(1H, d, OH), 2.31(2H, m), 4.62(1H, m), 4.81(1H, m), 5.66(1H, m), 7.53(3H, m), 7.68(1H, d), 7.82(1H, d), 7.91(1H,d), 8.06(1H, d); **^{13}C NMR** δ 35.1(CH_2), 67.6(CH), 70.5(CH_2), 122.6(CH, aromatic), 122.7(CH, aromatic), 125.4(CH, aromatic), 125.8(CH, aromatic), 126.5(CH, aromatic), 128.6(CH, aromatic), 129.1(CH, aromatic), 129.9(C, aromatic), 133.8(C, aromatic), 139.0(C, aromatic); **IR**($CHCl_3$) *v* 3601(-OH), 3018, 1633, 1281, 1216(s);

MS(EI) *m/e* 248(M+1, 2.6), 247(M, 26), 230(M-OH, 6.5), 157(M-$CH_2CH_2ONO_2$, 88), 129(100); **HRMS**(EI) $C_{13}H_{13}O_4N$, calc. 247.0845, expt'l 247.083969, error -2.0 ppm.

1-Bromo-4-cyclopropylnaphthalene. Into 50 mL round-bottomed flask was added 49.2 mg (0.2 mmol) of 1-Bromo-4-cyclopropylnaphthalene and 10 mL CH_3CN/CH_3OH (9:1, v/v). 219.2 mg (0.4 mmol) of CAN was than introduced into flask which was fitted with stirrer, circulated with N_2 and set in oil-bath. The reaction mixture was refluxed at a temperature of 55 ^oC for 9 hours and then poured into diethyl ether and water for workup. The combined ether layers was dried over anhydrous $MgSO_4$, filtered and concentrated. First PTLC using 7:1 (v/v) hexane/EtOAc as solvents gave 12.4 mg (25.2%) of starting material 1-bromo-4-cyclopropylnaphthalene, 22.6 mg (33.3%) 3-methoxy-3-(4-bromo-1-naphthyl)propylnitrate and a mixture of 1-(4-bromo-1-naphthyl)propyl-1,3-dinitrate and 1-(4-bromo-1-naphthyl)-1,3-dimethoxypropane. Second PTLC with $CHCl_3$ as solvent yielded 8.64 mg (14%) of 1-(4-bromo-1-naphthyl)-1,3-dimethoxypropane and 11.66 m g(15.6%) 1-(4-bromo-1-naphthyl)propyl-1,3-dinitrate.

3-Methoxy-3-(4-Bromo-1-naphthyl)propylnitrate **^{1}H NMR** δ 2.24(2H, m), 3.30(3H, s), 4.56(1H, m), 4.74(1H, m), 5.01(1H, t), 7.41(1H, d), 7.60(2H, m), 7.81(1H, d), 8.11(1H, d), 8.34(1H, d); **^{13}C NMR** δ 34.8(CH_2), 57.1(CH_3O), 70.2(CH_2), 77.3(CH), 123.05(CH, aromatic), 123.1(C, aromatic), 124.3(CH, aromatic), 127.16(CH, aromatic), 127.18(CH, aromatic), 128.3(CH, aromatic), 129.7(CH, aromatic), 131.97(C, aromatic), 132.2(C, aromatic), 136.4(C, aromatic); **IR**($CHCl_3$) *v* 3018, 1632(s, O-N asymmetric stretching), 1280(s, O-N symmetric stretching), 1116(s), 1112, 866(p bond N-O linkage); **MS**(EI) *m/e* 341(M+2, 9.0), 339(M^+, 8.6), 251(M+2-$CH_2CH_2ONO_2$, 100),

249(M-90, 97), 156(45), 152(69); **HRMS**(EI) $C_{14}H_{14}O_4NBr$, expt'l 339.0114, calc. 339.0106, error 2.2 ppm.

1-(4-Bromo-naphthyl)propyl-1,3-dinitrate **^{1}H NMR** δ 2.45(2H, m), 4.49(1H, m), 4.67(1H, m), 6.67(1H, t), 7.44(1H, d), 7.67(2H, m), 7.82(1H, d), 8.06(1H, m), 8.37(1H, m); **^{13}C NMR** δ 31.9(CH_2), 68.4(CH_2), 77.8(CH), 122.2(CH, aromatic), 123.7(CH, aromatic), 124.8(C, aromatic), 127.8(CH, aromatic), 128.1(CH, aromatic), 128.6(CH, aromatic), 129.6(CH, aromatic), 130.9(C, aromatic), 132.2(C, aromatic), 132.9(C, aromatic); **IR**($CHCl_3$) *v* 3018, 1645(s), 1279, 1215(s), 850; **MS**(EI) *m/e* 372(M+2, 3.6), 370(M^+, 3.3), 280(M-90, 7.8), 278(M+2-90, 7.5), 233(32), 152(100); **HRMS**(EI) $C_{13}H_{11}O_6N_2Br$, calc. 369.9800, expt'l 369.9807, error 1.8 ppm.

2-Cyclopropylnaphthalene. Into a 50mL round-bottomed flask was added 33.6 mg (0.2 mmol) of 2-cyclopropylnaphthalene and 10 mL CH_3CN/CH_3OH (9:1, v/v). 219.2 mg (0.4 mmol) of CAN was than introduced into flask which was fitted with stirrer, circulated with N_2 and set in oil-bath. The reaction mixture was refluxed at a temperature of 55 ^oC for 11 hours and then poured into diethyl ether and water for workup. The combined ether layers was dried over anhydrous $MgSO_4$, filtered and concentrated. First PTLC using 3:1 (v/v) hexane/EtOAc as solvents gave 3.9 mg (11.6%) of starting material 2-cyclopropylnaphthalene, 11.7 mg (22.4%) of 3-methoxy-3-(2-naphthyl)propylnitrate, 8.56 mg (18.6%) of 1- (2-naphthyl)-1,3-dimethoxypropane and a mixture of 1-(2-naphthyl)propyl-1,3-dinitrate and 3-hydroxy-3-(2-naphthyl). Second PTLC with $CHCl_3$ as solvent yielded 9.58 mg (16.4%) of 1-(2-naphthyl)propyl-1,3-dinitrate and 8.45 mg

(17.1%) of 3-hydroxy-3-(2-naphthyl)propylnitrate. It was noted that 3-hydroxy-3-(2-naphthyl)propylnitrate was produced in PTLC from 1-(2-naphthyl)propyl-1,3-dinitrate.

3-Methoxy-3-(2-naphthyl)propylnitrate **^{1}H NMR** δ 2.10(1H, m), 2.26(1H, m), 3.27(3H, s), 4.43(1H, m), 4.52(1H, m), 4.66(1H, m), 7.44(1H, d), 7.50(2H, m), 7.75(1H, s), 7.85(3H, d); **^{13}C NMR** δ 35.3(CH_2), 56.8(CH_3O), 70.2(CH_2), 79.9(CH), 123.8(CH, aromatic), 125.9(CH, aromatic), 126.1(CH, aromatic), 126.4(CH, aromatic), 127.7(CH, aromatic), 127.8(CH, aromatic), 128.8(CH, aromatic), 133.2(C, aromatic), 138.1(C, aromatic), 139.5(C, aromatic); **IR**($CHCl_3$) *v* 3018, 1633(s), 1281, 1216(s); **MS**(EI) *m/e* 261(M^+, 13.6), 171(M-90, 100); **HRMS**(EI) $C_{14}H_{15}O_4N$, calc. 261.1001, expt'l 261.0999, error -0.9 ppm.

1-(2-Naphthyl)propyl-1,3-dinitrate **^{1}H NMR** δ 2.34(1H, m), 2.53(1H, m), 4.47(1H, m), 4.62(1H, m), 6.07(1H, t), 7.47(1H, d), 7.54(2H, m), 7.86(3H, m), 7.91(1H, d); **^{13}C NMR** δ 31.9(CH_2), 68.4(CH_2), 81.4(CH), 123.1(CH, aromatic), 126.3(CH, aromatic), 126.9(CH, aromatic), 127.0(CH, aromatic), 127.8(CH, aromatic), 128.1(CH, aromatic), 129.3(CH, aromatic), 128.3(C, aromatic), 133(C, aromatic), 133.6(C, aromatic); **IR**($CHCl_3$) *v* 3018, 1642, 1281, 1216(s); **MS**(EI) *m/e* 292(M^+, 10.7), 127(100); **HRMS**(EI) $C_{13}H_{12}O_6N_2$, calc. 292.0695, expt'l 292.0695, error -0.0 ppm.

3-Hydroxy-3-(2-naphthyl)propylnitrate **^{1}H NMR** δ 2.09(1H, d, OH), 2.33(2H, m), 4.57(1H, m), 4.71(1H, m), 5.02(1H, m), 7.82(4H, m); **^{13}C NMR** δ 35.8(CH_2), 70.2(CH_2), 72.9(CH), 123.4(CH, aromatic), 124.5(CH, aromatic), 126.2(CH, aromatic), 126.5(CH, aromatic), 127.7(CH, aromatic), 127.9(CH, aromatic), 128.8(CH, aromatic), 133.1(C, aromatic), 133.2(C, aromatic), 140.6 (C, aromatic); **IR**($CHCl_3$) *v* 3605(-OH), 3018, 1636, 1281, 1215(s); **MS**(EI) *m/e* 248(M+1, 1.4), 247(M, 10),

230(M-OH, 6.5), 157(M-$CH_2CH_2ONO_2$, 30), 127(100); **HRMS**(EI) $C_{13}H_{13}O_4N$, calc. 247.0845, expt'l 247.0837, error -3.0 ppm.

7.4.3 Cyclopropylanthracenes

9-Cyclopropylanthracene. 26.6 mg (0.122 mmol) of 9-Cyclopropylanthracene was dissolved in 10 mL CH_3CN/CH_3OH (9:1, v/v) and 267.4 mg (0.488 mmol) CAN (mole ratio of CAN to 9-cyclopropylanthracene = 4) was than added. The reaction proceeded immediately. The orange color of the Ce(IV) solution disappeared and instead, a white solid (Ce(III) salt) in the solution was observed. The reaction mixture was stirred under nitrogen at room temperature for 20 minutes and then poured into water and extracted with diethyl ether. The ether layers was dried over anhydrous $MgSO_4$, filtered and concentrated. Products was separated by preparative thin layer chromatography CH_2Cl_2 as solvent, which yielded 6.5 mg (22%) of 9-cyclopropyl-10-methoxyanthracene, 15.4 mg (48%) of 9-cyclopropyl-9-methoxyanthrone. 21% of anthraquinone and 2% of 9-cyclopropyl-9-methoxy-10,10-dimethoxyanthracene were also obtained based on GC analysis.

Another run began with 49.05 mg (0.225 mmol) of 9-cyclopropylanthracene and 274 mg (0.50 mmol) of CAN. The reaction proceeded under same condition and the resulting solution was worked up with H_2O/diethyl ether. PTLC with 3:1 hexane/CH_2Cl_2 as solvents yielded 16.2 mg (29%) of 9-cyclopropyl-10-methoxyanthracene and 5.5 mg (10%) of starting material and a mixture of anthraquinone, 9-cyclopropyl-9-methoxyanthrone and 9-cyclopropyl-9-methoxy-10,10-dimethoxyxnthracene. Second PTLC of the mixture with 5:1 hexane/EtOAc as solvent yielded 5.7 mg (9%) of 9-

cyclopropyl-9-methoxy-10,10-dimethoxyxnthracene, 11.9 mg (17%) of 9-cyclopropyl-9-methoxyanthrone and 4.0 mg (9%) of anthraquinone (Table 5-1).

Product distribution of CAN oxidation of 9-cyclopropylanthracene in four different mole ratios of CAN to 9-cyclopropylanthracene were examined in the following experiment: Into each of four small vials was placed 5.6 mg (0.0257 mmol) and 1mL CH_3CN/CH_3OH (9:1, v/v). 13.7 mg (0.025 mmol), 27.4 mg (0.050 mmol), 41.4 mg (0.075 mmol) and 54.8 mg (0.10 mmol) of CAN were added to four vials, respectively. After 20 minutes, the reaction mixtures were worked up with H_2O/diethyl ether, dried over $MgSO_4$, filtered and evaporated to dryness. 5 mL CH_3CN was added into each of vials to dissolve the residue. 0.04 mL of the solution was taken and diluted into 2 mL with CH_3CN. HPLC was employed to analyze amount of products in each of four samples. The standard solutions of starting material 9-cyclopropylanthracene (0.01 mg/mL) and major product 9-cyclopropyl-10-methoxyanthracene (0.01 mg/mL) and 9-cyclopropyl-9-methoxyanthrone (0.04 mg/mL) in CH_3CH were prepared and HPLC correction factors for these compounds [1.0×10^{-4} (mg/mL)/area, 1.44×10^{-4} (mg/mL)/area and 1.41×10^{-4} (mg/mL)/area, respectively] were determined. The HPLC yields of products thus obtained were summarized in Table 5-2 (HPLC condition: CH_3CN/H_2O = 9:1, flow rate = 1 mL/min, UV detector: λ= 256 nm).

9-Bromo-10-cyclopropylanthracene. The reaction of 9-bromo-10-cyclopropylanthracene with CAN was performed in a similar procedure as that for 9-cyclopropylanthracene One run of reaction began with 42.2 mg (0.143 mmol) of 9-bromo-10-cyclopropylanthracene and 164.4 mg (0.30 mmol) of CAN. The reaction was

run in 10 mL 9:1(v/v) CH_3CN/CH_3OH for 20 min. The resulting solution was worked up and the products were isolated by PTLC with 3:1 hexane/CH_2Cl_2 as solvents, which gave 30.8 mg (60%) of 9-cyclopropyl-9-methoxyanthrone. 9% of anthraquinone was also obtained based on GC analysis.

Another run of reaction was performed in a 1 mL 9:1 (v/v) CH_3CN/CH_3OH containing 6.3mg (0.021mmol) of 9-bromo-10-cyclopropylanthracene and 24.7 mg (0.045 mmol) of CAN. The yield of product was determined by HPLC (HPLC condition: CH_3CN/H_2O = 9:1, flow rate = 1 mL/min, UV detector: λ= 256 nm). The standard curve method gave 4.3 mg (76.5%) of 9-cyclopropy-9-methoxyanthrone (0.01 mg/mL standard solution of 9-cyclopropy-9-methoxyanthrone). 8% of anthraquinone was also obtained based on GC analysis (Table 5-3).

7.4.4 9, 10-Dialkylanthracenes

9,10-Dimethylanthracne (DMA)

Run 1. 20 mg (0.097 mmol) of DMA was introduced into a 3-dram-vial and then 5 mL of CH_3CN/CH_3OH (9:1, v/v) was added. The solution (pale yellow) was stirred and kept in ice-bath (0 ^oC) for 5 min (DMA does not dissolve well in CH_3CN/CH_3OH). 101 mg (0.184 mmol, 1.9 equiv.of DMA) of CAN was added slowly and blue color of solution was noted at moment of CAN addition. The reaction mixture was stirred at 0 ^oC for 30 min and the resulting solution was colorless. The reaction mixture was poured into 20 mL diethyl ether and then water was added to do extraction. The ether layer was separated from water, dried over anhydrous $MgSO_4$, and filtered. White solid was obtained after concentrated. 0.6 mL $CDCl_3$ was added to rinse the solid

and $CDCl_3$ solution was then transferred into NMR tube. After 2 μL $[(CH_3)_3Si]_2O$ (internal standard) was introduced, ^1H NMR was run to determine the yields of products, according to

$$W_X = 0.1527\ (M_X\ V_S / N_X)(A_X / A_S)$$

where, W_X is weight of product X (mg), M_X molecular weight of X, V_S volume of internal standard S (μL), N_X number of protons integrated for product X, A_X area of integration for product X, and A_X area of integration for internal standard S. ^1H NMR showed that 9,10-dimethoxy-9,10-dimethylanthracene is only major product with a yield of 25.55 mg (98.3%). No trace of 9-methoxymethyl-10-methylanthracene was detected by ^1H NMR. PTLC was employed to isolate the product 9,10-dimethoxy-9,10-dimethylanthracene from reaction mixture and $CHCl_3$ was used as solvent.

9,10-Dimethoxy-9,10-dimethylanthracene **^{1}H NMR** δ 1.63(s, 6H, methyl), 2.79(s, 6H, methoxy), 7.41(m, 4H, aromatic), 7.68(m, 4H, aromatic); **^{13}C NMR** δ 35.9(methyl), 51.5(methoxy), 75.1(q-C), 126.0(CH, aromatic), 127.9(CH, aromatic), 138.6(C, aromatic); **IR**($CHCl_3$) *v* 1446, 1371, 1268, 1215(s), 1090, 1035; **MS**(CI) *m/e* 269(MH^+, 1.75), 253(M-15), 237(MH^+-32, 100), 205(MH^+-64, 35); **MS**(EI) *m/e* 268(M^+, trace), 253(M-15, 36), 237(M-31, 38), 222(M-46, 52), 207(M-61, 100), 206(M-62, 72).

Run 2. The experimental procedure is the same as that in run 1 except that reaction was controlled at 45 ^oC for 30 min. The reaction yielded 9.34 mg (40.8%) of 9-methoxymethyl-10-methylanthracene and 13.79 mg (53%) of 9,10-dimethoxy-9,10-dimethylanthracene. PTLC with $CHCl_3$ as solvent gave the pure 9-methoxymethyl-10-methylanthracene.

9-Methoxymethyl-10-methylanthracene **^{1}H NMR** δ 3.13(s, 3H, methyl), 3.55(s, 3H, methoxy), 5.44(s, 2H, methylene), 7.53(m, 4H, aromatic), 8.34(m, 2H, aromatic), 8.42(m, 2H, aromatic); **^{13}C NMR** δ 35.9(methyl), 58.3(methoxy), 66.8(methylene), 124.8(CH, aromatic), 124.9(CH, aromatic), 125.3(CH, aromatic), 125.6(CH, aromatic), 129.8(C, aromatic), 130.7(C, aromatic), 131.9(C, aromatic), 138.6(C, aromatic); **IR**($CHCl_3$) *v* 1463, 1279, 1214(s), 1092; **MS**(EI) *m/e* 237(M+1, 9.5), 236(M^+, 60), 221(M-15, 13), 205(M-31, 100), **HRMS**(EI) for $C_{17}H_{16}O$, calc. 236.1201, expt'l 236.1210, error 3.8 ppm.

The NMR tube containing pure 9-methoxymethyl-10-methylanthracene in $CDCl_3$ was placed in refrigerator. After several days some amount 9-methoxymethyl-10-methylanthracene was found converted to 9-methoxy-9-methyl-10-methyleneanthracene. PTLC with $CHCl_3$ as solvent gave the pure product.

9-Methoxy-9-methyl-10-methyleneanthracene **^{1}H NMR** δ 2.14(s, 3H, CH_3), 3.66(s, 3H, OCH_3), 4.54(s, 2H, $=CH_2$), 7.27(m, 4H, aromatic), 7.38(m, 2H, aromatic), 7.46(m, 2H, aromatic); **^{13}C NMR** δ 13.6(methyl), 60.2(methoxy), 69.6(methylene), 119.9(q-C), 120.7(CH, aromatic), 121.8(CH, aromatic), 127.3(CH, aromatic), 127.4(CH, aromatic), 130.7(q-C, methylene), 138.9(C, aromatic), 140.9(C, aromatic); **IR**($CHCl_3$) *v* 1463, 1223(s), 1122; **MS**(EI) *m/e* 237(M+1, 9.5), 236(M^+, 48), 221(M-15, 13), 205(M-31, 100); **HRMS**(EI) for $C_{17}H_{16}O$, calc. 236.1201, expt'l 236.1197, error -1.6 ppm.

Run 3. 40 mg (0.194 mmol) of DMA and 202 mg (0.368 mmol, 1.9 equiv. of DMA) of CAN reacted in 9:1 (v/v) CH_3CN/CH_3OH at 0 ^oC for 30 min (follow the procedure in run 1). The reaction mixture was equally divided into two portions. One

portion was directly worked up and products was analyzed by ^{1}H NMR, which exclusively yielded 24.54 mg (94.3%) of 9,10-dimethoxy-9,10-dimethylanthracene. Another portion was heated at 45^{o}C for 30min and was then worked up. The ^{1}H NMR analysis gave 9.85 mg (43.0%) of 9-methoxymethyl-10-methylanthracene and 12.75 mg (49.0%) of 9,10-dimethoxy-9,10-dimethylanthracene.

Run 4. The experimental procedure is the same as that in run 1 except that reaction was run in pure CD_3CN (no methanol) at 0 ^{o}C for 30 min. The reaction mixture was filtered through cotton to NMR tube and was subject to run ^{1}H NMR. ^{1}H NMR showed that there was no signal related to deprotonation product. The work up of this CD_3CN solution with water/ether gave deprotonation product. PTLC with $CHCl_3$ as solvent gave 9-(10-methylanthryl)methyl nitrate: ^{1}H NMR δ 3.18(s, 3H, methyl), 6.54(s, 2H, methylene), 7.62(m, 4H, aromatic), 8.36(m, 4H, aromatic).

9-Cyclopropyl-10-methylanthracene (**MCPA**)

Run 1. 20 mg (0.0862 mmol) of MCPA and 89.8 mg (0.0.164 mmol, 1.9 equiv. of MCPA) of CAN reacted in 9:1 (v/v) CH_3CN/CH_3OH at 0 ^{o}C for 30 min (following the procedure in run 1 of CAN oxidation of DMA in CH_3CN/CH_3OH). After work-up, 22.85 mg (90.5%) of 9-cyclopropyl-9,10-dimethoxy-10-methylanthracene was obtained as only major product, based on ^{1}H NMR analysis. PTLC with $CHCl_3$ as solvent gave pure product.

9-Cyclopropyl-9,10-dimethoxy-10-methylanthracene **^{1}H NMR** δ 0.35(m, 2H, cis-CP-methylene), 0.54(m, 2H, trans-CP-methylene), 1.14(m, 1H, methine), 1.71(s, 3H, methyl), 2.72(s, 3H, methoxy), 2.82(s, 3H, methoxy), 7.41(m, 4H, aromatic), 7.63(m,

2H, aromatic), 7.70(m, 2H, aromatic); **^{13}C NMR** δ 2.20(CP-methylene), 27.0(CP-methine), 35.8(methyl), 51.3(methoxy), 75.1(q-C), 76.3(q-C), 126.2(CH, aromatic), 126.5(CH, aromatic), 127.4(CH, aromatic), 127.9(CH, aromatic), 137.5(C, aromatic), 140.0(C, aromatic); **IR**($CHCl_3$) *v* 1476, 1446, 1216(s), 1087, 1062; **MS**(CI) *m/e* 295(MH^+, 3.5), 263(MH^+-32, 100); **MS**(EI) *m/e* 294(M^+, 0.75), 279(M-15, 6.5), 266(34), 253(31), 233(16), 222(54), 207(54), 192(100).

Run 2. The experimental procedure is the same as that in run 1 except that reaction was controlled at 45 ^oC for 30 min. The reaction yielded 8.42 mg (37.3%) of 9-cyclopropyl-10-methoxymethylanthracene and 14.55 mg (57.4%) of 9-cyclopropyl-9,10-dimethoxy-10-methylanthracene. PTLC with $CHCl_3$ as solvent gave pure 9-cyclopropyl-10-methoxymethylanthracene.

9-Cyclopropyl-10-methoxymethylanthracene **^{1}H NMR** δ 0.77(m, 2H, cis-CP-methylene), 1.46(m, 2H, trans-CP-methylene), 2.51(m, 1H, CP-methine), 3.56(s, 3H, methoxy), 5.42(s, 2H, methylene), 7.52(m, 4H, aromatic), 8.39(m, 2H, aromatic), 8.81(m, 2H, aromatic); **^{13}C NMR** δ 9.70(CP-methylene), 10.9(CP-methine), 58.4(methoxy), 66.7(methylene), 124.5(CH, aromatic), 124.6(CH, aromatic), 125.6(CH, aromatic), 126.5(CH, aromatic), 128.1(C, aromatic), 130.7(C, aromatic), 131.4(C, aromatic), 136.6(C, aromatic); **IR**($CHCl_3$) *v* 1663, 1601, 1447, 1317, 1279, 1215(s), 1091; **MS**(EI) *m/e* 263(M+1, 5), 262(M^+, 29), 231(M-31, 22), 230(35), 215(100); **HRMS**(EI) for $C_{19}H_{18}O$, calc. 262.1358, expt'l 262.1351, error -2.5 ppm.

The NMR tube containing pure 9-cyclopropyl-10-methoxymethylanthracene in $CDCl_3$ was placed in refrigerator. After several days some amount of 9-cyclopropyl-10-

methoxymethylanthracene was found converted to 9-cyclopropyl-9-methoxy-10-methyleneanthracene. PTLC with $CHCl_3$ as solvent gave the pure product.

9-Cyclopropyl-9-methoxy-10-methyleneanthracene **IR**($CHCl_3$) *v* 1553, 1419, 1215(s); **MS**(EI) *m/e* 263(M+1, 13), 262(M^+, 45), 231(M-31, 39), 230(52), 215(100); **HRMS**(EI) for $C_{19}H_{18}O$, calc. 262.1358, expt'l 262.1359, error 0.6ppm.

Control Experiment. 20 mg (0.0746 mmol) of 9,10-dimethoxy-9,10-dimethylanthracene in 0.9 mL $CDCl_3$ (colorless) was heated at 50°C for one hour. ^{1}HNMR showed that no reaction occurred. 2 drops of H_3PO_4 (98%) and 0.1 mL of CH_3OH were then added and heated at 50 °C for about 15min. The solution color changed into yellow. After work-up with diethyl ether and water. ^{1}H NMR was run to determine the yield of products. 57% of 9,10-dimethoxy-9,10-dimethylanthracene was converted into 9-methoxymethyl-10-methylanthracene and the yield was about 100%.

LITERATURE CITED

(1) a) Kaiser, E.; Kevan, L. (eds.), "*Radical Ions*", Interscience, New York, **1968**; b) Forrester, R.; Ishizu, K.; Kothe, G.; Nelson, S.; Ohya-Nishiguchi, H.; Watanabe, K.; Wilker, W., "*Organic Cation Radicals and Polyradicals*", in Landolt Bornstein, Numerical Data and Functional Relationships in Science and Technology, Springer Berlin, Heidelberg, New York, **1980**, Vol. IX, Part d2; c) Shida, T., "*Electronic Absorption Spectra of Radical Ions*", Elsevier, Amsterdam, **1988**.

(2) a) Shida, T.; Haselbach, E.; Bally, T., *Acc. Chem. Res.*, **1984**, 17, 180; b) Nelsen, S., *Acc. Chem. Res.*, **1987**, 20, 269; c) Roth, H., *Acc. Chem. Res.*, **1987**, 20, 343; d) Roth, H.; Schilling, M.; Wamser, C., *J. Am. Chem. Soc.*, **1984**, 106, 5023.

(3) Blankenship, R.; Parson, W., *Ann. Rev. Biochem.*, **1978**, 47, 635.

(4) Green, S., *Rev. Phys. Chem.*, **1981**, 32, 103.

(5) Wudl, F., *Acc. Chem. Res.*, **1984**, 17, 227.

(6) Maroulis A.; Shigemitsu, Y.; Arnold, D., *J. Am. Chem. Soc.*, **1978**, 100, 535.

(7) Bauld, N.; Bellville, D.; Hairirchian, B.; Lorenz, K.; Pabon, R.; Revnolds, D.; Wirth, D.; Chiou, H.; Marsh, B., *Acc. Chem. Res.*, **1987**, 20, 371.

(8) Kornblum, N., *Angew. Chem. Int. Ed. Engl.*, **1975**, 17, 180.

(9) Bard, A.; Ledwith, A.; Shine, H., *Advances in Physical Organic Chemistry*, **1976**, 13, 155.

(10) Eberson, L., *Advances in Physical Organic Chemistry*, **1982**, 18, 79.

(11) Hammerich, O.; Parker, V., *Advances in Physical Organic Chemistry*, **1984**, 20, 55.

(12) Roth, H., *Top. Curr. Chem.*, **1992**, 163, 133.

(13) Hixson, S., in "*Organic Photochemistry*", Padwa, A., ed., Marcel Dekker, New York, **1979**, Vol. 4, Chapter 3, pp191-326.

(14) Boche, G.; Walborsky, H., in "*Cyclopropane Derived Reactive Intermediates*", Patai, S.; Rappoport, Z., ed., John Wiley & Sons, New York, **1990**, Chapter 5, pp207-236.

(15) a) Ledwith A., *Acc. Chem. Res.*, **1972**, 5, 133; b) Mattes, S.; Farid, S., *Org. Photochem.*, **1983**, 6, 233; c) Mattay, J., *Angew. Chem. Int. Ed. Engl.*, **1987**, 26, 825.

(16) a) Yoshida, K., "*Electrooxidation in Organic Chemistry*", Wiley, New York, **1984**; b) Bard, A.; Faulkner, L.; "*Electrochemical Methods*", Wiley, New York, **1980**; c) Eberson, L., "*Electron Transfer Reactions in Organic Chemistry*", Springer Verlag, New York, **1987**.

(17) a) Kuwana, T.; Heineman, W., *Acc. Chem. Res.*, **1976**, 9, 241; b) Kuwana, T.; Winograd, N., in "*Electroanalytical Chemistry*" Bard, A., ed., Dekker, New York, **1974**, vol. 7, pp1.

(18) Eberson, L.; Utley, J.; Hammerich, O., in "*Organic Electrochemistry, An Introduction and A Guide, Third Edition, Reversed and Expanded*", **1994**, Marcel Dekker, Inc., New York, pp. 505-533.

(19) a) Nicholas, M.; Arnold, D., *Can. J. Chem.*, **1982**, 60, 2165; b) Nicholas, M.; Boyd, R.; Arnold, D., *Can. J. Chem.*, **1982**, 60, 3011.

(20) Eberson, L., *Tetrahedron*, **1978**, 34, 731.

(21) a) Shono, T.; Matsumura, Y., *J. Org. Chem.*, **1970**, 35, 4157; b) Shono, T.; Matsumura, Y.; Nakagawa, Y., *J. Org. Chem.*, **1971**, 36, 1771.

(22) Shono, T.; Matsumura, Y., *Bull. Chem. Soc. (jpn)*, **1975**, 48, 2861.

(23) a) Klehr, M.; Schafer, H., *Angew. Chem.*, **1975**, 87, 173; b) Torii, S.; Okamoto, T.; Ueno, N., *J. Chem. Soc. Chem. Communi.*, **1978**, 293; c) Torii, S.; Inokuchi, T.; Takahashi, N., *J. Org. Chem.*, **1978**, 43, 5020.

(24) Baggaley, A.; Brettle, R.; Sutton, J., *J. Chem. Soc. Perkin Trans. I*, **1975**,1055.

(25) a) Brettle, R.; Sutton, J., *J. Chem. Soc. Perkin Trans. I*, **1975**,1955; b) Gassman, P.; Yamaguchi, R., *J. Am. Chem. Soc.*, **1979**, 101, 1308.

(26) Matsubara, Y.; Uchida, T.; Ohnishi, T.; Kanehira, K.; Fujita, Y.; Hirashima, T.; Nishiguchi, I., *Tetrahedron Lett.*, **1985**, 26, 4513.

(27) Uchida, T.; Matsubara, Y.; Nishiguchi, I.; Hirashima, T.; Ohnishi, T.; Kanehira, K., *J. Org. Chem.*, **1990**, 55, 2938.

(28) Wayner, D.; Arnold, D., *J. Chem. Soc. Chem. Communi.*, **1982**.

(29) Wayner, D.; Arnold, D., *Can. J. Chem.*, **1985**, 63, 871.

(30) Wayner, D.; Arnold, D., *Can. J. Chem.*, **1986**, 64, 100, 1087.

(31) Rao, V.; Hixson, S., *J. Am. Chem. Soc.*, **1979**, 101, 6458.

(32) Mizuno, K.; Ogawa, J.; Kagano, H.; Otsuji, Y., *Chem. Lett.*, **1981**, 437.

(33) Mizuno, K.; Ogawa, J.; Otsuji, Y., *Chem. Lett.*, **1981**, 741.

(34) Mizuno, K.; Yoshioka, K.; Otsuji, Y., *Chem. Lett.*, **1983**, 941.

(35) Dinnocenzo, J.; Todd, W.; Simpson, T.; Gould, I., *J. Am. Chem. Soc.*, **1990**, 112, 2462.

(36) a) Gassman, P.; Olson, K.; Walter, L.; Yamaguchi, R., *J. Am. Chem. Soc.*, **1981**, 103, 4977; b) Gassman, P.; Olson, K., *J. Am. Chem. Soc.*, **1981**, 103, 4977; c) Gassman, P.; Hay, B., *J. Am. Chem. Soc.*, **1986**, 108, 4227; d) Gassman, P., in "*Photoinduced Electron Transfer*", Fox, M.; Chanon, M., Eds., Elsevier, Amsterdam, **1988**, Part C, Chapter 4.2, p70; e) Arnold, D.; Du, X., *Can. J. Chem.*, **1994**, 72, 403; f) Weng, H.; Roth, H., *J. Org. Chem.*, **1995**, 60, 4136; g) Weng, H.; Sethuraman, V.; Roth, D., *J. Am. Chem. Soc.*, **1994**, 116, 7021.

(37) Shaik, S; Dinnocenzo, J., *J. Org. Chem.*, **1990**, 55, 3434.

(38) Dinnocenzo, J.; Simpson, T.; Zuilhof, H.; Todd, W.; Heinrich, T., *J. Am. Chem. Soc.*, **1997**, 119, 987.

(39) Dinnocenzo, J.; Lieberman, D.; Simpson, T.; Gould, I., *J. Am. Chem. Soc.*, **1993**, 115, 366.

(40) Hammond, G., *J. Am. Chem. Soc.*, **1955**, 77, 334.

(41) Dinnocenzo, J.; Zuilhof, H.; Lieberman, D.; Simpson, T.; McKechney, M., *J. Am. Chem. Soc.*, **1997**, 119, 994.

(42) a) Mazzocchi, P.; Somich, C.; Edwards, M.; Morgan, T.; Ammon, H., *J. Am. Chem. Soc.*, **1986**, 108, 6828; b) Mazzocchi, P.; Somich, C., *Tetrahedron Lett.*, **1988**, 29, 513; c) Somich, C.; Mazzocchi, P.; Edwards, M.; Morgan, T.; Ammon, H., *J. Org. Chem.*, **1990**, 55, 2624.

(43) a) Maruyama, K.; Imahori, H.; Ozawa, Y., *Chem. Lett.*, **1989**, 2117; b) Takahashi, Y.; Endoh, F.; Ohaku, H.; Wakamatsu, K.; Miyashi, T., *J. Chem. Soc., Chem. Commun.*, **1994**, 1127.

(44) a) Dinnocenzo, J.; Schmittel, M., *J. Am. Chem. Soc.*, **1987**, 109, 1561; b) Dinnocenzo, J.; Conlon, D., *J. Am. Chem. Soc.*, **1988**, 110, 2324; c) Hixson, S.; Boyer, J.; Gallucci, C., *J. Chem. Soc., Chem. Commun.*, **1974**, 540; d) Wong, P.; Arnold, D., *Tetrahedron Lett.*, **1979**, 2101; e) Arnold, D.; Humphreys, R., *J. Am. Chem. Soc.*, **1979**, 2743; f) Roth, H.; Schilling, M., *J. Am. Chem. Soc.*, **1980**, 102, 7956; g) Qin, X.; Snow, L.; Williams, F., *J. Am. Chem. Soc.*, **1984**, 106, 7640; h) Roth, H.; Schilling, M., *J. Am. Chem. Soc.*, **1985**, 107, 1079.

(45) a) Mizuno, K.; Kamiyama, N.; Ichinose, N.; Otsuji, Y., *Tetrahedron*, **1985**, 41, 2207; b) Mizuno, K.; Ichinose, N.; Otsuji, Y., *Chem. Lett.*, **1985**, 455.

(46) a) Ouellette, R.; Robins, R.; South, A., *J. Am. Chem. Soc.*, **1968**, 90, 1619, and references therein.

(47) Young, L., *Tetrahedron Lett.*, **1968**, 5105.

(48) a) Baciocchi, E.; Mandolini, L.; Rol, C., *Tetrahedron Lett.*, **1973**, 3787; b) Baciocchi, E.; Mandolini, L.; Rol, C., *Tetrahedron Lett.*, **1976**, 3343; c) Baciocchi, E.; Rol, C.; Ruzziconi, R., *J. Chem. Research (s)*, **1984**, 334.

(49) Baciocchi, E.; D'Acunzo, F.; Galli, C.; Lanzalunga, O., *J. Chem. Soc., Perkin Trans. 2*, **1994**, 133.

(50) Baciocchi, E.; Rol, C., *J. Am. Chem. Soc.*, **1980**, 102, 7598.

(51) Fujita, M.; Fukuzumi, S., *J. Chem. Soc., Chem. Commun.*, **1993**, 1982.

(52) a) Onopchenko, A.; Schulz, J.; Seekircher, R., *J. Org. Chem.*, **1972**, 37, 1414; b) Onopchenko, A.; Schulz, J., *J. Org. Chem.*, **1972**, 37, 2564.

(53) Baciocchi, E.; Gabrielli, R.; Giancaspro, C.; Rol, C.; Sebastaini, G.; Speranza, M., *Tetrahedron Lett.*, **1985**, 26, 4269.

(54) a) Baciocchi, E.; Mattioli, M.; Romano, R.; Ruzziconi, R., *J. Org. Chem.*, **1991**, 56, 7154; b) Baciocchi, E.; Cort, A.; Eberson, L.; Mandolini, L.; Rol, C., *J. Org. Chem.*, **1986**, 51, 4544.

(55) Baciocchi, E.; Giacco, T.; Elisei, F., *J. Am. Chem. Soc.*, **1993**, 115, 12290.

(56) Baciocchi, E.; Bietti, M.; Mattioli, M., *J. Org. Chem.*, **1993**, 58, 7106.

(57) Baciocchi, E.; Rol, C.; Sebastiani, G., *Gazz. Chim. Ital.*, **1982**, 112, 513.

(58) Baciocchi, E.; Bietti, M.; Putignani, L.; Steenken, S., *J. Am. Chem. Soc.*, **1996**, 118, 5952.

(59) Kochi, J., *Tetrahedron Letter*, **1974**, 4305.

(60) Schlesener, C.; Amatore, C.; Kochi, J., *J. Am. Chem. Soc.*, **1984**, 106, 3567.

(61) Schlesener, C.; Amatore, C.; Kochi, J., *J. Phys. Chem.*, **1986**, 90, 3747.

(62) Schlesener, C.; Amatore, C.; Kochi, J., *J. Am. Chem. Soc.*, **1984**, 106, 7472.

(63) a) Parker, V., *Acta Chem. Scand.*, **1985**, B39, 227; b) Parker, V.; Tilset, M., *J. Am. Chem. Soc.*, **1986**, 108, 6371.

(64) a) Walling, C.; Zhao, C.; EI-Taliawi, G., *J. Org. Chem.*, **1983**, 48, 4910; b) Walling, C.; EI-Taliawi, G.; Zhao, C., *J. Org. Chem.*, **1983**, 48, 4914.

(65) Walling, C.; EI-Taliawi, G.; Amarnath, K., *J. Am. Chem. Soc.*, **1984**, 106, 7573.

(66) Sehested, K.; Holcman, J., *J. Phys. Chem.*, **1976**, 82, 651.

(67) Bciocchi, E.; Rol, C., *Gazz. Chim. Ital.*, **1983**, 113, 727.

(68) Tolbert, L.; Khanna, R., *J. Am. Chem. Soc.*, **1987**, 109, 3477.

(69) Tolbert, L.; Khanna, R.; Popp, A.; Gelbaum, L.; Bottomley, L., *J. Am. Chem. Soc.*, **1990**, 112, 2373.

(70) Sirimanne, S.; Li, Z.; VanderVeer, D.; Tolbert, L., *J. Am. Chem. Soc.*, **1991**, 113, 1766.

(71) Anzenbacher, P.; Niwa, T.; Tolbert, L.; Sirimanne, S.; Guengerich, F., *Biochemistry*, **1996**, 35, 2512.

(72) Camaioni, D.; Alnajjar, M., *J. Org. Chem.*, **1985**, 50, 4456.

(73) Deardurff, L.; Alnajjar, M.; Camaioni, D., *J. Org. Chem.*, **1986**, 51, 3686.

(74) Deardurff, L.; Camaioni, D., *J. Org. Chem.*, **1986**, 51, 3693.

(75) a) Silverman, R. B.; Hoffman, S. J. *J. Am. Chem. Soc.* **1980**, 102, 884; b) Silverman, R. B.; Hoffman, S. J.; Catus, W. B., III *J. Am. Chem. Soc.* **1980**, 102, 7126.

(76) a) Hanzlik, R. P.; Tullman, R. H. *J. Am. Chem. Soc.* **1982**, 104, 2048; b) Riley, P.; Hanzlik, R. P. *Tetrahedron Lett.* **1989**, 30, 3015.

(77) Macdonald, T. L.; Zirvi, K.; Burke, L. T.; Peyman, P.; Guengerich, F. P. *J. Am. Chem. Soc.* **1982**, 104, 2050.

(78) a) Castellino, A. J.; Bruice, T. C.; *J. Am. Chem. Soc.* **1988**, 110, 1313; b) Castellino, A. J.; Bruice, T. C. *J. Am. Chem. Soc.* **1988**, 110, 7512.

(79) a) Tanko, J. M.; Drumright, R. E. *J. Am. Chem. Soc.* **1990**, 112, 5362; b) Tanko, J. M.; Drumright, R. E. *J. Am. Chem. Soc.* **1992**, 114, 1844.

(80) a) Tanko, J. M.; Mas, R. H.; Suleman, N. K. *J. Am. Chem. Soc.* **1990**, 112, 5557; b) Arnold, J. C.; Gleicher, G. J.; Unruh, J. D. *J. Am. Chem. Soc.* **1974**, 96, 787; c) Tanko, J. M.; Suleman, N. K.; Blackert, J. F. *J. Org. Chem.* **1991**, 56, 6395.

(81) a) Creary, X., *J. Org. Chem.* **1980**, 45, 4653; b) Jason, M.; Kurzweil, P.; Leonard, K., *J. Org. Chem.* **1986**, 51, 2550.

(82) Shono, T. in "*Best Synthetic Methods: Electroorganic Synthesis*", Academic Press, **1991**, pp. 36-46.

(83) Bockmain, G.; Fritz, H., *Electrochim. Acta*, **1976**, 21, 1099.

(84) Yoshida, K.; Nagase, S., *J. Am. Chem. Soc.*, **1979**, 101, 4268.

(85) Achord, J.; Hussey, C., *J. Electtochem. Soc.*, **1981**, 128, 2556.

(86) Rozhkov, I.; Bukhtiarov, A. etc., *Dokl. Chem.* USSR (Engl. Trans.), **1970**, 193, 618.

(87) Eberson, L.; Hartshorn, M.; Persson, O., *J. Chem. Soc. Perkin Trans. 2*, **1995**, 409.

(88) a) Enkelmann, V.; Morra, B.; Krohnke, Ch.; Wegner, G., *Chem. Phys.*, **1982**, 66, 303; b) Terahara, A.; Ohya-nishiguchi, H.; Hirota, N.; Oku, A., *J. Phys. Chem.*, **1986**, 90, 1564.

(89) a) Nadjo, L.; Savéant, J., *Electroanal. Chem.*, **1973**, 48, 113; b) Andrieux, C.; Savéant, J., in "*Investigation of Rates and Mechanisms of Reactions, Part II, 4th Ed.*," Bernasconi, C., Ed., Wiley: New York, **1986**, pp 305 - 390.

(90) a) Parker, V., in *Topics in Organic Electrochemistry*, Fry, A.; Britton, W., Eds., Plenum Press, New York, **1986**, pp. 35 - 79; b) Parker, V., in *Comprehensive*

Chemical Kinetics, Vol. 26, Electrode Kinetics: Principles and Methodology; Bamford, C.; Compton, R., Eds., Elsevier, New York, **1986**, pp. 145 - 202

(91) $\partial\log(v_c)/\partial\log[\mathbf{2}] \approx 1$ is consistent with two rate laws: $k[\mathbf{2}^{+\cdot}]^2$ or $k[\mathbf{2}][\mathbf{2}^{+\cdot}]$. However, only the former is consistent with the LSV results.

(92) Simulations were performed using *DigiSim 2.1 (R) - A General Simulation Program for Cyclic Voltammetry*, Rudolph M.; Feldberg, S., Distributed by Bioanalytical Systems Inc., 2701 Kent Ave, West Lafayette 47906 USA.

(93) Butts, C.; Eberson, L.; Hartshorn, M.; Persson, O.; Robinson, W., *Acta Chem. Scand.*, **1995**, 49, 253.

(94) a) Peover, M., in "*Electroanalytical Chemistry*," Bard, A., Ed., Marcel Dekker, New York, **1967**, pp. 1→48; b) Phelps, J.; Santhanam, K.; Bard, A., *J. Am. Chem. Soc.* **1967**, 89, 1752.

(95) a) Bockman, T.; Kochi, J., *J. Am. Chem. Soc.*, **1989**, 111, 4669; b) Bockman, T.; Kochi, J., *J. Am. Chem. Soc.*, **1988**, 110, 1294.

(96) This kinetic analysis is based upon k_{dim} for $\mathbf{2}^{+\cdot}$. It is expected that k_{MeOH} for $\mathbf{1}^{+\cdot}$ is even slower. Dinnocenzo has shown that for substituted cyclopropylbenzene radical cations, the rate of nucleophile-induced ring opening correlates to σ^+ (and is facilitated by electron withdrawing groups). For Br, $\sigma^+ = 0.15$, vs. 0.0 for H.

(97) RSE's for $ArCH_2^{\cdot}$ were taken as the difference in the bond strength of $ArCH_2$-H (88.0, 85.1, and 85.7 kcal/mol for Ar = C_6H_5, α-, and β-$C_{10}H_7$, respectively) and CH_3CH_2-H (98.2 kcal/mol). Bond strengths were taken from McMillen, D.; Golden,

D., *Ann. Rev. Phys. Chem.*, **1982**, 33, 493. The BDE of β-$C_{10}H_7CH_2$-H was not available and was estimated using ΔH_f^o's obtained using SCF-MO theory (AM1).

(98) Benson, S., "*Thermochemical Kinetics*," Wiley: New York, **1976**, p309.

(99) Parker, V., *J. Am. Chem. Soc.*, **1992**, 114, 7458.

(100) Deno, N.; Gaugler, R.; Wisotsky, M., *J. Org. Chem.*, **1966**, 31, 1967.

(101) Deno, N.; Turner, J., *J. Org. Chem.*, **1966**, 31, 1969.

(102) Levin, R.; Lias, S., *Ionization Potential and Appearance Potential Measurements, 1971 – 1981* (NSRDS-NBS 71), U. S. Government Printing Office, Washington, D. C., **1982**.

(103) Wang, Y.; Tanko, J., Unpublished results at Virginia Polytechnic Institute and State University.

(104) For an excellent discussion of qualitative MO theory pertaining to arylcyclopropanes, see Takahashi, Y.; Ohaku, H.; Nishioka, N.; Ikeda, H.; Miyashi, T.; Gormin, D.; Hillinski, E., *J. Chem. Soc., Perkin Trans. 2*, **1997**, 303.

(105) Drumright, R.; Mas, R.; Merola, J.; Tanko, J., *J. Org. Chem.*, **1990**, 55, 4098.

(105) For a related discussion pertaining to reactions of nucleophiles with vinylcyclopropane radical cations, see Herbertz, T.; Roth, H., *J. Am. Chem. Soc.*, **1996**, 118, 10954.

(107) a) Maillard, B.; Forrest, D.; Ingold, K., *J. Am. Chem. Soc.*, **1976**, 98, 7024; b) Kinney, R.; Jones, R.; Bergman, R., *J. Am. Chem. Soc.*, **1978**, 100, 7902; c) Beckwith, A.; Moad, G., *J. Chem. Soc., Perkin Trans. 2*, **1980**, 1473; d) Effio, A.; Griller, D.; Ingold, K.; Beckwith, A.; Serelis, A., *J. Am. Chem. Soc.*, **1980**,

102, 1734; e) Mathew, L.; Warketin, J., *J. Am. Chem. Soc.* **1986**, 108, 7981; f) Beckwith, A.; Bowry, V.; Moad, G., *J. Org. Chem.*, **1988**, 53, 1632; g) Newcomb, M.; Glenn, A., *J. Am. Chem. Soc.*, **1989**, 111, 275; h) Beckwith, A.; Bowry, V., *J. Org. Chem.*, **1989**, 54, 2681.

(108) Tanner, D.; Chen, J.; Luelo, C.; Peters, P., *J. Am. Chem. Soc.*, **1992**, 114, 713.

(109) Simmons, H.; Cairns, T.; Vladuchick, S.; Hoiness, C., in "*Organic Reactions*", Dauben, W. etc. eds., **1973**, vol. 20, pp 1~132, John Wiley & Sons, Inc., New York.

(110) Marcoux, L.; Fritsch, J.; Adams, R., *J. Am. Chem. Soc.*, **1967**, 89, 5766.

(111) Phelps, J.; Santhanam, K.; Bard, A., *J. Am. Chem. Soc.*, **1967**, 89, 1752.

(112) Peover, M.; White, B., *J. Electroanal. Chem.*, **1967**, 13, 93.

(113) Parker, V., *Acc. Chem. Res.*, **1984**, 17, 243.

(114) Hammerich, O.; Parker, V., *Acta. Chem. Scand.*, **1982**, B36, 519.

(115) Parker, V., *Acta. Chem. Scand.*, **1970**, B24, 2757.

(116) Parker, V., *Acta. Chem. Scand.*, **1970**, B24, 3151.

(117) Parker, V., *Acta. Chem. Scand.*, **1970**, B24, 3162.

(118) Reitstoen, B.; Parker, V., *Acta. Chem. Scand.*, **1992**, 46, 464.

(119) Reitstoen, B.; Parker, V., *J. Am. Chem. Soc.*, **1991**, 113, 6954.

(120) Andrieux, C.; Nadjo, L.; Savéant, J., *J. Electroanal. Chem.*, **1970**, 26, 147.

(121) Simulations were performed using DigiSim 2.0, (Bioanalytical Systems, Inc., W. Lafayette, IN) for the rate laws $k_{obs}[A][B]$ and $k_{obs}[B]^2$, where $k_{obs} = k\,[CH_3OH]$. For the data in Figure 4-12→4-15, the cathodic current (I_{pc}) is measured from the

zero-current axis. The pseudo second order rate constant k_{obs} was found to vary with [CH_3OH]: $k_{obs} = 4.3 \times 10^3$, 1.1×10^4 , and 2.6×10^4 $M^{-1}s^{-1}$ at 0.25, 0.5, and 1.0 M CH_3OH, respectively. Thus, based upon CV analysis, the overall rate law is k[A][B][X] with $k = 2.9 \times 10^4$ $M^{-2}s^{-1}$.

(122) Zefirov, N.; Zhdankin, V.; Koz'min, A., *Russian Chem. Rev.*, **1988**, *57*, 1041, and references therein.

(123) The factors which affect whether radical cation decay might occur via disproportionation have been extensively discussed by Parker, see reference (112).

(124) Fujita, M.; Fukuzumi, S., *Chem Letters*, **1993**, 1911.

(125) As might be expected, the electron-donating methoxy in **7** causes the molecule to be more easily oxidized than starting compound **1**. The CV of **7** exhibits a peak potential of +676 mV (0.69 mM in $CH_3CN/LiClO_4$). Under analogous conditions, E_P for **1** is ca. 750 mV.

(126) Parker, V., *J. Chem. Soc. Chem. Commun.*, **1968**, 610.

(127) Norrsell, F.; Handoo, K.; Parker, V., *J. Org. Chem.* **1993**, 58, 4929.

(128) Dewar, M. J.; Zoebisch, E.; Healy, E.; Stewart, J. J., *J. Am. Chem. Soc.*, **1985**, 107, 3902.

(129) Closs, G.; Klinger, H., *J. Am. Chem. Soc.*, **1965**, 87, 3265.

(130) Bauld, N.; McDermed, J.; Hudson, C.; Rim, Y.; Zoeller, J.; Gordon, R.; Hyde, J., *J. Am. Chem. Soc.*, **1969**, 91, 6666.

(131) Spin desnities for the H(1s) orbital were determined using the keywords UHF and ESR, and converted to hyperfine coupling constants using the relationship: a_H =

$\rho_{H,1s}$ x 382 G. (The constant 382 G is derived from the experimentally observed a_H^{α} for the methyl radical (23.0G) and the AM1-calculated spin density in H(1s) (0.0602). Hyperfine coupling constants calculated in this manner nicely duplicate experimental values for several cyclopropane-containing radicals and radical ions. For example, the observed hyperfine couplings for the cyclopropylcarbinyl radical (which adopts the bisected conformation) are a_H^{α} = 20.74 G, a_H^{β} = 2.55 G, a_H^{χ} =2.01, 2.98 G (Kochi, J.; Krusic, P.; Eaton, D., *J. Am. Chem. Soc.*, **1969**, 91, 1877). The AM1-derived values are a_H^{α} = 21.8 G, a_H^{β} = 2.65 G, a_H^{χ} =0.68, 1.6 G. For 9-cyclopropylanthracene radical anion (which adopts the perpendicular conformation), AM1 predicts a_H^{β} = 5.9 G (experimentally, a_H^{β} = 6.64 G; reference 23).

(132) a) Parker, V., *Acta Chim. Scand.*, **1970**, 24, 2757; b) *ibid*, 2775; c) *ibid*, 3151; d) *ibid*, 3161; e) *ibid*, 3171; f) *ibid*, 3455.

(133) Parker, V., *Tetrahedron Lett.*, **1972**, 1450.

(134) Parker, V., *J. Chem. Soc., Chem. Commun.*, **1969**, 873.

(135) Fieser, L.; Putnam, S., *J. Am. Chem. Soc.*, **1947**, 69, 1038.

(136) Badger, G.Cook, J., *J. Chem. Soc.*, **1939**, 802.

(137) Criegee, R. in Wiberg, K. "*Oxidation in Organic Chemistry*", **1965**, Acedemic, New York.

(138) Li, Z.; Tolbert, L., *Gaodeng Xuexiao Huaxue Xuebao* (Chinese), **1995**, 16, 380.

(139) Li, Z.; Tolbert, L., *Acta Chimica Sinica* (Chinese), **1995**, 53, 1204.

(140) Li, Z.; Tolbert, L., *Youji Huaxue* (Chinese), **1995**, 15, 303.

(141) Camaioni, D., "*Electron Transfer and Ion Pair Formation During Oxidation and Gasification of Coal*", Final Report to Gas Research Institute (GRI-85/0056), **1985**, pp 1-65.

(142) Camaioni, D., "*Electron Transfer and Radical Cation Reactions of Coal Moodel Compounds*", Final Report to Gas Research Institute (GRI-88/0150), **1988**.

(143) Camaioni, D., "*Investigation of Carbon-Carbon Bond Cleavage in Radical Cations*", Final Report to Gas Research Institute (GRI-90/0000), **1990**.

(144) Sugiyama, T., *Chem. Lett.*, **1987**, 1013.

(145) Fujita, M. and Fukuzumi, S., *Chem. Lett.*, **1993**, 1911.

(146) Oyama, M.; Nozaki, K.; Okazaki, S., *J. Electroanal. Chem.*, **1991**, 304, 61.

(147) Oyama, M.; Nozaki, K.; Nagaoka, T.; Okazaki, S., *Bull. Chem. Soc. Jpn.*, **1990**, 63, 33.

(148) Bordwell, F.; Cheng, J., *J. Am. Chem. Soc.*, **1989**, 111, 1972.

(149) Zhang, X.; Bordwell, F.; Bares, J.; Cheng, J.; Petrie, B., *J. Org. Chem.*, **1993**, 58, 3051.

(150) Sehested, K.; Holcman, J., *J. Phys. Chem.*, **1978**, 82, 651.

(151) Still, W. Clark; Kahn, M.; Mitra, A. *J. Org. Chem.* **1978**, *43*, 2923.

(152) Drumright, R., " *Radical Anion Rearrangement. Aryl Cyclopropyl Ketyl Anions*", Ph. D. Dissertation, **1991**, Chapter 5, Virginia Polytechnic Institute and State University, Blacksburg, Virginia.

(153) Gordon, A.; Ford, R., "*The Chemist's Companion, A Handbook of Practical Data, Techniques, and References*", **1972**, John Wiley & Sons, New York.

(154) Rosemal, H. Mas, "*Stereoelectronic effects in the brominations of cyclopropylarenes and 9-alkylanthracenes*", Ph.D. Dissertation, **1989**, Chapter 5, pp101, Virginia Polytechnic Institute and State University, Blacksburg, Virginia.

(155) Hahn, R.; Howard, P.; Kong, S.; Lorenzo, G.; Miller, N., *J. Am. Chem. Soc.*, **1969**, 91, 3558.

(156) Simmons, H.; Cairns, T.; Vladuchick, S.; Hoiness, C., in "*Organic Reactions*", Dauben, W. etc. eds., **1973**, vol. 20, pp 1~132, John Wiley & Sons, Inc., New York.

VITA

Yonghui Wang was born on September 2, 1961 in Lingbao, China to Ximei Li and Fusheng Wang. He graduated from the Sixth High School of Lingbao in 1979 where he had a growing curiosity in chemistry.

In the Fall of 1979 he enrolled at Henan Normal University, Xinxiang, China with a dream of becoming a chemistry teacher. After receiving a Bachelor of Science in chemistry in1983, he was admitted to the graduate school at Northeast University, Shenyang, China. He studied analytical chemistry under the guidance of Prof. Shousong Zhang and quickly obtained his Master's degree in 1985.

In December of 1985 he became a faculty member of the Department of Environmental Engineering at Xian University of Architecture and Technology, Xian, China. He was promoted to Lecturer in 1988, vice-director of Environmental Engineering Division and associate professor in 1993.

In the fall of 1993 he entered the doctoral program at Virginia Polytechnic Institute and State University where he worked in the area of organic chemistry under the guidance of Prof. James M. Tanko. He received a Doctor of Philosophy in chemistry in June, 1997.

He married Ailian Wang on October 27, 1987 in Xian, China, and they currently have an eight-year-old son and a soon to be born second child. He will begin his postdoctoral research under the guidance of Prof. William von E. Doering in the Chemistry Department at Harvard University, Cambridge, Massachusetts, USA.